



University
of Glasgow

Koh-Tan, Han Hui Caline (2007) *Cardiovascular candidate genes within the oxidative stress pathway: rat and human studies*. PhD thesis.

<http://theses.gla.ac.uk/6293/>

Copyright and moral rights for this thesis are retained by the author

A copy can be downloaded for personal non-commercial research or study, without prior permission or charge

This thesis cannot be reproduced or quoted extensively from without first obtaining permission in writing from the Author

The content must not be changed in any way or sold commercially in any format or medium without the formal permission of the Author

When referring to this work, full bibliographic details including the author, title, awarding institution and date of the thesis must be given

CARDIOVASCULAR CANDIDATE GENES WITHIN THE OXIDATIVE STRESS PATHWAY: RAT AND HUMAN STUDIES

Thesis for the degree of Doctorate of Philosophy (Ph.D.)

BHF Glasgow Cardiovascular Research Centre
Division of Cardiovascular and Medical Sciences
Department of Medicine and Therapeutics
Faculty of Medicine
University of Glasgow

© Han Hui Caline Koh-Tan; *B.Sc, M.Res.*

1st November 2007

DECLARATION

I declare that this thesis has been written by myself and is a record of research performed by myself with the exception of superoxide and hydrogen peroxide production measurements (Dr. Carlene A. Hamilton), sacrifice of animals (Dr. Delyth Graham and Ms. Elisabeth Beattie), measurements of vascular compliance in association study subjects (Dr. Christian Delles, Dr. Lukas Zimmerli and Dr. David McGrane) and some of the work involving *in situ* hybridisation (Dr. Michelle O'Reilly). It has not been submitted previously for a higher degree. The research was carried out in the BHF Cardiovascular Research Centre, under the supervision of Prof. Anna Dominiczak and Dr. Delyth Graham. The research in the first year was carried out under the supervision of Dr. M. Julia Brosnan and Prof. Anna F. Dominiczak.

(Caline Tan)

ACKNOWLEDGEMENTS

First of all, I would like to thank my supervisors Prof. Anna F. Dominiczak and Dr. Delyth Graham for their guidance and advice. I have learnt much much more than just scientific research while under their guidance.

Although Dr. Brosnan was my supervisor only in my first year of PhD, I cannot thank her enough for helping to make my PhD a possibility.

I would like to thank Dr. Carlene Hamilton for being my advisor, listening to my whining and her help in obtaining the human tissue samples used in this project. Dr. Christian Delles, Dr. David McGrane and Dr. Lukas Zimmerli also helped tremendously in obtaining human varicose veins as control samples.

I would like to thank Dr. Wai Kwong Lee and Dr. Nick Brain for all their guidance and expertise in the molecular genetics work, helping me to understand more about genetics. Special thanks to Dr. Brain for helping to analyse the genotype data for eNOS intron 4 VNTR polymorphism in the initial population of case-control study.

Special thanks to Dr. Michelle O'Reilly, from the Department of Molecular Genetics, University of Edinburgh, for their help in my work involving *in situ* hybridisation, including different ways of using the data available in the genome database and the designing of probe target sequences for *in situ* hybridisation.

Special thanks to Prof. Irving Listowsky for his kind donation of antisera against the human *GSTM* (common) class and the specific antisera for human *GSTM4*, and Prof. John D. Hayes for his kind donation of antisera against rat *Gstm1*, *Gstm2* and human *GSTM3* antisera

Finally, very special thanks to my husband, parents and brother for the sacrifices and special support when I needed them most. I could not have done this without them.

CONTENTS	PAGE
Declaration	i
Acknowledgements	ii
Contents	iii
List of Figures	viii
List of Tables	x
Publications	xi
Abbreviations	xii
Abstract	1
1. Introduction	4
1.1. Cardiovascular Disease	4
1.1.1. Risk Factors	5
1.1.1.1. Hypertension	5
1.1.1.2. Genetics of Hypertension	8
1.1.1.3. Environmental Factors	10
1.1.2. Current Management	12
1.2. Animal Studies	13
1.3. Oxidative Stress in Cardiovascular Disease	20
1.3.1. Nitric Oxide	20
1.3.2. Endothelial Dysfunction	22
1.3.3. Reactive Oxygen Species	23
1.3.4. Oxidative Stress	24
1.3.5. Endothelial Nitric Oxide Synthase	27
1.3.6. Reactive Oxygen Species Sources and Stimuli	30
1.3.6.1. NAD(P)H oxidase	31
1.3.6.2. Other Sources of O ₂ ⁻	32
1.3.6.3. Angiotensin II and Other Stimuli	32
1.4. Anti-oxidant Enzymes – 1 st Line of Defence	33
1.4.1. Superoxide Dismutase	33
1.4.2. Catalase	35
1.5. Anti-oxidant Enzymes – 2 nd Line of Defence	36
1.5.1. Glutathione	36
1.5.2. Glutathione Peroxidase	38
1.5.3. Glutathione S-Transferases	39
1.5.3.1. Nomenclature of Glutathione S-Transferase μ Genes	41
1.5.3.2. Glutathione S-Transferase μ class	42
AIMS	45

2. Materials and Methods	46
2.1. Animal Strains	46
2.1.1. Congenic Breeding Strategy	46
2.1.2. Blood Pressure Measurement by Tail-Cuff Plethysmography	47
2.2. Rat Tissues	48
2.2.1. Preparation of Rat Tissues for Cryosections	48
2.2.2. Preparation of Rat Tissues for Paraffin Sections	48
2.2.2.1. Silanisation of Microscope Slides	49
2.3. Human Tissues	49
2.3.1. Vascular Tissues from Clinical Patients	49
2.3.2. Handling of Vascular Tissues	49
2.3.3. Preparation of Vascular Tissues for Cryosections	50
2.3.4. Preparation of Vascular Tissues for Paraffin Sections	50
2.4. General Molecular Biology	50
2.4.1. DNA Extraction	50
2.4.2. DNA Purification	51
2.4.3. Nucleic Acid Quantitation	51
2.4.4. Polymerase Chain Reaction (PCR)	52
2.4.5. Restriction Fragment Length Polymorphism (RFLP)	52
2.4.6. Sequencing	52
2.5. mRNA Expression	53
2.5.1. Total RNA Extraction	53
2.5.1.1. Total RNA Extraction using RNA Bee	53
2.5.1.2. Total RNA Extraction using Qiagen RNeasy Kit	54
2.5.2. DNase Treatment of Extracted Total RNA	54
2.5.2.1. DNase Treatment using RQ1 DNase	54
2.5.2.2. DNase Treatment using DNA-free™ kit	55
2.5.3. Reverse Transcription (RT) – PCR	55
2.5.4. Real-time RT-PCR	56
2.5.4.1. Real-time RT-PCR using Lightcycler™	56
2.5.4.2. Real-time RT-PCR using Taqman	56
2.5.5. Establishment of RT-PCR Products Identity	57
2.6. mRNA Localisation	57
2.6.1. Preparation of Cryosections	57
2.6.2. <i>In Situ</i> Hybridisation (ISH) using ³⁵ S-riboprobes	57
2.6.2.1. Preparation of Riboprobes	58
2.6.2.2. Pre-treatment of Tissue	59
2.6.2.3. Prehybridisation	59

2.6.2.4.	Hybridisation	59
2.6.2.5.	RNase Treatment and Washes	60
2.6.2.6.	Slide Dipping	60
2.6.2.7.	Haematoxylin and Eosin Counter Stain	62
2.7.	Protein Expression	62
2.7.1.	Protein Extraction	62
2.7.2.	Protein Quantitation	63
2.7.3.	Dot blot	63
2.8.	Protein Localisation	63
2.8.1.	Immunohistochemistry (IHC)	63
2.8.1.1.	Pre-treatment of Sections	64
2.8.1.2.	Antigen Retrieval	64
2.8.1.3.	Primary Antibody	64
2.8.1.4.	Secondary Antibody for IHC	64
2.8.1.5.	Enzymatic Colour Development	65
2.8.2.	Multiple Antigen IHC	65
2.8.2.1.	First Antigen IHC	65
2.8.2.2.	Second Antigen IHC	65
3.	Expression and Localisation of Rat Glutathione S-transferase μ Isoforms	67
3.1.	Introduction	67
3.2.	Materials & Methods	68
3.2.1.	Animal strains	68
3.2.2.	Human Samples	68
3.2.3.	Accession Numbers of Gene Sequences	68
3.2.3.1.	Rat <i>Gstm</i> Sequences	68
3.2.3.2.	Human <i>GSTM</i> Sequences	69
3.2.4.	mRNA Expression and Localisation	69
3.2.5.	Protein Expression and Localisation	74
3.2.6.	<i>hGSTM1*0</i> Genotyping of Human Vascular Tissues	74
3.2.7.	Statistical Analysis	74
3.3.	Results	75
3.3.1.	Systolic Blood Pressure of the Rat Strains	75
3.3.2.	Characterisation of Rat <i>Gstm</i> Genes	75
3.3.2.1.	Rat <i>Gstm</i> Sequences	75
3.3.2.2.	Expression of Rat <i>Gstm</i> Isoforms in Various Tissues	75
3.3.2.3.	Vascular Localisation and Expression of Rat <i>Gstm</i> Isoforms	79
3.3.2.4.	Renal Localisation and Expression of Rat <i>Gstm</i> Isoforms	85
3.3.3.	Characterisation of Human <i>GSTM</i> Genes	94

3.3.3.1.	Human <i>GSTM</i> Sequences	94
3.3.3.2.	Expression of Human <i>GSTM</i> Isoforms in Various Tissues	97
3.3.3.3.	Vascular Localisation of Human <i>GSTM</i> Isoforms	97
3.3.4.	Optimisation of In Situ Hybridisation on Vascular Tissues	97
3.3.5.	Lower Smooth Muscle α -Actin in Female Rats	103
3.4.	Discussion	103
4.	Effects of Antihypertensive Drugs on Expression Levels of Rat Glutathione S-transferase μ Isoforms	112
4.1.	Introduction	112
4.2.	Materials & Methods	113
4.2.1.	Animal Strains and Antihypertensive Therapy	113
4.2.2.	Superoxide Production Measurement	114
4.2.3.	Hydrogen Peroxide Production Measurement	114
4.2.4.	Gene Expression	116
4.2.5.	Statistical Analysis	116
4.3.	Results	116
4.3.1.	Olmesartan Reversal Study	116
4.3.1.1.	Effect of Drugs on Vascular Function and Gene Expression	118
4.3.1.2.	Effect of Drugs on Renal Function and Gene Expression	118
4.3.2.	Olmesartan Prevention Study	122
4.3.2.1.	Effect of Drugs on Vascular Function and Gene Expression	126
4.3.2.2.	Effect of Drugs on Renal Function and Gene Expression	126
4.4.	Discussion	133
4.4.1.	Vascular Effects of Antihypertensive Treatment	133
4.4.2.	Renal Effects of Antihypertensive Treatment	134
5.	Gene-Phenotype Interactions in the Oxidative Stress Pathway	136
5.1.	Introduction	136
5.1.1.	<i>CYBA</i> Polymorphisms	136
5.1.2.	<i>NOS3</i> Polymorphisms	137
5.1.3.	Arterial Stiffness and Vascular Compliance	138
5.2.	Materials & Methods	138
5.2.1.	Subjects	138
5.2.2.	Pulsewave Analysis	140
5.2.3.	DNA Samples	140
5.2.4.	PCR	141
5.2.5.	Genotyping	141
5.2.5.1.	Genotyping by Sequencing	141
5.2.5.2.	Genotyping by RFLP	141

5.2.5.3. Genotyping by PAGE Resolution	143
5.2.6. Statistical Analysis	143
5.3. Results	144
5.3.1. Genotype and Haplotype Analysis of <i>CYBA</i> Polymorphisms	144
5.3.2. <i>CYBA</i> Gene – Phenotype Interactions	147
5.3.3. Genotype and Haplotype Analysis of <i>NOS3</i> Polymorphisms	149
5.3.4. <i>NOS3</i> Gene – Phenotype Interactions	149
5.4. Discussion	152
6. Conclusions	155
References	158
Appendices	181
A – Recipes for Solutions	181
B – Suppliers and Catalogue Numbers	182
C – Multiple Alignment of Rat <i>Gstm</i> Sequences	185
D – Multiple Alignment of Human <i>Gstm</i> Sequences	193

LIST OF FIGURES	PAGE
Figure 1.1: Complex relationships for blood pressure regulation	7
Figure 1.2: Renin-angiotensin system enzymatic cascades	9
Figure 1.3: Genealogical background of the stroke-prone spontaneously hypertensive rat (SHRSP)	15
Figure 1.4: Marker-assisted “speed” congenic strategy	17
Figure 1.5: Chromosome 2 congenic strain SP.WKY _{Gla2c*}	18
Figure 1.6: Daytime and night-time average systolic (A) and diastolic (B) blood pressure	19
Figure 1.7: Schematic diagram to illustrate NO intracellular signalling processes across vascular wall	21
Figure 1.8: The roles of oxidative stress enzymes in maintaining the balance between O ₂ ⁻ and NO	25
Figure 1.9: Schematic diagram of a functionally active dimeric NOS	28
Figure 1.10: Regulation of NAD(P)H oxidase ROS production by rac1	28
Figure 1.11: Functional roles of glutathione	37
Figure 1.12: Organisation of the glutathione s-transferase mu genes in human and rat	43
Figure 3.1: Systolic blood pressure by tail-cuff plethysmography	76
Figure 3.2: Localisation of rGstm isoforms in vasculature	80
Figure 3.3: Vascular expression levels of <i>rGstm</i> isoforms	82
Figure 3.4: IHC of rGstm1 in male WKY, SHRSP and SP.WKY _{Gla2c*} carotid arteries	83
Figure 3.5: IHC of rGstm2 in male WKY, SHRSP and SP.WKY _{Gla2c*} carotid arteries	84
Figure 3.6: Effect of age on expression levels of vascular <i>rGstm</i> isoforms	86
Figure 3.7: Localisation of rGstm1 in kidney	87
Figure 3.8: Localisation of rGstm2 in kidney	89
Figure 3.9: Localisation of rGstm5 in kidney	90
Figure 3.10: Renal expression levels of <i>rGstm</i> isoforms	91
Figure 3.11: IHC of rGstm1 on male WKY, SHRSP and SP.WKY _{Gla2c*} kidney	92
Figure 3.12: Effect of age on expression levels of renal <i>rGstm</i> isoforms	95
Figure 3.13: Localisation of hGSTM isoforms in vasculature	99
Figure 3.14: Preliminary ISH experiments	101
Figure 3.15: Variations in pre-treatment of rat aorta for ISH	102
Figure 3.16: IHC of smooth muscle α -actin (<i>Acta2</i>) in carotid arteries	104
Figure 3.17: A schematic diagram of a juxtamedullary nephron	107

Figure 3.18: Phylogenetic tree of <i>GSTM</i> gene family from human, rat and mouse	110
Figure 4.1: Schematic for the prevention and reversal drug study	115
Figure 4.2: Reversal study systolic blood pressure	117
Figure 4.3: Reversal study vascular superoxide production	117
Figure 4.4: Effect of drugs on vascular gene expression in reversal study	119
Figure 4.5: Effect of drugs on vascular <i>rGstm</i> gene expression in reversal study	120
Figure 4.6: Reversal study – Superoxide and hydrogen peroxide production in renal cortex and medulla	121
Figure 4.7: Effect of drugs on renal gene expression in reversal study	123
Figure 4.8: Effect of drugs on renal <i>rGstm</i> gene expression in reversal study	124
Figure 4.9: Prevention study systolic blood pressure	125
Figure 4.10: Prevention study vascular superoxide production	125
Figure 4.11: Effect of drugs on vascular gene expression in prevention study	127
Figure 4.12: Effect of drugs on vascular <i>rGstm</i> gene expression in prevention study	128
Figure 4.13: Prevention study – Superoxide and hydrogen peroxide production in renal cortex and medulla	129
Figure 4.14: Effect of drugs on renal gene expression in prevention study	131
Figure 4.15: Effect of drugs on renal <i>rGstm</i> gene expression in prevention study	132

LIST OF TABLES	PAGE
Table 1.1: Classification of hypertension	5
Table 1.2: Mendelian forms of hypertension	11
Table 1.3: Properties of nitric oxide synthases (NOSs)	29
Table 1.4: Properties of superoxide dismutases (SODs)	34
Table 3.1: Accession numbers of sequences used to generate additional sequences for <i>rGstm</i> mRNA transcripts	70
Table 3.2: The primers and conditions for detection of <i>rGstm</i> genes expression	71
Table 3.3: The primers and conditions for detection of <i>hGSTM</i> genes expression	72
Table 3.4: Primers used for generating probe templates for <i>in situ</i> hybridisation	73
Table 3.5: (A) Percentage homology in coding sequences between <i>rGstm</i> isoforms	77
(B) Percentage homology in protein sequences between <i>rGstm</i> isoforms	77
Table 3.6: Expression of <i>rGstm</i> isoforms in various tissues	78
Table 3.7: Relative gene expression levels of <i>rGstm</i> isoforms in various tissues	78
Table 3.8: (A) Percentage homology in coding sequences between <i>hGSTM</i> isoforms	96
(B) Percentage homology in protein sequences between <i>hGSTM</i> isoforms	96
Table 3.9: Expression of <i>hGSTM</i> isoforms in various tissues	98
Table 5.1: Indices of arterial stiffness	139
Table 5.2: Genotyping primers for <i>CYBA</i> and <i>NOS3</i>	141
Table 5.3: Baseline characteristics of the study subjects	145
Table 5.4: Single SNP genotype distribution of <i>CYBA</i> gene	146
Table 5.5: Frequency of three-polymorphisms haplotypes of the <i>CYBA</i> gene	148
Table 5.6: Significance of the association between <i>CYBA</i> polymorphisms and clinical phenotypes as single polymorphisms	148
Table 5.7: Single SNP genotype distribution of <i>NOS3</i> gene	150
Table 5.8: Frequency of three-polymorphisms haplotypes of the <i>NOS3</i> gene	151
Table 5.9: Significance of the association between <i>NOS3</i> polymorphisms and clinical phenotypes as single polymorphisms	151

PUBLICATIONS

Abstracts

H.H.C Koh-Tan, D. Graham, C. Hamilton, M.W. McBride, A.F. Dominiczak. Do Pharmacological Interventions Reduce Oxidative Stress in a Model of Genetic Hypertension? *21st Scientific Meeting of the International Society of Hypertension, Fukuoka (Japan), 15th – 19th October 2006*. In: *J. Hyper.* 2006, 24(S6):S54.(Oral communications)

H.H.C Koh-Tan, D. Graham, C. Hamilton, M.W. McBride, A.F. Dominiczak. Do Pharmacological Interventions Reduce Oxidative Stress in a Model of Genetic Hypertension? *Annual Scientific Meeting of the British Society of Hypertension, Cambridge, 18th – 20th September 2006*. (Oral communications)

Expression and Localisation of Human and Rat *Gstm* Isoforms. **H.H.C Koh-Tan**, D. Graham, M.W. McBride, A.F. Dominiczak. *XVI European Meeting of Hypertension, Madrid (Spain), 12th – 15th June 2006*. In: *J. Hyper.* 2006, 24(S4):S332. (Poster communications)

Expression of Glutathione S-Transferase in Human Blood Vessels. **Koh-Tan HHC**, Brosnan MJ, Hamilton CA, Lee WK, Brain N, Al-Benna S & Dominiczak AF. *Scottish Society for Experimental Medicine, Dundee, June 2004*. (Poster communications)

ABBREVIATIONS

μM	micromolar (micromoles per litre)
ACE	angiotensin converting enzyme
ACE2	ACE-related carboxypeptidase
ACh	acetylcholine
ACTA2	smooth muscle α -actin
Agtr1a	angiotensin II receptor type 1 α subunit
AIx	augmentation index
AMPD2	adenosine monophosphate deaminase 2
ANOVA	analysis of variance
Ang 1-7	angiotensin 1-7
Ang 1-9	angiotensin 1-9
Ang I	angiotensin I
Ang II	angiotensin II
AP1	activator protein 1
AP2	activator protein 2
APES	3-aminopropyltriethoxysilane
APS	ammonium persulphate
ARBs	AT ₁ R blocker
ARE	antioxidant response element
AS	antisense
AT	annealing temperature
ATP	adenosine triphosphate
AT ₁ R	angiotensin type 1 receptor
AT ₂ R	angiotensin type 2 receptor
BCA	bicinchoninic acid
BH ₄	tetrahydrobiopterin
BN	Brown Norway
bp	base pair
BP	blood pressure
C1	large artery compliance
C2	small artery compliance
CA	carotid artery (ies)
Ca ²⁺	calcium ions
CAD	coronary artery disease
CABG	coronary artery bypass graft
CCB	calcium channel blockers

cDNA	complementary DNA
cGMP	cyclic guanosine monophosphate
CHD	coronary heart disease
CI	confidence interval
CRE	cyclic AMP response element
Cu/Zn-SOD	copper/zinc superoxide dismutase
CVD	cardiovascular disease
CYBA	cytochrome <i>b</i> ₂₄₅ , α polypeptide
Cyt _{b558}	cytochrome _{b558}
COX	cyclo-oxygenase
DAB	3,3' – diaminobenzidine
DBP	diastolic blood pressure
DEPC	diethyl pyrocarbonate
DEPC- dH ₂ O	DEPC- treated dH ₂ O
dH ₂ O	distilled water
DMSO	dimethyl sulphoxide
DNA	deoxyribonucleic acid
DNase	deoxyribonuclease
dNTPs	deoxyribonucleotide triphosphates
DOCA	deoxycorticosterone acetate
dsDNA	double-stranded DNA
dsRNA	double-stranded RNA
dTT	dithiothreitol
ecSOD	extracellular superoxide dismutase
EDHF	endothelium-derived hyperpolarising factor
EDRF	endothelium-derived relaxing factor
EDTA	ethylenediaminetetraacetic acid
EGF(-R)	epidermal growth factor (receptor)
EH	essential hypertension
eNOS	endothelial nitric oxide synthase
EPS8L3	epidermal growth factor receptor pathway substrate 8-like protein 3.
ERE	oestrogen response element
ESRD	end-stage renal disease
FAD	flavin adenine dinucleotide
FMN	flavin mononucleotide
GCS	γ -glutamyl-cysteine synthetase
GPx	glutathione peroxidase
GRE	glucocorticoid response element

GS	glutathione synthetase
GSH	reduced glutathione/glutathione
GSSG	oxidised glutathione
GSTM	glutathione S-transferase mu type
GTP	guanosine triphosphate
H ₂ O ₂	hydrogen peroxide
HDL	high density lipoprotein
hGSTM	human glutathione s-transferase mu
HOCl	hypochlorous acid
HPLC	high performance liquid chromatography
HRP	horse radish peroxidase
HSP	heat shock protein
HWE	Hardy Weinberg equilibrium
Igs	immunoglobulins
IHC	immunohistochemistry
IL	interleukin
ISH	<i>in situ</i> hybridisation
LDL	low density lipoprotein
L-NMMA	N-monomethyl-L-arginine
LO ⁻ or LOO ⁻	lipid radicals
MAPK(s)	mitogen-activated protein kinase(s)
Mg ²⁺	magnesium ion
mBeq	milliBequerel
mg	milligrams
mM	millimolar (millimoles per litre)
mmHg	millimetres of mercury
Mn-SOD	manganese superoxide dismutase
MRP	multidrug resistance-associated protein
mRNA	messenger RNA
NAD(P)H	reduced nicotinamide adenine dinucleotide (phosphate)
NAD(P)+	oxidised nicotinamide adenine dinucleotide (phosphate)
NaOAc	sodium acetate
Ncf1	neutrophil cytosolic factor 1
NH ₄ OAc	ammonium acetate
nM	nanomolar (nanomoles per litre)
NO	nitric oxide
NO ₂ ⁻	nitrite
NO ₃ ⁻	nitrate

NOS	nitric oxide synthase
NP-40	Nonidet P-40
O ₂	molecular oxygen
O ₂ ⁻	superoxide anion
OH ⁻	hydroxyl radical
ONOO ⁻	peroxynitrite
PBS	phosphate buffered saline
PCR	polymerase chain reaction
PDE	phosphodiesterases
PDGF(-R)	platelet-derived growth factor (receptor)
PG	prostaglandin
PGI ₂	prostacyclin
PKG	cGMP-dependent protein kinase
PLG-H	Phase Lock Gel Heavy
PP	pulse pressure
PWV	pulse-wave velocity
QTL(s)	quantitative trait locus (loci)
rac1	ras-related C3 botulinum toxin substrate 1
RAS	renin-angiotensin system
RE	restriction enzymes
RFLP	restriction fragment length polymorphisms
rGstm	rat glutathione s-transferase mu
rATP	riboadenosine triphosphate
rCTP	ribocytosine triphosphate
rGTP	riboguanosine triphosphate
RNA	ribonucleic acid
RNase	ribonuclease
ROS	reactive oxygen species
rpm	revolutions per minute
RT-PCR	reverse-transcription polymerase chain reaction
SBP	systolic blood pressure
SD	standard deviation
SDS	sodium dodecyl sulphate
sdH ₂ O	sterile distilled water
SEM	standard error of the mean
SHR	spontaneously hypertensive rat
SHRSP	stroke-prone spontaneously hypertensive rat
SNP(s)	single nucleotide polymorphism(s)

SOD	superoxide dismutase
SRE	sterol regulatory element
SSC	standard saline citrate
SSRE	shear stress response element
ssRNA	single-stranded RNA
SV	saphenous vein
TA	thoracic aorta
TBE	Tris-borate EDTA
TBS	Tris-buffered saline
TE	Tris-EDTA
TEMED	tetramethylethylenediamine
TGF β	transforming growth factor β
TNF α	tumour necrosis factor α
tPA	tissue plasminogen activator
VLDL	very low density lipoprotein
VNTR	variable number of tandem repeats
VSMC(s)	vascular smooth muscle cell(s)
VV	varicose vein
WHO	world health organisation
WKY	Wistar-Kyoto rat
XRE	xenobiotics response element

ABSTRACT

Oxidative stress has been implicated in cardiovascular disease (CVD) including hypertension. We hypothesise that oxidative stress-related genes and their functional polymorphisms influence the risk of developing hypertension and coronary artery disease. Combined congenic breeding strategy and microarray expression profiling studies from our group previously identified rat glutathione s-transferase mu type-1 (*rGstm1*) as a functional and positional candidate gene implicated in hypertension. In the previous studies, expression of *rGstm1* was lower in the kidney from the hypertensive rat model, stroke-prone spontaneously hypertensive rat (SHRSP), compared to the normotensive Wistar Kyoto (WKY) and a chromosome 2 congenic strain (SP.WKY_{Gla2c*}). The *rGstm1* belongs to a family of *Gstm* genes, encoding for dimeric enzymes known to detoxify oxidised lipids and provide secondary defence against oxidative stress. This project aims to characterise *Gstm* gene family in rat and human tissues and investigate functional roles of *rGstm* genes using pharmacological intervention studies. Association between functional polymorphisms in two other genes (*CYBA* and *NOS3*), encoding for enzymes involved in oxidative stress, and coronary artery disease are also investigated.

I have characterised the expression profiles of the *rGstm* gene family in rat vascular and renal tissues. Five of the possible eight *rGstm* genes are expressed in thoracic aorta and kidney. Results from this thesis demonstrate reduced mRNA expression of several members of *rGstm* gene family, in vascular and renal tissues. Most notably, expression of vascular and renal *rGstm1* mRNA and protein, (the latter analysed by IHC), are lower in the SHRSP compared to WKY and SP.WKY_{Gla2c*}. Vascular mRNA expression of *rGstm2*, *rGstm5* and *rGstm7* were reduced in the SHRSP males compared to the WKY males and SP.WKY_{Gla2c*} males but not in the females. Vascular mRNA expression of *rGstm3* in SHRSP males was lower than SP.WKY_{Gla2c*} males but not WKY males, while SHRSP and SP.WKY_{Gla2c*} females expressed higher levels of *rGstm3* than WKY females. There were also trends towards reduced renal mRNA expression of *rGstm2*, *rGstm3*, *rGstm5* and *rGstm7* in the SHRSP compared to WKY and SP.WKY_{Gla2c*}. In the carotid artery, expression of *rGstm1* protein has been detected in all vascular cell types. In the kidney, expression of *rGstm1* protein has

been detected widely across cortex and medulla. Renal *rGstm1* expression is reduced in tissues from SHRSP rats compared to WKY and SP.WKY_{Gla2c*} at 5-weeks of age suggesting that the differential gene expression is not a consequence of increased blood pressure (BP). This reduction in renal *rGstm1* gene expression is not compensated for by other members of the *rGstm* gene family. In addition, there is also gender-specific differential expression of several vascular and renal *rGstm* genes.

The expression profile of the human *GSTM* (*hGSTM*) gene family in vascular tissue from varicose vein and saphenous vein have also been characterised in an attempt to identify the true human orthologue of *rGstm1*. There are five known members in the *hGSTM* gene family, all of which were expressed in vascular tissues. Results from characterisation of the vascular *hGSTM* gene family show that four *hGSTM* members are homologous to *rGstm1*. These four *hGstm* genes remain as potential orthologue for *rGstm1*.

Functional roles of vascular and renal *rGstm* genes have been investigated using two pharmacological intervention studies. Olmesartan (AT₁R antagonist) or hydralazine plus hydrochlorothiazide (direct vasodilator and diuretic) have been used to evaluate the oxidative stress status and gene expression of *rGstm* genes, in the reversal and prevention studies. Both drug treatments improved the BP of SHRSP rats in reversal study and prevented the rise in BP in the prevention study. Olmesartan-treated SHRSP rats demonstrated reduced superoxide (O₂⁻) and hydrogen peroxide (H₂O₂) production in both reversal and prevention studies. Minor effects by both drug treatments were observed for the *rGstm* gene family in the prevention but not the reversal study. Both drug treatments did not influence vascular or renal *rGstm1* expression in either reversal or prevention studies. Improvement in BP did not improve *rGstm1* gene expression. The *rGstm1* was not responsive to pharmacological interventions due to strain-dependent genetic abnormalities.

Polymorphisms in oxidative stress related enzymes have often been associated with coronary artery disease (CAD). It is likely that each polymorphism imparts small effects that add up to alter the balance between reactive oxygen species (ROS) and nitric oxide (NO). Functional polymorphisms in two key enzymes

involved in ROS and NO balance were investigated for association with CAD and vascular compliance as single polymorphism and as haplotypes. The two genes selected were *CYBA*, which encodes the p22^{phox} subunit of NADPH oxidase, and *NOS3*, which encodes for endothelial nitric oxide synthase (eNOS). The polymorphisms investigated were *CYBA* A-930G, C242T and A640G; and *NOS3* T-786C, intron 4A/4B and G894T. There was an association between *CYBA* A-930G with CAD, with the A allele being recessive. There was also an association between *NOS3* G894T with CAD, only when G allele was dominant. The T-786C of *NOS3* was associated with small artery compliance index (C2), in both CAD and control groups. There were no difference in haplotype frequencies of the three polymorphisms in both genes between the CAD and control groups. There were no associations between the *CYBA* or *NOS3* haplotypes with vascular compliance.

In conclusion, this thesis provides the most detailed characterisation of the *Gstm* gene family in terms of CVD to date. It has confirmed previously identified reduction in *rGstm1* expression in SHRSP, which could not be improved by antihypertensive treatment despite significant improvements in BP and oxidative stress levels. Despite careful human characterisation, four members of human *GSTM* gene family remain as potential orthologues for *rGstm1*. In addition, a relatively small association study identified significant association between CAD and polymorphisms in two key enzymes involved in NO and O₂⁻ balance.

CHAPTER 1: INTRODUCTION

1.1. Cardiovascular Disease

According to the most recent World Health Report released in 2003, nearly 147.4 million people in the world are burdened by cardiovascular disease based on estimates from 2002 alone (1). An estimated 16.7 million people died of cardiovascular diseases (CVD), particularly heart attacks and strokes, which constituted about 29.2% of death world-wide in 2002. CVD, aptly described as one of the world's neglected epidemics, is a problem in industrialised countries as well as the poorest countries and is still a growing problem. Apart from its impact on morbidity and mortality, it also has an impact on social and economic developments. According to the British Heart Foundation (BHF) 2006 statistics on the website, CVD is the main cause of death in the UK having accounted for just over 216,000 deaths (37%) in 2004 (2). The death rate from coronary heart disease (CHD) has been highest in Scotland consistently for over 25 years. CVD cost the health care system in the UK around £14,750 million in 2003, of which hospital care of CVD patients accounted for 76% and 18% for costs of drugs and dispensing them (3). Production losses due to mortality and morbidity associated with CVD cost the UK over £6,200 million in 2003. In 2004, the costs of prescriptions for lipid lowering and antihypertensive drugs came to a total of £1.379 billion. Overall CVD is estimated to cost the UK economy just under £26 billion a year. For these reasons, it is desirable to identify the mechanisms, including genetic factors, that leads to cardiovascular disease.

CVD are diseases of the heart and circulatory system, stroke, coronary heart disease, heart failure, peripheral vascular disease and renal failure/end-stage renal disease (ESRD) (2). Hypertension, atherosclerosis and diabetes mellitus are risk factors, often seen in early development of CVD. The major modifiable risk factors of CVD are high blood pressure (BP), hypercholesterolaemia, smoking, lack of exercise, unhealthy diets, obesity and diabetes mellitus (2;4). Other modifiable risk factors include low socioeconomic status, mental ill-health, psychosocial stress, alcohol consumption and use of certain medication (4). While one can try to reduce risk factors such as these, there are also risk factors for CVD that cannot be changed. Non-modifiable risk factors include aging, known family

history of CVD, gender and ethnicity. The major CVD risk factors explain at least 75–85% of new cases of coronary heart disease (1), and illustrate the need for research into risk factors such as hypertension.

1.1.1. Risk Factors

Hypertension, a major risk factor for many CVD and the most important risk factor for stroke, and its genetic components will be the main focus of this project.

1.1.1.1. Hypertension

Hypertension is defined clinically as systolic blood pressure (SBP) of over 140mmHg and diastolic blood pressure (DBP) of over 90mmHg in adults aged ≥ 18 (5). There are three grades of hypertension, from mild to moderate and severe (*Table 1.1*) (5). Hypertension can be primary/essential hypertension or secondary to other causes. Essential (idiopathic causes) hypertension (EH) refers to a lasting increase in BP with genetic and environmental causes. Certain hypertension occurs as a consequence of rare mutations that result in drastic physiological perturbations. These mutations will be discussed in the next section. Secondary hypertension is due to renal causes, such as renal artery stenosis, or adrenal causes, such as Conn's disease and phaeochromocytoma. These will not be discussed further in this thesis.

Table 1.1: Classification of hypertension

Blood Pressure (BP) Category	Systolic BP (mmHg)	Diastolic BP (mmHg)
Normal	<120	<80
High-normal	135 – 139	85 – 89
Mild hypertension (Grade 1)	140 – 159	90 – 99
Moderate hypertension (Grade 2)	160 – 179	100 – 109
Severe hypertension (Grade 3)	≥ 180	≥ 110

Adapted from (5)

Diastolic blood pressure (DBP) increases with age until approximately 50 years of age while systolic blood pressure (SBP) increases with age until approximately 80 years of age. Mean systolic blood pressure increases with age in both men and women, rising from 127mmHg in men aged 16-24 to 145mmHg in men aged 75 and over, and from 119mmHg to 149mmHg in women (1). According to the Scottish Health Survey, 33% of Scottish men and 33% of Scottish women are hypertensive or are treated for hypertension (2). The prevalence of EH rises with age, affecting up to 60-70% of those 70-years old or more (6). The epidemiological relationship between SBP and DBP and risk of developing CVD is continuous but is only one of the important components (7). The World Health Report 2002 estimates that around 11% of all disease burden in developed countries is caused by raised blood pressure, and that over 50% of CHD and almost 75% of stroke in developed countries is due to high SBP (8). Both epidemiological studies and clinical trials provide compelling evidence that antihypertensive therapy effectively reduce the risk of CVD. A reduction in blood pressure by an average of 12/6 mmHg can be expected to reduce stroke by 40% and coronary heart disease (CHD) by 20% (9).

The specific underlying mechanisms involved in the development of hypertension are still incompletely understood but it is a major risk factor for stroke, myocardial infarction, congestive heart failure and ESRD. A wide variety of physiological systems that have pleiotropic effects and interact in a complex manner have been found to influence BP (*Figure 1.1*) (10;11). Sodium and fluid balance, and vasomotor tone are important in BP regulation. Both of these mechanisms are affected by numerous genetic and environmental factors, controlled by hormonal, non-sympathetic, paracrine and intracellular feedback loops. One of the best examples is the renin–angiotensin system (RAS). Interactions between these factors change with age.

RAS is well known for its regulation of blood pressure and fluid homeostasis, The RAS comprises a cascade of enzymatic reactions resulting in the formation of the main effector molecule angiotensin II (Ang II). Ang II can act either as a systemic hormone (endocrine) or as a locally generated factor (paracrine, autocrine) (12;13).

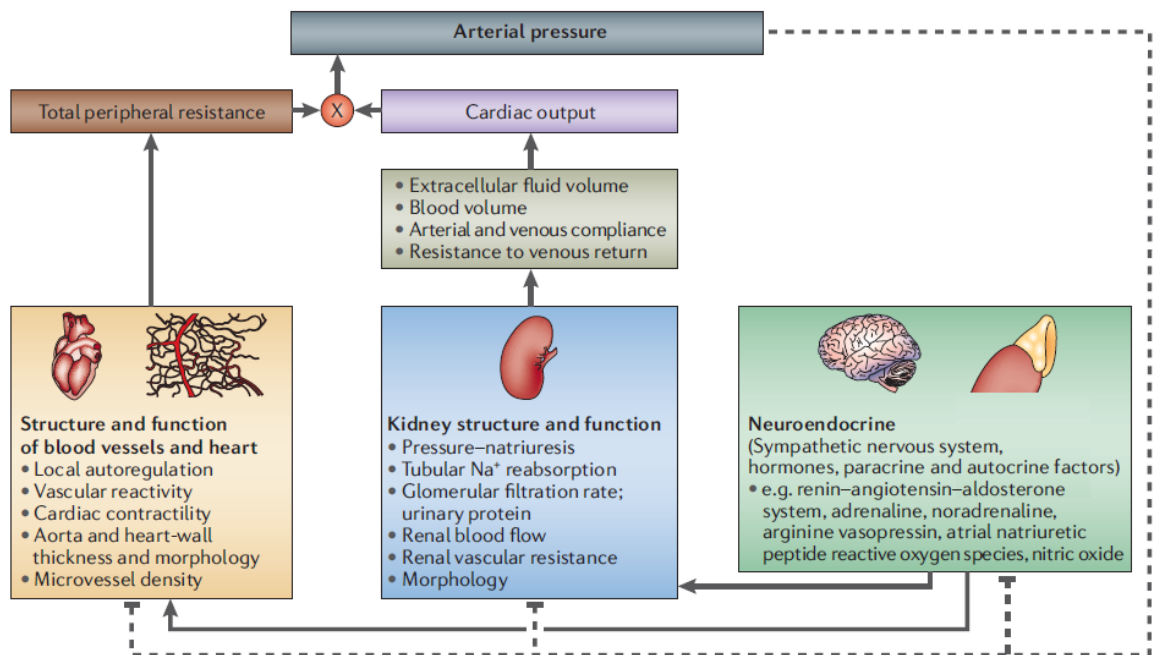


Figure 1.1: Complex relationships for blood pressure regulation

Arterial pressure can be computationally defined as the product of cardiac output and the total peripheral resistance. Cardiac output is determined by the complex relationships between extracellular fluid volume, blood volume, arterial and venous compliance and resistance of blood flow around the systemic circulation. The kidney is the primary controller of both extracellular fluid volume and arterial pressure through the pressure-natriuresis mechanism. The total peripheral resistance is determined by the structure and function of the vasculature and by local autoregulatory mechanisms. Both kidney and vascular functions are influenced by neuroendocrine factors. Homeostatic negative feedback (dotted lines) also has an important role in the regulation of arterial pressure. A variety of sensors of arterial pressure produce signalling response outputs that feed back to control neuroendocrine, vascular and kidney function. Taken from Ref. (11)

Ang II production can be angiotensin converting enzyme (ACE)–dependent or –independent (*Figure 1.2*). ACE-dependent Ang II formation is catalysed by a two-step reaction, first to angiotensin I (Ang I) by renin and subsequently by ACE. ACE-independent conversion to Ang II can be from angiotensinogen directly by enzymes tissue plasminogen activator (tPA), cathepsin G and tonin, or from Ang I by chymase and cathepsin G. Ang II then binds to Ang II type 1 receptor (AT₁R) or type 2 receptor (AT₂R) located on cell membrane, mediating its physiological effects. A recently discovered novel ACE-related carboxypeptidase (ACE2) converts Ang I to angiotensin 1-9 (Ang 1-9) and subsequently to angiotensin 1-7 (Ang 1-7), a known vasodilator (14). ACE2 expression was found to be decreased in three different hypertensive rat models (15) while ACE2 knock-out mice exhibited increased systolic blood pressure (16). AT₁R has been implicated in the regulation of ACE2 and Ang 1-7 expression (17).

The AT₁R and AT₂R display a heterogeneous distribution in peripheral tissues and brain but differ markedly in their signalling cascades and biological activities, and thus their role in blood pressure regulation (13). In general, AT₁R expression is present in adult cardiovascular tissues, whereas AT₂R is highly expressed during foetal development (18). There are two subtypes AT_{1a} and AT_{1b} that are pharmacologically indistinguishable and are thought to signal identically (19;20). The two subtypes are differentially expressed and regulated with AT_{1a} being the predominant receptor in most organs, whereas AT_{1b} is more abundant in the adrenal and pituitary glands (21). AT₁R mediate vasoconstrictor responses whereas AT₂R mediate vasodilator responses (12). Ang II binding to AT₁R mediates vasoconstriction as well as modulating renal sodium and water reabsorption.

1.1.1.2. Genetics of Hypertension

Data generated from animal models, human twin and family studies suggested that inherited factors contribute to 30% of the variation in BP (22). Evidence for genetic influences comes from twin studies, population studies, adoptive studies and monogenic diseases. Twin studies documented greater concordance of blood pressures in monozygotic than dizygotic twins (23;24), and population studies show greater similarity in BP within families than between families (25). Adoption

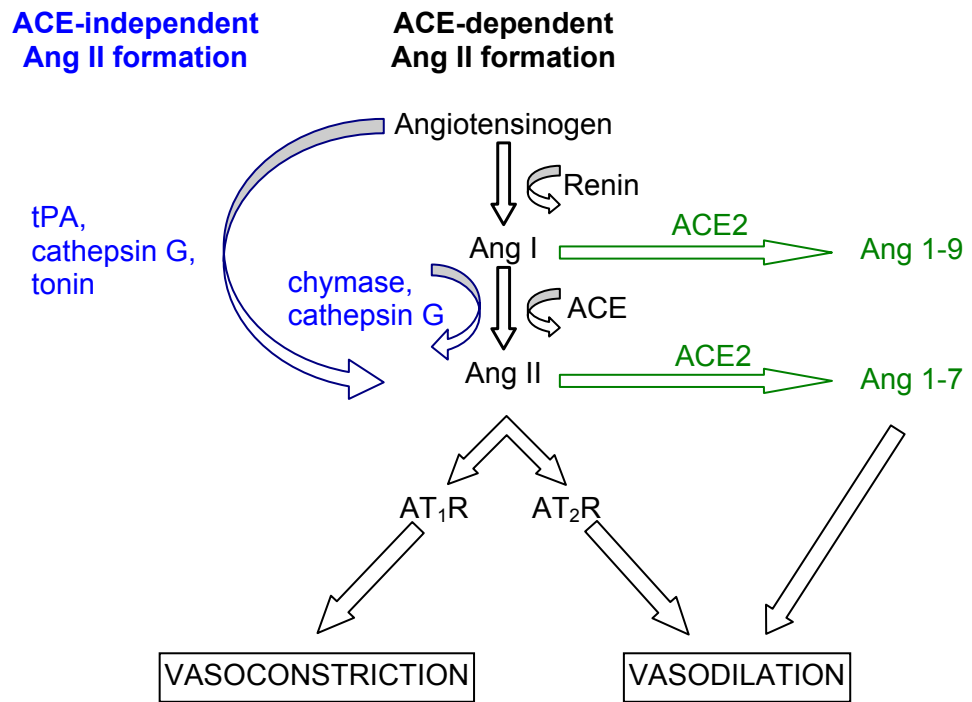


Figure 1.2: Renin-angiotensin system enzymatic cascades

ACE = angiotensin converting enzyme; ACE2 = ACE-related carboxypeptidase; Ang = angiotensin; AT₁R = angiotensin II type 1 receptor; AT₂R = angiotensin II type 2 receptor; tPA = tissue plasminogen activator. Adapted from Ref. (12;216).

studies demonstrate greater concordance of BP among biological siblings than adoptive siblings living in the same household (26). Mutations in single genes can have major effects on BP, accounting for the rare Mendelian forms of blood pressure dysregulation. Ten genes have been identified containing mutations resulting in hypertension and nine genes have been identified containing mutations resulting in hypotension (*Table 1.2*), mostly by altering renal salt handling (11;27). However, these rare alleles account for less than 1% of human hypertension and have not been found to be associated with essential hypertension.

Genome-wide linkage analysis has identified over 100 hypertension-related quantitative trait loci (QTLs) (reviewed in (11)). This suggests involvement of multiple loci, each imparting small effects on the trait in the general population. Candidate gene association studies use the statistical power of linkage analysis for identifying genetic variants that underlie susceptibility to hypertension. Genes investigated have been from the renin-angiotensin system (RAS), renal sodium handling system, signal transduction pathways, cholesterol metabolism pathways, inflammation, and oxidative stress (22). Genetic variants include single nucleotide polymorphism (SNP), variable number of tandem repeats (VNTR), insertion, deletion and duplication (28). Many genetic variants/allelic polymorphisms were found to be associated with primary phenotype (e.g. blood pressure), intermediate phenotype (e.g. arterial stiffness) and end-point phenotypes (e.g. stroke) of cardiovascular disease. For example, A1166C, a commonly investigated SNP in AT₁R gene was found to be associated with essential hypertension (29), arterial stiffness (30) and stroke (31).

Gender is a well-known genetic risk factor for hypertension. BP was shown to be higher in men than in women of similar ages (32) while the Y chromosome harbors gene(s) that contribute to BP variation in hypertensive and normotensive men (33).

1.1.1.3. Environmental Factors

Lifestyle choices such as smoking, heavy alcohol consumption, physical inactivity and diet are examples of environmental risk factors. Smoking is an independent cardiovascular risk factor but also through interaction with other risk factors,

Table 1.2: Mendelian forms of hypertension

Disorder	Mode of inheritance	Genes	Mutation and functional consequences
Glucocorticoid-remediable aldosteronism	Autosomal dominant	<i>CYP11b1</i> & <i>CYP11b2</i>	Ectopic expression of aldosterone synthase activity in adrenal fasciculata
Apparent mineralocorticoid excess	Autosomal recessive	<i>11bHSD</i>	Loss-of-function mutation resulting in excess stimulation of the mineralocorticoid receptor (MR); hypertension mediated by increased renal cortical collecting tubule epithelial sodium channel (ENaC) activity
Mutations in mineralocorticoid receptor	Autosomal dominant	<i>NR3C2</i>	S810L missense mutation in the ligand-binding domain converts receptor antagonists (such as progesterone) to agonists; pregnancy exacerbates hypertension
Liddle syndrome	Autosomal dominant	<i>SCNN1B</i> <i>SCNN1G</i>	<i>De novo</i> missense mutation of the β -subunit of ENaC Mutation in the γ -subunit of ENaC that deletes the cytoplasmic C terminus, resulting in excess sodium retention
Gordon's syndrome	Autosomal dominant	<i>WNK1</i> & <i>WNK4</i>	WNK serine–threonine kinase defects resulting in hyperkalaemia and hypertension
Mutations in peroxisome proliferator-activated receptor- γ	Autosomal dominant	<i>PPARG</i>	Loss-of-function mutation resulting in insulin resistance, diabetes mellitus and hypertension
Hypertension with brachydactyly	Autosomal dominant	Not yet identified	Complex chromosome 12p rearrangement, including deletion, insertion and inversion. Severe hypertension, neurovascular anomalies and death from stroke around 50 years of age
Syndrome of hypertension, hypercholesterolaemia and hypomagnesaemia	Mitochondrial inheritance	Not yet identified	Maternal inheritance of a homoplasmic mutation causes a cytidine substitution in the mitochondrial tRNA

CYP11b1 = cytochrome P450, subfamily 11B, polypeptide 1; CYP11b2 = cytochrome P450, subfamily 11B, polypeptide 2; NR3C2 = mineralocorticoid receptor (aldosterone receptor); PPARG = peroxisome proliferator activated receptor- γ ; SCNN1B = sodium channel non-voltage-gated 1 β (epithelial); SCNN1G = sodium channel, non-voltage-gated 1 γ ; tRNA = transfer ribonucleic acid; WNK1 = lysine deficient protein kinase 1; WNK4 = lysine deficient protein kinase 4; 11bHSD = hydroxysteroid 11- β dehydrogenase. Adapted from Ref. (11;217;218)

including blood pressure (34). Smokers demonstrate significantly higher blood pressure than non-smokers (35). Even the effects of passive smoking are comparable to that of chronic active smoking (36). Studies have demonstrated dose-dependent impairment of endothelial function in smokers and passive smokers (37).

Alcohol is a threshold risk factor where the risk is low when alcohol consumption is moderate but high with heavy alcohol consumption (38). Abstinence in heavy alcohol drinkers significantly reduces BP, suggesting that heavy alcohol consumption is a risk factor (39).

Population studies show an inverse relation between physical activity and blood pressure levels and cardiovascular morbidity and mortality (40-42). Increased physical fitness has a more prominent correlation with a favorable coronary risk profile for women than men (43)

It is well recognised that obesity is linked to hypertension from experimental studies showing that weight gain is associated with increase in BP (44). Clinical studies have shown that weight loss is effective in lowering BP in most hypertensive patients, and population studies showing that excess weight gain is one of the best predictors for development of hypertension (44). Multiple studies showed that most hypertensive patients are overweight providing evidence that obesity is a major cause of hypertension. Results from the Framingham Heart Study suggested that approximately 65% to 75% of the risk for hypertension can be directly attributed to excess weight (45).

1.1.2. Current Management

According to the Joint British Societies' (JBS) guidelines on prevention of cardiovascular disease, the specific objective is to reduce the risk of CVD and its complications, including the need for percutaneous or surgical revascularisation procedures (coronary artery bypass grafting (CABG)), and to improve quality of life and life expectancy (5). Recommendations for reducing risk factors include change of lifestyle and therapies that reduce risk factors such as high blood pressure or provide cardioprotective effects. The JBS guidelines aim to emphasise

a total risk approach to CVD risk assessment in the asymptomatic population; and to define lifestyle and risk factor interventions with thresholds and targets. Similarly, the European guidelines on cardiovascular disease prevention in clinical practice published in 2004 recommended management of total cardiovascular risk (46). The roles of lifestyle changes such as smoking, the management of major cardiovascular risk factors such as diabetes and the use of different prophylactic drug therapies such as anti-hypercholesterolaemia in the prevention of clinical CVD should be addressed.

There are seven classes of antihypertensive drugs used to lower blood pressure. They are the ACE inhibitors, Ang II receptor blockers (ARBs), α -blockers, β -blockers, calcium channel blockers (CCBs), diuretics and direct vasodilator (47). ACE inhibitors (e.g. captopril) block the cleavage of Ang I to the potent vasoconstrictor, Ang II, by ACE. ARBs (e.g. losartan) are Ang II receptor antagonists that results in vasodilation. The α -adrenergic blockers (e.g. Prazosin) competitively block α 1-adrenoceptors causing the relaxation of both arterial and venous smooth muscle. The β -adrenoceptor blockers can act on both β 1 and β 2 receptors (e.g. propranolol) or selectively for β 1 receptors (e.g. atenolol), decreasing cardiac output. Calcium channel blockers (e.g. nifedipine) cause relaxation of vascular smooth muscle, dilating mainly arterioles. Diuretics (e.g. hydrochlorothiazide) lower blood pressure by increasing sodium and water excretion, resulting in a decrease in cardiac output and renal blood flow. Direct vasodilators act primarily on arteries or arterioles (e.g. hydralazine) or equally on arterial and venous smooth muscle (e.g. sodium nitroprusside).

1.2. Animal Studies

Animal models have already been used extensively in the investigation of genes involved in BP regulation. The most commonly used species in hypertension research is the rat (48). There are animal models for the study of the different types of hypertension, including non-genetic and genetic models (49;50). Non genetic models such as 2-kidney 1-clip and the deoxycorticosterone acetate (DOCA)-salt models are used for investigating secondary hypertension, due to renal and endocrine causes, respectively. Genotype-driven genetic models e.g. transgenic animals (mostly mice) are often used to investigate the mechanisms

behind Mendelian hypertension. Phenotype-driven genetic models are animal models of heritable hypertension, such as the spontaneously hypertensive rat (SHR), which are used to identify underlying genes or mechanisms contributing to development of hypertension (49;50).

Animal models of heritable hypertension offer more favourable investigative opportunities compared to studies in humans because of reduced genetic heterogeneity, controlled breeding and greater scope for interventional study (48). The SHR is the most commonly used model that displays hypertension as an inherited trait (48). Other rat strains include the stroke-prone SHR (SHRSP), the Dahl salt-sensitive rats, Sabra hypertensive-prone rats, Milan, Lyon, fawn-hooded and Prague hypertensive rats.(48;51).

The SHR was obtained by inbreeding Wistar rats with persistently high systolic blood pressure (*Figure 1.3*) (52;53). The SHR blood pressure increases at 5-6 weeks of age and then continues steadily to SBP of 180-200mmHg at 12-16 weeks of age.(48). The SHRSP is a further developed substrain of the SHR with even higher levels of blood pressure and a strong preponderance to die from stroke (52;53). In addition to increasing BP with age, the SHR and SHRSP also show gender-dependent BP effects similar to human hypertension (54). Both SHR and SHRSP exhibited many features of hypertensive pathological characteristics including impaired endothelium-dependent relaxations of isolated arteries, cardiac hypertrophy, heart failure, and renal dysfunction (48;50). These similarities are also found in human essential hypertension, making them excellent models for studying the mechanisms involved in the development of hypertension.

Genome-wide scan in rodents are commonly used to identify regions within the genome containing gene or genes that are linked to hypertension. At least one BP quantitative trait locus (QTL), has been identified on almost every chromosome in the rat genome (51). Following the identification of a QTL, congenic and consomic rat strains are developed to confirm presence of the QTL and begin narrowing down the implicated region (55). Congenic strains have a chromosomal segment transferred from a donor strain to a recipient strain background by backcrossing. Consomic strains have an entire chromosome transferred from a donor strain to a recipient strain background by backcrossing. Congenic substitution mapping is

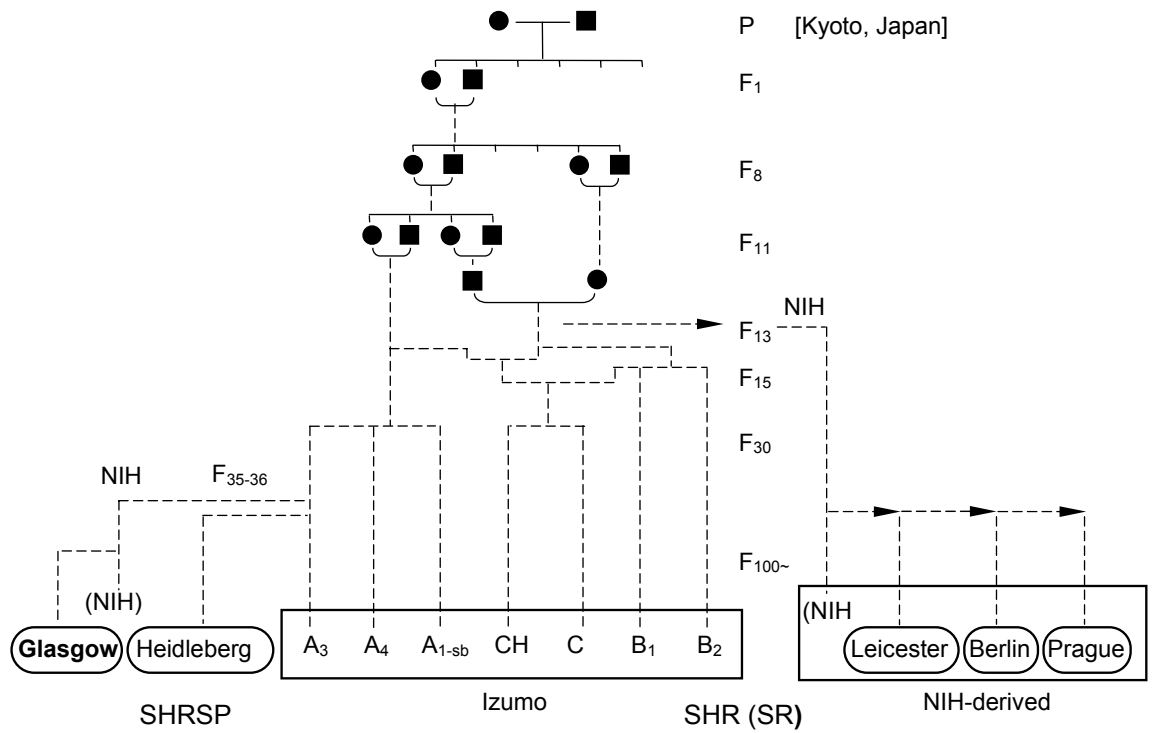


Figure 1.3: Genealogical background of the stroke-prone spontaneously hypertensive rat (SHRSP).

The SHRSP strain, maintained at Glasgow University (Gla), was obtained after filial generation 35-36. Personal communication & Ref. (52;53)

then used to reduce the chromosomal region in which the QTL resides and subsequently identify causal genes. The first successful example of congenic strategy in the identification of a causal gene is the identification of *Cd36* as an insulin-resistance gene by Aitman et. al (56).

Aitman et. al. identified QTL linkages for hypertension, hypertriglyceridaemia, reduced high density lipoprotein (HDL) phospholipid and metabolic defects in adipocytes mapped to a region on chromosome 4 in SHR x Brown Norway(BN) (56). The group went on to replace the region of the chromosome 4 QTL in SHR with the corresponding region from the BN genome. By using a combination of cDNA microarrays, characterisation of a congenic strain and transgenic rescue, Aitman et. al. identified *Cd36* as a causative gene for glucose and fatty acid metabolism. *Cd36* encodes a fatty acid receptor/transporter involved in the transmembrane transport of long-chain fatty acids in adipose tissue and in cardiac and skeletal muscle. The *Cd36* gene was deleted in the SHR (56). Importance of this gene, however, was strain-dependent since the gene deletion in SHR is not observed in SHRSP (57). The congenic strain displayed lower SBP and DBP; and improved fructose-induced glucose intolerance, hyperinsulinemia, and hypertriglyceridemia (57). Overexpression of *Cd36* gene improved glucose tolerance, insulin-stimulated glucose incorporation into muscle glycogen, and serum fatty-acid levels (58).

Similarly, previous work in our laboratory identified two blood pressure QTLs mapping to a region on rat chromosome 2 (59), which have been implicated in several other crosses (60). To confirm the chromosome 2 QTL, our group generated a panel of congenic strains by speed congenic strategy (*Figure 1.4*) One of the congenic strain (SP.WKY_{Gla2c*}) as depicted in *Figure 1.5* contains a single introgressed region from WKY into SHRSP, which encompasses one of the two chromosome 2 QTLs. SP.WKY_{Gla2c*} strain has significantly lower blood pressure than the SHRSP but higher than the WKY (*Figure 1.6*), suggesting that the genes within this QTL region affect blood pressure homeostasis (61). QTL within the same region has been confirmed in different congenic strains by introgressing the relevant region from Milan normotensive or WKY into the Dahl salt-sensitive (62-64).

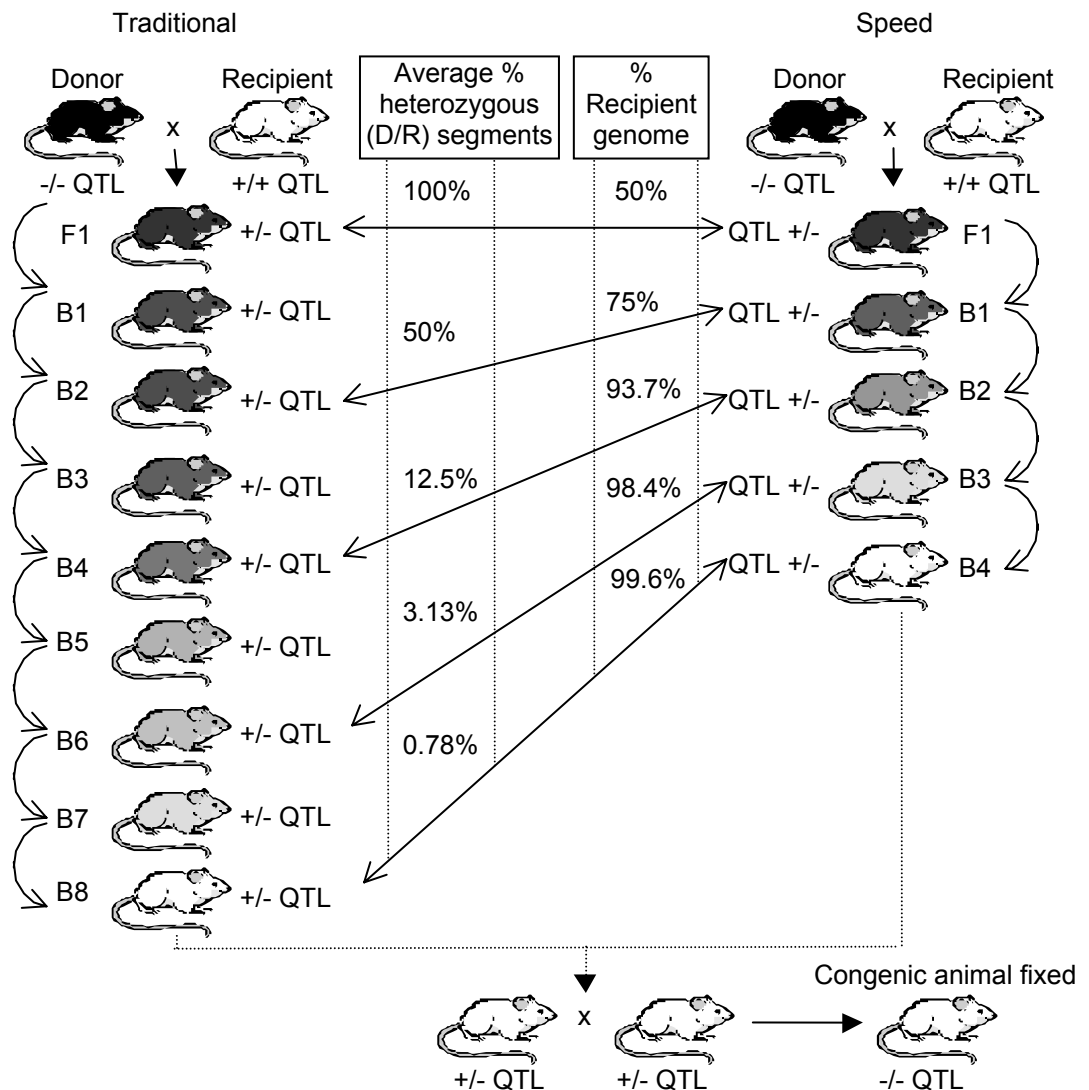


Figure 1.4: Marker-assisted “speed” congenic strategy

Congenic strain construction, illustrating the difference between the traditional and marker-assisted speed congenic approach. The arrows indicate the backcross at which background heterozygosity is theoretically the same. Decreasing shades of grey to white represent the serial dilution of the donor genome in the genetic background. D = donor strain alleles, R = recipient strain alleles, B = backcross, F1 = first filial generation; QTL = quantitative trait locus

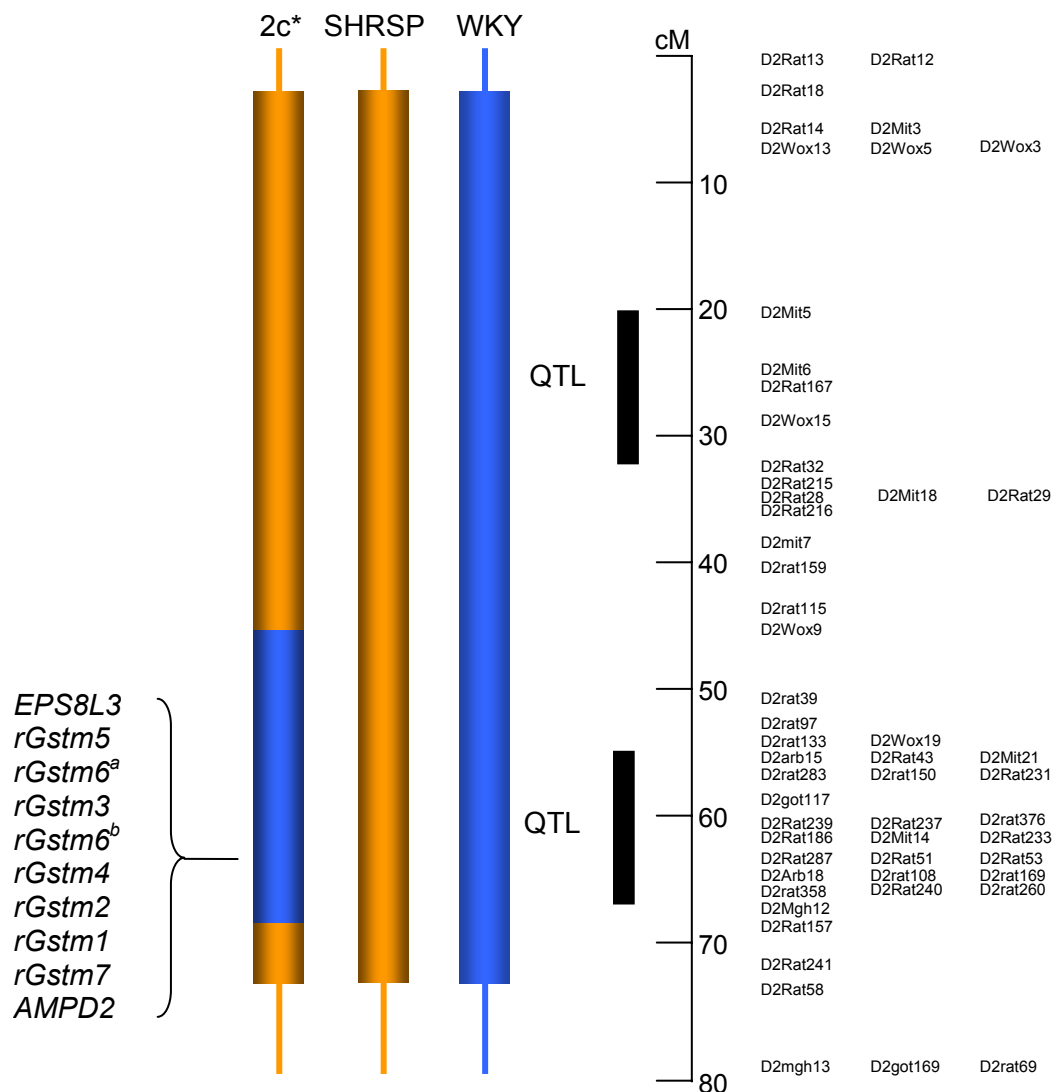


Figure 1.5: Chromosome 2 congenic strain SP.WKY_{Gla}2c*

The congenic strain contains a 22-cM segment, encompassing a quantitative trait locus (QTL), transferred from WKY (donor strain; blue) to the genetic background of SHRSP (recipient strain; orange) between the markers D2Wox9 and D2Mgh12. The congenic strain described is the SP.WKY_{Gla}2 (D2Wox9 – D2Mgh12) and is abbreviated to SP.WKY_{Gla}2c* for simplicity, and 2c* in figures. The *rGstm* family gene locus is encompassed within the congenic region, under the quantitative trait locus (QTL). AMPD2 = adenosine monophosphate deaminase 2; EPS8L3 = epidermal growth factor receptor pathway substrate 8-like protein 3. Adapted from (61).

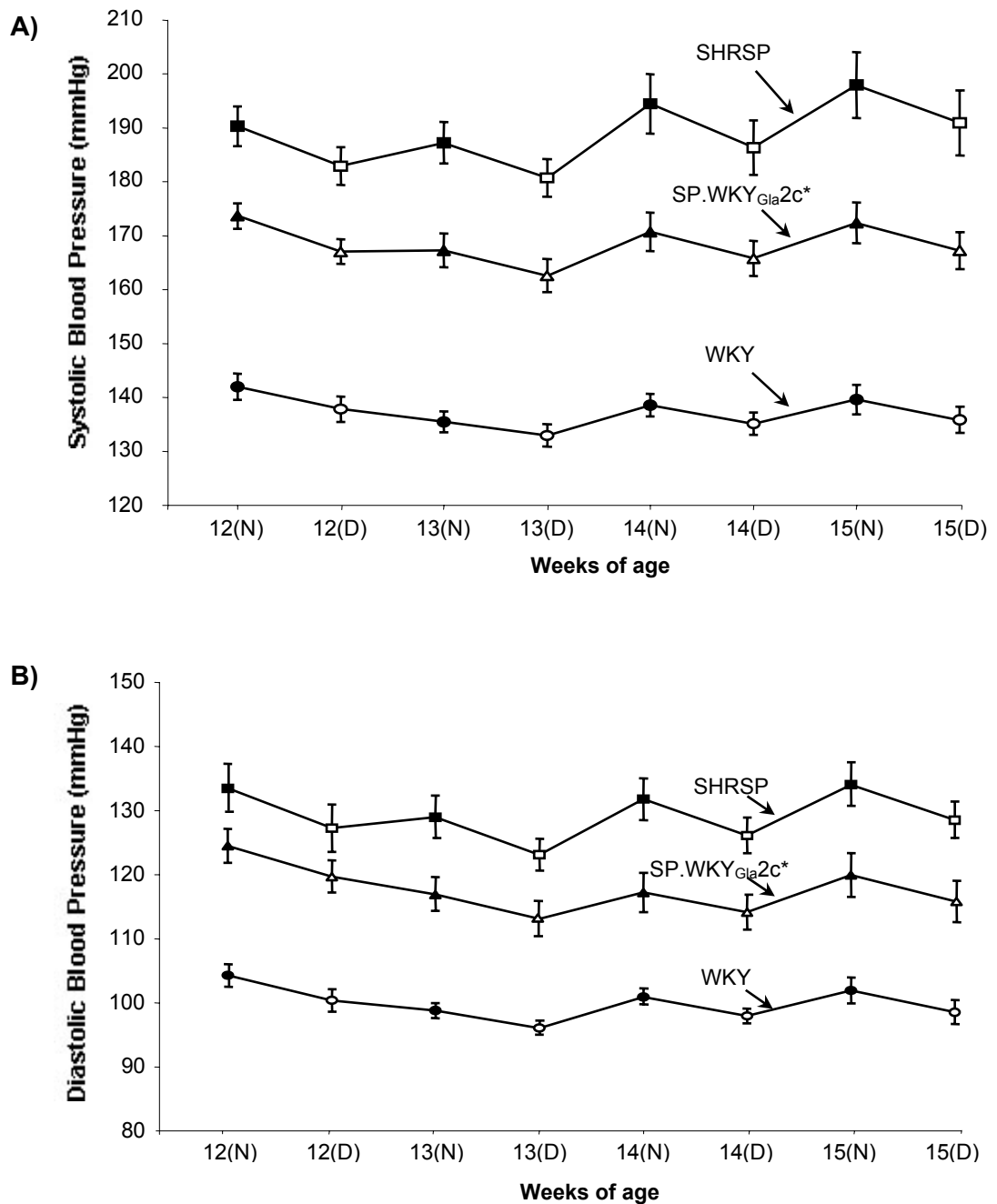


Figure 1.6: Daytime and night-time average systolic (A) and diastolic (B) blood pressure.

The systolic and diastolic blood pressures, measured by radiotelemetry over a 3-week period, for WKY, SHRSP and congenic strain SP.WKY_{Gla2c*} (n=8-11 per group) D = day, N = night. Taken from Ref. (61)

Microarray analysis of gene expression in kidney homogenates from 16-week old rats showed reduction in glutathione s-transferase mu type-1 (*rGstm1*) expression by about 4-fold in SHRSP compared to WKY and SP.WKY_{Gla2c*} (61). A similar microarray study by Okuda et. al. of kidneys from 10-week old SHR and WKY also showed down-regulation of *rGstm1* (65) (please note that in this study, the gene was mis-named as *GSTM4*). Another microarray study by Okuda et. al. in seven different rat strains also identified *rGstm1* (please note that the gene was mis-named as *Gstm2*) as differentially expressed (66). Subsequent Western blot analysis in our laboratory confirmed differential expression of rGstm1 protein in SHRSP, WKY and SP.WKY_{Gla2c*} (67). These results suggest that *rGstm1* is a positional and functional candidate gene for blood pressure regulation.

1.3. Oxidative Stress in Cardiovascular Disease

1.3.1. Nitric Oxide

Nitric oxide (NO) first identified as endothelium-derived relaxing factor (EDRF), is responsible for vasorelaxation by its effect on the vascular smooth muscle cells (VSMCs) (68). The release of paracrine vasodilators from endothelial cells is a critical determinant of vascular tone and an integral regulatory mechanism involved in maintenance of local blood flow and systemic blood pressure (69). Endothelium-dependent agonists, including acetylcholine (ACh) and bradykinin, stimulate endothelial cells to release NO, prostacyclin (PGI₂) and endothelial-derived hyperpolarisation factor (EDHF) (70). The relative contribution of each mediator to endothelial-dependent dilation is inversely related to vessel calibre, with NO- and PGI₂-mediated responses predominating in large conduit vessels while EDHF is more prominent in peripheral resistance vessels. As NO has a half-life of only 3.8 to 6.2 seconds and is released upon synthesis, vascular NO levels are mainly regulated through alterations in expression and activity of constitutive endothelial nitric oxide synthase (eNOS) (71).

Major physiologic stimulus of vascular NO production is blood-flow induced shear stress on endothelial cells (72). NO is produced by nitric oxide synthases (NOSs) by conversion of L-arginine to L-citrulline and NO (*Figure 1.7*) (73). Established mechanisms of NO action include vasodilation, inhibition of platelet aggregation,

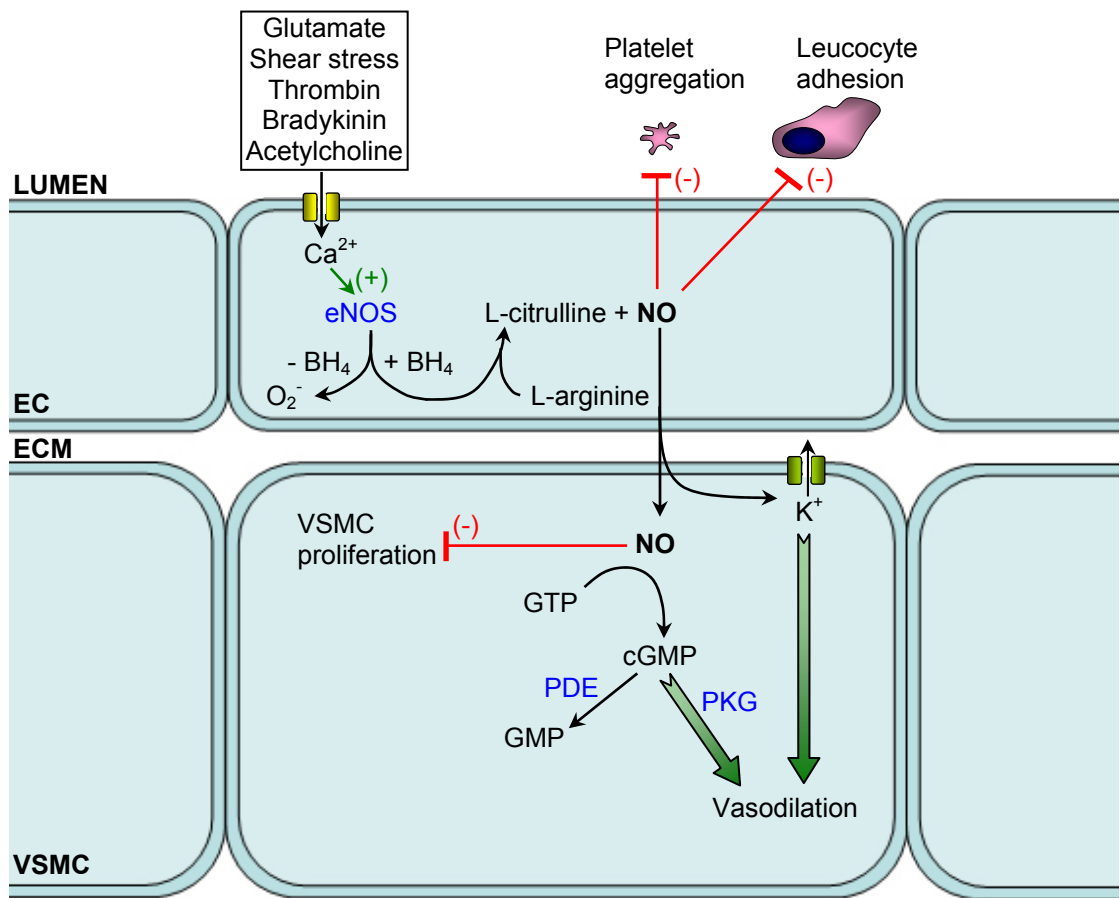


Figure 1.7: Schematic diagram to illustrate NO intracellular signalling processes across the vascular wall.

BH₄ = tetrahydrobiopterin; cGMP = cyclic guanosine monophosphate; ECM = extracellular matrix; eNOS = endothelial nitric oxide synthase; GMP = guanosine monophosphate; GTP = guanosine triphosphate; NO = nitric oxide; O₂⁻ = superoxide anion; PDE = phosphodiesterases; PKG = cGMP-dependent protein kinase; VSMC = vascular smooth muscle cell

leucocyte adhesion, and smooth muscle proliferation and antioxidative effects. Vasodilation is the best documented activity of NO in the cardiovascular system. NO mediates vasodilation through activation of cyclic guanosine monophosphate (cGMP)-dependent protein kinases (PKG I and PKG II) mainly via PKG I (74;75). The activity of cGMP is terminated by rapid conversion to GMP which is catalysed by various phosphodiesterases (PDE), specifically PDE₅ (73). The vasodilation effect of NO can also be independent of PKG I activation (76). Platelets have the ability to aggregate and form a haemostatic plug but this effect must be carefully balanced against the necessity to maintain the fluid state of the blood and to avoid thrombosis (73). Atherosclerotic changes are often followed by hyperactivity associated with thrombosis, myocardial infarction and stroke. NO-induced inhibition of platelet aggregation is mainly through activation of PKG I. Increased leucocyte adhesion is a major step in the pathogenesis of atherosclerosis and NO is an important endogenous mediator which inhibits leucocyte adhesion. The mechanism of the anti-adhesive action of NO most likely involves anti-oxidative effects (73). Proliferation of smooth muscle cells plays a key role in narrowing the lumen of blood vessels in CAD and disappearance of contractile activity. NO also has been shown to inhibit smooth muscle proliferation. Vascular oxidative stress contributes to pathophysiology of cardiovascular diseases. The antioxidative effects of NO are in part mediated by inducing expression of ferritin, haem oxygenase-1 and extracellular superoxide dismutase (ecSOD), the activities of which decrease superoxide levels and formation of highly reactive radical peroxynitrite in the vascular wall (73).

1.3.2. Endothelial dysfunction

Endothelial dysfunction describes impaired endothelium-dependent vasorelaxation caused by a loss of NO bioactivity in the vessel wall (77;78), as a consequence of decreased NO bioavailability. Evidence includes blunting of forearm vasodilator response to mental tasks following NO synthesis inhibition with N-monomethyl-L-arginine (L-NMMA) (79;80), a reduction in NO activity in both primary and secondary hypertension (81;82), and even in normotensive offspring of hypertensive parents (83). Basal NO production, as measured by plasma nitrate levels, was shown to be lower in patients with essential hypertension (84). Racial difference has been found to influence NO-dependent vasodilator response (85).

Altered endothelium-dependent vascular relaxation has been shown in all animal models of cardiovascular disease (48). Anti-oxidant vitamins have been shown to enhance endothelium-dependent vasodilation in experimental models (86;87) but not in large human studies (88;89). There has been accumulating evidence in animal models and humans that endothelial dysfunction and decreased NO bioavailability may contribute to hypercholesterolaemia, diabetes and hypertension (90). Overexpression of eNOS by gene transfer in animal studies and substrate L-arginine supplementation in human studies have been shown to improve endothelium-dependent relaxation (91-94), further supporting the importance of NO in endothelial function.

1.3.3. Reactive Oxygen Species

Many cells that comprise the vasculature generate reactive oxygen species (ROS) (*Figure 1.8*). Reactive oxygen species (ROS) include free radicals, such as superoxide anion (O_2^-), hydroxyl radical (OH^-), nitric oxide (NO), lipid radicals (LOO^-), which possess unpaired electrons or molecules that possess oxidising effects, such as hydrogen peroxide (H_2O_2), hypochlorous acid (HOCl) and peroxynitrite ($ONOO^-$) (77). ROS regulate cellular signalling systems in both VSMCs and/or endothelial cells (78;95;96). ROS production induced by agonists has been shown in VSMCs, endothelial cells and adventitial fibroblasts. ROS mediate cell responses to agonist by activation of specific signalling cascades, through redox-sensitive proteins. These include tyrosine kinase receptors such as platelet-derived growth factor receptor (PDGF-R), epidermal growth factor receptor (EGF-R) and G-coupled receptor agonists such as phenylephrine and thrombin. H_2O_2 has been shown to activate several mitogen-activated protein kinases (MAPKs), a family of serine/threonine kinases that control cellular responses to growth, apoptosis and stress signals. ROS have also been shown to be necessary for VSMCs survival and even apoptosis (97). O_2^- appears to induce cell growth while H_2O_2 appears to lead to cell death in *in vitro* studies. Similarly, in endothelial cells, ROS appear to be required for survival as well as apoptosis (78). ROS generation by different sources can suppress endothelial cell death or promote endothelial cell apoptosis.

The vascular superoxide level is determined by the balance between its rate of formation by various oxidases, auto-oxidation processes and its rate of removal and reaction with various molecules (96). Vascular tissue contains multiple oxidases whose activity and expression appear to be highly regulated, thus the tight control of ROS metabolism. Superoxide dismutase (SOD) dismutate O_2^- at a rate of $2.4 \times 10^9 \text{ mol.L}^{-1}.\text{s}^{-1}$ to the more stable hydrogen peroxide (H_2O_2), which is then converted to water by catalase or glutathione peroxidase (GPx) (78;95;98). Since NO reacts with O_2^- forming $ONOO^-$ at a rate of $6.7 \times 10^{-9} \text{ mol.L}^{-1}.\text{s}^{-1}$, it becomes an important scavenger of O_2^- (77). Additionally, anti-oxidants such as ascorbate scavenge superoxide but many of these substances may not be present at sufficient levels (96). Finally, the expression of ROS-producing enzymes can be altered by hormones such as angiotensin II (Ang II) or cytokines such as tumour necrosis factor (TNF) $-\alpha$ and interleukin (IL) -1β (95)

1.3.4. Oxidative stress

Oxidative stress occurs when ROS and its derivatives are produced excessively, outstripping endogenous anti-oxidant defence mechanisms (*Figure 1.8*) (77). The imbalance between NO and ROS results in reduced NO bioavailability, leading to endothelial dysfunction, which is the basis of many other vascular diseases. Endothelial dysfunction and oxidative stress are common features in human and rat hypertension (48). Reduction of NO bioavailability in the endothelium, can be the result of decreased NO production or increased ROS production (77). Decreased NO production might be a consequence of reduced expression of eNOS (99), lack of substrate or cofactor (100-102), or alterations of cellular signalling resulting in the eNOS not being activated (103). Increased O_2^- production can be due to increased expression or activity of O_2^- -producing enzymes, shear stress or excess stimulation (77). Even eNOS, in the absence of sufficient key co-factor tetrahydrobiopterin (BH_4), produce O_2^- and H_2O_2 instead (*Figure 1.7*) (104;105).

Overproduction of the first reactive oxygen radical O_2^- , can lead to a radical chain reaction generating more ROS (*Figure 1.8*). Due to its rapid reaction with NO, O_2^- can consume NO rapidly, thus decreased NO bioavailability, and prevents its interaction with the signalling mechanisms normally regulated by NO, leading to

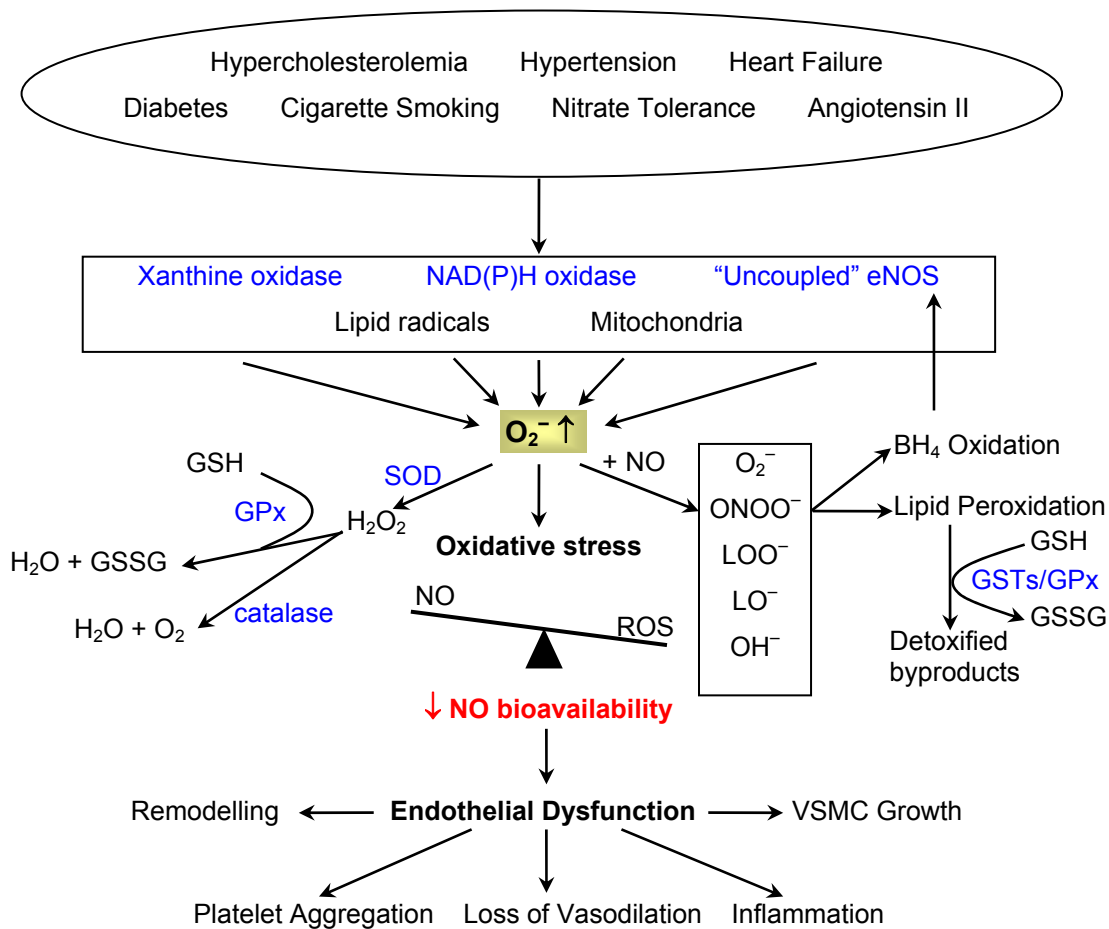


Figure 1.8: The roles of oxidative stress enzymes in maintaining the balance between O_2^- and NO.

BH₄ = tetrahydrobiopterin; eNOS = endothelial nitric oxide synthase; H₂O = water; H₂O₂ = hydrogen peroxide; GPx = glutathione peroxidase; GSH = glutathione; GSSG = oxidised glutathione; GSTs = glutathione s-transferases; LO⁻ or LOO⁻ = lipid radicals; NAD(P)H = nicotinamide adenine dinucleotide (phosphate); NO = nitric oxide; O₂ = molecular oxygen; O₂⁻ = superoxide anion; ONOO⁻ = peroxynitrite; ROS = reactive oxygen species; SOD = superoxide dismutase; VSMC = vascular smooth muscle cell. Adapted from Ref. (77)

endothelial dysfunction. Agonists-induced activation of vascular NAD(P)H oxidases produce H_2O_2 in large quantities, which in turn amplifies its own production, resulting in compensatory or detrimental consequences (106). H_2O_2 either mediates endothelium-dependent vasodilatation in hypertension when NO is substantially reduced as a compensatory mechanism, or may be involved in VSMC proliferation and hypertrophy over long period of time. At least five different mechanisms are implicated in self-propagation of H_2O_2 in vascular cells.

One of the most important ROS is $ONOO^-$, the by-product of NO and O_2^- . It is a highly reactive radical, strong oxidant and it is more stable than either NO or O_2^- (96;107). $ONOO^-$ activates signalling-like mechanisms such as (a) inactivation of mitochondrial electron transport and respiration, (b) increased potency of O_2^- as inhibitor of mitochondrial respiration, (c) stimulation of cyclooxygenase production of prostaglandin (PG) H_2 , a prothrombotic vasoconstrictor, (d) inhibition of PGI_2 synthase, (e) the potential to convert production of endothelium-derived PGI_2 , an antithrombotic vasodilator to PGH_2 . $ONOO^-$ has been shown to irreversibly inhibit protein tyrosine phosphatases, thus disrupting balance maintained between cellular kinase and phosphatase activity. Inhibition of anti-oxidant enzymes GPx, catalase and manganese (Mn) SOD by $ONOO^-$ probably affect redox control mechanisms, promoting O_2^- generation leading to decreased anti-oxidant defence, which is likely to promote activation of apoptosis.

ROS are implicated in oxidation of biological macromolecules, such as DNA, protein, carbohydrates and lipids (*Figure 1.8*). ROS oxidation of lipid can lead to production of other lipid radical chain reactions, whereby oxidised fatty acids generates fatty acid peroxy radicals, which attack adjacent fatty acid side chains (77). Lipid radicals accumulate in cell membrane causing leakage of plasmolemma and dysfunction of membrane-bound receptors. In addition, the end-products of lipid peroxidation have cytotoxic and mutagenic effects. The effects of ROS vary depending on the oxidative stress levels and the cell types involved (108). A number of enzymes play important roles in the maintaining the balance between the levels of O_2^- and NO including eNOS

1.3.5. Endothelial Nitric Oxide Synthase

Nitric oxide synthases (NOSs) are haem containing oxido-reductases that convert L-arginine to NO and by-product L-citrulline in the presence of nicotinamide adenine dinucleotide phosphate (NADPH) and O₂ (109-113). Each NOS polypeptide is comprised of an N-terminal oxygenase domain and a C-terminal reductase domain (*Figure 1.9*) (110;112;113). The core region of NOS oxygenase domain binds haem, BH₄ and L-arginine as well as forming the active site where NO synthesis takes place. The C-terminal reductase domain binds flavin mononucleotide (FMN), flavin adenine dinucleotide (FAD), and NADPH. During NO synthesis the reductase flavins acquire electrons from NADPH and transfer them to the haem iron, which permits it to bind and activate O₂⁻ and catalyse NO synthesis.

There are three distinct enzyme isoforms (*Table 1.3*), which are neuronal NOS (nNOS), inducible NOS (iNOS) in phagocytic cells and eNOS (109-113). All three NOSs expression have been detected in other cell types, in addition to the suggestion from its name (111). The gene encoding for nNOS is *NOS1*, located on chromosome 12q24; iNOS, encoded by *NOS2* on chromosome 17q11-12; and eNOS encoded by *NOS3* on chromosome 7q35-36 (109;113). Both nNOS and eNOS are constitutively expressed while iNOS expression is typically synthesised in response to inflammatory mediators (109-113). NO is usually produced by eNOS in the vasculature, but can also be produced by iNOS in pathological states by macrophages. In the cardiovascular system, eNOS is a major player in the control of endothelial function and therefore will be the focus of subsequent discussion.

eNOS was first purified and its corresponding cDNA cloned from endothelial cells but was subsequently found to be expressed in other cells of the cardiovascular system (111). *NOS3* containing 26 exons spanning approximately 21kb of genomic DNA encodes for a 135kDa polypeptide (109). No alternative splice variants have been characterised but a number of allelic variants have been associated with cardiovascular disease. The gene expression of *NOS3* is regulated at transcriptional and post-transcriptional level (109;111;113). Transcriptional regulation includes allelic variant in the promoter with binding sites

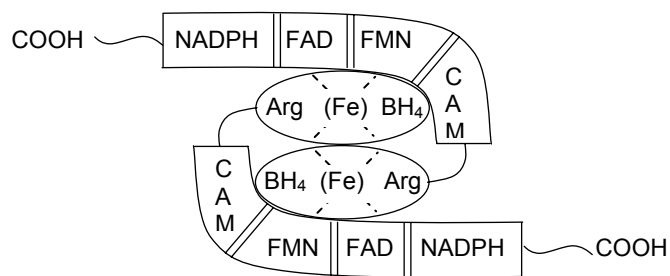


Figure 1.9: Schematic diagram of a functionally active dimeric NOS

Arg = L-arginine; BH₄ = tetrahydrobiopterin; CAM = calmodulin; FAD = flavin adenine dinucleotide; FMN = flavin mononucleotide; (Fe) = haem; NADPH = nicotinamide adenine dinucleotide phosphate. Taken from Ref. (112)

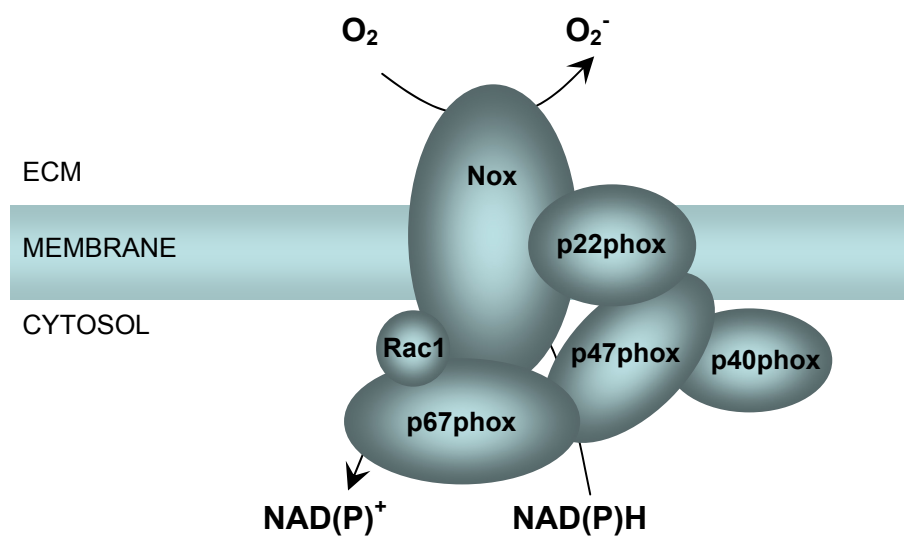


Figure 1.10: Regulation of NAD(P)H oxidase ROS production by rac1

NAD(P)H oxidase consists of 5 subunits, 3 cytoplasmic subunits (p67^{phox}, p47^{phox} and p40^{phox}), and 2 membrane subunits (Nox and p22^{phox}), which are also known as cytochrome_{b558} (Cyt_{b558}). NAD(P)H oxidase production of O₂⁻ is regulated by rac1 protein. ECM = extracellular matrix; NAD(P)⁺ = oxidised nicotinamide adenine dinucleotide (phosphate) ; NAD(P)H = reduced nicotinamide adenine dinucleotide (phosphate). Adapted from Ref. (127)

Table 1.3: Properties of nitric oxide synthases (NOSs)

Gene	Enzyme	Monomeric size (Molecular weight)	Human chromosomal location	Rat chromosomal location	Principal tissue distribution under basal conditions
<i>NOS1</i>	nNOS	1439 a.a. (161kDa)	12q24.2–q24.31	12q16	Neurons Skeletal muscle Macula densa segment Bronchial and tracheal epithelium
<i>NOS2</i>	iNOS	1153 a.a. (131kDa)	17q11.2–q12	10q25	Bronchial airway, epithelium, alveolar, macrophages Ileum Uterus Platelets
<i>NOS3</i>	eNOS	1203 a.a. (133kDa).	7q35–q36	4q11	Endothelium Hippocampal CA1 neurons Cardiac myocytes

The monomeric size and molecular weight of the enzymes are represented by the human proteins. a.a. = amino acid; NOS = nitric oxide synthase; nNOS = neuronal NOS; iNOS – inducible NOS; eNOS = endothelial NOS; kDa = kiloDalton.

Adapted from Ref. (109;113)

for transcription factors such as Sp1, activator proteins 1 and 2 elements (AP1, AP2), a nuclear factor-1 element (NF-1), and regulatory sequences for stimuli such as sterol regulatory element (SRE), partial oestrogen responsive elements (ERE), a cyclic AMP response element (CRE) and a putative shear stress response element (SSRE) (111;114). Lysophosphatidylcholine is the most potent activator of eNOS mRNA expression, in a dose- and time- dependent manner (115), while oxidised low density lipoproteins (oxLDL) decrease eNOS mRNA, probably involving mRNA stabilisation (116). Transforming growth factor (TGF)- β increase eNOS mRNA, protein and activity (117) while TNF- α does the opposite (118). Oestrogen and other hormones have also been found to influence the expression of eNOS (114).

Covalent modifications of eNOS by palmitoylation, myristoylation, phosphorylation and acetylation have been reported (112;113). These modifications might influence the activity of the enzyme. eNOS is able to synthesise NO in response to increased calcium ions (Ca^{2+}), and in some cases, to shear stress (*Figure 1.7*) (110;112). Functionally active eNOS is made of homodimeric subunits (*Figure 1.9*) and dimer stability may also regulate eNOS activity. Interactions of eNOS and other proteins, such as caveolins, calmodulin and heat shock protein (HSP)-90 have been shown to alter the activity of eNOS. Activity of eNOS is also regulated by a feedback inhibition through binding of NO to haem in a reversible manner. One of the most important factors regulating activity of eNOS is physiological concentration of BH_4 , an essential redox cofactor permanently bound to eNOS. BH_4 stabilises the dimeric form of eNOS and directly increases production of NO (119). Insufficient BH_4 can result in uncoupling of the electron transfer from NADPH to L-arginine by eNOS, which produces O_2^- instead (*Figure 1.7*) (100). Low concentrations of ONOO^- can oxidise BH_4 at physiological conditions (120). Consequently low levels of BH_4 can mediate eNOS-dependent ONOO^- formation. BH_4 also inhibits O_2^- production by eNOS and xanthine oxidase in a dose-dependent manner (119).

1.3.6. Reactive Oxygen Species: Sources and Stimuli

It is now established that sources of ROS are mitochondrial respiration, arachidonic acid pathway enzymes (e.g. lipoxygenase and cyclooxygenase),

cytochrome p450s, xanthine oxidase, nicotinamide dinucleotide / nicotinamide dinucleotide phosphate (NAD(P)H) oxidase, NOS, peroxidase and haemoproteins (77). In cardiovascular research, NAD(P)H oxidase, xanthine oxidase and NOS are the enzymes studied most extensively because they have been proven to contribute to development of hypertension.

1.3.6.1. NAD(P)H oxidase

All cell types found in the vessel wall are equipped with NAD(P)H oxidases, which are active under basal physiological conditions, participate in redox-sensitive mechanisms that control both vascular function and adaptive gene expression responses (96). The majority of available data show the use of nicotinamide dinucleotide (NADH) but there is also evidence of the utilisation of the nicotinamide dinucleotide phosphate (NADPH) as a substrate for O_2^- production. The NAD(P)H oxidase has been confirmed to be the predominant O_2^- producing enzyme and the major source of O_2^- in vascular tissues (77). Studies in animal models have shown that NAD(P)H oxidase generation of O_2^- is greater in vascular tissues from hypertensive strains and tend to be higher in older animals (121). Endothelium from male rats also produced higher NAD(P)H oxidase-dependent O_2^- than from female rats in aorta and microvessels (122;123).

The membrane-associated NAD(P)H oxidase enzyme consists of 5 subunits, 3 cytoplasmic subunits and 2 membrane subunits (124-127). The membrane components are p22^{phox} and Nox more commonly known as cytochrome b558 (Cyt_{b558}) or flavohaemoprotein while the cytoplasmic components consist of p40^{phox}, p47^{phox} and p67^{phox} (Figure 1.10). Vascular NAD(P)H oxidases are similar in structure to the neutrophil NAD(P)H oxidase, but produce less O_2^- for a longer period (98). Activation of NAD(P)H oxidase requires guanosine triphosphate (GTP) binding protein rac1, through interaction of rac1 with p67phox subunit. Rac1 is a 21kDa protein, which regulates the production of O_2^- by NAD(P)H oxidase and is required for the assembly of the NAD(P)H oxidase subunits. ROS generated by a rac1-regulated oxidase, such as NAD(P)H oxidase is crucial in suppressing endothelial cell death while ROS produced independently of rac1 promote endothelial cell apoptosis (78).

O_2^- production in aorta of adult SHR was associated with upregulation of p22^{phox} mRNA, with evidence pointing to VSMCs as potential source (128) Luciferase activity of VSMCs from SHRs was higher than WKY, preferring NADH to NADPH as substrate. The p22^{phox} subunit is an essential component of the vascular NAD(P)H oxidase. This is further confirmed by decreased O_2^- production following inhibition of p22^{phox} mRNA expression by stable transfection of antisense cDNA into VSMCs (125).

1.3.6.2. Other Sources of O_2^-

Other sources include xanthine oxidase, myeloperoxidase, cyclooxygenase, lipoxygenase, mitochondrial respiration, cytochrome p450 isoenzymes, haem oxygenase, and glucose oxidase (77;129).

Xanthine oxidase generates O_2^- and H_2O_2 by catalysing oxidation of hypoxanthine and xanthine to uric acid during purine metabolism (129;130). Under pathophysiological conditions, it is another major source of vascular oxidative stress. Xanthine oxidase is not only expressed in vascular cells but also circulates in the plasma and binds to endothelial cell extracellular matrix.

During inflammation, neutrophils and monocytes are activated and can be a major source of reactive oxygen species (129). For example, activated neutrophils and monocytes secrete myeloperoxidase, a haemoprotein that localises in and around endothelial cells after leukocyte degranulation. This enzyme uses H_2O_2 peroxide to produce HOCl. Myeloperoxidase can also oxidise tyrosine and nitrite (NO_2^-) to form tyrosyl radicals and nitrogen dioxide radicals, respectively. These reactions lead to formation of reactive nitrogen species and protein nitration, for example, nitrotyrosine formation.

1.3.6.3. Angiotensin II and Other Stimuli

Ang II is, perhaps, the most widely investigated and potent stimulus for the production of ROS in vascular cells. Ang II can increase O_2^- in cultured VSMCs from rats (131;132) as well as human arteries and veins (133), mediated through NAD(P)H oxidase. Ang II stimulation of AT₁R in the vascular wall leads to

activation of NAD(P)H oxidase in vascular cells (134). This is due to the assembly of enzyme subunits and the upregulation of expression of oxidase subunits and rac1 (135-140). Other enzymes also contribute to Ang II-induced oxidative stress in the vasculature. Modulation of AT₁R expression levels by various agonists influences Ang II-induced ROS production in vascular cells.

Several growth factors such as platelet-derived growth factor (PDGF) (141), epidermal growth factor (EGF) (142) and thrombin (143) lead to increased ROS. The pro-inflammatory cytokines such as IL-1 (144) and TNF- α (144;145) activate NAD(P)H oxidase and xanthine oxidase in vascular cells. During endotoxaemia, lipopolysaccharides induce oxidative stress by enhancing xanthine oxidase and NAD(P)H oxidase expression and activity (146). ROS and their oxidised by-products such as H₂O₂, lipid peroxides and oxidised low density lipoprotein (oxLDL) have been shown to activate NAD(P)H oxidase O₂⁻ production in vascular smooth muscle cells and fibroblasts (147-150). Mechanical stimuli such as shear stress have been shown to increase endothelial cells O₂⁻ production in a manner requiring both NAD(P)H oxidase and xanthine oxidase (151;152).

1.4. Anti-oxidant Enzymes – 1st Line of Defence

There are several anti-oxidant enzymes that help to balance the levels of nitric oxide and reactive oxygen species by converting ROS into less harmful compounds. Superoxide dismutase (SOD) and catalase provide the first line of defence, while glutathione peroxidase (GPx) and glutathione s-transferase (GSTs) provide the second line of defence (*Figure 1.8*) (153-155).

1.4.1. Superoxide Dismutase

Superoxide dismutases (SODs) are the first and most important line of anti-oxidant enzyme defence, particularly against O₂⁻ (153;156). SODs catalyse the conversion of two O₂⁻ and two hydrogen ions to H₂O₂ and molecular O₂ at a diffusion-limited rate (153). Vascular tissue contains three isoforms of SOD which accelerate the dismutation of superoxide into H₂O₂ and O₂⁻ (*Table 1.4*) (157). The first isoform is cytosolic copper zinc (Cu/Zn)-SOD encoded by *SOD1*, which is thought to lower O₂⁻ levels from the nanomolar to picomolar concentration range. Mitochondria

Table 1.4: Properties of superoxide dismutases (SODs)

Gene	Enzyme	Monomeric size (Molecular weight)	Human chromosomal location	Rat chromosomal location	Cellular localisation under basal conditions
<i>SOD1</i>	Cu/Zn-SOD	154 a.a. (17kDa)	21q22.11	11q11	Cytosol
<i>SOD2</i>	Mn-SOD	222 a.a. (26.6kDa)	6q25.3	1q21	Mitochondria
<i>SOD3</i>	ecSOD	240 a.a. (26kDa)	4p15.3-p15.1	14q11	Extracellular matrix

The monomeric size and predicted molecular weight of the enzymes are represented by the human proteins. a.a. = amino acid; SOD = superoxide dismutase; Cu/Zn-SOD = copper/zinc SOD; Mn-SOD = manganese SOD; ecSOD = extracellular SOD; kDa = kiloDalton.

contain a second isoform, manganese (Mn)–SOD encoded by *SOD2*, and lastly, arterial smooth muscle cells are the principal source of the extracellular isoform of the Cu/Zn–SOD enzyme in the vascular wall, commonly known as extracellular SOD (ecSOD) encoded by *SOD3*. Although the enzymes are related, the genes are localised on different chromosomes, with human *SOD1* on chromosome 21q22, *SOD2* on 6q25 and *SOD3* on 4p-q21 (157).

Cu/Zn–SOD and ecSOD have copper (Cu) and zinc (Zn) in their catalytic centre while Mn–SOD has manganese as a cofactor (156). Cytosolic Cu/Zn-SOD functions as a homodimer, Mn–SOD as homotetrameric enzyme while ecSOD is made up of homotetrameric glycoproteins with a high affinity for heparin sulphate. The importance of SODs as anti-oxidant enzymes was shown by gene transfer experiments where overexpression of the SODs reduced oxidation of low density lipoprotein (LDL) in endothelial cells (158-160), improved endothelial function (161) and provided protection against myocardial infarction (157). Gene expression levels of SODs can be upregulated by mechanical, chemical and biological stimuli or downregulated in certain pathophysiological conditions (153;156;157). In addition, Mn–SOD expression is also regulated at post-transcriptional level by a RNA-binding protein (162).

1.4.2. Catalase

Catalase is a homotetrameric haemin-enzyme containing four ferriprotoporphyrin groups (153;156). Catalase is an intracellular anti-oxidant enzyme, mainly located in cellular peroxisomes and to some extent in the cytosol. It catalyses the heterolytic decomposition of two H_2O_2 molecules to water and O_2 . Catalase contains 4 tightly bound NADPH molecules, which function to prevent the accumulation of an inactive Fe(IV) form of the enzyme (163-165). Catalase is one of the most efficient enzymes with the capability to deal with H_2O_2 in the millimolar range of concentration (166). Catalase prevents the accumulation of H_2O_2 in peroxisomes, without which, the cells would undergo immediate cell death.

A rare inherited autosomal recessive disease in the human catalase gene is located on chromosome 11p13 and results in catalase deficiency in Hungarian families associated with increased cardiovascular risk (154). A variant in the

promoter region of catalase gene was found to be associated with essential hypertension. These human studies support the importance of catalase as an anti-oxidative enzyme. However, studies in animals and humans have only provided evidence for moderate protection by catalase against oxidative stress (167). ROS production was reduced by gene transfer of both SOD and catalase but the relative contribution of each gene is still not clear (168). A number of transcription factors are involved in the regulation of catalase gene expression in a tissue-specific manner (169;170). Catalase itself is also involved in the regulation of cyclooxygenase gene expression in rat aortic smooth muscle cells (171).

1.5. Anti-oxidant Enzymes – 2nd Line of defence

Interaction of ROS with macromolecules does occur, generating highly reactive products that are capable of damaging DNA, protein and lipid (172). Extended chain reaction from these secondary oxidation products can result in degradation of cellular components and ultimate death of the cell so there is a need to detoxify these secondary oxidation products. Secondary line of protection is provided by enzymes such as glutathione peroxidase (GPx), glutathione s-transferase (GSTs), aldo-keto reductase and aldehyde dehydrogenase.

1.5.1. Glutathione

Glutathione (GSH) is a small molecular weight organic donor molecule used by a number detoxifying enzymes, namely GPx and GSTs. Since its discovery in 1920s biochemical and functional studies in parallel with developments in protein biochemistry and enzymology has placed glutathione in the centre of drug and foreign substance detoxification and multi-drug resistance (173). Functional roles of glutathione can include anti-oxidant defence mechanisms as well as metabolic and regulatory functions (*Figure 1.11*) (173). The anti-oxidant function of glutathione is probably due to the unique redox chemistry of the cysteinyl–thiol of the molecule (155;173).

Glutathione is the principal intracellular non-protein thiol, present in concentrations up to 10mM in cells (174). Concentrations of glutathione in various cells are relatively constant in physiological conditions but intracellular concentrations can

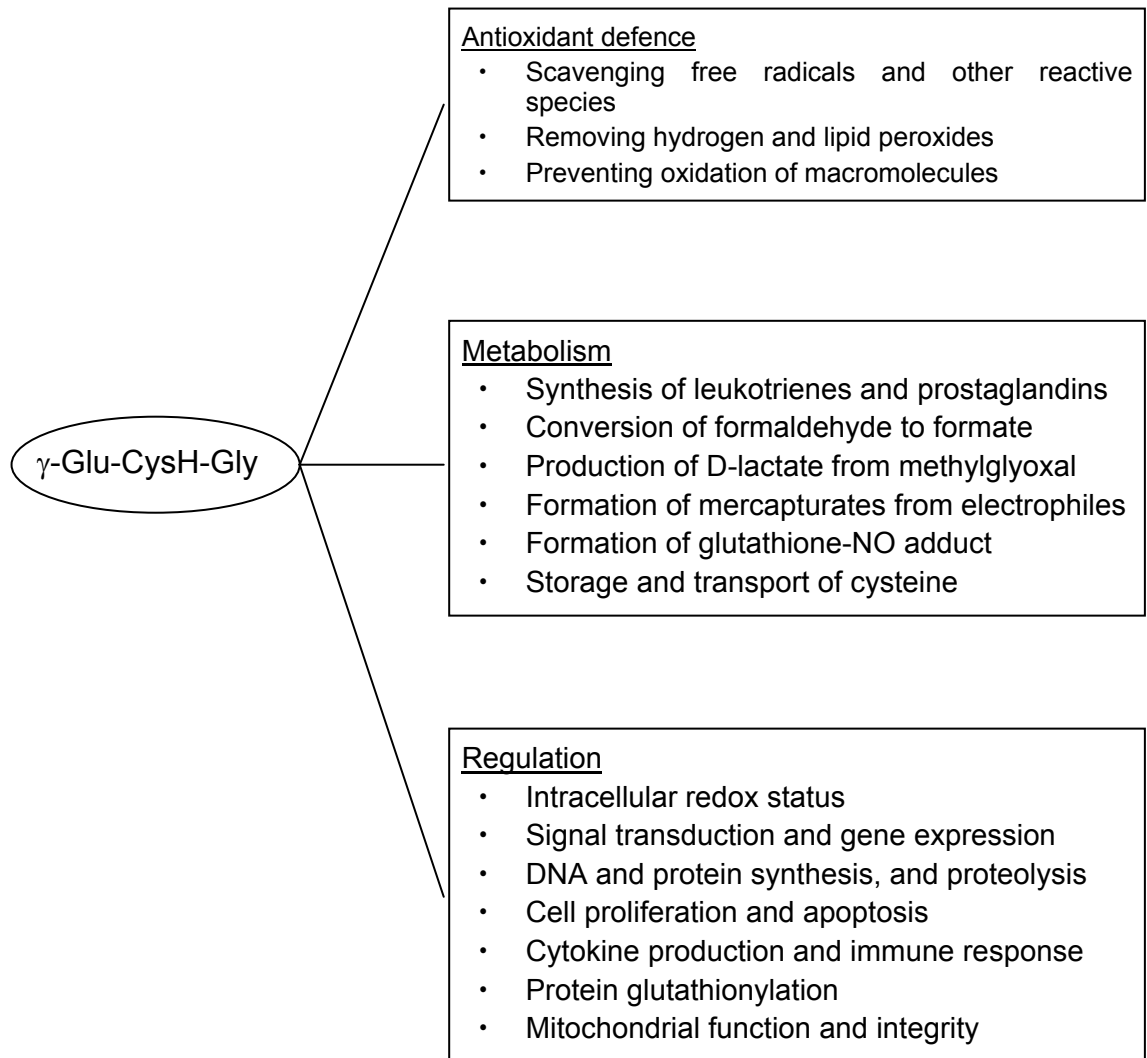


Figure 1.11: Functional roles of glutathione

Adapted from Ref. (173)

be affected in various pathologies (155;173). Plasma glutathione arises largely from the liver. Glutathione exists in reduced form and is a tri-peptide γ -Glu-CysH-Gly synthesised in a two-step reaction (174). L-glutamate and L-cysteine is first catalysed by γ -glutamyl-cysteine synthase (GCS), in the presence of adenosine triphosphate (ATP) and magnesium ion (Mg^{2+}), to form L- γ -glutamyl-L-cysteine in a rate-limiting step. L- γ -glutamyl-L-cysteine and glycine is then catalysed by glutathione synthase (GS), in the presence of ATP and Mg^{2+} , to form glutathione. Less than 0.2% of total glutathione occurs in oxidised form as glutathione disulphide (GSSG), which is potentially highly cytotoxic. This form is reduced by glutathione reductase in the presence of NADPH. The [GSH]:[GSSG] ratio, often used as an indicator of the cellular redox state, is the major redox couple that determines the antioxidative capacity of cells (173). Its value can, however, be affected by other redox couples including NADPH/NADP⁺ and thioredoxin_{red}/thioredoxin_{ox}. Metabolites detoxified via glutathione conjugation are eliminated from cells by energy-dependent efflux pumps such as glutathione s-conjugate transporter, which is also known as multidrug resistance-associated protein (MRP).

1.5.2. Glutathione Peroxidases

GPxs plays a role in both first line of defence, by reducing H_2O_2 to water and second line of defence, by reducing organic peroxides such as lipid hydroperoxide to water and lipid alcohol, via conjugation of glutathione, forming GSSG (175;176). There are four known GPxs which contain selenocysteine at the active site and at least two other proteins with over 40% sequence identity to cytosolic GPx that do not contain selenocysteine (175). GPx1 and GPx2 are homotetrameric proteins, GPx3 is a homotetrameric glycoprotein while GPx4 is a monomeric enzyme (175). Cytosolic or cellular GPx (GPx1 or GSHPx-1), encoded by *GPx1* on chromosome 3p21.3, can metabolise H_2O_2 and a variety of organic peroxides, including cholesterol and long-chain fatty acid peroxides. The fatty acid metabolism by GPx1 requires phospholipase A2 activity as well. GPx2 found mainly in the epithelium of gastrointestinal tract (GSHPx-GI), encoded on chromosome 14q24.1 has similar activities to GPx1. *GPx3*, encoded on chromosome 5q23, was first purified from plasma, thus GSHPx-P. *GPx3* mRNA was later found to be expressed predominantly in kidney, particularly the proximal tubular epithelial

cells. GPx4, encoded on chromosome 19p13.3, can react with phospholipid hydroperoxide (PHGPx)

GPx1 knockout mice show increased susceptibility to ROS-induced oxidative stress (177) while induction of GPx1 has been shown to protect endothelial cells against oxidative stress (178), and transgenic GPx1 expression improved endothelial dysfunction (179). GPx1 is also important for modulation of ROS and consequently transcription factor activation (175). Cellular and tissue location of the GPxs are critical for their biological functions. The unusual distribution of GPx2 suggests a specific function in metabolising ingested lipid hydroperoxides. Regulation of GPx2, unlike GPx1, is less restricted by selenium deficiency. GPx3 also has activity against phospholipid hydroperoxides. GPx4 is responsible for protection of membranes against oxidative damage and also control of cell function. Although GPxs are important, there are also non-selenocysteine enzymes that have peroxidase activity, most notably the GSTs.

1.5.3. Glutathione S-Transferases

The soluble dimeric glutathione s-transferases (GSTs) are major phase II detoxification enzymes, with the ability to conjugate xenobiotics and reactive oxygen species using donor molecule glutathione (155;180-184). There are two distinct families encoding proteins with GSTs activities, the first consists of cytosolic proteins and the second consists of membrane-bound proteins (185;186). The cytosolic proteins are the *bona fide* GSTs, having both GSTs_N and GSTs_C domains (186) while the membrane-bound enzymes are not part of the GSTs gene superfamily. In the human, the GSTs gene family comprises 16 genes in six classes – one pi (π) gene (*GSTP1*) on chromosome 11q13, five mu (μ) genes (*GSTM1-GSTM5*) on chromosome 1p13.3, five alpha (α) genes (*GSTA1-GSTA5*) on chromosome 6p12, two omega (ω/Ω) genes (*GSTO1, GSTO2*) on chromosome 10q25, one zeta (ζ) gene (*GSTZ1*) on chromosome 14q24 and two theta (θ) genes (*GSTT1, GSTT2*) on chromosome 22q11.

GSTs are dimeric proteins, each subunit about 26kDa, formed only from subunits within the same class (181). GSTs are 2-domain structures made of structurally conserved nucleophilic glutathione binding sites (G-sites) and the diverse

hydrophobic binding sites (H-sites) that determines the substrate specificities (184). The G-sites are largely made up through interactions with N-terminal residues while the H-sites involve C-terminal residues and other parts of the protein. Substrates are electrophilic compounds that are able to react with the thiol moiety of glutathione (181). GSTs catalyse binding of a large variety of electrophiles to sulphhydryl group of glutathione, generally resulting in less harmful, more water-soluble molecules (155). Expression of GSTs seems to be under control of responsive elements such as glucocorticoid response element (GRE), xenobiotics response element (XRE) or antioxidant response element (ARE) (182;187). The major role of GSTs is detoxification of α,β -unsaturated carbonyls, epoxides, hydroperoxides and electrophilic metabolites of xenobiotics (155). Particular isoenzymes are extremely efficient at conjugating glutathione with 4-hydroxynonenal aldehyde formed from lipid peroxidation of polyunsaturated fatty acids. Certain GSTs can catalyse conjugation of glutathione with cholesterol α -oxide, a mutagenic compound generated during oxidation of membranes. Some GSTs exhibit selenium -independent peroxidase, isomerase and thiol transferase activity (184). While some GSTs are active with phospholipid hydroperoxides, many are active with free fatty acid hydroperoxides (155). Generally, the reductase activity of GSTs can arrest lipid peroxidation. In DNA, thymines are likely targets of free radical damage as they have the highest electron affinity and will form thymine hydroperoxides (155). Certain GSTs conjugate glutathione with adenine and thymine propenals, which are reactive purine and pyrimidine bases formed during oxidative damage to DNA. Although the biological significance of GSTs' ability to reduce DNA hydroperoxides is not clear, GSTs in rat liver appear to translocate to the nucleus during periods of drug-induced oxidative stress. In addition to their role in catalysing the conjugation of electrophilic substrates to glutathione, these enzymes also carry out a range of other functions. These include removal of ROS, regeneration of S-thiolated proteins, catalysis of conjugations of endogenous ligands and catalysis of reactions in metabolic pathways not associated with detoxification (187). GSTs represent a second line of defence against highly toxic spectrum of substances produced by ROS-mediated reactions due to their broad substrate specificity.

SODs are the most studied anti-oxidant enzymes, with catalase and GPx also increasingly becoming a focus of several studies. The role of GSTs as protectors

of cardiovascular system is beginning to emerge. Most of the studies on GSTs have been in cancer research. However, the rat *Gstm1* was identified to be differentially expressed in the genetic models of hypertension (61;65;66). The following sections will discuss the *GSTM* gene family in greater detail.

1.5.3.1. Nomenclature of Glutathione S-Transferase μ Genes

The current nomenclature used for the GSTs was standardised in 1992 (188). *GSTM1* null is referred to as *GSTM1*0*. As the current study does not look at the different alleles of each GSTs μ isoenzymes, *GSTM1*A* or *GSTM1*B* are referred to as only *GSTM1* without differentiating between the two alleles of *GSTM1*. Likewise, *GSTM3* is used instead of *GSTM3*A* or *GSTM3*B*. For the isoforms without known alleles such as *GSTM2-2*, *GSTM2* is used instead of *GSTM2-2*. However, it should be noted that in the literature pre-dating the standardised nomenclature, *GSTM1*, *GSTM2* and *GSTM5* were previously referred to as GST1, GST4 and GST5 respectively. Likewise, the rat *Gstm* genes were and are still referred to as the Yb genes, with *Gstm1*, *Gstm2*, *Gstm3* and *Gstm4* corresponding to Yb1, Yb2, Yb3 and Yb4, respectively. Subsequently, more rat *Gstm* genes have been identified and are named as *Gstm* rather than Yb. With the confusion of GST nomenclature in the literature as well as discovery of new GSTs, there is a continuous effort to update the nomenclature of human soluble GSTs by researchers around the world (189).

To avoid any confusion, for this thesis, a prefix 'r' followed by *Gstm* (capital 'G', lower case 'stm') i.e. *rGstm*, is used to describe the rat *Gstm* isoform. A prefix 'h' followed by *GSTM* (all capital letters) i.e. *hGSTM*, is used to describe human *GSTM* isoform. The *hGSTM1* null allele will be described as *hGSTM1*0*. When referring to genes, italics is used. When referring to the gene family in either rat or human, *rGstm* and *hGSTM* will be used, respectively. When referring to either rat or human version of gene or protein, *GSTM* is used instead. A rat *Gstm* gene described as similar to *GSTM7-7* in the NCBI database will be referred to as *rGstm7*. A predicted rat *Gstm* gene described as *Gstm6_predicted* in the NCBI database will be referred to as *rGstm6^a*. A second predicted gene described as similar to *Gstm6* protein will be referred to as *rGstm6^b*. As the enzyme isoforms

are not studied as dimeric proteins but as individual subunits, the proteins will be referred to as GSTM1 and so on.

1.5.3.2. Glutathione S-Transferase μ Class

There are five members in the GSTM class in human and possibly eight in the rat. Each *GSTM* gene consists of 8 exons and 7 introns. The sequences of these genes and their encoded amino acid sequences are highly homologous, suggesting gene duplication in the evolution of the *GSTM* genes.

The 155kb cluster of rat *Gstm* locus is located to chromosome 2q34, in the order of M7-M1-M2-M4-M6^b-M3-M6^a, followed by M5 in an inverted orientation (*Figure 1.12A*). It should be noted that *rGstm6^a*, *rGstm6^b* and *rGstm7* have only been identified and named within the past two years. There are no published studies involving these three genes to-date. There is extensive literature on the biochemistry of rat GSTs as well as their roles as phase II detoxification enzymes. With the recent identification of new GST classes and members of the earlier known classes, results from literature, pre-dating the late 1990s and probably the early 2000s, should be interpreted with caution. The *rGstm1* has been identified as a positional and functional candidate gene for hypertension by our group (61). There are also data on differential expression of this gene in other hypertensive rat strains as compared to normotensive reference strains (65;66) but there have been very few follow up studies until now.

Similarly the 85kb cluster of human *GSTM* locus is situated on chromosome 1p13.3 (190;191), in the order M4-M2-M1-M5 followed by M3 in an inverted orientation (*Figure 1.12A*) (192). The *hGSTM3* gene is most distantly related to others and the *hGSTM3* subunit is also structurally distinct from the other *GSTM* with 4 residue extensions at N-terminus and 3 residue extensions at C-terminus (193). Early work on *hGSTM* shows that in the *hGSTM1* gene alone, reported polymorphisms include a single base change giving rise to the functionally identical *hGSTM1*A* and *hGSTM1*B* alleles (194); a duplication of the *hGSTM1* gene (195); and deletion of the *hGSTM1* gene resulting in the *hGSTM1* null allele (*hGSTM1*0*) (*Figure 1.12B*) (196;197). Numerous studies have demonstrated weak associations between the *hGSTM1*0* polymorphism with an increased risk to

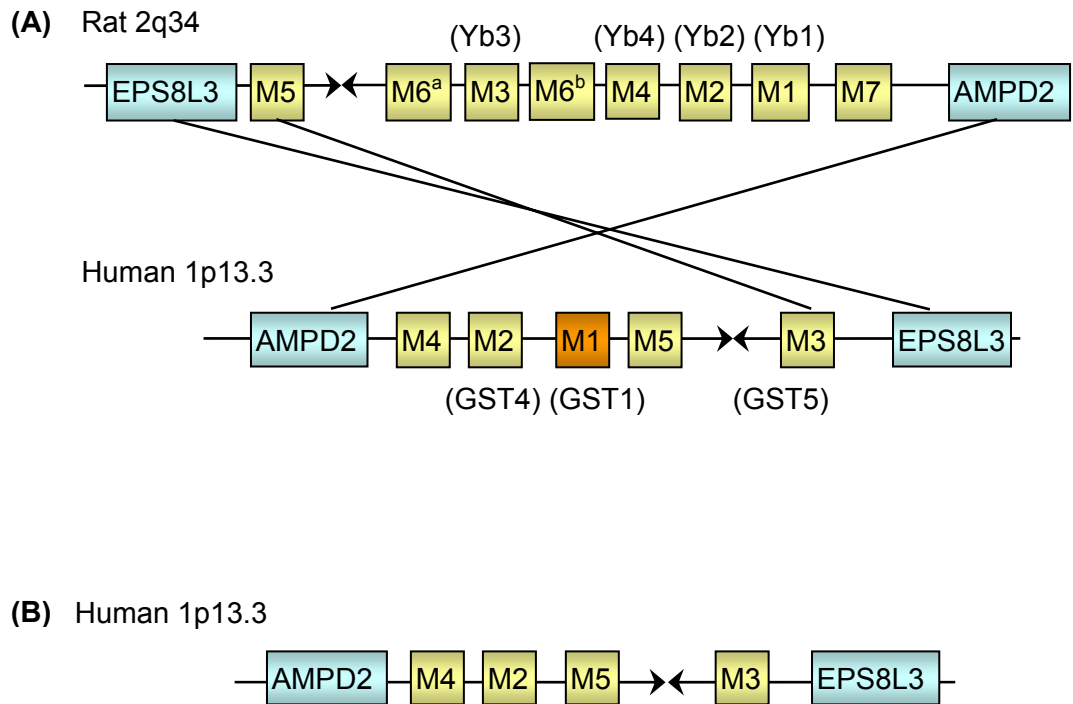


Figure 1.12: Organisation of the glutathione s-transferase mu genes in human and rat

(A) Synteny between rat *Gstm* gene cluster on chromosome 2 and human *GSTM* gene cluster on chromosome 1. The names in brackets are the alternate names for the respective genes in earlier literature. AMPD2, adenosine monophosphate deaminase 2; EPS8L3, epidermal growth factor receptor pathway substrate 8-like protein 3; GSTs, glutathione S-transferase;

(B) Organisation *hGSTM* genes in individuals missing *hGSTM1* gene.

various epoxide induced cancers (198;199). The *hGSTM1*0* polymorphism has also been associated with increased cardiovascular risk (200-203). An alternative non-functional splice variant of *hGSTM1* also exists. A polymorphism in the *hGSTM3* gene consisting of two alleles, *hGSTM3*A* and *hGSTM3*B*, is distinguished by a three base pair deletion in intron 6 (204). The *hGSTM3*B* has been associated with altered expression levels of hGSTM3-3 and, in linkage with the *hGSTM1*A* allele, has been shown to reduce the risk of developing epoxide induced cancers (204;205). In *hGSTM4*, two alternatively spliced, non-functional transcripts have been identified (206). A recent study described many more polymorphisms in the *hGSTM* genes (207) but in this thesis, the polymorphisms in the *hGSTM* genes are not the main focus.

There are no readily available isoform-specific antibodies against each of the GSTM isoforms, and probably due to unavailable substrate specificities between the GST classes, and isoform within a GST class, most studies measured GST expression and activities as a class rather than as individual isoforms (208-212). Any known enzyme activities previously attributed to any one rGstm isoform might also include the activities of the recently identified rGstm members. When the activities of the isoforms were measured, it is often not all the isoforms of a GST class that were investigated (213-215). When such studies were done, the results showed that the substrates specificities were not mutually exclusive; but rather the different isoforms have different affinities for the same substrates.

AIMS

We hypothesise that oxidative stress-related genes and their functional polymorphisms influence the risk of developing hypertension and thus coronary artery disease. Previous gene expression profiling combined with congenic strategies identified *rGstm1* as a positional and functional candidate gene for blood pressure regulation (61;219). However, *rGstm1* is one of eight members of the *rGstm* family of genes that actively provide a second line of defence against oxidative stress. We hypothesise that the *Gstm* gene family are important anti-oxidant enzymes that help to regulate the balance of ROS and NO in the kidney as well as vasculature. There is also no consensus of which human *GSTM* is a true orthologue of rat *Gstm1*. It will be of interest to find the human orthologue of *rGstm1*, to determine if there is also differential expression of *hGSTM* genes and proteins in human vasculature. As CVD are polymorphic diseases, there is also a need to determine if the reduced renal *rGstm1* expression in SHRSP is a secondary effect of increased blood pressure or play a primary functional role in pathogenesis of hypertension. Human *GSTM1*0* polymorphisms and polymorphisms in oxidative stress related enzymes are often associated with CVD. It is likely that each polymorphism impart small effects that add up to regulate the balance of ROS and NO.

The aims of this study are :

- (1) To characterise the vascular and renal expression of the rat *Gstm* genes as well as human *GSTM* genes in vascular tissues.
- (2) To investigate the functional role of *rGstm* genes in the major sites of action for blood pressure regulation – vessel and kidney – different classes of antihypertensive drug treatments will be used to evaluate the oxidative stress status and gene expression of *rGstm* genes.
- (3) To establish if functional polymorphisms in two key enzymes involved in ROS and NO balance are associated with CAD as single polymorphism and as haplotypes.

CHAPTER 2: MATERIALS & METHODS

The details for all the equipments, chemicals, reagents and consumables used in this study are listed in *Appendix B*.

2.1. Animal Strains

The animal strains used in this thesis are WKY_{Gla}, SHRSP_{Gla} and a chromosome 2 congenic strain (SP.WKY_{Gla}2c*). All animals were housed under controlled environmental conditions, where the temperature was maintained at 21°C, 12 hour light/dark cycles were from 7am to 7pm and the rats were fed standard rat chow (rat and mouse No.1 maintenance diet, Special Diet Services) and water provided *ad libitum*. The offspring were weaned after 3 weeks of age when they were sexed, ear-tagged (National Band and Tag Co.) and caged (maximum 3 animals per cage) according to sibling group and sex.

Work with experimental animals was in accordance with the Animals Scientific Procedures Act 1986 under the project license held by Prof. A.F. Dominiczak. Inbred colonies of the SHRSP and WKY strains have been maintained in Glasgow by brother-sister mating since 1991, when 6 males and 7 females of each strain were given as a gift by Dr. D.F. Bohr from the Department of Physiology at the University of Michigan, USA. These colonies originated from National Institutes of Health, Bethesda, USA and were subsequently maintained as inbred colonies for over 15 years at the University of Michigan (219). Maintenance of the integrity of the colonies as well as the hypertensive and normotensive phenotypes was undertaken by selection of SHRSP adult breeders with blood pressures 170-190 mmHg (males) and 140-170 mmHg (females), and WKY adult breeders of 120-140 mmHg (males) and 100-130 mmHg (females). Routine microsatellite screening was used to confirm homozygosity of all loci within a group of animals from each strain, selected at random.

2.1.1. Congenic breeding strategy

The congenic SP.WKY_{Gla}2c* strain was produced and published by the group using a marker-assisted “speed” congenic strategy (*Figure 1.4*), prior to the

beginning of this project (219). The congenic strain used in the present study contains a 22-cM segment transferred from WKY (donor strain) to the genetic background of SHRSP (recipient strain). The nomenclature of the strains consists of the first abbreviation belonging to the recipient strain and the second to the donor: Gla denotes that strains originate from the Glasgow colonies, and the number 2 refers to rat chromosome 2. Thus, the congenic strain described is the SP.WKY_{Gla}2 (D2Wox9-D2Mgh12) and is abbreviated to SP.WKY_{Gla}2c* for simplicity (*Figure 1.5*). Five backcrosses were required to produce the congenic strain with no detectable heterozygosity of background markers. The SP.WKY_{Gla}2c* strain incorporated only the lower blood pressure QTL on rat chromosome 2.

Genomic DNA was isolated from a 4-mm tip from the tail of congenic animals and genotyping as described previously. Genotyping was performed by polymerase chain reaction (PCR) amplification of microsatellite markers, and the genotypic results obtained were mapped relative to each other using the MAPMAKER/ EXP 3.0 computer package with an error-detection procedure (220). A genetic linkage map of rat chromosome 2 was constructed, consisting of 74 microsatellite markers (polymorphic between the WKY and SHRSP strains) by genotyping F2 animals. Genetic distances were calculated with the Haldane mapping function. PCR was performed using the rat genome T55 radiation hybrid (RH) panel obtained from Research Genetics. Of the 74 markers scored, 55 were accurately positioned on the RH map of rat chromosome 2. The markers covered a distance of 1224 centiRays and were all placed with a logarithm of odds ratio (LOD) – 10, which equates to 10¹⁰ odds for linkage. Scored consensus data were submitted to the RHMAPPER program (<http://rgd.mcw.edu/RHMAPSERVER/>).

2.1.2. Blood Pressure Measurement by Tail-Cuff Plethysmography

Systolic blood pressure was measured by tail-cuff plethysmography in conscious, restrained animals as previously described (221). Rats were placed in a 37°C incubation chamber for 15-20min to allow vasodilation, wrapped in a cloth for restrain purposes, and an inflatable cuff placed on their tail along with a piezoceramic transducer (Hartmann & Braun type 2) for pulse detection. The pressure in the cuff could be controlled in 1mmHg steps over a 300mmHg range

and the resulting pulsation detected by the transducer was amplified and filtered before being displayed on computer using IBM compatible software. This signal was visualised as a function of pressure and an estimation of the systolic pressure was marked. A minimum of six readings were taken for each rat per sitting and the average was taken for the systolic blood pressure value for that animal.

2.2. Rat Tissues

Rat tissues freshly removed from rats under deep terminal anaesthesia (halothane), for total RNA and protein extraction, were immediately snapped frozen in liquid nitrogen.

2.2.1. Preparation of Rat Tissues for Cryosections

A small cup was made using aluminium foil over the base of a Bijoux container and filled with optimal cutting temperature (O.C.T.) compound. Vascular tissues (e.g. carotid arteries, aorta) were cleaned of the surrounding connective tissues, slowly inserted into the compound, kept upright and placed on top of dry ice to freeze the specimens in the O.C.T. compound. Sterile pipette tips were used to hold the vessel upright when necessary. The frozen tissue blocks were then kept at -70°C until required. Transverse cross-section of a kidney from the each rat was cut and the kidney was then embedded (cut surface facing the bottom of the well) in the O.C.T compound. 6-10µm thick sections were cut using the Thermo cryostat and thaw-mounted on RNase-free silanised slides. The slides were then kept at -70°C until required.

2.2.2. Preparation of Rat Tissues for Paraffin Sections

The tissues were rinsed with PBS to remove excess blood and the connective tissue surrounding vascular tissues were removed. The tissues were then fixed in 10% formalin solution overnight or 1hr for carotid arteries (CA) at room temperature (RT), after which the formalin solution was replaced with PBS. The fixed samples were later embedded into paraffin blocks by trained technical staff in the laboratory. Paraffin sections of 6µm thickness were cut and baked onto silanised slides at 60°C for 3hr followed by 40°C overnight. Both the paraffin

blocks and paraffin sections were then kept at RT in appropriate boxes. For kidney, transverse cross-sections were used.

2.2.2.1. Silanisation of Microscope Slides

The microscope slides were first placed in racks and immersed in a trough of distilled water (dH₂O) containing 0.1% diethylpyrocarbonate (DEPC) to deactivate RNases in fume cupboard for 1hr at RT. Excess water were drained and the racks were then wrapped in foil and autoclaved. The autoclaved slides were then coated in freshly prepared 2% solution of 3-aminopropyltriethoxysilane (APES) in dry acetone for 5s, in a fume hood. The slides were then rinsed once in dry acetone for 5s and twice in DEPC- treated dH₂O (DEPC-dH₂O) for 5min each. The slides were then wrapped in foil, sealed and dried overnight at 42°C and stored until required. Slides used for immunohistochemistry (IHC) did not require treatment with DEPC-dH₂O or be wrapped in foil.

2.3. Human Tissues

2.3.1. Vascular Tissues from Clinical Patients

The study was approved by the local ethics committee, and all of the patients gave written informed consent. Freshly collected saphenous veins (SVs) and internal mammary arteries (IMAs), from patients undergoing CABG operation were collected in sterile saline solution by the surgical team at Western Infirmary, and control veins (VVs), from patients undergoing varicose vein removal, by the surgical team at the Gartnavel Hospital in Glasgow.

2.3.2. Handling of Vascular Tissues

Vessels were trimmed of connective tissues and transferred into Bijoux containers containing RNA/ater® solution. Any sections of control veins that were varicose were discarded. The samples were kept at -20°C until further use.

2.3.3. Preparation of Vascular Tissues for Cryosections

When sufficient tissues was available, cryosections of human internal mammary arteries, saphenous veins and varicose veins were prepared as described in section 2.2.1.

2.3.4. Preparation of Vascular Tissues for Paraffin Sections

Paraffin sections were prepared as described in section 2.2.2.

2.4. General Molecular Biology

The water used in molecular biology work is distilled water (dH₂O) that has been autoclaved, and are referred to as sterile dH₂O (sdH₂O). Any experiments involving RNA used autoclaved DEPC-treated dH₂O (DEPC-dH₂O). All plasticware or glassware used for RNA work were pre-soaked in 0.1% DEPC water for at least 2hr at RT (in fume hood) and then autoclaved. Glassware used for *in situ* hybridisation (ISH) in Edinburgh was baked at 180°C for at least 8hrs. Filtered RNase-free tips were used in all RNA work.

2.4.1. DNA Extraction

Approximately 0.5cm of human vessels were minced briefly with sterile blades and placed into Eppendorf tubes containing 500µl of DNA extraction solution containing a final concentration of 50mM of Tris pH 8.0, 100mM EDTA pH 8.0, 100mM NaCl, 1% SDS and 0.5mg/ml Proteinase K. The samples were incubated at 55°C overnight. The entire solution was transferred to a pre-spun Eppendorf Phase Lock Gel heavy (PLG-H) tube and 500µl of phenol:chloroform:isoamyl alcohol (25:24:1) was added and mixed by gentle inversion. The tubes were centrifuged at 14,000rpm for 5min. The aqueous phase was transferred to a fresh pre-spun PLG-H tube, 500µl of chloroform:isoamyl alcohol added and mixed by gentle inversion. The tubes were centrifuged at 14,000rpm for 5min and the aqueous phase transferred to a fresh Eppendorf tubes. 100µl pf 10M ammonium acetate (NH₄OAc) and 500µl of ice cold 100% ethanol were added and mixed gently. The tubes were then centrifuged 10,000rpm for 2min. The ethanol was

decanted with care taken to avoid disrupting the DNA pellet. 500 μ l of ice cold 70% ethanol was added to the pellet, mixed gently and the tubes centrifuged at 10,000rpm for 2min. The ethanol was again decanted with care and excess ethanol drained onto a clean paper towel. The samples were air-dried in a rack at 4°C for 15min to remove residual ethanol. The DNA pellet was dissolved in 100 μ l of sdH₂O and quantified. The DNA was diluted to a working concentration of 5ng/ μ l.

2.4.2. DNA Purification

If the concentrations of the extracted samples were too diluted or contaminated with lipids, the samples were purified and reconstituted in smaller volume of 1X Tris/EDTA (TE) buffer (10mM Tris, 5mM ethylenediaminetetraacetic acid (EDTA)). 40 μ l of 3M sodium acetate (NaOAc) was added to the DNA sample and the total volume was made up to 400 μ l with 1X TE buffer. 800 μ l of ice-cold 100% ethanol was added to the sample. The sample was then incubated at -20°C overnight. The sample was then centrifuged at 14,000 rpm for 2min and the supernatant discarded carefully without disturbing the DNA pellet. 1ml of 70% ethanol was added to the pellet and mixed gently. The sample was then centrifuged at 14,000rpm for 2min and the supernatant discarded carefully without disturbing the DNA pellet. The pellet was then air-dried at 4°C and re-suspended in 1X TE. The concentration of the sample was then re-quantified.

2.4.3. Nucleic Acid Quantitation

The RNA samples were quantified using RiboGreen™ RNA Quantitation Reagent and Kit while DNA samples were quantified using PicoGreen™ dsDNA Quantitation Kit according to the manufacturer's instructions. The plate was read using the Wallac 1420 Victor machine.

The samples for real-time RT-PCR were quantified with a method that is technologically more advanced, less time-consuming and requires less sample. 1 μ l of the RNA/DNA samples was quantified using the NanoDrop ND-1000 spectrophotometer and the programme ND-1000 v3.1.0

2.4.4. Polymerase Chain Reaction (PCR)

The genes of interest were amplified by polymerase chain reaction (PCR) set up in a PCR plate with 2µl of template cDNA, 1.5mM MgCl₂, 1X Mg-free buffer (10mM TrisHCl pH 9, 25mM KCl and 0.1% Triton-X-100), 1µl 10mM forward primers, 1µl 10mM reverse primers, 3.2µl 1.25mM dNTPs, 0.2µl *Taq* DNA polymerase (5U/ml) and made up with sdH₂O to a final volume of 20µl. The PCR reactions were run on the Peltier Thermal Cycler (PTC-225). 5µl of the PCR reactions were then electrophoresed with 1µl of 6X loading dye in a 2% agarose gel at 100V for 1hr, alongside 100bp DNA ladder.

2.4.5. Restriction Fragment Length Polymorphism (RFLP)

The PCR products of the genes of interest were digested with restriction enzymes (RE) at the appropriate temperature for 2hr. A typical reaction was set up with 15µl PCR products, 1u/µl RE and 1X RE buffer and made up to 20µl with sdH₂O. The digested reactions were then run in a 2% agarose gel at 100V for 1hr, alongside the 100bp DNA ladder. For fragments between 10 – 150bp, the digested reactions were run in 3.5% Metaphor agarose gel, alongside pUC18 *Msp* I digest DNA ladder.

2.4.6. Sequencing

For PCR products of longer than 200bp, the products were cleaned using the Nucleofast 96 PCR plate according to the manufacturer's instructions. The cleaned PCR products were then re-solubilised in 50µl of sdH₂O. For PCR products 200bp or shorter, the products were cleaned using the microCLEAN reagent according to the manufacturer's instructions. Pellets of PCR products were then re-solubilised in 15µl of sdH₂O. 5µl of cleaned PCR products were electrophoresed in a 1.5% agarose gel to check for the efficacy of the cleaning procedure.

Two sequencing reactions were set up for each sample, each containing a final concentration of 3.2µM of forward or reverse primer, 0.5µl of Big Dye® Terminator

v3.1 Cycle sequencing kit, 0.875X sequencing buffer, 4-8µl of cleaned PCR product and sdH₂O to a final volume of 20µl. The reactions were sequenced at 96°C for 45s, 50°C for 25s and 60°C for 4min for 25 cycles. The sequencing reactions were cleaned using the genCLEAN DYE Terminator Removal plate according to the manufacturer's instructions. 7µl of the cleaned sequencing reaction were mixed with 10µl of formamide in a bar-coded plate and analysed on the Applied Biosystems 3730 DNA analyser and Seqscape v2.5 software.

2.5. mRNA Expression

The following two methods were used for total RNA extraction. The second method was used later on in the project due to improvement of technology, which gives better quality than the first method.

2.5.1. Total RNA Extraction

2.5.1.1. Total RNA Extraction using RNA Bee

Frozen tissue samples (0.5cm to 1cm) were homogenised completely in 2ml of ice-cold RNA Bee in a Bijoux container using a Polytron. 200µl of chloroform was added to the samples and mixed by brief vortexing. The homogenates of each sample were transferred into 2 labelled pre-spun 1.5ml PLG-H tubes and placed on ice for 5min. The PLG-H tubes were centrifuged at 12,000rpm at 4°C for 15min in a pre-cooled centrifuge. The top aqueous layers of both PLG-H tubes were transferred into 1 labelled 2ml Eppendorf tube. An equal volume of isopropanol (~1ml) were added to the samples and mixed by brief vortexing. The samples were centrifuged at 12,000rpm at 4°C for 15min. The supernatants were removed carefully without disturbing the pellet. 1ml of 70% ethanol in DEPC-dH₂O was added to the samples and vortexed briefly. The tubes were centrifuged at 10,000rpm at 4°C for 10min. The supernatants were removed carefully and the RNA pellets were air-dried at 4°C, covered with a clean paper towel. The pellets were then re-suspended in 100µl of DEPC-dH₂O. The RNA samples were then quantified as described in section 2.4.3. and 1µl of the sample was diluted to a final concentration of 100-500ng/µl and integrity of the extracted RNA checked on the Agilent at MBSU, University of Glasgow.

2.5.1.2. Total RNA Extraction using Qiagen RNeasy Kits

The total RNA from samples was extracted using Qiagen RNeasy kits accordingly to the manufacturer's recommended instructions for fibrous tissues (Appendix C of RNeasy Handbooks) with the following exceptions. The columns were left to stand at RT for 5min instead of 1min to elute the clean total RNA. The first eluate was pipetted back onto the membrane in the columns and left to stand for another 1min. The resulting eluate was then quantified as described in section 2.4.3., 1 μ l of each samples was diluted to a final concentration of 100-500ng/ μ l and integrity of the extracted RNA checked on the Agilent.

2.5.2. DNase Treatment of Extracted Total RNA

The following two methods were used for DNase treatment of total RNA. The second method was used in later experiments due to improvement of technology, which gives better retrieval of total RNA or equivalent quality.

2.5.2.1. DNase Treatment using RQ1 DNase

The RNA samples extracted were treated using RQ1 RNase-free DNase before further experiments. For each RNA samples, a reaction were set up with 1X RQ1 buffer, total RNA and RQ1 DNase (1u/ μ l) to a concentration of 1u/ μ g RNA and DEPC-dH₂O to a final volume of 100 μ l if necessary. The samples were incubated at 37°C for 1hr. 100 μ l of phenol were added to the samples, vortexed for 15s and centrifuged at 14,000rpm at 4°C for 5min. The top layer were transferred to a new Eppendorf tube, 100 μ l of phenol:chloroform (1:1) were added to the samples, vortexed for 15s and centrifuged at 14,000rpm at 4°C for 5min. The top layer were transferred to another new Eppendorf tube, 100 μ l of chloroform were added to the samples, vortexed for 15s and centrifuged at 14,000rpm at 4°C for 5min. To each sample, 10 μ l of 3M NaOAc and 300 μ l of ice-cold 100% ethanol were added and placed in -20°C overnight. On the following day, the samples were centrifuged at 14,000rpm at 4°C for 5min and the supernatant discarded. 300 μ l of 70% ethanol in DEPC-dH₂O was added to the samples, vortexed briefly and centrifuged at 14,000rpm at 4°C for 5min. The supernatants were removed carefully and the

RNA pellets were air-dried at 4°C, covered with a clean paper towel. The pellets were then re-suspended in appropriate volume of DEPC-dH₂O, depending on the amount of starting total RNA used for the treatment.

2.5.2.2. DNase Treatment using DNA-free™ kit

Alternatively, extracted total RNA was treated with DNase using the DNA-free™ kit from Ambion. RNA aliquot of up to 50µg or 44µl was transferred to RNase-free tube containing 5µl of 10X buffer and 1µl of DNase I and incubated at 37°C for 20-30min. After incubation, 5µl of inactivation reagent was added to the tubes and left at RT for 2min and centrifuged at 12,000rpm for 2min at 4°C. The supernatant containing the cleaned total RNA was then transferred into new tubes. The RNA samples were then re-quantified, 1ug aliquoted into fresh tubes for reverse transcription reaction and the remaining samples stored at -70°C.

2.5.3. Reverse Transcription (RT) – PCR

All RT-PCR experiments were carried out in a two-step protocol. The Reverse Transcription system from Promega was used to obtain cDNA from commercial and patients' total RNA samples. 1 µg of DNase-treated total RNA for each sample was incubated at 70°C for 10min, spun briefly and placed on ice for 5min. The RNA samples were reverse transcribed to cDNA in a 20µl reaction containing a final concentration of 5mM of MgCl₂, 1X RT buffer, 1mM of dNTP mixture, 1u/µl of RNasin, 15u of AMV reverse transcriptase and 0.5µg of random primers. A few selected samples were used for negative control cDNA reactions without AMV reverse transcriptase. The reverse transcription reactions were carried out at 42°C for 1hr. The reactions were stopped by incubating the samples at 99°C for 5min and then placed on ice for 5min. The samples were diluted to a final volume of 100µl. When not used immediately, the samples were stored at -20°C.

The genes of interest were amplified by PCR, using specific primers as described in section 2.4.4. The PCR products of the genes of interest obtained were cleaned and sequenced as described in section 2.4.6., to confirm the identity of the amplicons.

2.5.4. Real-time RT-PCR

Initial experiments was performed using the first method (Lightcycler) but due to limited number of samples that could be done in each experimental run, later experiments (which contained much larger sample size) were performed using the second method (Taqman).

2.5.4.1. Real-time RT-PCR using Lightcycler™

Real-time RT-PCR quantitation of the samples was carried out in a two-step RT-PCR assay. The reactions were prepared using the LightCycler™ DNA Master SYBR Green I kit. Each reaction consists of 2µl of cDNA sample, 2µl of SYBR master mix, 4mM MgCl₂, 0.5µM sense primer, 0.5µM antisense primer in a 20µl reaction. The real-time RT-PCR reaction was carried out at 95°C for 60sec, 35 cycles of 95°C for 3sec, annealing temperature for 15sec, 72°C for 10sec and 80°C-83°C for signal acquisition, continuous acquisition of signal during melting curves of samples from 99°C to 40°C. The melting curves were used to assess the quality of each run. A standard curve of purified RT-PCR products was included in each assay for the calculation of absolute number of template copies. The gene of interest was expressed as a percentage of β-actin.

An optimisation RT-PCR and an efficiency assay was performed for each gene prior to real-time RT-PCR experiments. The optimisation PCR was set up in duplicates, with each reaction capillary set up and carried out as described above, with the exception of annealing temperature of 50°C to 65°C. The efficiency assay involved setting up seven serial dilutions of a random sample and the dilutions were plotted against the crossing points. The results were acceptable is the calculated r is >0.9.

2.5.4.2. Real-time RT-PCR using Taqman

Relative real-time RT-PCR quantitation of the samples was carried out in a two-step RT-PCR assay using the Taqman Gene Expression Assays from Applied Biosystems in a multiplex reaction (if the gene of interest and β-actin reacts with the same efficiency). Each reaction consists of 2.5µl of Taqman Universal PCR

Master Mix, 1X VIC-labelled β -actin probe, 1X FAM-labelled probe for genes of interest and 2 μ l of cDNA in a final volume of 5 μ l, in barcoded 384-well plate. For genes of interest that do not run with the same efficiency as β -actin, the gene of interest was run in a singleplex reaction within the same plate as β -actin. The $\Delta\Delta$ Ct comparative method was used for the relative quantitation of gene expression, normalised to β -actin according to manufacturer's instructions (ABI PRISM 7700 Sequence Detection System User Bulletin #2)

An efficiency assay was performed for each gene of interest in various tissues prior to real-time RT-PCR experiments. A serial dilution of a random sample was set up in singleplex or multiplex reactions as described above. The slope as calculated according to manufacturer's instructions (ABI PRISM 7700 Sequence Detection System User Bulletin #2) was considered to be valid if the absolute value was < 0.1.

2.5.5. Establishment of RT-PCR Product Identity

The RT-PCR product identities were confirmed using RFLP (as described in section 2.4.5.) and/or direct sequencing (section 2.4.6.). The digested fragments were electrophoresed in 2.5% agarose at 100V for 1hr 20min.

2.6. mRNA Localisation

2.6.1. Preparation of Cryosections

The frozen sections were cut to 6-10 μ m thickness and thaw-mounted on RNase-free silanised slides. The slides were then kept at -70°C until required.

2.6.2. *In Situ* Hybridisation using ^{35}S -riboprobes

The majority of ISH experiments were carried out in the Department of Molecular Genetics, in Western General Hospital in Edinburgh. The last batch of slides were dipped at the Yoshitomi Research Institute of Neuroscience Glasgow (YRING) with help from Dr Susan Cochran.

2.6.2.1. Preparation of Riboprobes

The templates used for generating the RNA probes were obtained by two PCR reactions. The first PCR amplified the gene of interest from several cDNA samples in a 20 μ l PCR reaction containing a final concentration of 1.5mM MgCl₂, 1X buffer, 1X Q-solution, 0.2mM dNTPs, 0.5 μ M of each primer, 0.01u/ μ l of Qiagen HotStar Taq polymerase and 2 μ l of cDNA for *hGSTM* and *rGstm*; or 1 μ l of cDNA for *ACTA2*. The PCR reaction was set at 95°C for 15min followed by 35 cycles of 95°C for 1min, 62°C for 90 sec, 72°C for 2min, followed by 72°C for 10min and finally 60°C for 20min. The PCR products were then cleaned and sequenced to check the specificity of the PCR reaction. The specific cleaned PCR products were pooled.

A second nested PCR was performed on the first cleaned PCR products using primers with integrated binding sites for T3 and T7 RNA polymerase. The nested PCR consists of a 20 μ l PCR reaction containing a final concentration of 1.5mM MgCl₂, 1X buffer, 1X Q-solution, 0.2mM dNTPs, 0.5 μ M of each primer, 0.01u/ μ l of Qiagen HotStar Taq polymerase and 2 μ l of 1/100 dilution of the pooled 1st PCR. The PCR reaction was set at 95°C for 15min followed by 4 cycles of 95°C for 1min, 62°C for 90 sec, 72°C for 2min, followed by 29 cycles of 95°C for 1min, 72°C for 2min, and finally 72°C for 10min and 60°C for 20min. The nested PCR reactions were checked by electrophoresis in 1% agarose gel, cleaned as described in section 2.4.6. and quantified as described in section 2.4.3. If required the samples were concentrated by incubating at 50°C for 10-20min.

Two reaction mixtures were prepared for each probe, containing a final concentration of 0.9X Transcription buffer, 8.9mM of dithiothreitol (freshly prepared), 5.3U of RNasin, 0.3mM rNTPs (ATP, CTP and GTP), 1.85mBeq ³⁵S-UTP, 5U of T3 RNA polymerase for sense probes or T7 RNA polymerase for antisense probes and at least 200ng of PCR template. The reactions were incubated at 37°C for 90min, after which 1 μ l of RNase-free DNase was added to each reaction, mixed gently and incubated at 37°C for 10min. The probes were then purified through Nick™ columns in 400 μ l of 1X TE buffer, pH 8.0. The amount of radioactive-labelled probe was quantified by counting 1 μ l of purified probe in

1ml of scintillation fluid in a beta-counter. The probes were then frozen at -20°C until required. The probes were never kept for more than 1 month before use in experiments.

2.6.2.2. Pre treatment of Tissue

The frozen sections were removed from the freezer and fixed immediately in a fume hood, in freshly prepared cold 4% paraformaldehyde in 0.1M phosphate buffer for 10min, washed in PBS for 5min twice. This was followed by acetylation of positively-charged amino groups in 0.1M triethanolamine containing 0.25% of acetic anhydride (added prior to transfer of slides, mixed by agitating rack in solution) for 10min. The slides were then washed in PBS for 3min and dehydrated in 70% ethanol for 2min, 80% ethanol for 2min and 95% ethanol for 2min. Each solution was changed after 2 racks, except for triethanolamine which was replaced after each rack of slides. The slides were allowed to dry briefly before pre-hybridisation.

2.6.2.3. Prehybridisation

The sections on each slide were covered with 200µl of prehybridisation buffer containing 1:1 (RNase-free deionised formamide: 2X prehybridisation buffer) and any bubbles were removed. The slides were then incubated in a humid box lined with two pieces of Whatman 3M filter paper soaked in box buffer (4X SSC, 50% deionised formamide) at 50°C for 3hr.

2.6.2.4. Hybridisation

Hybridisation solution containing 50% RNase-free deionised formamide and probes of 10^7 counts/ml were prepared for each probe and 2X hybridisation buffer was used to make up to the final volume of the hybridisation mix required for each probe. The hybridisation solution were mixed well and incubated at 75°C for 10min and cooled on ice for 10min. Next, 10µl of 1M dithiothreitol was added for every ml of hybridisation mix, mixed well and placed on ice. The prehybridisation buffer was drained from the slides onto tissue (2-3 slides at a time to avoid excess drying of slides). Lens tissues were used to wipe around the sections to remove excess

prehybridisation buffer (one slide at a time). 200µl of the appropriate hybridisation mix was then added to each slide (remove any bubbles), covering the sections and returned to humid box. Care was taken to ensure each humid box has sufficient box buffer (damp but not soaking). The boxes were sealed with autoclave tape and incubated at 50°C for 14-16hr.

2.6.2.5. RNase Treatment and Washes

The hybridisation mix was drained onto the filter paper in the box and slides were transferred into slide racks and washed in 2X SSC for 5min thrice. The slides were kept in the last wash before the RNase buffer was added. RNase buffer was prepared by adding 3µl of 10µg/ml RNase A per ml of RNase box buffer (0.5M NaCl, 0.01M Tris pH 7.5 and 1mM EDTA). The slides (2-3 at a time) were drained onto tissues and excess SSC was wiped off using lens tissue and 200µl of RNase buffer was added to the slides, covering the sections (remove any bubbles). The slides were then placed in the RNase humid boxes lined with one piece of Whatman 3M filter paper soaked in RNase box buffer. The slides were then incubated at 37°C for 1hr.

The washes were carried out in Omnibaid *in situ* wash system. The slides were drained onto tissues as before, transferred to slide racks and placed into the first wash sleeve, containing 2X SSC, at RT for 1hr. The second wash was carried out in 0.1X SSC at 60°C for 1hr. For the third wash, the sleeve containing 0.1X SSC was pre-heated to 60°C. The slide rack was transferred from the second wash to the third wash, agitated up and down a few times and the third wash sleeve was removed and let stand in ambient rack for 1hr. The slides were then dehydrated by passing through 50% ethanol in ammonium acetate for 2min, 70% ethanol in ammonium acetate for 2min and 95% ethanol in ammonium acetate for 2min. The slides were then air-dried in the fume hood. When dried, the slides were placed against Kodak BioMax MR film in cassette.

2.6.2.6. Slide Dipping

While the experiments were carried out in Edinburgh, the slides were dipped by Dr. Michelle O'Reilly. The nuclear emulsion used was the Kodak NTB2. A Falcon

tube of dH₂O and about 20ml of emulsion (sufficient for ~50 slides) in another Falcon tube were warmed in a 42°C water bath for 20min in the darkroom, alongside an empty slide mailer. The emulsion volume is measured briefly and an equivalent amount of the pre-warmed dH₂O is added to the emulsion and mixed gently by rocking back and forth. The emulsion mixture was then poured into the pre-warmed slide mailer and left for about 20min in the water bath or until the bubbles dispersed. Each slide was then dipped evenly, inserted into alternate slide spaces of a black plastic rack on its side with the tissue side facing up and left to dry for 3-4hr. The slide box was then wrapped in tin foil and black bag, taped up, labelled and placed in the fridge for exposure (~5 times the length of time they were exposed to film for). When the dipped slides were ready for developing, the slide box was removed from the fridge and allowed to come to RT. The slides were brought through troughs of developer for 4min, water for 10sec, fixer for 5min and water for 5min, all solutions at 15°C. The slides were then left to dry for 1hr. Each trough of solutions was used for only two racks.

For experiments where the slides were dipped in Glasgow, the slides were dipped in Ilford K5 nuclear emulsion (under the Kodak 6B/Ilford 905 filter). A Falcon tube of 0.5% glycerol in dH₂O and the dipping chamber were pre-warmed in a 45°C water bath in the darkroom. About 20ml of emulsion was measured into another Falcon tube, the glycerol solution added to the emulsion and mixed well. The tube was then wrapped in aluminium foil and placed back in the water bath for 15-30min. The emulsion mix was then filtered through damp muslin via a filter funnel into the pre-warmed dipping chamber. The slides were dipped evenly and left to dry in slide tray for 2-3hr. The slides were then stored in a slide box with silica gel, sealed, labelled and kept in fridge for exposure. For development, the slide boxes were taken out of the fridge and warmed to RT. The slides were transferred to a slide rack and brought through troughs of developer (D19) for 10min with occasional agitation, dH₂O for 30sec with continuous agitation, fixer (30% sodium thiosulphate made up fresh on day of use) for 5min with occasional agitation and dH₂O for 30min under continuous stream of running water. The developer and the first wash were changed after each rack of slides.

The dipped slides were observed with dark field microscopy using equipment in either laboratory. The exposed films were scanned using Microtek Phantom 336

CX and the pictures obtained and adjusted using Adobe Photoshop 7.0 software. Adjustments include brightness and cropping of scanned pictures.

2.6.2.7. Haematoxylin and Eosin Counter Stain

The dipped and developed slides were counterstained with Mayer's haematoxylin for 1min, washed with dH₂O for 20sec and the nuclei blue colour development was done by bringing the sections through 0.03% ammonium hydroxide for 1min. The slides were washed in dH₂O for 1min, followed by 70% ethanol for 1min and the cytoplasm was then stained with Eosin (solution Y) for 1min. The slides were then brought through 95% ethanol for 1min twice, 100% ethanol twice and HistoClear for 1min twice. The slides were dripped dry and cover slip-mounted with Histomount. The emulsion on the back of the slides was scrapped off with a scalpel blade before analysing the slides microscopically.

The slides were viewed with bright field microscopy on the Olympus BX40 microscope and pictures obtained using the Hitachi HV-C20A 3-CCD colour camera and Image Pro Plus version 5 software. The Adobe Photoshop 7.0 software was used for subsequent adjustments, such as brightness and cropping.

2.7. Protein Expression

2.7.1. Protein Extraction

Protein from tissues were extracted using the Ripa lysis buffer (150mM NaCl, 0.05% Nonidet P-40 (NP-40), 0.5% sodium deoxycholate, 0.1% SDS, 5mM EDTA, 20mM TrisHCl pH 7.5). On the day of use, for every 10 ml of lysis buffer used, a tablet of Roche complete EDTA-free protease inhibitors cocktail was added. The samples were homogenised in the Ripa buffer (900µl of Ripa buffer for up to 0.3g tissue). The homogenates were made up to 1% NP-40 (add 100µl of 10% NP-40 for every 900µl of Ripa buffer), vortexed hard and placed on ice for 5min. The samples were centrifuged at 14,000rpm for 10min at 4°C and the supernatant containing the proteins were transferred to new tubes and kept on ice. 5µl of the supernatant was removed for determining the protein concentration while the rest of the protein samples were stored at -70°C until needed.

2.7.2. Protein Quantitation

The protein concentrations were determined using Pierce BCA (bicinchoninic acid) protein assay kit, according to the manufacturer's instructions. The bovine serum albumin (BSA) standard was diluted in 10X dilution of appropriate buffer while the samples were diluted 10X before quantitation.

2.7.3. Dot blot

1µl of recombinant protein samples diluted in PBS was spotted onto nitrocellulose membrane at the centre of appropriately labelled-grids (drawn with pencil). The protein spots were applied little by little to minimize the area that the solution penetrates. When the spots have dried, the membrane was blocked with 5% milk in PBS for 1hr at RT. The membrane was then incubated with primary antibody diluted in 5% milk/PBS for 1hr at RT. The membrane was then washed three times with PBS for 5min each. The membrane was then incubated with horse radish peroxidase (HRP)-conjugated secondary antibody diluted in 5% milk/PBS for 30min at RT and washed three times with PBS for 5min each. The protein spots were detected with Amersham ECL detection system according to the manufacturer's instructions and the signals developed on Hyperfilm.

2.8. Protein Localisation

The microscope slides were silanised as described in section 2.2.2.1., with the exception that the slides need not be soaked in DEPC-containing water, wrapped in foil and autoclaved.

2.8.1. Immunohistochemistry (IHC)

Total protein concentration of antisera and normal serum were determined as described in section 2.7.2. Dilutions of antisera and normal serum were made to contain equivalent amount of total protein. For antisera and antibodies without recommended dilution for IHC, serial dilutions of both antisera and negative controls were performed to determine the best dilution to use for IHC.

2.8.1.1. Pre-treatment of Sections

Frozen sections were air dried for 1hr at RT, fixed in acetone for 10min, air dried for 10min and washed in PBS for 5min addition of blocking serum. The paraffin sections were deparaffinised and hydrated by bringing the slides through HistoClear for 7min twice, 100% ethanol for 7min, 95% ethanol for 7min, 70% ethanol for 7min and dH₂O for 7min. Endogenous peroxidase activity was first quenched by incubating the slides in 0.3% H₂O₂ in methanol for 30min and washed in dH₂O for 10min twice.

2.8.1.2. Antigen Retrieval

Antigen retrieval was performed when detection of cell surface antigen was required. A glass coplin jar or Pyrex glass beaker containing 0.01M citrate buffer pH 6.0 was heated to 95°C in a waterbath. The slides from previous step were then place into the coplin jar and incubated at 95°C for 15min. The slides were then washed with dH₂O for 10min twice.

2.8.1.3. Primary Antibody

The sections were then blocked with 0.01% normal serum of the animal the secondary antibody was raised in (diluted in PBS) for 1hr, in humidified trays at RT. The blocking serum was drained off and the primary antibody or antisera at appropriate dilutions; or negative control immunoglobulins (Igs) or negative control serum in blocking solution was then added and incubated overnight in humidified trays. The sections were washed in PBS for 5min thrice.

2.8.1.4. Secondary Antibody for IHC

For primary antibodies or antisera raised in either rabbit or mouse, the Vectastain Elite ABC Universal kit was used. Biotinylated secondary antibody in 0.02% blocking serum/PBS was added and incubated for 30min in humidified trays. The sections were washed in PBS for 5min thrice. The Vectastain ABC reagent, pre-incubated for 30min at RT, was added, incubated for 30min in humidified trays and washed in PBS for 5min thrice. For primary antibodies raised in other animals,

appropriate HRP-conjugated secondary antibody in 0.02% blocking serum/PBS was added and incubated for 1hr at RT. The sections were washed in PBS for 5min thrice.

2.8.1.5. Enzymatic Colour Development

The Vector Lab DAB (3,3'-diaminobenzidine) substrate kit was used for colour development. The substrate (DAB) reagent was added, incubated for 5min in humidified trays and washed in dH₂O for 5min. The sections were then counterstained with Harris's modified haematoxylin and washed in running cold tap water for 5min for "blue" staining the nucleus. The sections were finally dehydrated by bringing the slides through 70% ethanol for 10min, 95% ethanol for 10min, 100% ethanol for 10min and HistoClear for 10min twice. The slides were then cover slip-mounted with Histomount.

2.8.2. Multiple Antigen IHC

Sections were pre-treated as described in section 2.8.1.1. and antigen retrieval step was undertaken when required as described in section 2.8.1.2.

2.8.2.1. First Antigen IHC

The sections were blocked, primary antibody/antisera or the negative controls were added as described in section 2.8.1.3. Secondary antibodies were added as described in section 2.8.1.4. The Vector Lab DAB substrate kit was used for colour development. The substrate (DAB-Nickel) reagent was added, incubated for 5min in humidified trays and washed in dH₂O for 5min.

2.8.2.2. Second Antigen IHC

Immediately following section 2.8.2.1, the sections were blocked and primary antibody/antisera or the negative controls added as described in section 2.8.1.3. Secondary antibodies were added as described in section 2.8.1.4. The Vector Lab DAB substrate kit was used for colour development. The substrate (DAB) reagent was added, incubated for 5min in humidified trays and washed in dH₂O for 5min.

The sections were then counterstained, dehydrated and mounted as described in section 2.8.1.5.

The slides were viewed with bright field microscopy on the Olympus BX40 microscope and pictures obtained using the Hitachi HV-C20A 3-CCD colour camera and Image Pro Plus v5 software. The Adobe Photoshop 7.0 Professional software was used for subsequent adjustments, such as brightness and cropping. Changes to brightness settings were made only after the appropriate negative control pictures were added to the figures.

CHAPTER 3: EXPRESSION AND LOCALISATION OF RAT AND HUMAN GLUTATHIONE S-TRANSFERASE μ ISOFORMS

3.1. Introduction

Previously, gene expression profiling combined with congenic strain construction by our group identified *rGstm1* as a positional and functional candidate gene for blood pressure regulation (61;67). In these studies, expression of renal *rGstm1* was significantly reduced in SHRSP compared to WKY and a chromosome 2 congenic strain (SP.WKY_{Gla2c*}). The *rGstm1* gene is one of possibly eight members of a closely related family of genes that lie on an important pathway of endogenous cellular defences against oxidative stress induced damage of macromolecules. Even though renal *rGstm1* was identified as differentially expressed in the microarray expression profiling, not all of the other *rGstm* genes were represented on the microarray chip. As the *rGstm* gene family locus falls within the introgressed chromosome 2 congenic region (as defined on page 16 and *Figure 1.5*), it is possible that the expressions of the other members of the *rGstm* gene family may also be reduced in the SHRSP kidney. However, the contribution of the other members of the *rGstm* gene family is as yet unknown. Vascular oxidative stress is also an important contributory factor in development of essential hypertension. Thus, it is of interest whether *rGstm* gene expression is also reduced in vascular tissues.

SHRSP is an excellent model of human essential hypertension, showing many characteristics in common with the human disease. Therefore identification of defective oxidative stress defence mechanisms in the rat may be directly applicable to human hypertension. Furthermore, new genes identified in animal studies, such as *rGstm1*, provide potentially new targets for pharmacogenomic therapy. At present, there is uncertainty as to which *hGSTM* is the true orthologue of *rGstm1*. While there are possibly eight members in the *rGstm* gene family, there are only five known members in the *hGSTM* gene family. The *rGstm5* and *hGSTM3* are the only known true orthologues leaving the remainder four *hGSTM* genes as homologues of *rGstm1*. It is likely that one of the *hGSTM* isoforms is a true orthologue or plays a similar functional role as *rGstm1*.

The aims of this study were **(1)** to characterise the expression profile of the *rGstm* gene family in the vascular and renal tissues; and **(2)** to characterise the expression profile of the *hGSTM* gene family in vascular tissue in an attempt to identify the true human orthologue of *rGstm1*.

3.2. Materials & Methods

The details for all the equipment, chemicals, reagents and consumables used in this study are listed in *Appendix B*.

3.2.1. Animal Strains

Baseline characteristics were investigated in both male and female, 16-week-old SHRSP, WKY, and SP.WKY_{Gla2c*} congenic strains (n=3-6). Systolic blood pressure was measured using tail-cuff plethysmography within 1 week of sacrifice as described in section 2.1.2. Thoracic aorta, carotid artery, heart, liver, kidney and brain taken from rats sacrificed under deep terminal anaesthesia were snapped frozen in liquid nitrogen and stored at -70°C for further experiments. The effect of age was investigated using RNA samples from thoracic aorta and kidney from 5-week-old and 21-week old male SHRSP and WKY (n=3).

3.2.2. Human Samples

Human saphenous and varicose veins were obtained as described in section 2.3.1. Total RNA from human heart, kidney, testes and liver were obtained commercially from Ambion.

3.2.3. Accession of Gene Sequences

3.2.3.1. Rat Gstm Sequences

The GenBank accession numbers for the *rGstm* transcript used are BC063172.1 (*rGstm1*), NM_177426.1 (*rGstm2*), BC059130.1 (*rGstm3*), NM_020540.1 (*rGstm4*), NM_172038.1 (*rGstm5*), XM_215682.4 (*rGstm6^a*), XM_575012.2 (*rGstm6^b*) and NM_001024304.1 (*rGstm7*). Some additional sequences obtained

from other known mRNA accession numbers, EST database or genomic sequences for the rat *Gstm* isoforms were added to the above accession numbers (Table 3.1), using the Vector NTI Suite 9. A multiple alignment of all 8 *rGstm* transcript sequences are in Appendix C.

3.2.3.2. Human GSTM Sequences

The GenBank accession numbers for the *hGSTM* mRNA transcript used for the design of primers are NM_000561.2 (*hGSTM1*), NM_000848.2 (*hGSTM2*), NM_000849.3 (*hGSTM3*), NM_000850.3 (*hGSTM4*) and NM_000851.2 (*hGSTM5*). For this study, the previously reported alternate transcripts of *hGSTM1* and *hGSTM4* were not explored. A multiple alignment of all 5 *hGSTM* transcript sequences are in Appendix D.

3.2.4. mRNA Expression and Localisation

RNA was extracted, quantified, DNase treated and reverse transcribed as described in section 2.5. Distribution of the *rGstm* family of genes in various tissues from 16-week-old WKY female was detected by RT-PCR. Sequencing of the RT-PCR amplicons was performed to confirm the specificity of the RT-PCR reactions. The mRNA expression levels of *rGstm* gene were assessed by Taqman Gene Expression Assays or Lightcycler (section 2.5.4). The primers and conditions used for detection of *rGstm* gene expression, real-time RT-PCR by Lightcycler and the sequencing of RT-PCR amplicons are as in *Table 3.2*. The primers and conditions used for detection of *hGSTM* gene expression are as in *Table 3.3*. The PCR products for *hGSTM* genes can also be digested with restriction enzymes (REs) for 2hr at the appropriate temperatures to confirm the identity of the RT-PCR sequence.

The primers and conditions used for generating riboprobes used for ISH are as in *Table 3.4*. The smooth muscle alpha actin gene (*ACTA2*) was included as positive control for every experiment. The accession numbers for rat and human *ACTA2* are X06801 and NM_001613, respectively. The primers used for amplifying target region of the rat *Acta2* are the same primers used for the human *ACTA2* gene.

Table 3.1: Accession numbers of sequences used to generate additional sequences for rat *Gstm* mRNA transcripts

Genes	Accession Numbers
<i>rGstm1</i>	Contig of BC063172.1 + M28241.1
<i>rGstm2</i>	Contig of NM_177426.1, J02592.1 + EST sequence CB313254
<i>rGstm3</i>	Contig of BC059130.1, EST sequences CB313357 + CB315738
<i>rGstm4</i>	NM_020540.1 modified*
<i>rGstm5</i>	NM_172038.1 + EST sequence BM422714
<i>rGstm6^a</i>	XM_215682.4
<i>rGstm6^b</i>	XM_575012.2
<i>rGstm7</i>	NM_001024304.1

*Additional sequences for both the 5' and 3' ends of the mRNA transcript sequences were added by compiling a contig of the reference sequence with genomic sequence and then used for design of primers.

Table 3.2: The primers and conditions for detection of rat *Gstm* gene expression

Gene	Primers	Sequences (5' – 3')	AT	PCR size
<i>rGstm1</i>	WM1F WM1R	TCAAACCTGGGCCTGGACTTCC AGTAGAGCTTCATCTTCTCAG	58°C	264bp
<i>rGstm1</i>	rGSTM1-S rGSTM1-AS	CAAATTGAGAAGACCACAGC TTCTCCTCATAGCTTGAGTC	53°C	120bp
<i>rGstm2</i>	WM2F WM2R	TATGAGGACAAGAAGTACAGC TAAACAAGAAAATCCACATAC	52°C	401bp
<i>rGstm3</i>	WM3F WM3R	ATGGTGCTGGCGAGACTTTGC TGGTTCCTCTCAAGAACATCG	59°C	180bp
<i>rGstm4</i>	WM4F WM4R	CCCGCATACATCTCATGATAG GCACTCGGGCTCAAACATACG	59°C	203bp
<i>rGstm4</i>	rM4F2 rM4R2	CTGCGGTATCTTAGTAAACAC CTGCGGTATCTTAGTAAACAC	57°C	621bp
<i>rGstm5</i>	WM5F WM5R	TGAAGAGAAACAGTACACGTG CTTGTTCTTCCCCTCCATAAG	56°C	124bp
<i>rGstm6^a</i>	rMNOV1F2 rMNOV1R2	AGCCCTGAGTTTGAGAAACG TGTCTTCAAATACACAGGGCC	56°C	289bp
<i>rGstm6^b</i>	WMNOV1F WMNOV1R	TTGGGTCACGCCATCCGGCTG CTTCAAGAACTCAGGCTTCCG	62°C	351bp
<i>rGstm7</i>	WMNOVF WMNOVR	ATGCTATTCGATTACTCCTGG GCTGATTGGAGACATCCATAG	56°C	288bp

AT = annealing temperature

Table 3.3: The primers and conditions for detection of human *GSTM* genes expression

Gene	Primer	Sequence (5' – 3')	AT	PCR size	RE
<i>hGSTM1</i>	hGSTM1F hGSTM1R	AGA CCA TGG ACA ACC ATA TGC A AGC ACT TGG GCT CAA ATA TAC G	59°C	218bp	<i>Mwo I</i>
<i>hGSTM2</i>	hGSTM2F hGSTM2R	AGT TTA TGG ACA GCC GTA TGC A AGG CAG CTG GGC TCA AAT ACT T	62°C	217bp	<i>Pst I</i>
<i>hGSTM3</i>	hGSTMF hGSTM3R	ACA AGA TCA CCC AGA GCA A CAG GCT TGT TGC CCC ACT GG	51°C	456bp	<i>Eco RV</i>
<i>hGSTM4</i>	hGSTM4F hGSTM4R	AGG CTA TGG ACG TCT CCA AT ATT ACT TGT TGC CCC AGA CA	55°C	351bp	<i>Msp I</i>
<i>hGSTM5</i>	hGSTMF hGSTM5R	ACA AGA TCA CCC AGA GCA A GCC CTA TTT GCT GTT CCA TGT A	51°C	458bp	<i>Mwo I</i>
<i>hGSMT1*0</i>	P1 P2 P3	CGCCATCTTGCTGCTACATTGCCCCG ATCTTCTCCTCTTCTGTCTC TTCTGGATTGTAGCAGATCA	52°C	<i>GSTM1 & GSTM4</i> : 230bp (P1 + P2) <i>GSTM1</i> : 157bp (P1 + P3)	

AT = annealing temperature

Table 3.4: Primers used for generating probe templates for *in situ* hybridisation

Gene	Primers	Sequences (5' -- 3')	AT	PCR size	Target size
<i>ACTA2</i>	hACTA2-IS-F1	CACCAACTGGGACGACATGG	62°C 90 min	392bp	
	hACTA2-IS-R1	CACGCTCAGCAGTAGTAACG			
	hACTA2-IS-F2	<u>TCTAGATTAACCCTCACTAAAGGGACCCTGCTCACGGAGG</u>	55°C 90 min	310bp	
	hACTA2-IS-R2	<u>GGATCCTAATACGACTCACTATAGGGAGGTAGTCAGTGAGATCTC</u>			
<i>hGSTM4</i>	hM4IS-F1	GGACCTTGCTCCCTGAACACTC	62°C 90 min	250bp	
	hM4IS-R1	CCTCAGCTGGGCTGAACTGC			
	hM4IS-F2	<u>TCTAGATTAACCCTCACTAAAGGGATGGATCTTACTCCTTCCAGC</u>	55°C 90 min	251bp	
	hM4IS-R2	<u>GGATCCTAATACGACTCACTATAGGGCTGCGACCTCCTCTGG</u>			
<i>rGstm1</i>	rM1IS-F1	TTTGTCCGGCCCACGTTTCTCTG	62°C 90 min	761bp	
	rM1IS-R1	CAAGGGCCTACTTGTTACTCCATTGG			
	rM1IS-F2	<u>TCTAGATTAACCCTCACTAAAGGGATTTGTCCGGCCCACG</u>	55°C 90 min	130bp	
	rM1IS-R2	<u>GGATCCTAATACGACTCACTATAGGGCGCTGTGGTCTTCTCAATTTG</u>			

The underlined sequences are the binding site for T3 and T7 RNA polymerases.

3.2.5. Protein Expression and Localisation

The antisera used to assess the protein expression and localisation of the rGstm1, rGstm2, rGstm5 and hGSTM3 by immunohistochemistry were gifts from Prof. John D. Hayes. The hGSTM4-specific antiserum was a gift from Prof. Irving Listowsky. The hGSTM1-specific monoclonal antibody was from Abnova (Taiwan), hGSTM1/2 polyclonal antibody was from Abcam. Assessment of the localisation of rGstm proteins were analysed by Dr. Barbara Young, a consultant histopathologist at the Western Infirmary Glasgow.

3.2.6. *hGSTM1*0* Genotyping of Human Vascular Tissues

Due to high homology between hGSTM1 and hGSTM2, there are no specific antibodies available for these two isoenzymes. Specific detection of hGSTM2 can be carried out by IHC on samples from *hGSTM1*0* patients therefore all human vascular samples were genotyped for the *hGSTM1*0* allele. DNA was extracted from approximately 0.5cm section of each biological sample as described in section 2.4.1, purified as described in section 2.4.2 and quantified as described in section 2.4.3. The samples were then diluted to 5ng/ μ l working concentration.

A 20 μ l PCR reaction was set up containing a final concentration of 1.5mM MgCl₂, 1X buffer, 0.2mM dNTPs, 0.5 μ M of primer P1, 0.25 μ M of primers P2 and P3, 0.01u/ μ l of Qiagen HotStar Taq polymerase and 25ng of DNA. The PCR reaction was set at 95°C for 15min followed by 35 cycles of 95°C for 1min, appropriate annealing temperature for 1min, 72°C for 1min and finally 60°C for 30min. The primers used for detection of *hGSTM1*0* genotype are as in *Table 3.3*.

3.2.7. Statistical Analysis

Results are shown as mean \pm SEM. 2-sample t-test was used to test for significance in expression level between the males and females of each strain. One-way ANOVA with Tukey's comparison was used to test for significance between the SHRSP and WKY or SP.WKY_{Gla2c*} (2c*) strain, in either males or females only. For the effect of age on *rGstm* gene expression, 2-sample t-test was used to test for significance between WKY and SHRSP at each time points.

3.3. Results

3.3.1. Systolic Blood Pressure of the Rat Strains

The SBP of SHRSP males was significantly higher than WKY males ($p = 0.006$; confidence interval (CI) = $-44.12, -7.52$) and congenic SP.WKY_{Gla2c*} males (CI = $8.64, 49.56$) (*Figure 3.1*). The SBP of SHRSP females was non-significantly higher than WKY females ($p = 0.200$; CI = $8.52, -41.69$). There was no difference in SBP between SHRSP and SP.WKY_{Gla2c*} females ($p = 0.200$; CI = $27.57, -25.09$). There was also a gender-specific difference in WKY ($p = 0.007$; CI = $8.23, 38.30$) and SHRSP ($p = 0.016$; CI = $8.44, 56.56$) but not SP.WKY_{Gla2c*} ($p = 0.631$; CI = $-18.66, 27.94$)

3.3.2. Characterisation of Rat Gstm

3.3.2.1. Rat Gstm Sequences

Multiple alignment of the mRNA transcript sequences from the databases NCBI and Ensembl shows that this family of genes are highly homologous both in mRNA and peptide sequences (*Appendix C*). The *rGstm1* gene shares between 71% to 89% homology for coding sequences and 64% to 82% for peptide sequences with other members of *rGstm* family (*Table 3.5*). The least homologous isoform is *rGstm5* ranging from 70% to 74% for coding sequences and 59% to 68% for peptide sequences. The untranslated region (UTR) of the mRNA transcripts at both 5' and 3' ends of the genes also share high homology.

3.3.2.2. Expression of Rat Gstm Isoforms in Various Tissues

Semi-quantitation of *rGstm* genes in various tissues, from 16-week-old WKY female rats (due to lack of male), based on intensities of RT-PCR product bands are given in *Table 3.6*. Expression of *rGstm1* gene was highest in liver and brain, followed by kidney, heart and least in thoracic aorta. The *rGstm2* gene was expressed most in liver followed by kidney, and least in heart and thoracic aorta. The *rGstm3* gene was expressed highly in the brain, to a lesser extent in thoracic aorta and little in heart, kidney and liver. Expression of *rGstm5* was highest in

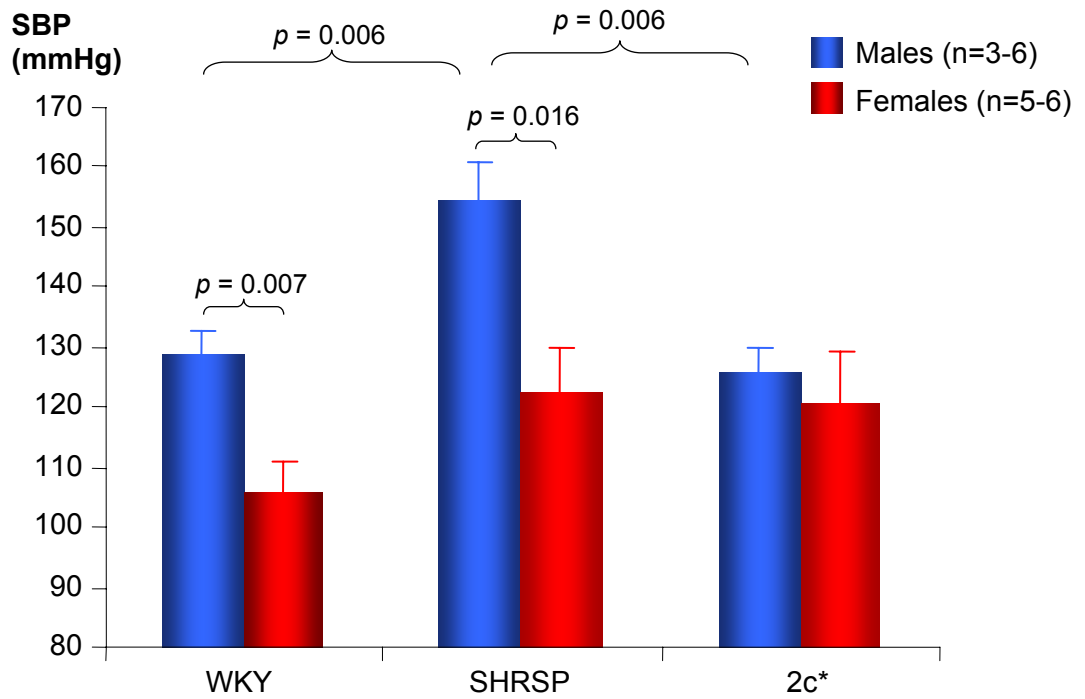


Figure 3.1: Systolic blood pressure by tail cuff plethysmography

Systolic blood pressures (SBP) from 16-week old rats were measured using tail cuff plethysmography. 2c* = SP.WKY_{Gla}2c*

Table 3.5: (A) Percentage homology in coding sequences between *rGstm* isoforms

	<i>rGstm1</i>	<i>rGstm2</i>	<i>rGstm3</i>	<i>rGstm4</i>	<i>rGstm5</i>	<i>rGstm6^a</i>	<i>rGstm6^b</i>	<i>rGstm7</i>
<i>rGstm1</i>								
<i>rGstm2</i>	84%							
<i>rGstm3</i>	85%	85%						
<i>rGstm4</i>	89%	84%	82%					
<i>rGstm5</i>	71%	72%	74%	70%				
<i>rGstm6^a</i>	83%	88%	83%	83%	72%			
<i>rGstm6^b</i>	86%	86%	83%	86%	74%	84%		
<i>rGstm7</i>	82%	84%	83%	80%	74%	83%	83%	

(B) Percentage homology in protein sequences between *rGstm* isoforms

	<i>rGstm1</i>	<i>rGstm2</i>	<i>rGstm3</i>	<i>rGstm4</i>	<i>rGstm5</i>	<i>rGstm6^a</i>	<i>rGstm6^b</i>	<i>rGstm7</i>
<i>rGstm1</i>								
<i>rGstm2</i>	78%							
<i>rGstm3</i>	77%	80%						
<i>rGstm4</i>	82%	76%	76%					
<i>rGstm5</i>	64%	67%	68%	59%				
<i>rGstm6^a</i>	75%	83%	77%	75%	66%			
<i>rGstm6^b</i>	75%	79%	76%	75%	66%	80%		
<i>rGstm7</i>	74%	80%	81%	71%	68%	78%	80%	

Table 3.6: Expression of *rGstm* isoforms in various tissues

Gene	Thoracic A.	Brain	Heart	Kidney	Liver
<i>rGstm1</i>	++	+++++	+++	++++	+++++
<i>rGstm2</i>	+	–	+	++	+++
<i>rGstm3</i>	++	+++	+	+	+
<i>rGstm4</i>	–	–	–	–	–
<i>rGstm5</i>	++	+++	++	+++	+
<i>rGstm6^a</i>	–	–	–	–	–
<i>rGstm6^b</i>	–	++	–	–	–
<i>rGstm7</i>	++	++++	+	+++	+++

The *rGstm* genes are expressed at varying levels in different tissues from WKY female rat, with (+) being present to high levels (++++), and the scale being compared across tissue for each gene. The grading of the expression was based on the intensities of the RT-PCR product band. (–) denotes that the gene was not expressed in the tissue in question.

Table 3.7: Gene expression levels of *rGstm* isoforms in selected tissues

Gene	Aorta	Kidney	Liver
<i>rGstm1</i>	1.000 ± 0.333	6.548 ± 0.416	891.509 ± 375.360
<i>rGstm2</i>	1.000 ± 0.164	1.731 ± 0.162	160.975 ± 25.260
<i>rGstm3</i>	1.000 ± 0.081	0.343 ± 0.049	2.529 ± 0.521
<i>rGstm5</i>	1.000 ± 0.183	0.256 ± 0.016	0.142 ± 0.040
<i>rGstm7</i>	1.000 ± 0.070	1.008 ± 0.026	4.063 ± 0.826

Each gene is expressed as fold-change, relative to vascular expression levels for consistency.

heart and kidney, followed by thoracic aorta and heart, least in liver. The *rGstm6^b* gene expression was detected only in the brain. Expression of *rGstm7* gene was highest in brain, slightly less in kidney and liver, to a lesser extent in thoracic aorta and least in heart. Expression of *rGstm4* and *rGstm6^a* was not detected in any of the tissues examined.

Real-time relative quantitation of the *rGstm* genes in thoracic aorta, kidney and liver from 16-week-old WKY male rats are shown in *Table 3.7*. Liver expressed up to nearly 900-fold more *rGstm1* while kidney expressed 6-7 fold more than aorta. Liver expressed nearly 200-fold more *rGstm2*, whereas kidney expressed nearly 2-fold more than aorta. Liver expressed 2-3 fold more *rGstm3* than aorta. In contrast, kidney expressed only 0.343-fold the *rGstm3* expression in aorta. Expression of *rGstm5* was highest in aorta, with kidney expressing only 0.256-fold and liver expressing only 0.142-fold the level of expression in aorta. Aorta and kidney expressed equivalent levels of *rGstm7* but liver expressed approximately 4-fold higher.

3.3.2.3. Vascular Localisation and Expression of Rat *Gstm* Isoforms

Due to lack of *rGstm* isoform-specific antibodies, localisation of *rGstm* subunits were available only for *rGstm1*, *rGstm2* and *rGstm5*. Localisation of *rGstm1*, *rGstm2* and *rGstm5* in carotid arteries from 16-week-old rats were done by IHC using isoform-specific antisera. Expression of *rGstm1* protein by IHC was detected in all of the vascular cell types (*Figure 3.2A*). Expression of *rGstm2* protein was localised to the endothelium (*Figure 3.2C*) while *rGstm5* expression was detected only in the VSMCs (*Figure 3.2E*). *Figures 3.2 (B), (D) and (F)* were the respective negative control IHC.

Real-time absolute quantitation of *rGstm* isoforms measured in 16-week-old WKY male rats were expressed as a percentage of β -actin expression level. There was no predominant isoform in aorta, with *rGstm1* (0.554% \pm 0.062%), *rGstm2* (0.690% \pm 0.023%), *rGstm3* (0.501% \pm 0.057%) and *rGstm5* (0.763% \pm 0.041%) expressed at similar levels but the least expressed isoform was *rGstm7* (0.080% \pm 0.006%).

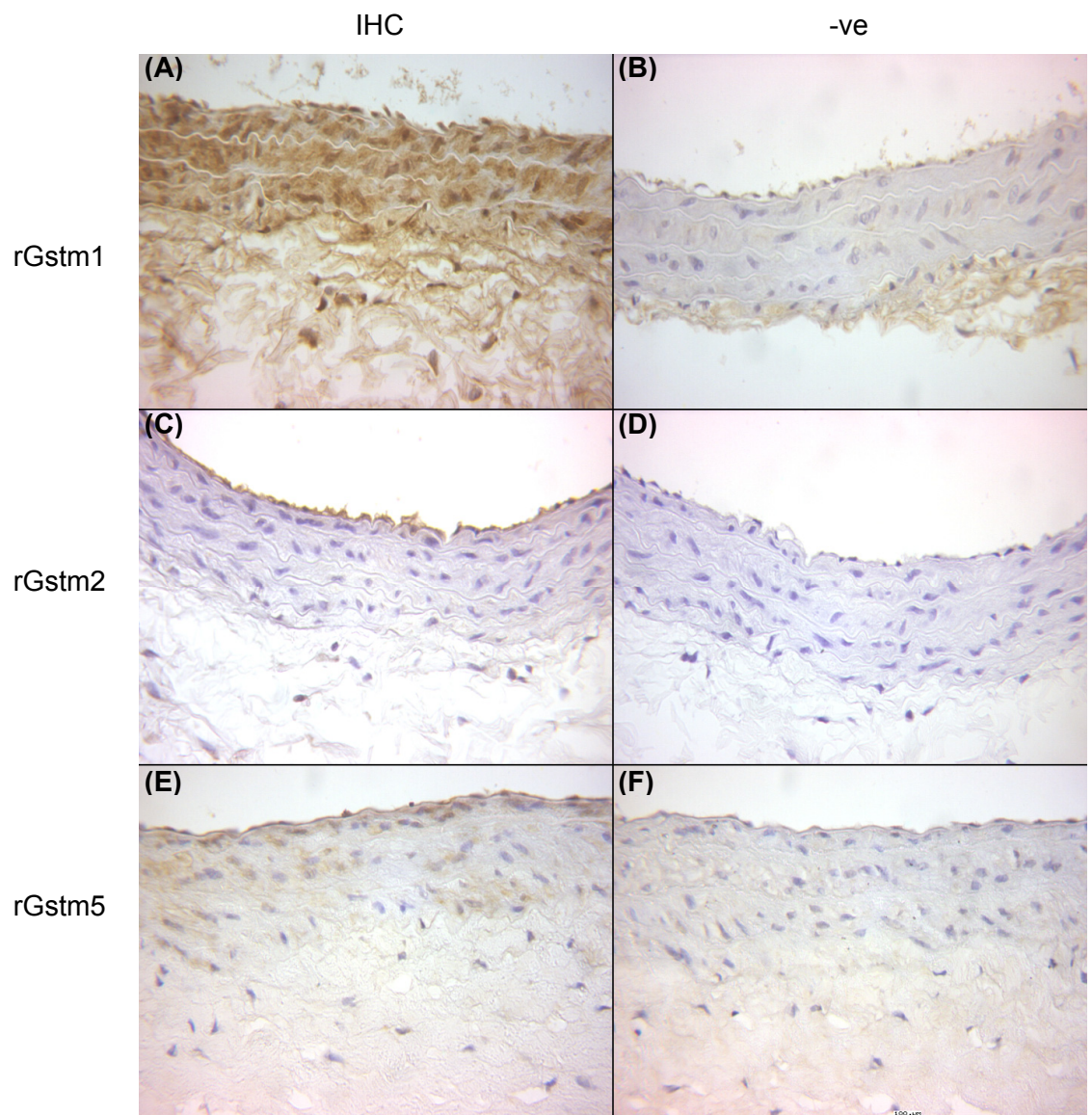


Figure 3.2: Localisation of rGstm isoforms in vasculature

(A), (C) and (E) represent the localisation of rGstm1, rGstm2 and rGstm5 in carotid artery from WKY male rat by immunohistochemistry, respectively. (B), (D) and (F) are the appropriate negative (-ve) controls. Magnification = x400.

Real-time relative quantitation of *rGstm* mRNA expression levels in 16-week-old rats, relative to *rGstm7* in SHRSP male as fold-changes are shown in *Figure 3.3*. There were no significant differences in *rGstm1* expression between the SHRSP and WKY or SP.WKY_{Gla2c*} strains in either male or female rats. However, there was a trend towards reduced *rGstm1* in SHRSP compared to WKY or SP.WKY_{Gla2c*} in both male and female rats. IHC of *rGstm1* in carotid arteries from WKY, SHRSP and SP.WKY_{Gla2c*} male rats showed reduced *rGstm1* expression in SHRSP compared to WKY and congenic SP.WKY_{Gla2c*} strains (*Figure 3.4*). There was no significant difference in *rGstm1* mRNA expression between male and female rats in all three strains (*Figure 3.3*).

There were no significant differences in *rGstm2* mRNA expression between the SHRSP and WKY or SP.WKY_{Gla2c*} strains in either male or female rats (*Figure 3.3*). There was a trend towards reduced *rGstm2* in SHRSP compared to WKY and SP.WKY_{Gla2c*}, in males only. There was no significant difference in *rGstm2* expression between male and female rats in all three strains. IHC of *rGstm2* in carotid arteries from WKY, SHRSP and SP.WKY_{Gla2c*} male rats showed reduced *rGstm2* expression in SHRSP compared to WKY and congenic SP.WKY_{Gla2c*} strains across the vessel wall (*Figure 3.5*). However, *rGstm2* was shown to be localised to endothelium (*Figure 3.2*). In order to investigate the specificity of the anti-*rGstm2* serum, a dot blot was performed on recombinant *rGstm1* and *rGstm2* proteins. The antiserum detected both *rGstm1* and *rGstm2* recombinant proteins.

SHRSP male rats expressed non-significantly lower *rGstm3* than WKY male ($p = 0.414$; CI = $-0.46, 1.04$) and significantly lower *rGstm3* than SP.WKY_{Gla2c*} males ($p = 0.018$; CI = $-2.10, -0.29$) (*Figure 3.3*). The *rGstm3* expression in SHRSP female rats was significantly higher than WKY females ($p = 0.003$; CI = $-2.51, -0.60$) but not the SP.WKY_{Gla2c*} female rats ($p = 0.998$; CI = $-1.01, 1.01$). Expression of *rGstm3* gene showed gender-specific difference in the SHRSP rats ($p = 0.005$; CI = $0.71, 2.59$) but not in the WKY ($p = 0.359$; CI = $-0.68, 0.28$) or SP.WKY_{Gla2c*} ($p = 0.293$; CI = $-0.68, 1.59$).

There was no significant difference in *rGstm5* expression levels between strains (*Figure 3.3*). In males only, there was a trend towards lower *rGstm5* expression in the SHRSP compared to WKY or SP.WKY_{Gla2c*}. There was no significant

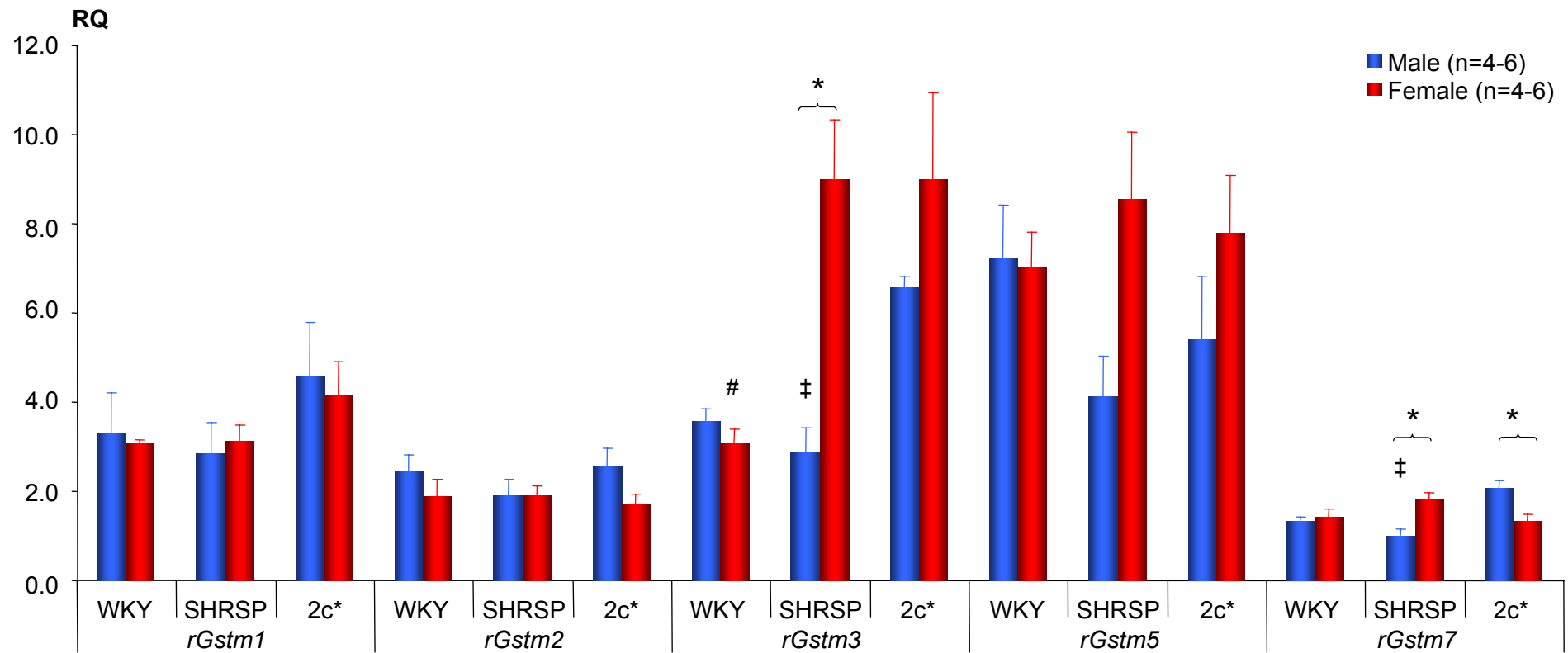


Figure 3.3: Vascular expression levels of *rGstm* isoforms in male and female rats

RQ = relative quantitation; 2c* = SP.WKY_{Gla}2c*;

‡ SHRSP males vs. 2c* males, $p < 0.02$; # SHRSP females vs. WKY females, $p = 0.003$; * male vs. female, $p < 0.05$

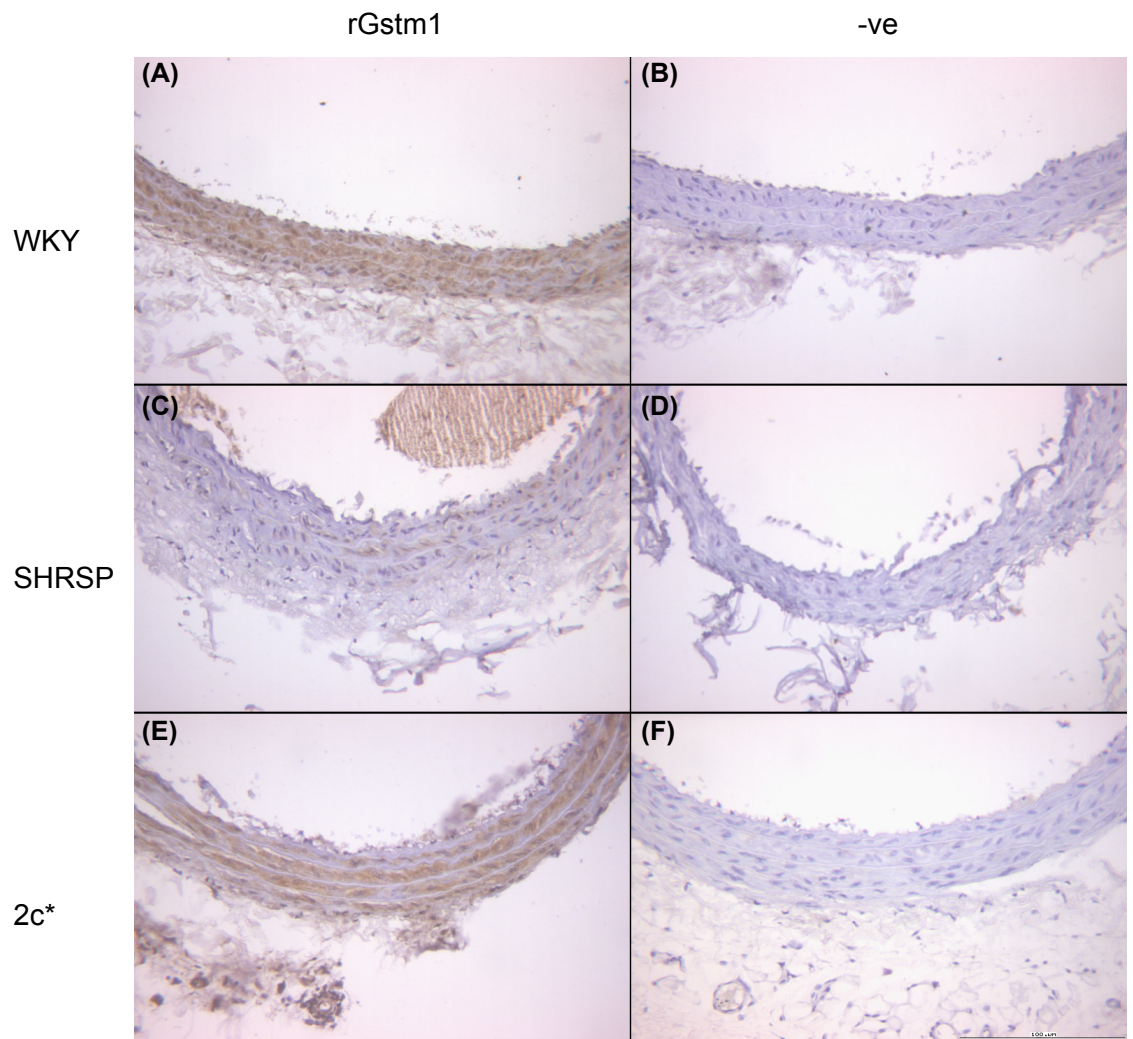


Figure 3.4: IHC of rGstm1 in male WKY, SHRSP and SP.WKY_{Gla}2c* carotid arteries
 IHC of rGstm1 protein in carotid arteries from WKY, SHRSP and SP.WKY_{Gla}2c* (2c*) male rats. Magnification = x200; -ve = negative controls.

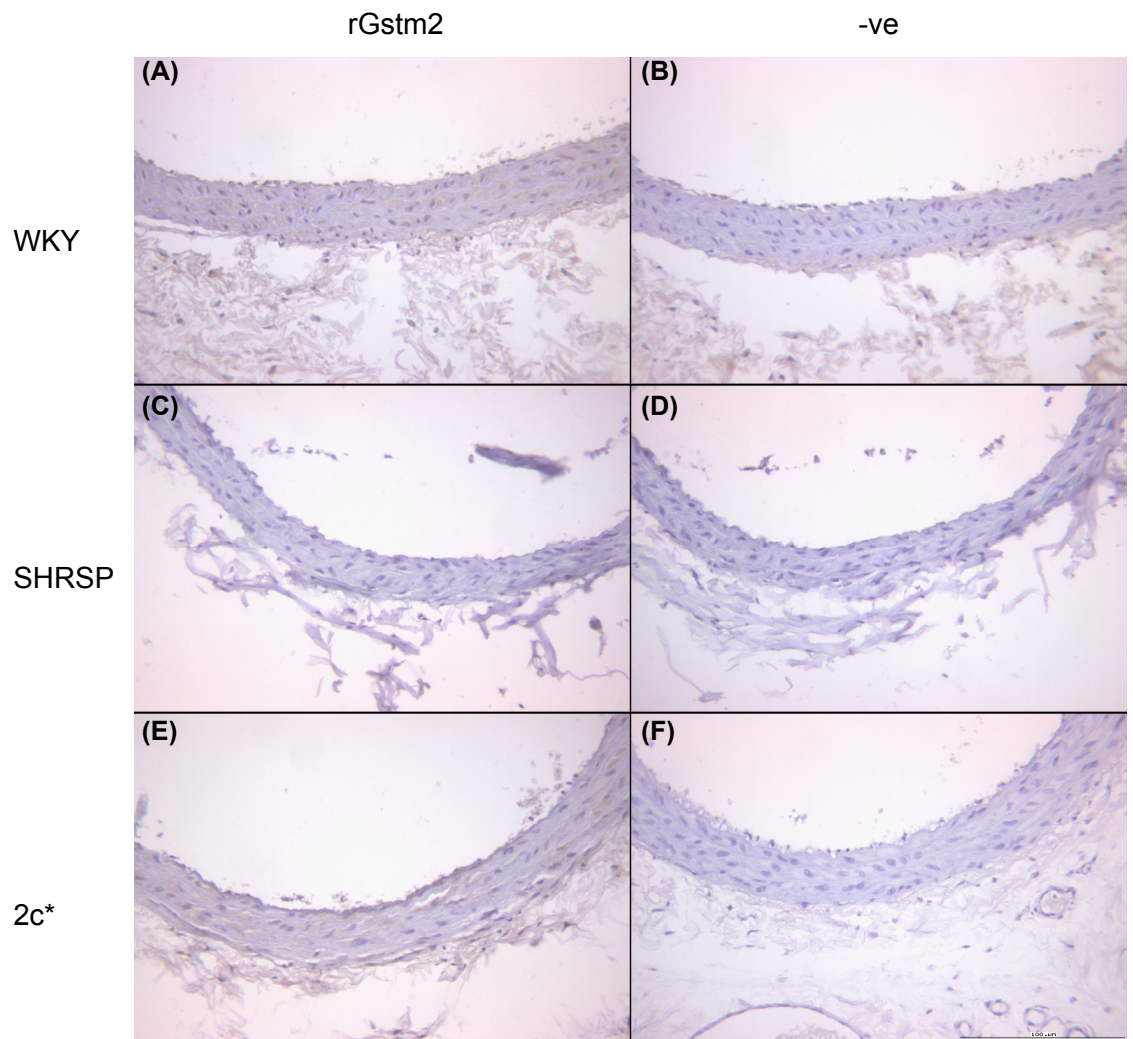


Figure 3.5: IHC of rGstm2 in male WKY, SHRSP and SP.WKY_{Gla}2c* carotid arteries
 IHC of rGstm1 protein in carotid arteries from WKY, SHRSP and SP.WKY_{Gla}2c* (2c*) male rats. Magnification = x200; -ve = negative controls.

difference in *rGstm5* expression levels between males and females, though there was a trend towards lower expression in male compared to female rats.

The slightly lower *rGstm7* expression level in SHRSP males compared to WKY males was not significant ($p = 0.148$; CI = $-0.16, 0.99$) but reached statistical significance when compared to SP.WKY_{Gla2c*} male ($p = 0.008$; CI = $-1.67, -0.40$) (*Figure 3.3*). This strain effect was not observed in the female rats. There were gender-specific differences in *rGstm7* expression levels between SHRSP ($p = 0.02$; CI = $0.20, 1.52$) and SP.WKY_{Gla2c*} ($p = 0.043$; CI = $-1.22, -0.03$) rats but not the WKY rats.

The effect of age on real-time relative quantitation of vascular *rGstm* expression levels in 5-week-old, 16-week-old and 20-week-old rats, relative to 5-week-old SHRSP males following normalisation to β -actin expression for each gene are shown in *Figure 3.6*. The expression of *rGstm1*, *rGstm2*, *rGstm5* increased gradually with age, while *rGstm7* increased after 16 weeks of age in both SHRSP and WKY rats. Expression of *rGstm3* gene increased gradually in WKY rats but increased more sharply after 16 weeks of age in SHRSP, resulting in significantly higher *rGstm3* expression in SHRSP rats at 20 weeks of age ($p = 0.003$; CI = $0.43, 1.52$).

3.3.2.4. Renal Localisation and Expression of Rat Gstm Isoforms

Previous work from our laboratory demonstrated co-localisation of rGstm1 protein with aquaporin-2, which localised specifically to the principal cells of collecting ducts (67). In this study, multiple antigen IHC for aquaporin-2 and rGstm1 on kidney sections from WKY rat co-localised rGstm1 expression to the principal cells of collecting ducts (*Figure 3.7*). In addition, rGstm1 expression was also detected in the distal convoluted epithelial cells (personal communications with Dr. Barbara Young). The proximal convoluted tubules (PCTs) can be identified in the renal cortex by their lining of a single layer of cuboidal epithelial cells with a prominent brush border composed of microvilli [(222) & personal communications with Dr. Barbara Young]. The cytoplasm of these cells is eosinophilic and granular due to their high content of mitochondria. In contrast, the distal convoluted tubules (DCTs) are lined by cuboidal epithelial cells of fewer microvilli and therefore no

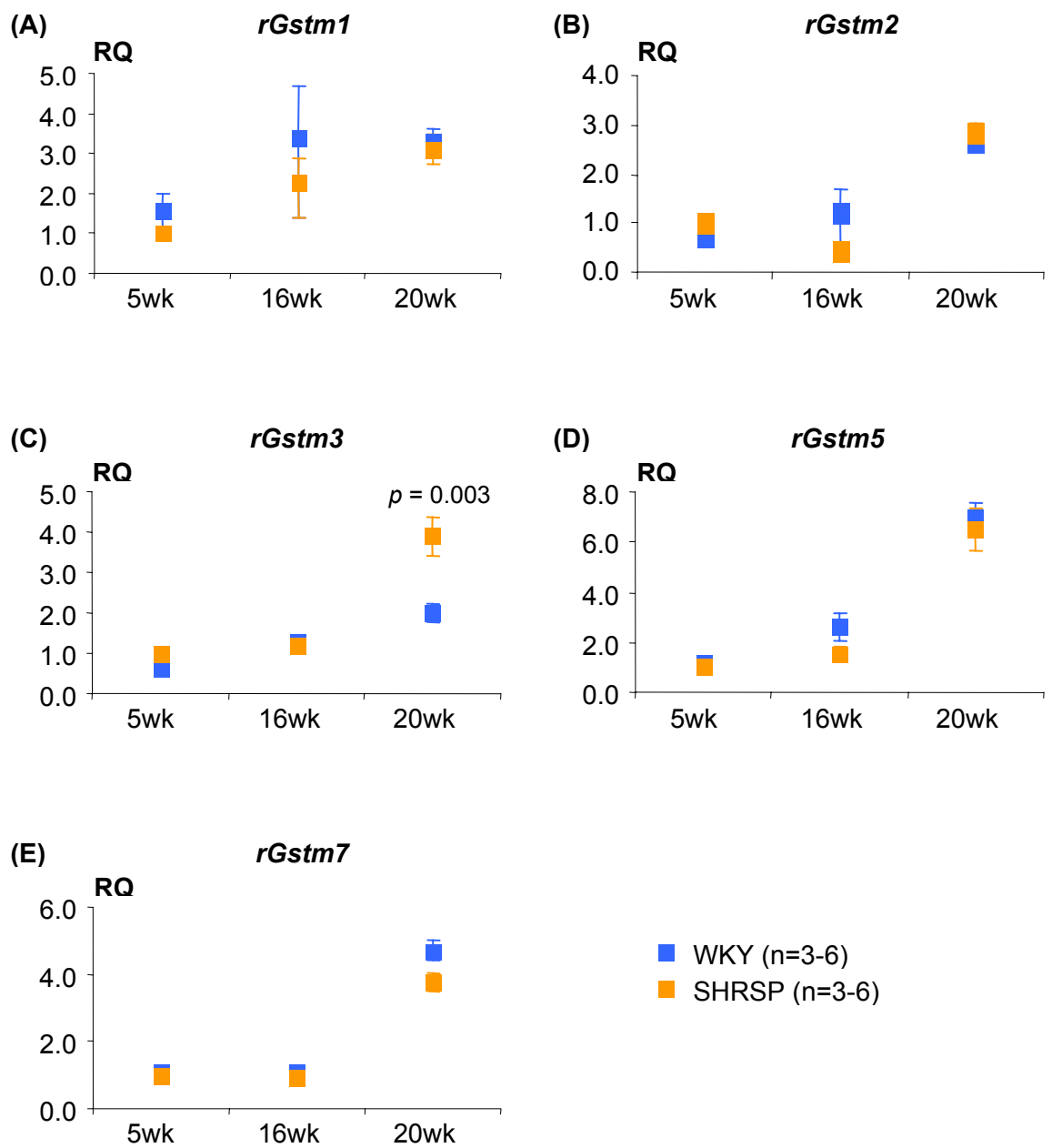


Figure 3.6: Effect of age on expression levels of vascular *rGstm* isoforms

The values are represented by mean \pm SEM. Quantitation of each gene is expressed as fold-change relative to 5-week-old SHRSP expression. *p*-value denotes significance between WKY and SHRSP at time point indicated.

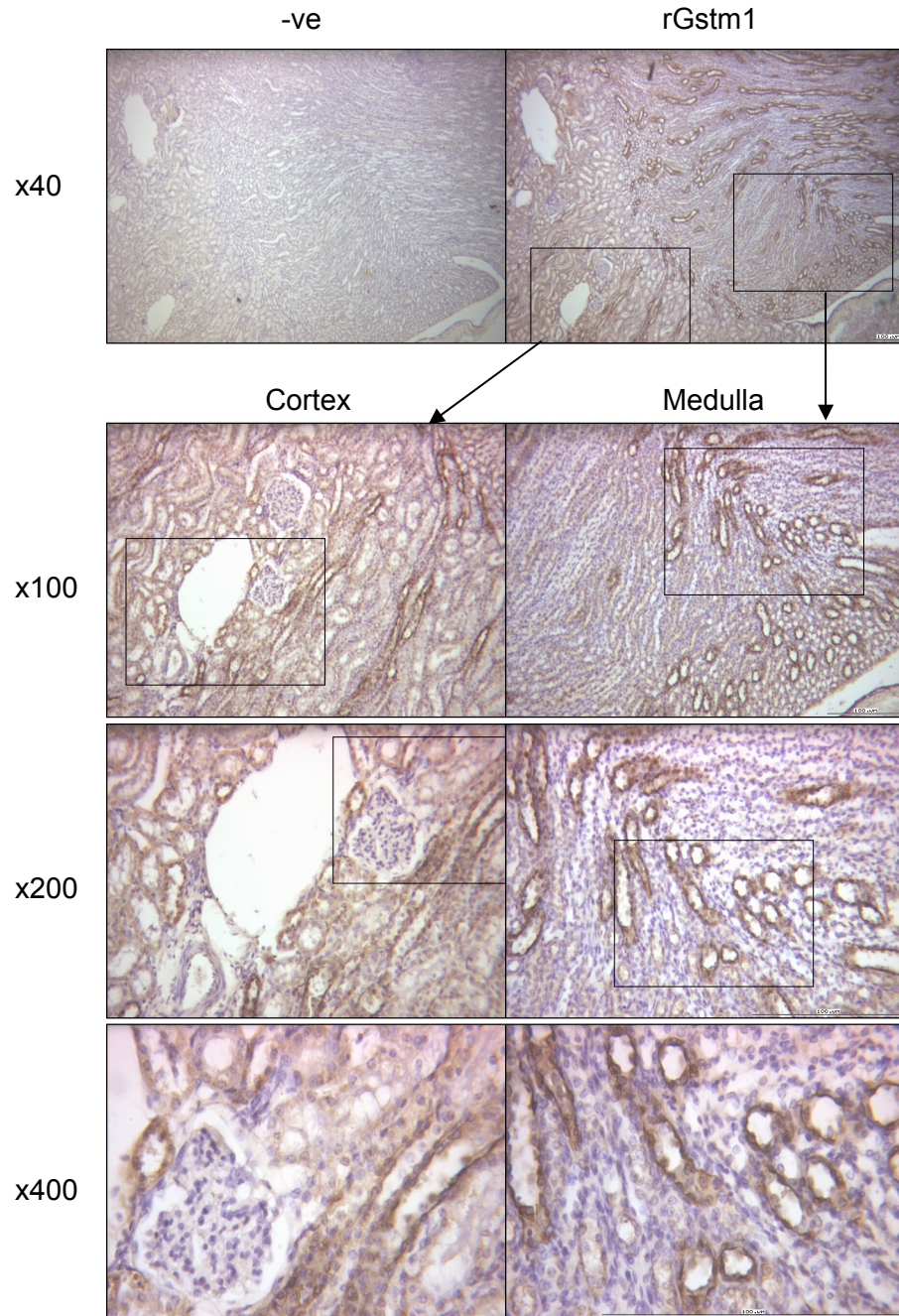


Figure 3.7: Localisation of rGstm1 in kidney

Aquaporin-2 stains grey-black, rGstm1 stains brown and nucleus counterstains blue. The sections were analysed at magnification as indicated on the left of the pictures. The rectangle in the positively-stained pictures were magnified and shown immediately below. -ve = negative controls.

brush border which leaves the lumen more open. There are also fewer mitochondria so that the cytoplasm is less eosinophilic. The thick ascending limb, which makes up the majority of thick loop of Henle in the renal medulla can be identified as simple cuboidal cells, often round in cross-section. The thick loop of Henle can be differentiated from the larger diameter of collecting tubules and collecting ducts. Similarly, expression of rGstm2 and rGstm5 protein co-localised with aquaporin-2, to the principal cells of collecting ducts (*Figure 3.8* and *3.9*, respectively). In addition, rGstm2 expression was detected in DCTs and rGstm5 expression was detected in PCTs and DCTs (personal communications with Dr. Barbara Young).

Real-time absolute quantitation of *rGstm* isoforms in 16-week-old WKY male rats, expressed as a percentage of β -actin expression level, showed that the predominant isoform in kidney was *rGstm1* ($1.468\% \pm 0.034\%$) and the least expressed isoform was *rGstm7* ($0.007\% \pm 0.001\%$). The *rGstm2* ($0.199\% \pm 0.015\%$), *rGstm3* ($0.034\% \pm 0.004\%$) and *rGstm5* ($0.024\% \pm 0.002\%$) isoforms were expressed at approximately one-tenth the expression level of *rGstm1*.

Real-time relative quantitation of *rGstm* expression levels in 16-week-old rats, relative to *rGstm7* in SHRSP male as fold-changes are shown in *Figure 3.10*. Expression of *rGstm1* gene in SHRSP was significantly reduced compared to WKY and SP.WKY_{Gla2c*}, in both male ($p \leq 0.008$; CI = 2.04, 3.64 and -3.78 , -2.17 , respectively) and female rats ($p < 0.001$; CI = 1.78, 2.69 and -2.72 , -1.77 , respectively). In addition, there was also a significantly lower *rGstm1* gene expression in the WKY females ($p = 0.002$; CI = -1.05 , -0.36) than WKY males. There was also a trend towards lower *rGstm1* expression in the SP.WKY_{Gla2c*} females ($p = 0.057$; CI = -1.73 , 0.06) compared to SP.WKY_{Gla2c*} males. This gender-specific effect was not observed in the SHRSP rats. There was no significant difference in *rGstm1* expression between SHRSP and WKY males or SP.WKY_{Gla2c*} males; or SHRSP and WKY females. IHC of whole kidney sections from WKY, SHRSP and SP.WKY_{Gla2c*} showed reduced rGstm1 expression in SHRSP compared to WKY and congenic SP.WKY_{Gla2c*} strains (*Figure 3.11A*). The reduced rGstm1 expression was observed in cortex, outer and inner medulla (*Figure 3.11B*), especially in the principal cells of collecting ducts.

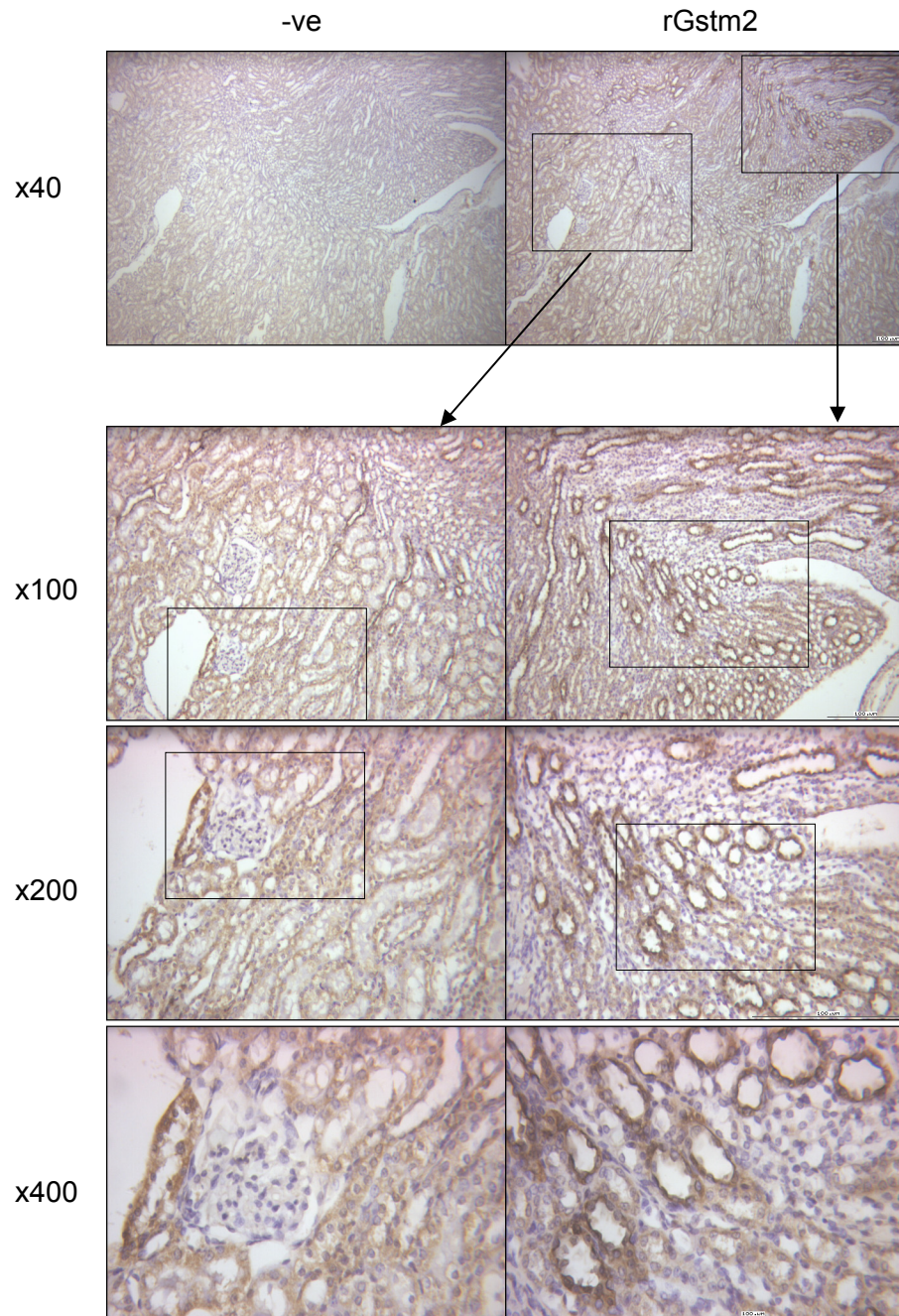


Figure 3.8: Localisation of rGstm2 in kidney

Localisation of rGstm2 in kidney. Aquaporin-2 stains grey-black, rGstm2 stains brown and nucleus counterstains blue. The sections were analysed at magnification as indicated on the left of the pictures. The rectangle in the positively-stained pictures were magnified and shown immediately below. –ve = negative controls.

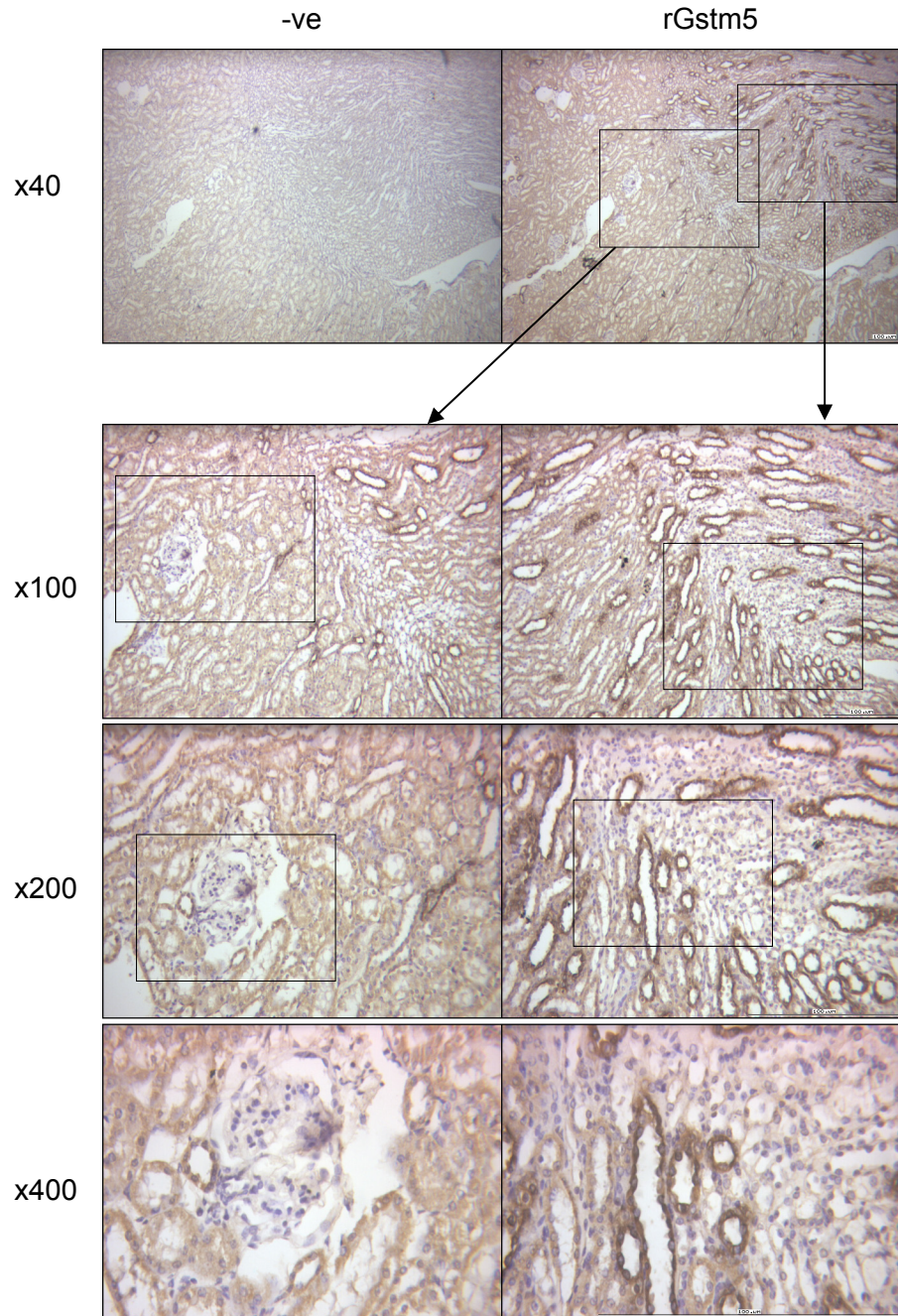


Figure 3.9: Localisation of rGstm5 in kidney

Localisation of rGstm5 in kidney. Aquaporin-2 stains grey-black, rGstm5 stains brown and nucleus counterstains blue. The sections were analysed at magnification as indicated on the left of the pictures. The rectangle in the positively-stained pictures were magnified and shown immediately below. -ve = negative controls.

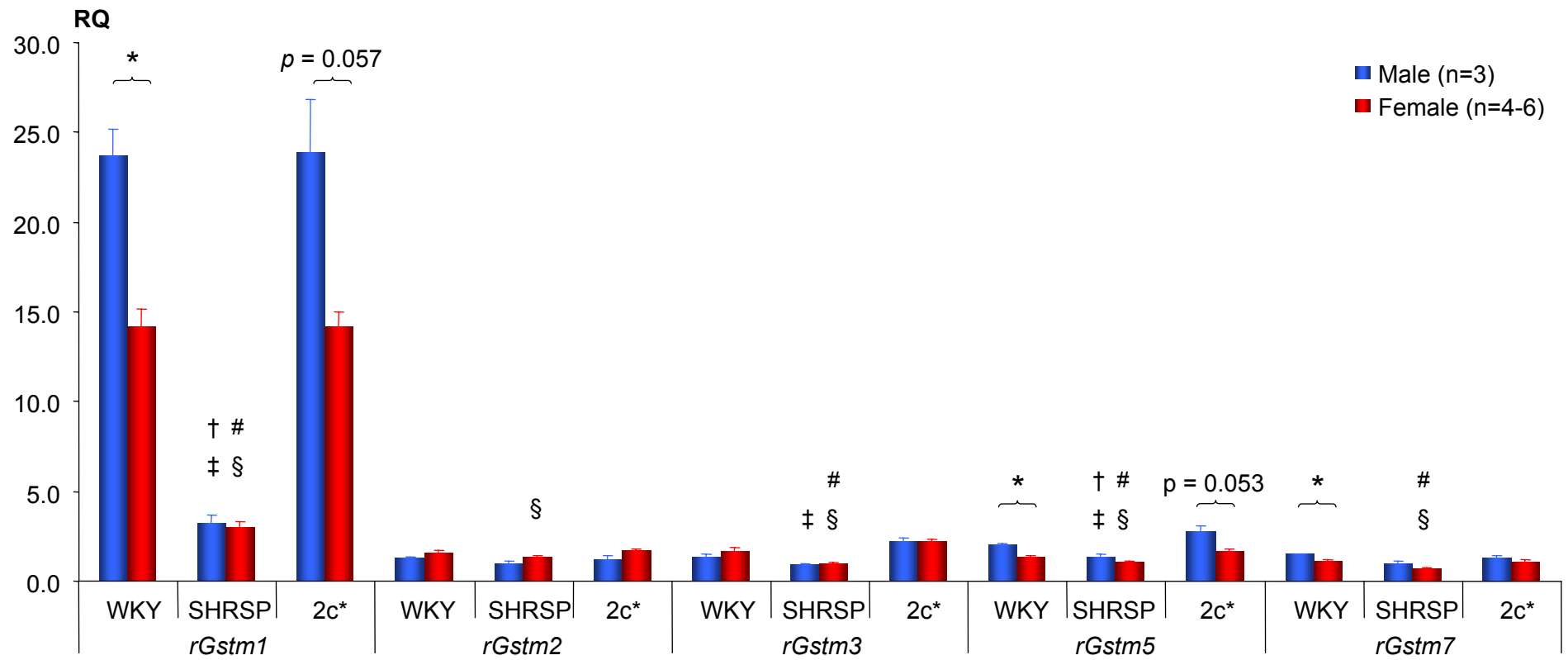


Figure 3.10: Renal expression levels of *rGstm* isoforms in male and female rats

RQ = relative quantitation; 2c* = SP.WKY_{Gla}2c*;

† SHRSP male vs. WKY male, $p < 0.05$; ‡ SHRSP male vs. 2c* male, $p < 0.05$; # SHRSP female vs. WKY female, $p < 0.05$; § SHRSP female vs. 2c* female, $p < 0.05$; * male vs. female, $p < 0.05$

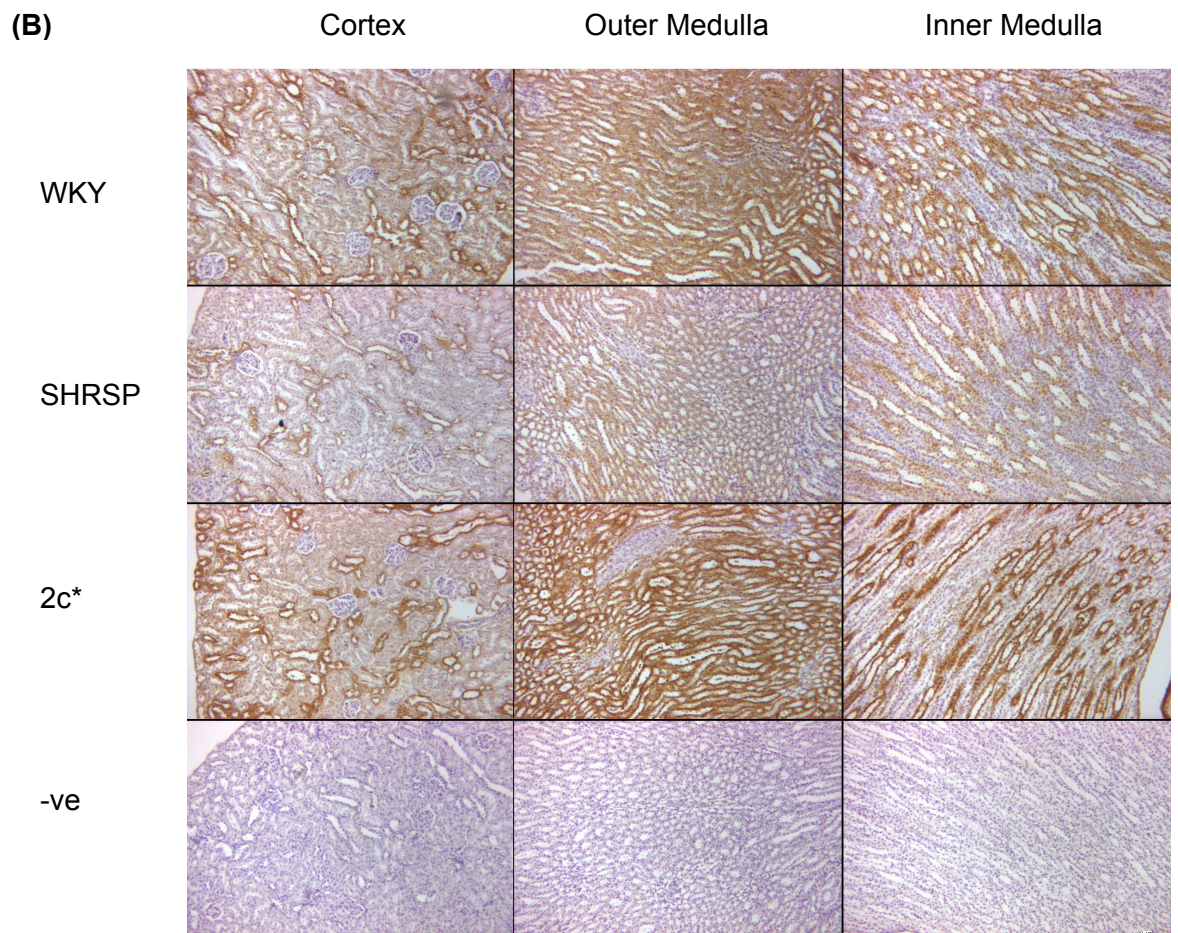
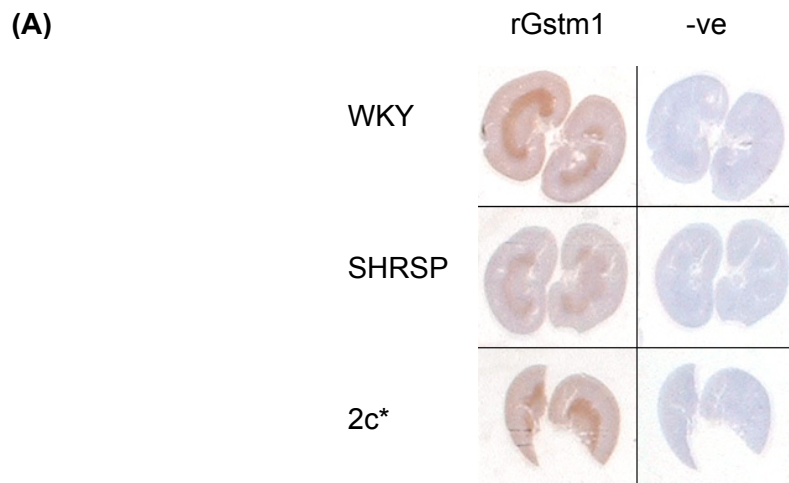


Figure 3.11: IHC of rGstm1 on male WKY, SHRSP and SP.WKY_{Gla}2c* kidney

(A) IHC of rGstm1 protein on whole kidney sections from WKY, SHRSP and SP.WKY_{Gla}2c* (2c*) male rats and (B) magnified x100.

There was no significant difference in *rGstm2* expression between SHRSP and WKY or SP.WKY_{Gla2c*} in males (*Figure 3.10*). SHRSP female expressed significantly lower *rGstm2* mRNA than SP.WKY_{Gla2c*} females ($p = 0.024$; CI = -0.70, -0.07) and non-significantly lower *rGstm2* than WKY females ($p = 0.169$; CI = -0.61, 0.12). There was no gender-specific difference in *rGstm2* expression in any of the three strains.

SHRSP rats expressed lower *rGstm3* than WKY and SP.WKY_{Gla2c*} in both male and female rats but the difference between SHRSP males and WKY males did not reach statistical significance (*Figure 3.10*). There was no gender-specific difference in *rGstm3* expression in any of the three strains.

The *rGstm5* expression pattern was similar to *rGstm1*, where SHRSP expressed significantly lower *rGstm5* than WKY or SP.WKY_{Gla2c*} in both male ($p \leq 0.031$; CI = -1.17, -0.11 and 0.21, 1.49, respectively) and female rats ($p \leq 0.032$; CI = -0.60, -0.08 and 0.08, 1.12, respectively) (*Figure 3.10*). There were significantly lower *rGstm5* expression in WKY females compared to males ($p = 0.005$; CI = -0.96, -0.32). There was also a trend towards lower *rGstm5* expression in SP.WKY_{Gla2c*} females ($p = 0.053$; CI = -1.18, 0.01) compared to SP.WKY_{Gla2c*} males but this gender-specific difference was not observed in the SHRSP rats.

The pattern of *rGstm7* expression was similar to *rGstm1* and *rGstm5* but at much lower levels (*Figure 3.10*). However, the difference in *rGstm7* expression levels between SHRSP and WKY males ($p = 0.070$; CI = -0.12, 1.29) or SP.WKY_{Gla2c*} males ($p = 0.164$; CI = -0.30, 1.11) did not reach statistical significance. The difference in *rGstm7* expression between SHRSP and WKY females or SP.WKY_{Gla2c*} females were statistically significant ($p < 0.001$; CI = 0.32, 1.05 and -1.00, -0.23, respectively). The gender-specific difference in *rGstm7* expression levels was statistically significant only in WKY rats ($p = 0.006$; CI = -0.63, -0.16) but not in SHRSP ($p = 0.099$; CI = -1.23, 0.23) or SP.WKY_{Gla2c*} ($p = 0.237$; CI = -0.86, 0.27) rats.

The effect of age on real-time relative quantitation of renal *rGstm* expression levels in 5-week-old, 16-week-old and 20-week-old rats, relative to 5-week-old SHRSP males following normalisation to β -actin expression for each gene are shown in

Figure 3.12. The SHRSP rats expressed significantly lower *rGstm1* than WKY rats at 5-weeks of age ($p = 0.002$; CI = $-2.78, -1.55$), remaining significantly lower at 16-weeks of age ($p = 0.008$; CI = $2.04, 3.64$) and 21-weeks of age ($p = 0.009$; CI = $-3.89, -1.67$). The *rGstm1* expression in WKY rats increased gradually with age but not in SHRSP rats. There were no significant differences in *rGstm2* expression between SHRSP and WKY at all time points studied and remained constant with age. The *rGstm3* expression in SHRSP rats remained constant with age while the expression in WKY rats increased after 16-weeks of age to a significantly higher *rGstm3* expression in WKY than SHRSP at 21-weeks of age ($p = 0.023$; CI = $-3.16, -0.48$). The expression of *rGstm5* increased in both SHRSP and WKY rats after 5-weeks of age and plateau after 16-weeks of age. However, the increase of *rGstm5* mRNA expression in WKY was more pronounced resulting in a significantly higher *rGstm5* expression than SHRSP at 16-weeks of age ($p = 0.031$; CI = $-1.17, -0.11$) and 21-weeks of age ($p = 0.009$; CI = $-1.00, -0.26$). There was no change in *rGstm7* expression in the SHRSP with increasing age but there was an increase in *rGstm7* expression in WKY rats after 5 weeks of age, reaching a plateau between 16 weeks and 21 weeks of age. This resulted in higher *rGstm7* expression in the WKY than SHRSP at 16-weeks of age ($p = 0.056$; CI = $-1.54, 0.059$) and 21-weeks of age ($p = 0.001$; CI = $-1.35, -0.65$).

3.3.3. Characterisation of Human GSTM Genes

3.3.3.1. Human GSTM Sequences

Multiple alignment of the mRNA transcript sequences from NCBI and Ensembl databases showed that hGSTM1 shares between 77% to 92% homology for coding sequences and 73% to 87% for peptide sequences with other members of GSTM family (*Table 3.8*). The least homologous isoforms was hGSTM3 ranging from 70% to 74% for coding sequences and 59% to 68% for peptide sequences. The untranslated region (UTR) of the mRNA transcripts at both 5' and 3' ends of the genes also share high homology.

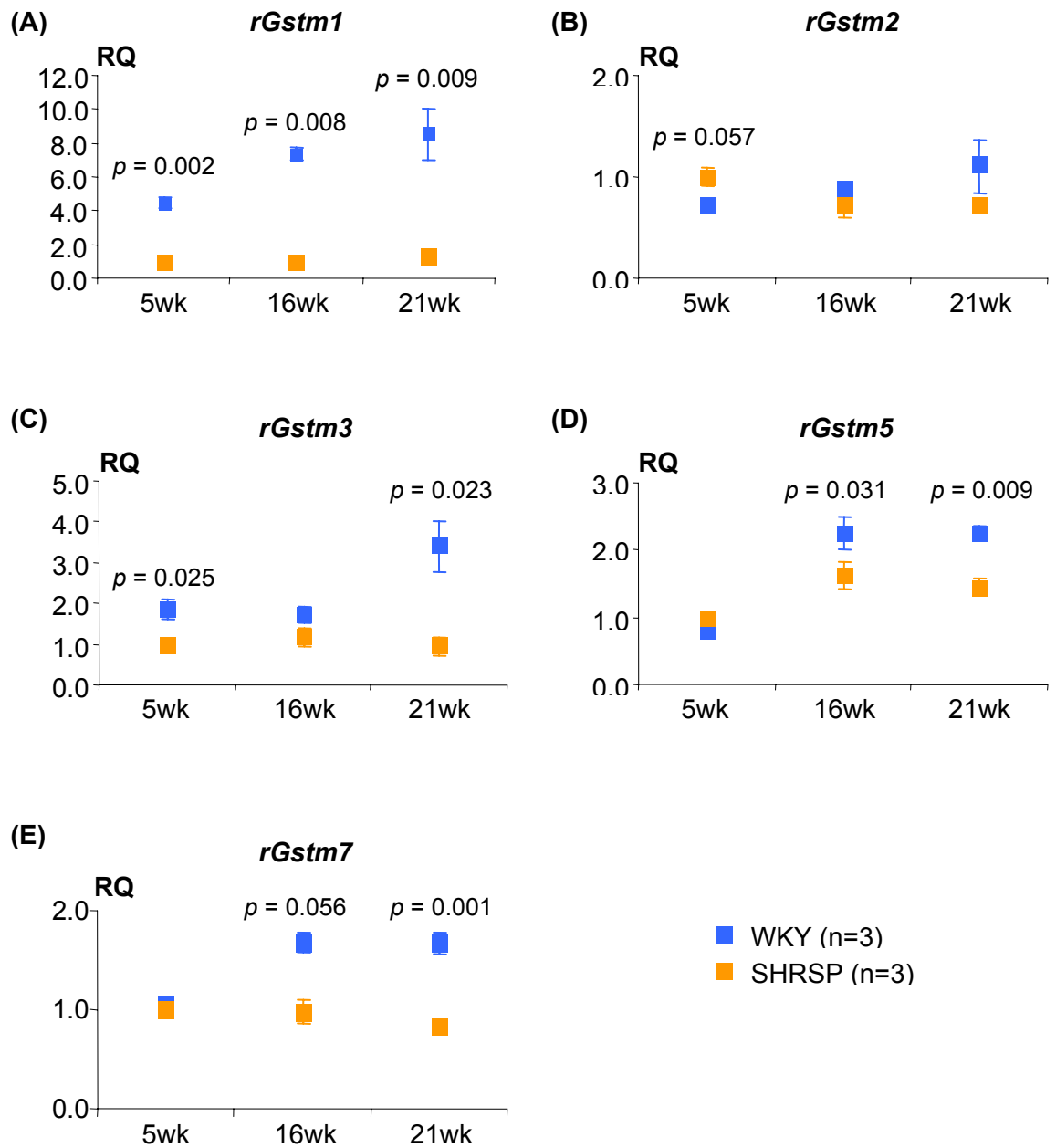


Figure 3.12: Effect of age on expression levels of renal *rGstm* isoforms

The values are represented by mean \pm SEM. Quantitation of each gene is expressed as fold-change relative to 5-week-old SHRSP expression. 2-sample t-test was used to test for significance between WKY and SHRSP at each time points. *p*-value denotes significance between WKY and SHRSP at time point indicated.

Table 3.8: (A) Percentage homology in coding sequences between *hGSTM* isoforms

	<i>hGSTM1</i>	<i>hGSTM2</i>	<i>hGSTM3</i>	<i>hGSTM4</i>	<i>hGSTM5</i>
<i>hGSTM1</i>					
<i>hGSTM2</i>	89%				
<i>hGSTM3</i>	77%	74%			
<i>hGSTM4</i>	92%	89%	77%		
<i>hGSTM5</i>	92%	89%	77%	90%	

(B) Percentage homology in protein sequences between *hGSTM* isoforms

	<i>hGSTM1</i>	<i>hGSTM2</i>	<i>hGSTM3</i>	<i>hGSTM4</i>	<i>hGSTM5</i>
<i>hGSTM1</i>					
<i>hGSTM2</i>	84%				
<i>hGSTM3</i>	73%	68%			
<i>hGSTM4</i>	86%	83%	72%		
<i>hGSTM5</i>	87%	81%	72%	83%	

3.3.3.2. Expression of Human GSTM Isoforms in Various Tissues

The *hGSTM1* was expressed in kidney, testes and saphenous vein (SV) but expression data was inconclusive in heart and liver (*Table 3.9*) as the RNA for these tissues were commercial RNA and may have come from individuals who were *hGSTM1*0*. The *hGSTM1* was expressed at higher level in testes than kidney or SV. The *hGSTM2* was expressed most in heart, followed by testes, kidney and least in SV and was not in the liver. The *hGSTM3* was expressed most in testes, followed by heart, kidney or liver, and least in the SV. The *hGSTM4* was expressed in roughly equivalent levels in kidney, testes and SV and less in heart and liver. The *hGSTM5* was expressed only in the testes and vascular tissues.

3.3.3.3. Vascular Localisation of Human GSTM Isoforms

As there was no specific antibody for hGSTM2 protein, the localisation of the protein was detected using an antibody that recognises both hGSTM1 and hGSTM2 on sections from subjects with the *hGSTM1*0* polymorphism. Since subjects with *hGSTM1*0* polymorphism do not have the *hGSTM1* gene, the antibody will only bind to hGSTM2 protein. The specificity of the antibodies and antisera were also confirmed by dot blot analysis with recombinant hGSTM proteins. *Figure 3.13* shows that expression of hGSTM1 (A), hGSTM2 (C) and hGSTM4 (G) were detected in all the vascular cell types while hGSTM3 was expressed only in VSMCs (E). *Figures 3.13* (B), (D), (F) and (H) show the respective negative control IHC.

3.3.4. **Optimisation of *In Situ* Hybridisation on Vascular Tissue**

As part of the characterisation of the rGstm in vascular and renal tissues, as well as *hGSTM* genes in vascular tissues, *in situ* hybridisation was chosen as the technique of choice to localise the expression of each of the *Gstm* isoforms. This was due to the high homology of the sequences both at coding and protein levels, and lack of readily available isoform-specific antibodies. Even though Prof. I. Listowsky's group have previously published work using hGSTM isoform-specific antisera, most of their subsequent work have used reverse-phase high performance liquid chromatography (HPLC) (223). There were also other isoforms

Table 3.9: Expression of *hGSTM* isoforms in various tissues

Gene	Heart	Kidney	Liver	Testes	SV
<i>hGSTM1</i>	?	+	?	++	+
<i>hGSTM2</i>	++++	++	–	+++	+
<i>hGSTM3</i>	+++	++	++	++++	+
<i>hGSTM4</i>	+	++	+	++	++
<i>hGSTM5</i>	–	–	–	++	+

The *hGSTM* genes are expressed at varying levels in different tissues, with (+) being present to high levels (++++), and the scale being compared across tissue for each gene. The grading of the expression was based on the intensities of the RT-PCR product band. It is unclear (?) if these tissues expressed *hGSTM1*. (–) denotes that the gene was not expressed in the tissue in question. SV = saphenous vein

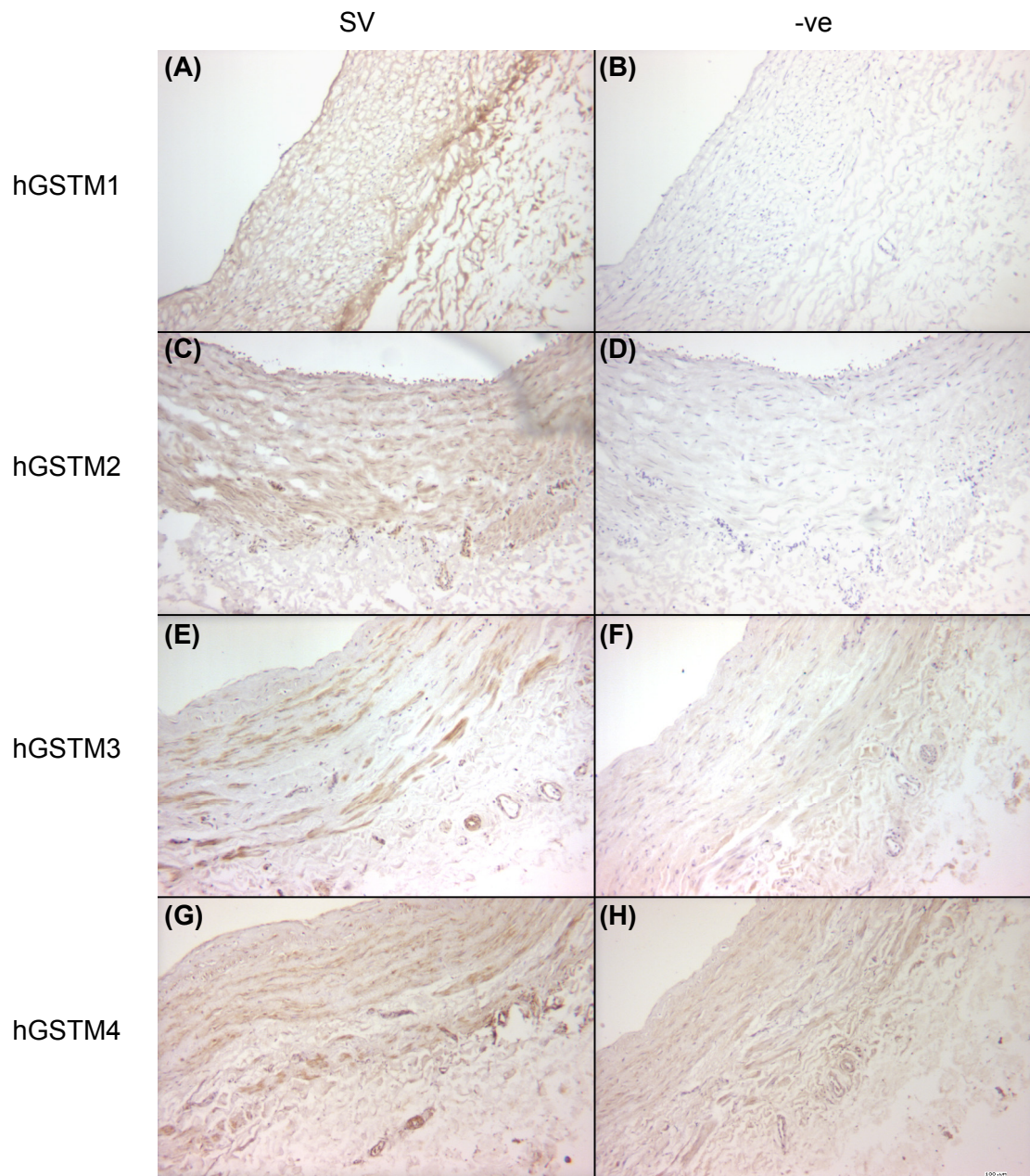


Figure 3.13: Localisation of hGSTM isoforms in vasculature

(A), (C), (E) and (G) represent the localisation of hGSTM1, hGSTM2, hGSTM3 and hGSTM4 in saphenous veins by IHC. (B), (D), (F) and (H) are the appropriate negative controls. Magnification = x100; SV = saphenous vein; -ve = negative control.

that could not be localised using immunohistochemistry, due to lack of available GSTM-specific antisera in both rat and human. In addition, the later described rGstm6^a, rGstm6^b and rGstm7 meant that the specificity of the available antisera was in question. Thus, a more specific method was required to localise the expression of these genes.

Riboprobes were used for hybridisation to mRNA transcripts in 10µm frozen sections of thoracic aorta (TA) and kidney from rats and varicose veins from human subjects. Preliminary ISH experiments to detect *hGSTM4* in varicose vein yielded unsuccessful results due to high background signals in the negative control sections (*Figure 3.14A*) while *rGstm1* in thoracic aorta and kidney yielded very low detectable signal (*Figure 3.14B*). The smooth muscle α -actin (*ACTA2*) used as a positive control gene in the rat and human vascular tissues confirmed the high background signal (*Figure 3.14C*). The use of *ACTA2* probes on kidney sections suggested that the protocol was adequate for the kidney sections (*Figure 3.14D*) and so the lack of *rGstm1* signal in kidney was probably due to unsuitable target sequence or yet-to-be identified problem of *in situ* detection of *rGstm1* gene.

Variations in a number of steps were introduced in an attempt to improve the *Gstm* signals while reducing the background signals. The results of the variations compared to the initial protocol are shown in *Figure 3.15*. The changes compared to the (A) initial protocol were (B) reducing the paraformaldehyde fixing time from 10min to 5min to reduce cross-linking of proteins to allow more access by riboprobes to target mRNA; (C) increase acetylation with acetic anhydride from 10min to 15min to reduce non-specific binding of probes to the highly positively charged vascular tissue; (D) introduction of antigen retrieval using 10mM citrate buffer, pH 6.0 after PBS washes following formaldehyde fixing to break some of the bonds between proteins formed during cross-linking; (E) introduction of second RNase incubation following the first wash at 60°C after the first RNase digestion to digest any non-specifically bound or trapped riboprobes that might be more accessible following washing at 60°C; (F) combination of increased acetylation with additional RNase digestion; and (G) combination of decreased fixation with increased acetylation. Increased acetylation of the sections increased the positive/antisense signal while two RNase digestions reduced the non-specific/sense signal. Decreased fixation did not improve the signal to background

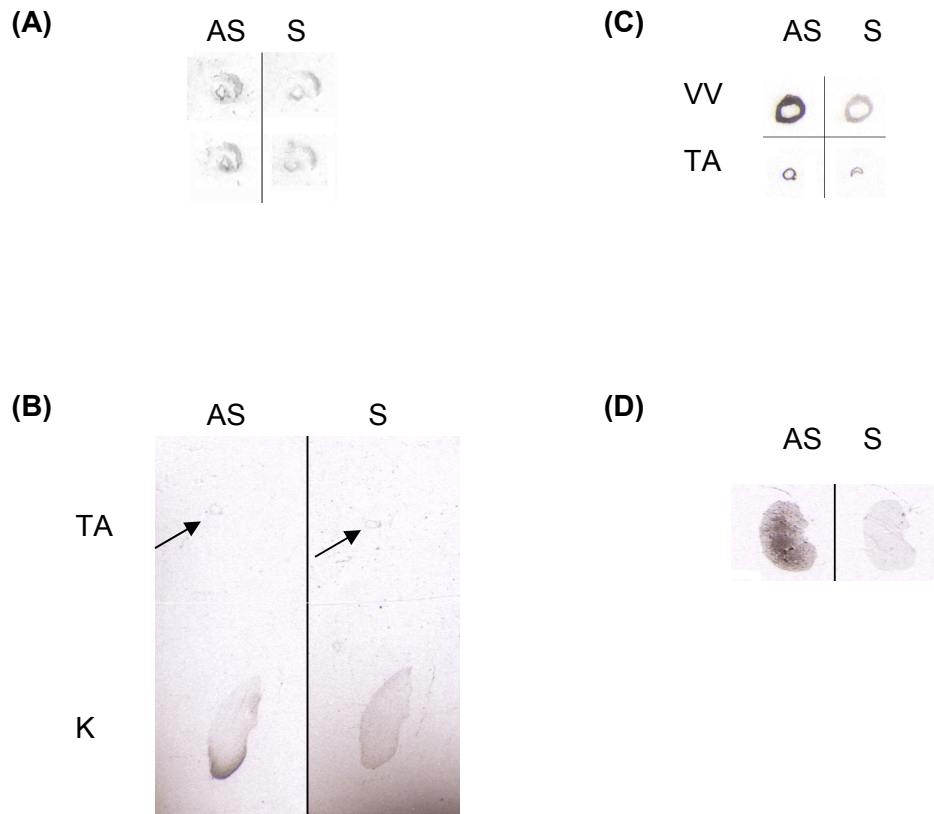


Figure 3.14: Preliminary *in situ* hybridisation experiments

In situ hybridisation for (A) *hGSTM4* in human varicose vein (VV); (B) *rGstm1* in rat thoracic aorta (TA) and kidney (K); (C) smooth muscle α -actin (*ACTA2*) in human varicose vein and rat thoracic aorta; and (D) *Acta2* in rat kidney. AS = antisense, S = sense.

	AS	S	<u>Variations</u>
(A)			No change
(B)			Fixing for 5min
(C)			Acetylation for 15min
(D)			Antigen Retrieval
(E)			2 x RNase
(F)			Acetylation for 15min & 2 x RNase
(G)			Fixing for 5min & Acetylation for 15min

Figure 3.15: Variations in pre-treatment of rat aorta for ISH

Changes to the ISH protocol are (B) reducing the fixing of tissue sections in 4% paraformaldehyde from 10min to 5min; (C) increase acetylation of tissue sections with acetic anhydride from 10min to 15min; (D) introducing antigen retrieval with citrate buffer following acetylation; (E) an additional RNase step following first wash at 60°C; (F) a combination of variations C and E; and (G) a combination of variations B and C. AS = antisense; S = sense

ratio. In contrast, antigen retrieval reduced both specific and non-specific signals. A combination of reduced fixation and increased acetylation did not improve the signal:background ratio more than increased acetylation alone. A combination of increased acetylation and additional RNase digestion appeared to improve the antisense signal while reducing the sense signal.

Due to time and practicality constraints optimisation of ISH method was not investigated further. Consequently localisations of *rGstm* and *hGSTM* genes by ISH are not available.

3.3.5. Lower Smooth Muscle α -Actin in Female Rats

While comparing the protein expression levels of *rGstm* isoforms in the vascular tissues using IHC, control IHC using smooth muscle α -actin (*Acta2*) was also carried out on carotid artery sections from male and female rats of SHRSP, WKY and congenic SP.WKY_{Gla2c*} strains (*Figure 3.16*). Surprisingly, there was a lower *Acta2* protein expression in the smooth muscle layer in the carotid arteries from female rats than their male counterparts, regardless of strains. This gender effect is an important observation, which should be taken into account when using *Acta2* as a house-keeping protein (control) in studies using both males and females.

3.4. Discussion

Previous work in our group has shown that SBP and DBP of the congenic SP.WKY_{Gla2c*} strain was significantly lower than SHRSP but higher than WKY (61). In that study, BP was measured by radiotelemetry only in male rats. In this project, SBP of the congenic strain was significantly lower than SHRSP but not higher than WKY. This discrepancy could be due to the different methods of SBP measurement. Results generated by tail cuff plethysmography may be subject to stress artifacts due to warming and handling and therefore cannot be directly compared with telemetry. In addition, there were significant gender-specific difference in WKY and SHRSP but not the congenic strain.

Analysis of *rGstm* sequences at transcriptional and protein level showed that there was high homology between the family members. The expression of *rGstm1*,

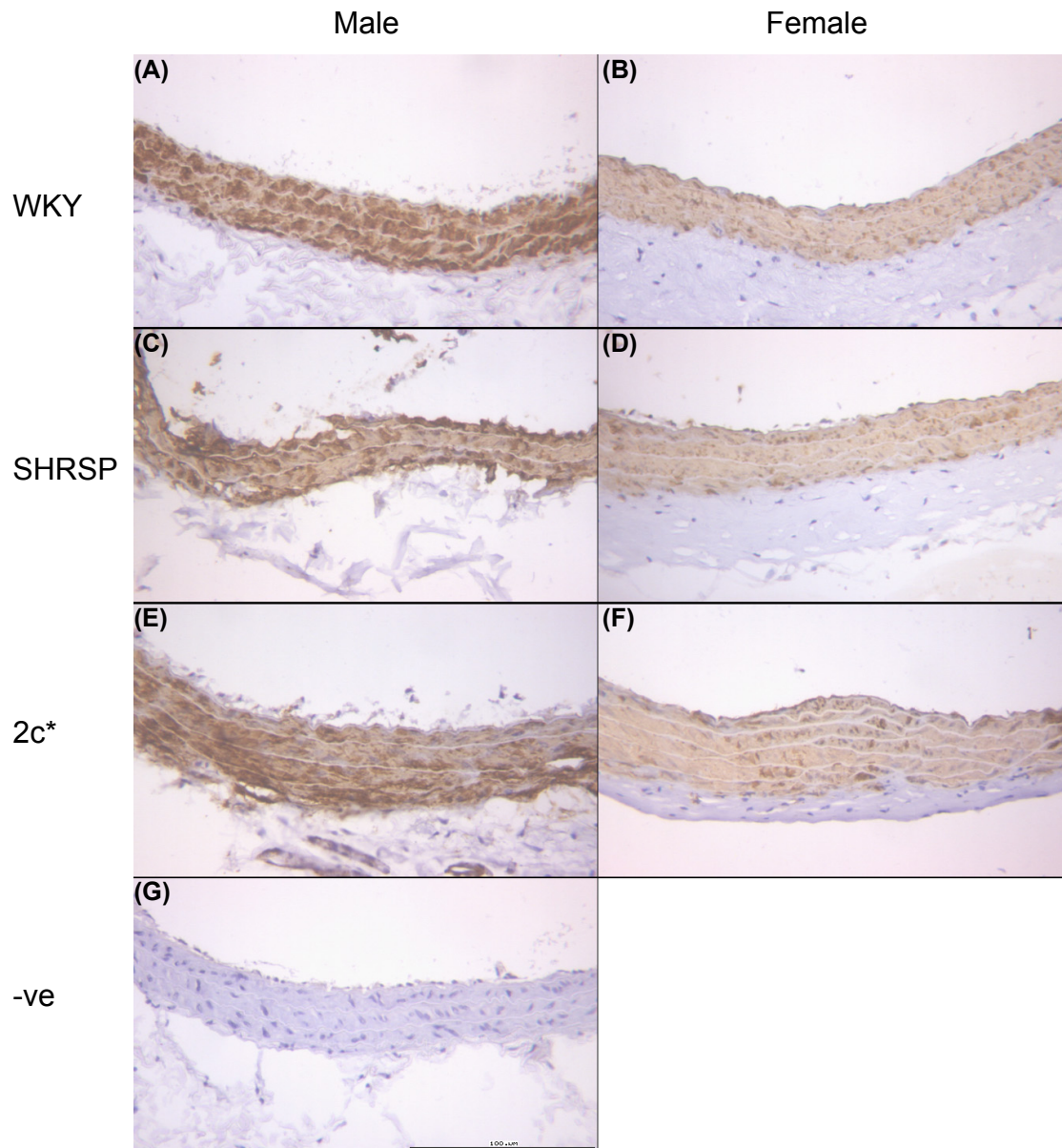


Figure 3.16: IHC of smooth muscle α -actin (Acta2) in carotid arteries

(A), (C), (E) are IHC of Acta2 gene in male WKY, SHRSP and SP.WKY_{Gla}2c* (2c*), while (B), (D), (F) are the female counterparts and (G) is a representative negative (-ve) control. Magnification = x200

rGstm2, *rGstm3*, *rGstm5* and *rGstm7* were detected in thoracic aorta, brain, heart, kidney and liver. In addition to the five *rGstm* genes, expression of *rGstm6^b* was also detected in brain. However, the expression of *rGstm4* and *rGstm6^a* were not detected in all the tissues examined. The original paper that first characterised rat *Gstm4* gene from a genomic DNA clone did not detect any mRNA transcripts (224). A study that attempted to characterise expression of the *rGstm* gene family in various tissues also failed to detect any mRNA transcripts or corresponding protein (225). A search through the EST databases did not provide any “hits” for either *rGstm4* or *rGstm6^a*, suggesting that these two genes may be pseudogenes. It is also possible that these genes are expressed in tissues yet to be looked at or in certain developmental stages only. The latter explanation seems likely as a recombinant rat *Gstm4* (*rGstm4*) protein expressed in *Escherichia coli* showed the S-glutathiolated form of the enzyme was catalytically active (226). Antibodies raised against unique C-terminal undecapeptide or tridecapeptide of *rGSTM4* reacted with rat and mouse liver GSTs revealing an orthologous mouse *GSTM4* (*mGSTM4*). The *mGSTM4* was present at low basal levels but was inducible in mouse liver. It is likely that *rGSTM4* is also present at very low levels in rat liver and is inducible. However, in the major cardiovascular tissues (e.g. kidney and vasculature) the expression of *rGSTM4* was not detected in either the WKY or SHRSP rat.

Generally, vascular *rGstm* gene expressions were lower in SHRSP compared to WKY and/or SP.WKY_{Gla2c*}. There were also gender-specific differential expression of *rGstm3* and *rGstm7*. Despite the significant differential expression, the differences were less than 1-fold and the variations within groups were high. A search through the literature revealed that no known studies have attempted to characterise the entire *rGstm* gene family. This study is the most comprehensive study of *rGstm* gene family expression in vascular tissues. The data from this study provides a reference guide for future vascular *rGstm* studies.

Differences in mRNA expression levels may not be translated equally to protein levels and so it was necessary to investigate vascular *rGstm* protein expression. The expression of *rGstm1* protein was detected in all the vascular cell types. The SHRSP vascular *rGstm1* protein expression was lower than WKY and SP.WKY_{Gla2c*}.

The rGstm2 protein was initially localised to endothelium. Unexpectedly, attempts to compare rGstm2 protein expression in thoracic aortas from the three strains by IHC revealed rGstm2 expression in all vascular cell types. Subsequent dot blot of anti-rGstm2 serum showed that the antiserum is non-specific, detecting both rGstm1 and rGstm2 recombinant proteins, suggesting that the observed difference in rGstm2 expression was probably a consequence of the difference in rGstm1 protein expression. The rGstm5 protein was localised to VSMCs.

As there were no available recombinant proteins or peptides available for the entire rGstm gene family that could be used to confirm the specificity of the antisera, an alternative localisation method for rGstm expression would be required to confirm the current findings. Even though ISH detects mRNA expression, it provides the opportunity for specific localisation of *rGstm* isoforms. Optimisation experiments for ISH gave promising results. However, the length of time required for an experiment is extremely long (e.g. approximately 7 weeks for hGSTM4 in SV), when using radioactive detection method. Thus the opportunity for repeated experiments and optimisation steps is limited. It would be beneficial for further optimisation of ISH and, perhaps, using a more rapid detection method such as enzymatic colour change or fluorochrome detection system (227). *In situ* RT-PCR is another option for detecting transcripts present at very low amounts, below detection limit of the usual IHC or ISH (228).

IHC co-localised rGstm1, rGstm2 and rGstm5 expression with aquaporin-2 in the principal cells of collecting duct. Expression of rGstm1, rGstm2 and rGstm5 protein were also detected in other cell types within the kidney. To further determine the localisation of these rGstm proteins in the kidney, co-localisation with other genes expressed specifically in different regions of nephron would be required. An example is aquaporin-1, which was localised to renal proximal tubule and descending limb of the loop of Henle (*Figure 3.17*) (229). However, since the non-specificity of the anti-rGstm2 antiserum and possibly the other antisera remains to be clarified, an alternative localisation method would be required to confirm the current findings.

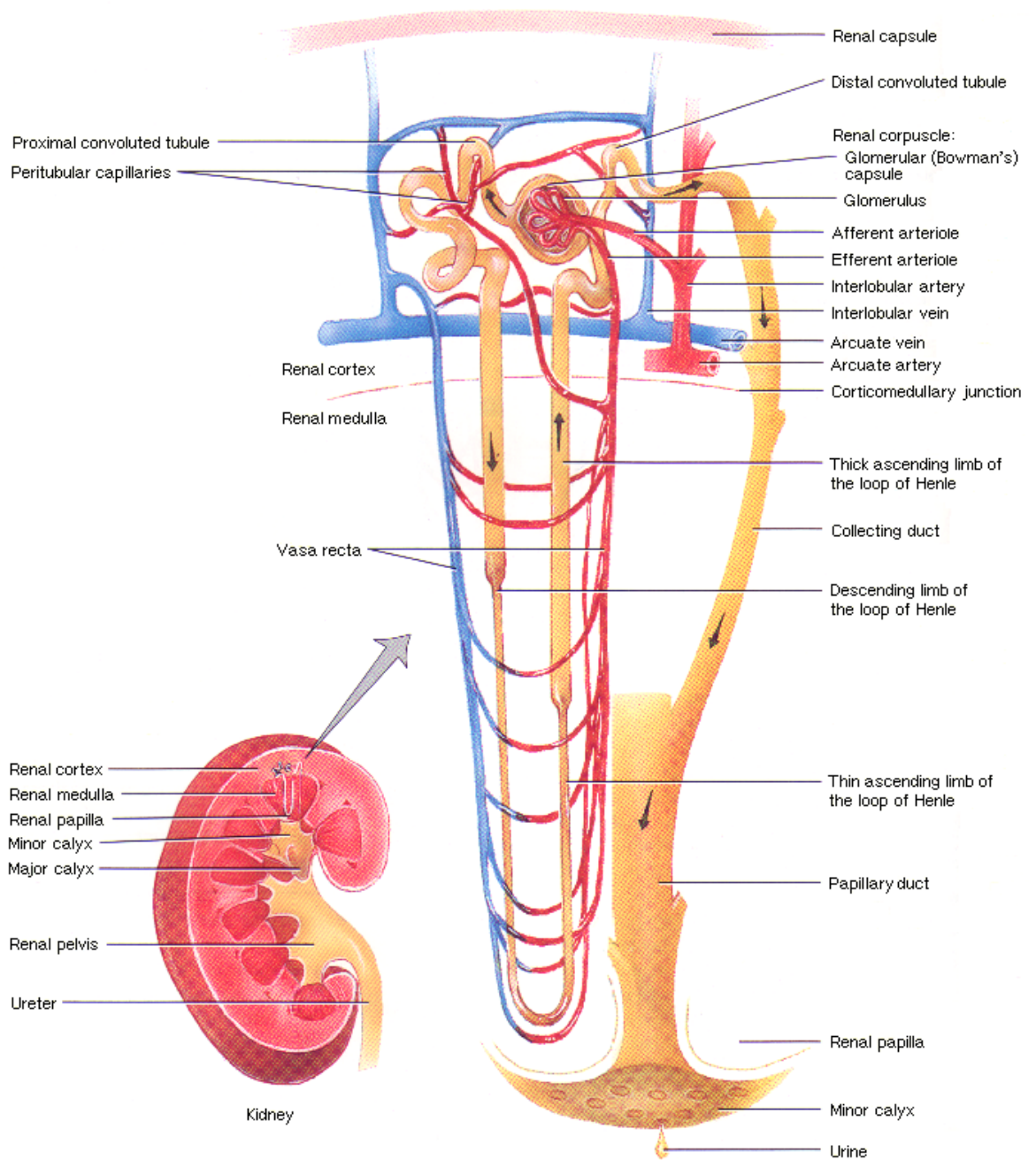


Figure 3.17: Schematic diagram of a juxtamedullary nephron.

Taken from Ref. (237)

Previous microarray analysis of gene expression in kidney homogenates from 16-week old rats showed reduction in *rGstm1* mRNA and protein expression (61;67). It is likely that decreased expression of one isoform may be compensated by increasing expression of another isoforms. This is highly likely since the enzymes consist of homo- and hetero-dimeric subunits, which can be formed between members of the same class of GSTs (184). In this project, renal expression of *rGstm1* was highest, followed by *rGstm2*, *rGstm3*, *rGstm5* and *rGstm7*. Expression of *rGstm1* mRNA was approximately 7.5 times higher than *rGstm2* mRNA. In this project, the differential *rGstm1* expression at mRNA and protein levels identified in previous studies were confirmed. IHC of *rGstm1* protein in kidneys from male rats showed reduced cortical and medullary expression by SHRSP, compared to WKY and SP.WKY_{Gla2c*}. The mRNA expression of other members of *rGstm* gene family were also reduced in SHRSP compared to WKY and SP.WKY_{Gla2c*}, except for *rGstm2*. However, the differences between SHRSP and WKY or SP.WKY_{Gla2c*} were small compared to *rGstm1*. From these data, we can conclude that there is no compensatory increase in other *rGstm* isoforms and there is a general reduction in expression of *rGstm* family members with the greatest effect in *rGstm1*.

In addition to strain-specific differences, gender-specific differences were also observed in this project. WKY and SP.WKY_{Gla2c*} female expressed significantly lower *rGstm1* expression than their male counterparts. This gender-specific difference was not observed in SHRSP. This was probably because the extent of the reduction in SHRSP eliminated the gender effect observed in the WKY and SP.WKY_{Gla2c*}. Expression of *rGstm5* in WKY female and SP.WKY_{Gla2c*} female; and *rGstm7* in WKY female were also lower than their male counterparts. This effect may be the result of hormonal regulation of *rGstm* gene expression as gender-specific difference was also previously reported in rat liver (230). Several α and μ class GSTs were expressed in a sex-dependent fashion in adult rat liver, where they were regulated by multiple pituitary-dependent hormones through pre-translational mechanisms.

The expression of *rGstm1* was reduced in SHRSP even at 5 weeks of age. This difference in *rGstm1* mRNA expression became larger with age. The expression of *rGstm3*, *rGstm5* and *rGstm7* increased with age in WKY but less so in SHRSP.

Reduced expression of *rGstm1* exists before the onset of hypertension indicating a primary cause rather than secondary effect of BP. There is evidence for renal oxidative stress in hypertensive rat models (67;231). Superoxide levels in the kidney medulla and cortex, measured by lucigenin chemiluminescence, were significantly higher in SHRSP compared to WKY, with that of SP.WKY^{Gla2c*} being intermediate. Overall, the results point to *rGstm* as important enzymes in hypertension, especially *rGstm1* in the kidney. It is likely that *rGstm* enzymes are important for reducing renal oxidative stress.

Analysis of *hGSTM* sequences at transcriptional and protein level showed that the homology between the gene family members are high. Distribution of *hGSTM* genes and localisation of *hGSTM1*-*hGSTM4* did not provide any further indication as to which of the *hGSTM* genes is the orthologue of *rGstm1*. Analysis of *Gstm* gene sequences from rat, mouse and human suggested that the *hGSTM* gene family evolved independently of rodent *Gstm* genes, except for *hGSTM3*. (Figure 3.18). Despite this, the *hGSTM* enzymes could still play important roles in protection against vascular oxidative stress in hypertension.

Obtaining good quality vascular tissues from human subjects was problematic. In this study, tissues were obtained from two sources, SV from CAD patients undergoing CABG surgery and VV from patients undergoing varicose vein removal. In both cases, removal and maintenance of vessels before receiving them in the laboratory was not optimal for RNA extraction procedures. Samples from CAD patients were kept in sterile saline for a long period of time before they could be snap frozen for further processing. The method of removal of VV often results in inversion of the vessel potentially causing loss of the endothelial layer. This mechanical stress could also prompt inflammatory responses which could render the results unreliable. The expression data generated in the human subjects may be less reliable than those obtained for the rats.

It has been shown that approximately 50% of Caucasians have a deletion of the entire *hGSTM1* gene (232). This results in the lack of the relevant protein expression. There is no known *rGstm* gene deletion in the rats, which also have more members in the gene family. The *hGSTM1* was associated with altered expression of *hGSTM3* (204). The Medical Research Council British Genetics of

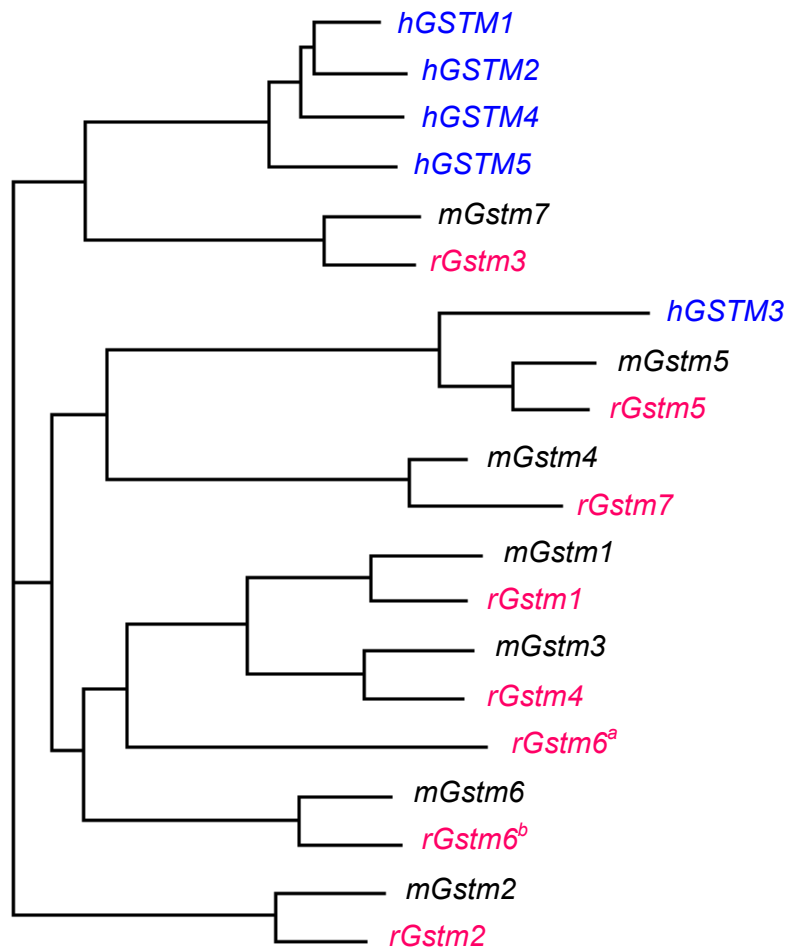


Figure 3.18: Phylogenetic tree of Gstm gene family from human, rat and mouse

HyperTension (BRIGHT) study aimed to identify genes that confer susceptibility to essential hypertension, consisted of 1599 severely hypertensive families (233). Sequencing and genotyping of DNA samples from the BRIGHT study implicated *hGSTM5* as an important candidate gene in hypertension (234).

As an aside to the GSTM results presented in this study, an interesting observation was also made regarding Acta2 protein expression. Surprisingly, Acta2 protein expression in thoracic aorta was lower in female compared to male, regardless of strain. A search through the literature did not provide any previous report of differential Acta2 expression between males and females. To my knowledge, this is the first report of gender-specific differential Acta2 expression in VSMC from rats. Acta2, more commonly known as smooth muscle α -actin, is one of the contractile proteins important for the differentiated function of VSMCs (235). There is a higher ratio of α -actin to γ -actin in aortic tissues than venous tissues, emphasising the importance of α -actin in contractile function. Acta2 knock-out mice demonstrated lower SBP than wild-type mice (236). Despite the importance of Acta2 protein, it is not required for the development of the cardiovascular system. The observed gender-specific difference in Acta2 expression could possibly account, in part, for the observed difference in SBP between male and female rats.

The majority of studies investigating GSTMs have focussed on biochemical properties and role in cancer, since GSTs are phase II drug-metabolising enzymes. In contrast, this study provided a detailed characterisation of the GSTM gene family in terms of cardiovascular tissue expression. These data provide an important basis for further functional investigation of the role of GSTM in the development of hypertension in both rat models and humans.

CHAPTER 4: EFFECTS OF ANTIHYPERTENSIVE DRUGS ON THE EXPRESSION LEVELS OF RAT GLUTATHIONE S-TRANSFERASE μ ISOFORMS

4.1. Introduction

In the previous chapter, characterisation of the rGstm family confirmed differential expression of rGstm1 at both mRNA and protein levels in SHRSP. Furthermore, *rGstm3*, *rGstm5* and *rGstm7* were also shown to be significantly reduced in the SHRSP compared to WKY. It is unknown whether the observed differences in rGstm gene expression are secondary effects due to changes in pathophysiological mechanisms involved in the development of hypertension or whether rGstm expression can be manipulated by preventing or reversing elevated BP.

The SHRSP is an excellent model for investigating the functional role of the rGstm family. Previous studies in our laboratory have identified increased levels of vascular O_2^- and reduced NO bioavailability in SHRSP (121;238;239). We have also shown that significant improvements in NO bioavailability in SHRSP can be achieved using AT₁R antagonists (240;241).

The aims of this study were to carry out pharmacological intervention studies to investigate the role of rGstm enzymes in oxidative stress and determine whether reduced rGstm expression in SHRSP can be improved with antihypertensive treatment. Two different classes of antihypertensive drugs were used for mechanistic assessment of the role of the rGstm family in oxidative stress and hypertension. We compared the effects of AT₁R antagonist (olmesartan) (242) with a vasodilator and diuretic combination (hydralazine and hydrochlorothiazide, H + H) on SBP, O_2^- and H_2O_2 production and expression levels of *rGstm* genes. AT₁R blockers (ARBs) reduce oxidative stress in models of hypertension and atherosclerosis by inhibiting Ang II stimulated O_2^- production through Ang II receptor blockade (240;243;244), whereas H + H act through different mechanisms by causing direct vasodilation and diuresis (47;245;246). As Ang II is a potent stimulator of O_2^- production by NADPH oxidase, measurement of the gene expression of *CYBA* (which encodes for p22^{phox} subunit of NAD(P)H

oxidase), *Ncf1* (which encodes for p47^{phox} subunit of NAD(P)H oxidase) and *Rac1* (which encodes for GTP-binding protein rac1) were also carried out. The expression of p22^{phox} and p47^{phox} subunits have both been detected in all the vascular cell layers (247). The p22^{phox} subunit represents membrane component of the NAD(P)H oxidase while p47^{phox} subunit represents the cytoplasmic component of the NAD(P)H oxidase. The rac1 protein is the ubiquitously expressed regulator required for the activation of non-phagocytic NAD(P)H oxidases (247). Furthermore, to ensure that any observed effects of olmesartan were not due to the amount of AT₁R present, the expression of *Agtr1a* gene, which encodes for α subtype of AT₁R was also measured.

Two study protocols were undertaken (prevention and reversal) to allow investigation of different aspects of BP control and development of hypertension on gene expression. The reversal study allows identification of non-reversible changes occurring due to hypertension and the prevention study allows investigation of functional effects in *rGstm* expression when hypertension is prevented from developing.

4.2. Materials & Methods

The details for all the equipments, chemicals, reagents and consumables used in this study are listed in *Appendix B*.

4.2.1. Animal Strains and Antihypertensive Therapy

In the reversal drug study, 16-week-old male SHRSP were treated orally with olmesartan (20 mg/kg per day; n = 8) or hydralazine plus hydrochlorothiazide (H + H) (16 mg/kg per day; n = 8) or vehicle (n = 9) for 4 weeks. In the prevention drug study, 8-week-old male SHRSP were treated orally with olmesartan (20 mg/kg/day; n = 7) or H + H (16 mg/kg/day; n = 7) or vehicle (n = 7) for 8 weeks. The WKY strain (n=6) was also treated with vehicle in parallel. Olmesartan (courtesy of Sankyo Pharma GmbH, marketed as olmesartan medoxomil), first described as CS-866, is a pro-drug that de-esterifies to its active form (242). As olmesartan is poorly water soluble, a suspension of the drug was prepared daily in a commercially available preparation of custard baby food, which was eaten by the

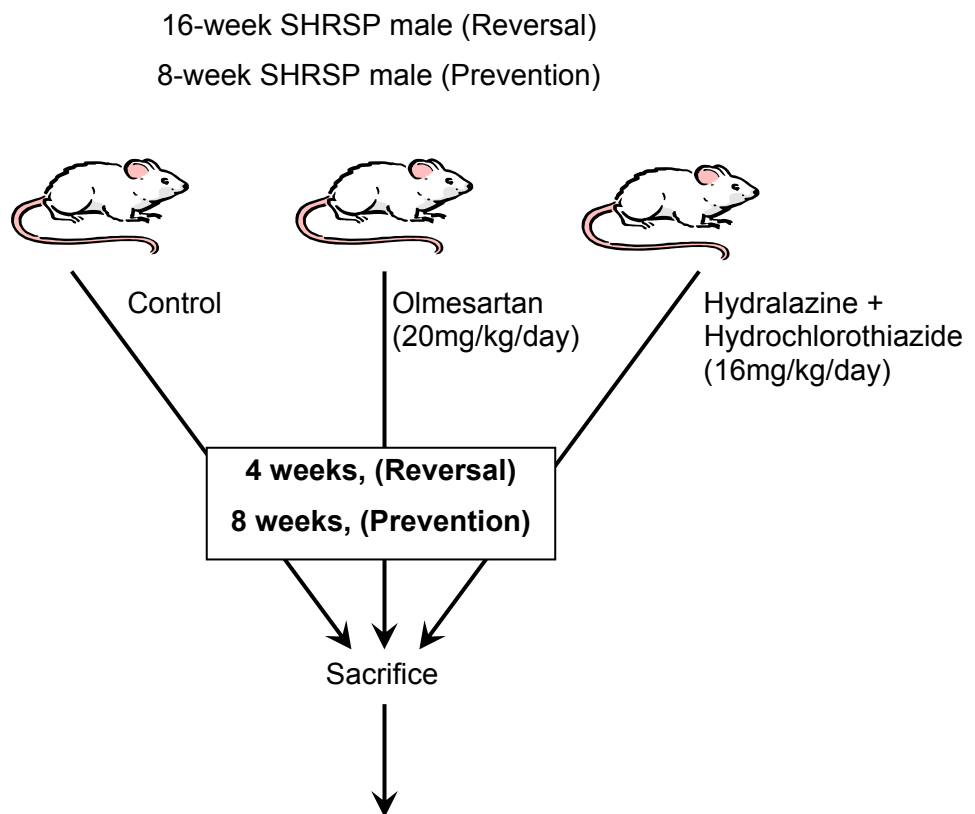
rats immediately. For consistency, the other drugs were administered in the same manner. Control animals received custard but no drugs. Drug doses were chosen to achieve equipotent blood pressure-lowering effects as determined in preliminary experiments in males. The animals were weighed weekly to adjust the drugs accordingly. SBP was measured weekly by tail-cuff plethysmography as described in section 2.1.2.

At sacrifice, thoracic aorta and kidney were removed and snap-frozen in liquid nitrogen for total RNA and protein extraction. Abdominal arteries and a quarter of kidney dissected into cortex and medulla were removed for measurement of superoxide production by lucigenin. One half of a kidney from each animal was embedded into frozen blocks, as described in section 2.2.1., and one half formalin-fixed and embedded into paraffin blocks, as described in section 2.2.2. The carotid arteries were also formalin-fixed and embedded into paraffin blocks. A schematic diagram of the drug studies are shown in *Figure 4.1*.

4.2.2. Superoxide Production Measurement

Abdominal aortas were cleaned, cut into segments of approximately 5mm, weighed and placed in a scintillation vial containing 2ml of Krebs buffer. Quartered sections of kidney which had been dissected into renal cortex and medulla were homogenised separately in 0.05M phosphate buffer pH7.8 (20mls buffer/0.1g tissue) containing protease inhibitors. The samples were centrifuged at 1000g for 5min and the supernatant stored in aliquots at -70°C . For the lucigenin assays, 0.2 – 0.5 μl of renal samples, depending on protein concentrations, was added to 2ml of Krebs buffer in a scintillation vial.

Lucigenin was added and the samples counted immediately in liquid scintillation analyzer TRI-CARB 2100TR. Readings were taken every 10 seconds for 3min. A standard curve was prepared with every assay by addition of 20 μl of xanthine oxidase (0.1U/ml), 20 μl of lucigenin (25 μM for vessels; 5 μM for kidney homogenates) and increasing volume of 20nM xanthine into a scintillation vial containing 2ml of Krebs buffer.



- SBP was measured weekly by tail-cuff plethysmography.
- O_2^- production was measured by lucigenin chemiluminescence.
- H_2O_2 production was measured by Amplex Red Hydrogen Peroxide/Peroxidase Assay Kit
- Gene expression was measured by relative quantitative RT-PCR.

Figure 4.1: Schematic protocol for the reversal and prevention drug study

WKY rats of the same age given vehicle control were ran in parallel in both studies. SBP = systolic blood pressure.

4.2.3. Hydrogen Peroxide Production Measurement

Hydrogen peroxide production was measured using the Amplex Red Hydrogen Peroxide/Peroxidase Assay Kit [Molecular Probes] according to the manufacturer's instructions. The plate was read using the Wallac 1420 Victor plate reader.

4.2.4. Gene Expression

The gene expression levels were measured as described in section 2.5.4.2. In addition to *rGstm* genes, we also measured the gene expression of AT₁R, NADPH subunit p22^{phox}, p47^{phox} and regulator rac1.

4.2.5. Statistical Analysis

Results are shown as mean \pm SEM. SBP of WKY or either drug-treated groups were all compared to the SHRSP control group using repeated measures ANOVA, general linear model. The superoxide production, hydrogen peroxide production and gene expression measurements of WKY or drug-treated groups were all compared to the untreated SHRSP control group using one-way ANOVA with Dunnett's comparison for 95% confidence interval. The statistically significant *p*-values compared to untreated SHRSP control group are shown, when available. Non-significant *p*-values are not shown.

4.3. Results

4.3.1. Olmesartan Reversal Study

At 16 weeks of age, all the SHRSP rats had fully developed hypertension with SBP of 173mmHg \pm 20mmHg compared to SBP of normotensive WKY (122mmHg \pm 13mmHg). After 1 week of treatment, both olmesartan (green line) and H + H (red line) treatments significantly reduced the SBP of the SHRSP to levels equivalent as the WKY (*p* < 0.001) (*Figure 4.2*). This reduction in SBP was maintained at levels equivalent to the WKY for the course of the study. The SBP of the SHRSP control (yellow line) remained high (>170mmHg) for the course of the study.

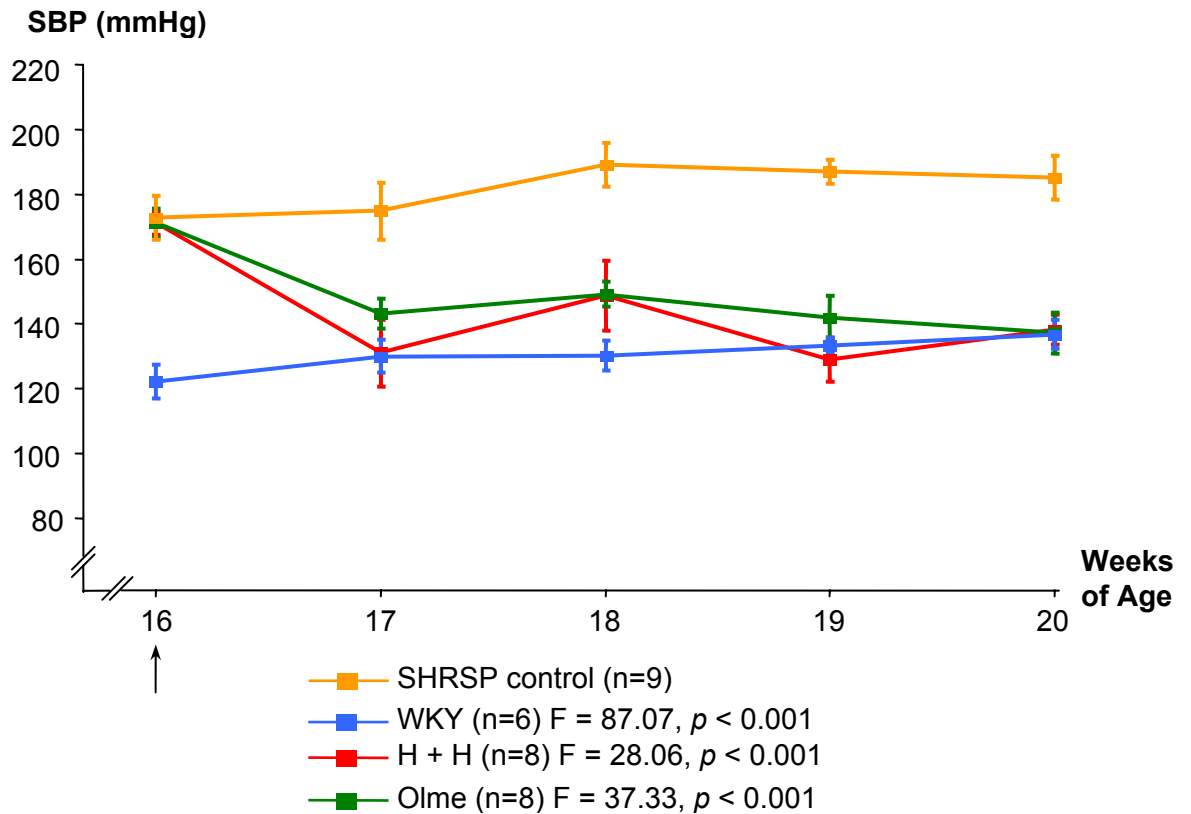


Figure 4.2: Reversal study systolic blood pressure

16-week-old SHRSP males were treated with either drug at for 4 weeks. WKY rats of the same age were included in parallel. H + H = Hydralazine + hydrochlorothiazide; Olme = olmesartan.

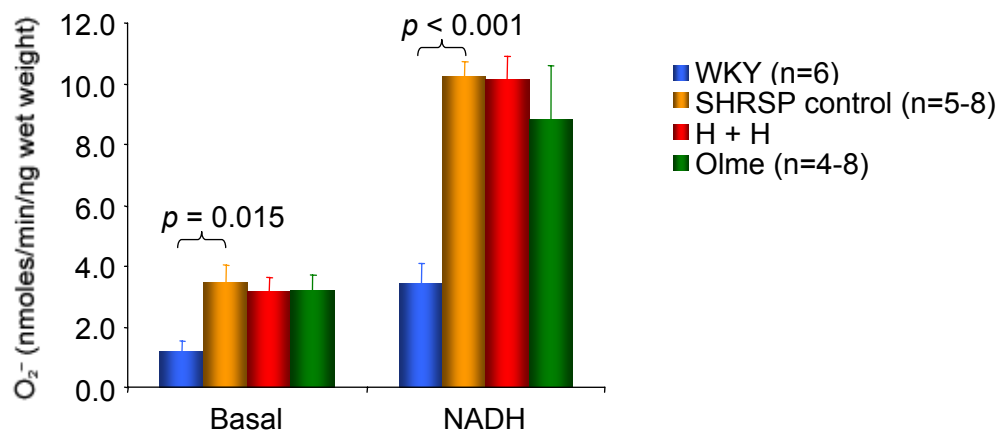


Figure 4.3: Reversal study vascular superoxide production

Basal and NADH-stimulated O_2^- production in abdominal aorta from WKY and SHRSP rats treated with vehicle, hydralazine + hydrochlorothiazide (H + H) or olmesartan (Olme).

4.3.1.1. Effect of Drugs on Vascular Function and Gene Expression

The vascular basal and NADH-stimulated O_2^- production were measured as a marker of oxidative stress (Figure 4.3). Abdominal aorta from SHRSP control demonstrated significantly higher levels of basal ($p = 0.015$; CI = $-4.06, -0.54$) and NADH-stimulated ($p < 0.001$; CI = $-10.07, -3.51$) O_2^- production than WKY rats. Neither drug treatments affected O_2^- production in SHRSP rats at basal or with NADH stimulation.

In order to determine if the difference in O_2^- production between SHRSP and WKY was due to differential expression of vascular NAD(P)H oxidase subunits or Ang II stimulation, the gene expression of p22^{phox}, p47^{phox}, rac1 and AT₁R were measured (Figure 4.4). There were no significant differences in the vascular gene expression levels for p22^{phox}, p47^{phox}, rac1 or AT₁R mRNA between untreated SHRSP controls and WKY rats. Neither of the drug treatments significantly affected the gene expression of p22^{phox}, p47^{phox}, rac1 or AT₁R. The apparent increase in p47^{phox} gene expression by H + H treatment was not statistically significant ($p = 0.088$; CI = $-1.77, 0.13$), probably due to the large variability within the group.

SHRSP rats expressed significantly higher levels of vascular *rGstm3* than WKY but there were no significant differences in *rGstm1*, *rGstm2*, *rGstm5* and *rGstm7* expression (Figure 4.5). Neither of the drug treatments affected the vascular gene expression of *rGstm1*, *rGstm2*, *rGstm3*, *rGstm5* or *rGstm7*.

4.3.1.2. Effect of Drugs on Renal Function and Gene Expression

Basal, NADH- and NADPH-stimulated O_2^- production was significantly higher in the SHRSP renal cortex ($p < 0.05$; CI = $-0.14, -0.02$; $-2.89, -1.52$ and $-1.43, -0.13$, respectively) and medulla than WKY ($p < 0.05$; CI = $-0.14, 0.02$; $-3.29, -0.76$ and $-1.62, -0.11$, respectively) with the exception of basal O_2^- production in renal medulla (Figure 4.6A). Neither of the drug treatments significantly affected the levels of O_2^- production but there was a trend for reduced NADH-stimulated O_2^- production in renal cortex from olmesartan-treated rats. H_2O_2 production following NADH or NADPH stimulation were measured to see if the similar trends

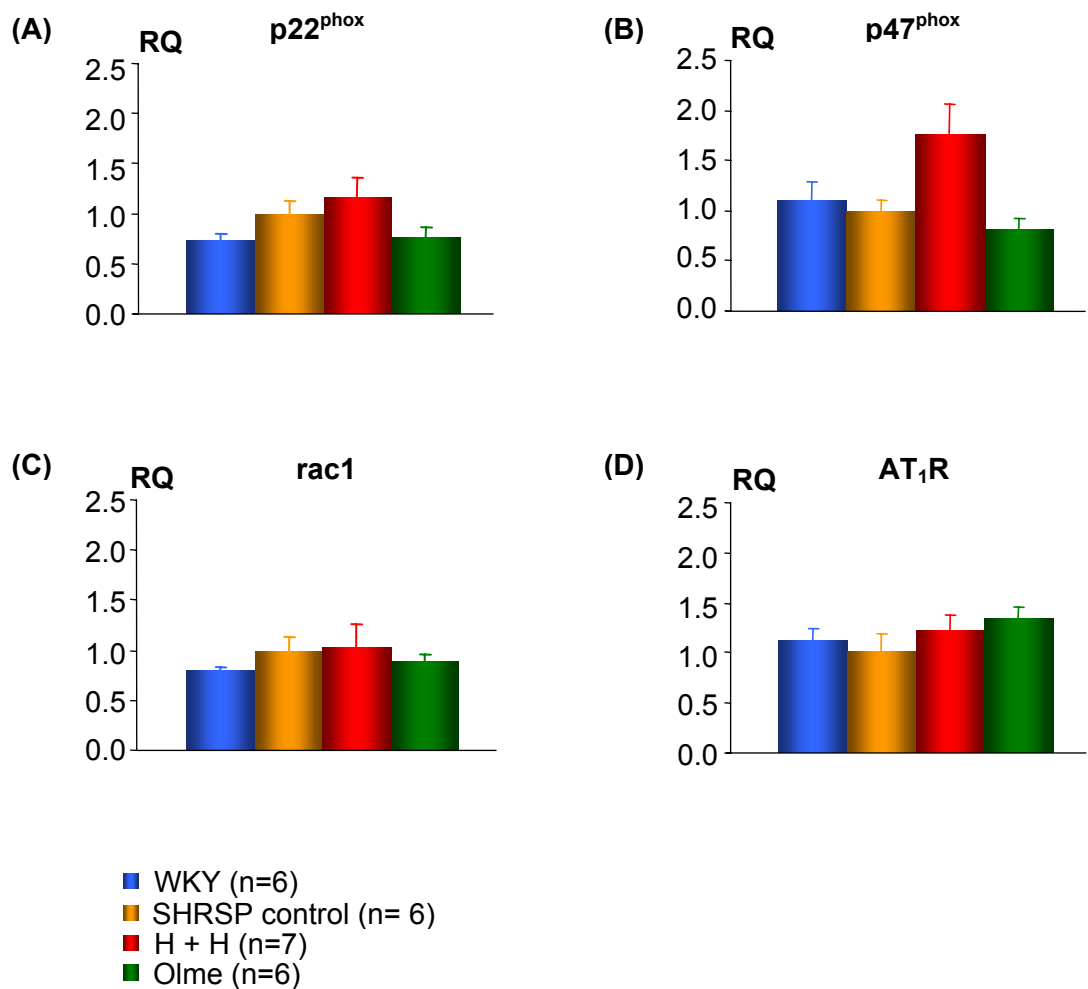


Figure 4.4: Effect of drugs on vascular gene expression in reversal study

Gene expression of p22^{phox}, p47^{phox}, rac1 and AT₁R relative to SHRSP expression levels. RQ = relative quantitation; H + H = Hydralazine + hydrochlorothiazide; Olme = olmesartan.

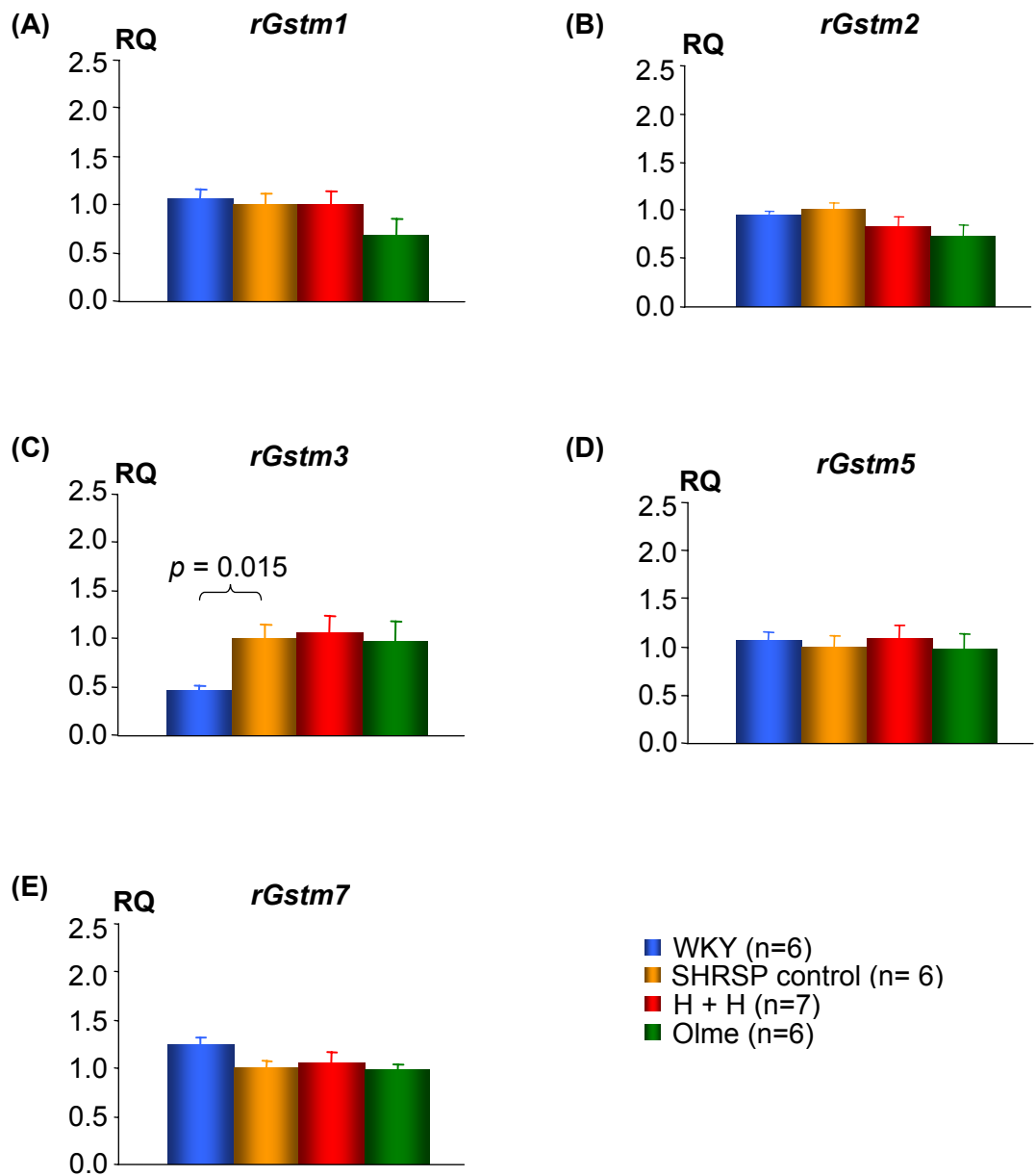


Figure 4.5: Effect of drugs on vascular *rGstm* gene expression in reversal study
 Gene expression of *rGstm1*, *rGstm2*, *rGstm3*, *rGstm5* and *rGstm7* relative to SHRSP expression levels. RQ = relative quantitation; H + H = Hydralazine + hydrochlorothiazide; Olme = olmesartan.

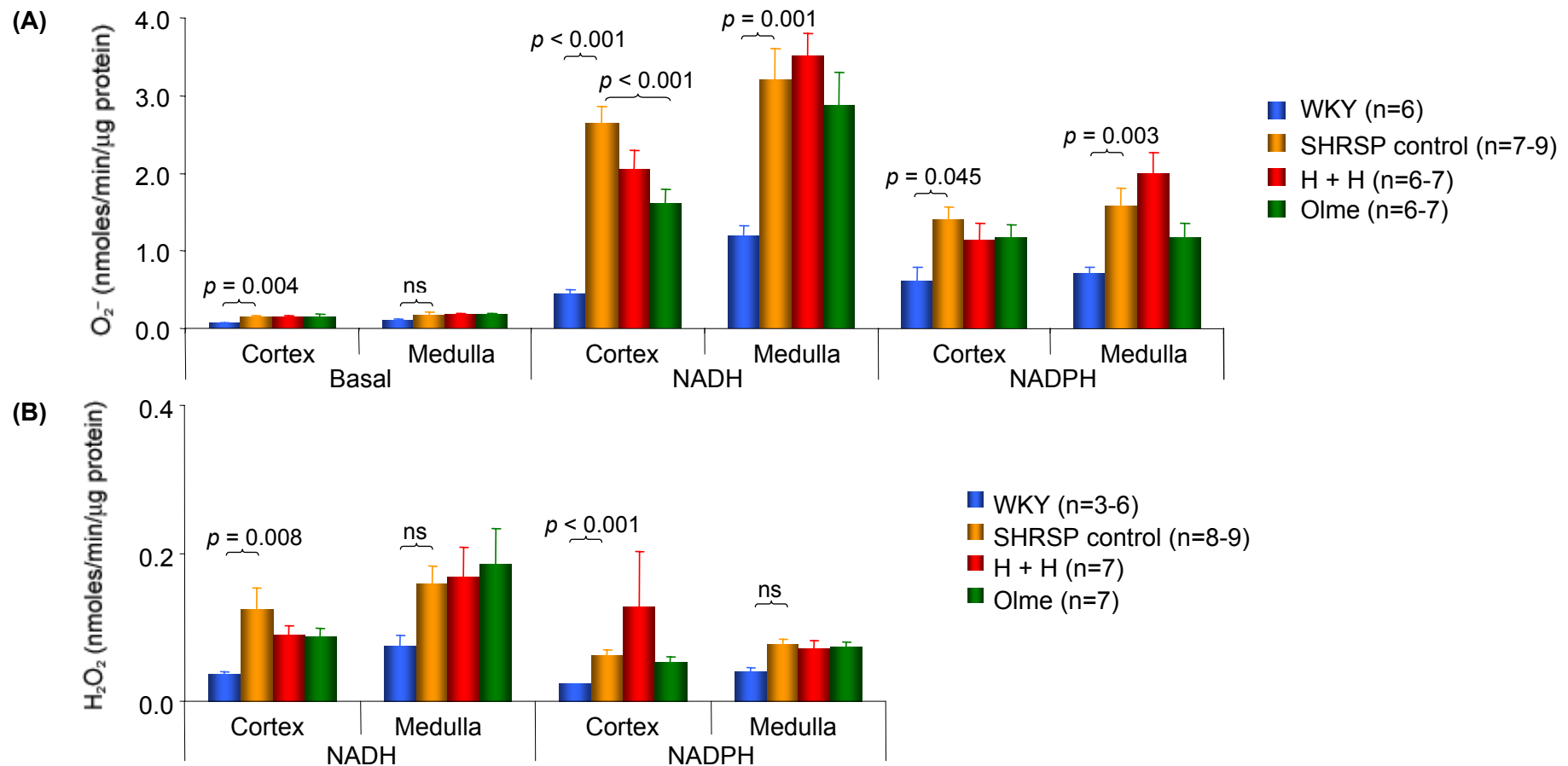


Figure 4.6: Reversal study – Superoxide and hydrogen peroxide production in renal cortex and medulla

(A) Basal, NADH- and NADPH-stimulated O_2^- production in renal cortex and medulla.

(B) H_2O_2 production stimulated with NADH or NADPH in renal cortex or medulla. H + H = Hydralazine + hydrochlorothiazide; Olme = olmesartan; SHRSP = stroke-prone spontaneously hypertensive rat; WKY = Wistar Kyoto; ns = non-significant.

could be observed. SHRSP rats produced significantly higher levels of H₂O₂ in renal cortex with both NADH and NADH stimulation compared to WKY. There was also a non-significant trend towards higher levels of H₂O₂ production in renal medulla from SHRSP compared to WKY (*Figure 4.6B*). A small reduction in NADH-stimulated H₂O₂ production in renal cortex was obtained by both drug treatments but these effects did not reach statistical significance.

As with vascular tissues, gene expression levels of renal NAD(P)H oxidase subunits, regulatory protein rac1 and AT₁R gene expression were measured to determine if the difference in ROS production between SHRSP and WKY was due to differences in gene expression levels (*Figure 4.7*). SHRSP expressed significantly higher level of p47^{phox} mRNA than WKY ($p = 0.032$; CI = 0.12, 1.07) but there were no significant differences in gene expression of p22^{phox}, rac1 or AT₁R. The expression levels of AT₁R, p22^{phox}, p47^{phox} or rac1 were not affected by either drug treatments.

SHRSP expressed significantly lower *rGstm1* than WKY in renal tissue by approximately 5-fold ($p < 0.001$; CI = -2.69, -2.02), *rGstm3* by approximately 1-fold ($p = 0.002$; CI = -1.45, -0.25) and *rGstm7* by approximately 0.5-fold ($p < 0.001$; CI = -0.90, -0.27) (*Figure 4.8*). There were no significant difference in *rGstm2* or *rGstm5* expression between SHRSP and WKY. Neither drug treatments affected the expression levels of the *rGstm* isoforms.

4.3.2. Olmesartan Prevention Study

At 8 weeks of age, the SBP of prehypertensive SHRSP rats was 130mmHg \pm 10mmHg, similar to WKY SBP of 129mmHg \pm 13mmHg (*Figure 4.9*). The SHRSP rats SBP began to rise, reaching 188mmHg \pm 21mmHg by 11 weeks of age and remained at this level for the rest of the duration of the study. The WKY SBP remained between 125mmHg and 137mmHg for the course of the study. Olmesartan and H + H significantly prevented the rise in SBP observed in control SHRSP over the course of the 8-week treatment period ($p < 0.001$). SBP of olmesartan and H + H treated rats were maintained at equivalent levels to that of WKY rats.

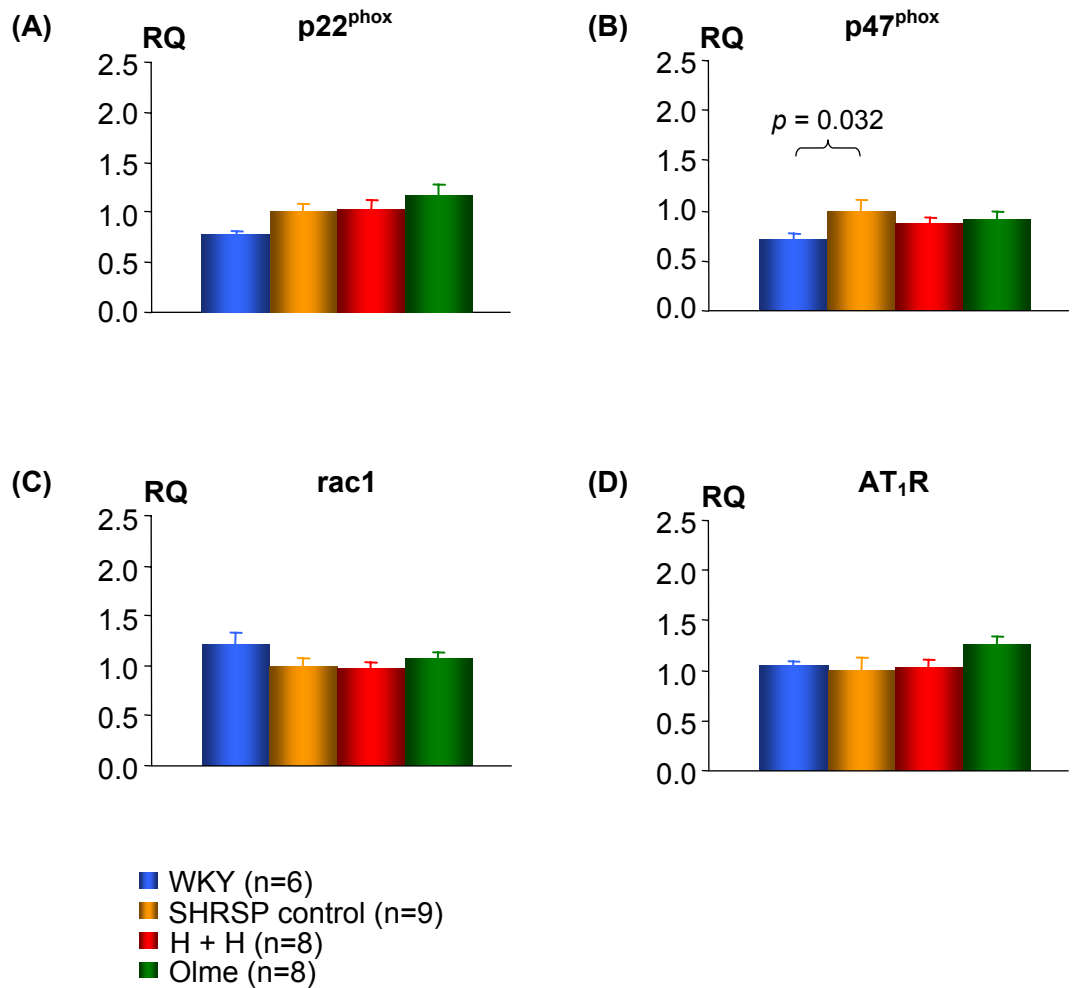


Figure 4.7: Effect of drugs on renal gene expression in reversal study

Gene expression of p22^{phox}, p47^{phox}, rac1 and AT₁R relative to SHRSP expression levels. RQ = relative quantitation; H + H = Hydralazine + hydrochlorothiazide; Olme = olmesartan.

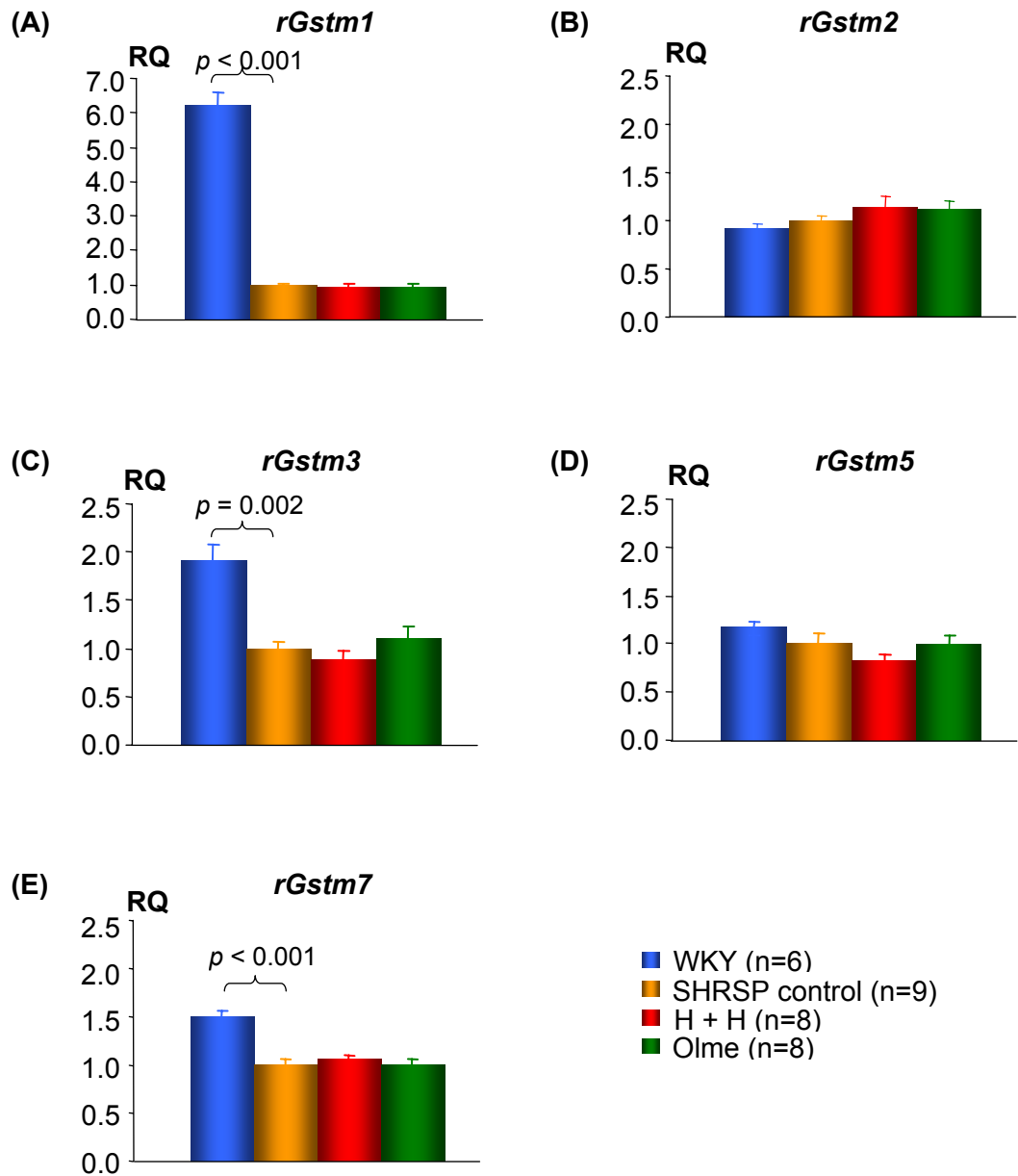


Figure 4.8: Effect of drugs on renal *rGstm* gene expression in reversal study

Gene expression of *rGstm1*, *rGstm2*, *rGstm3*, *rGstm5* and *rGstm7* relative to SHRSP expression levels. RQ = relative quantitation; H + H = Hydralazine + hydrochlorothiazide; Olme = olmesartan.

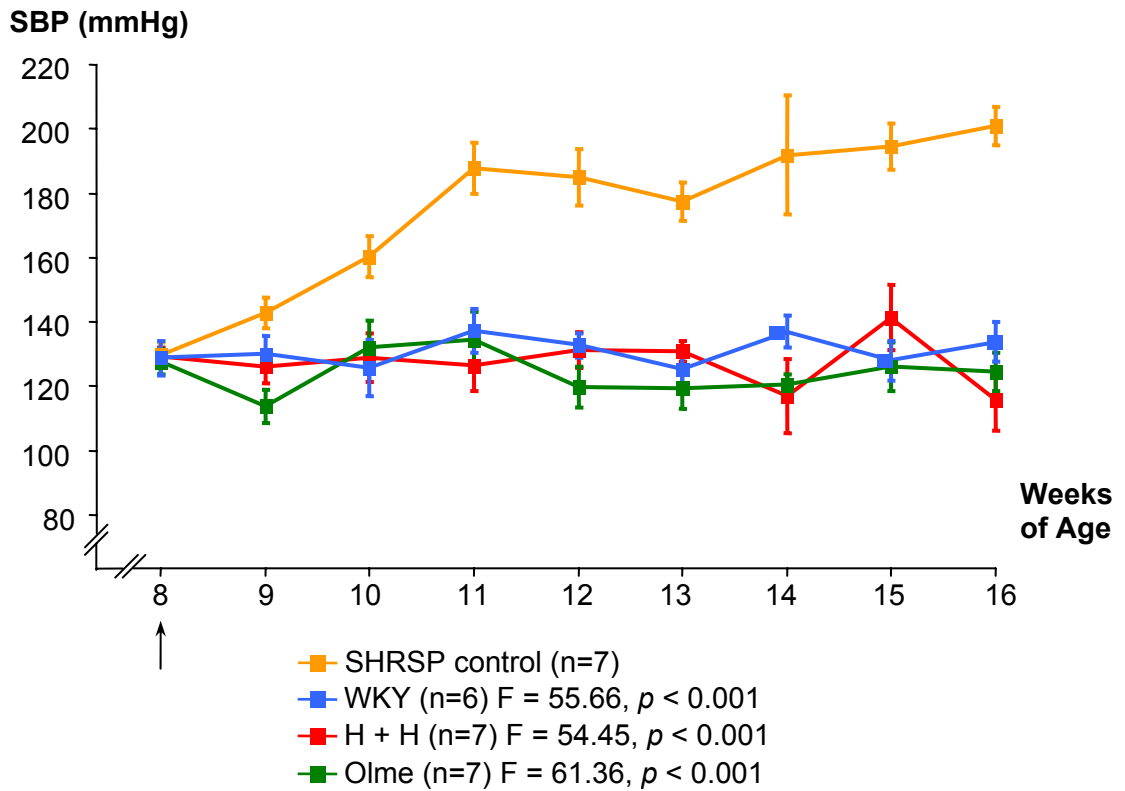


Figure 4.9: Prevention study systolic blood pressure

Prehypertensive 8-week-old SHRSP males were treated with either drug for 8 weeks. WKY rats of the same age were included in parallel. H + H = Hydralazine + hydrochlorothiazide; Olme = olmesartan.

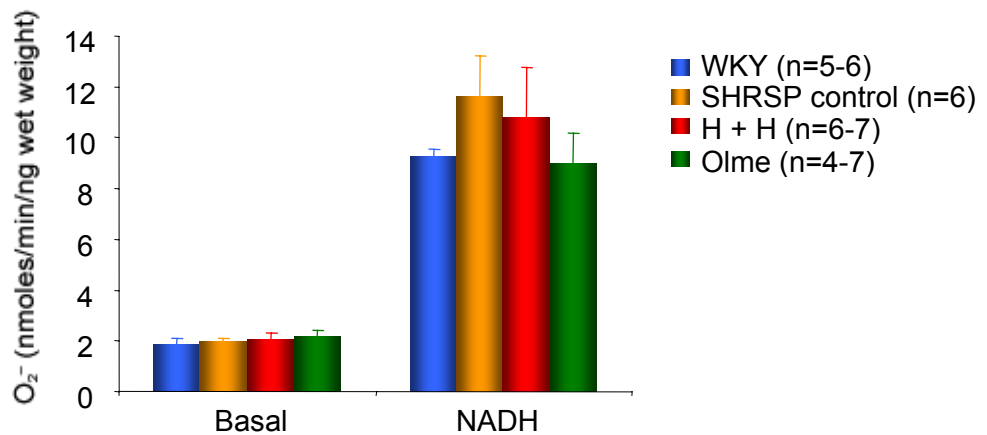


Figure 4.10: Prevention study vascular superoxide production

Basal and NADH-stimulated O_2^- production in aorta from WKY and SHRSP rats treated with vehicle, hydralazine + hydrochlorothiazide (H + H) or olmesartan (Olme).

4.3.2.1. Effect of Drugs on Vascular Function and Gene Expression

As with the reversal study, basal and NADH-stimulated O_2^- productions were measured as a marker of oxidative stress (Figure 4.10). There was no significant difference in basal O_2^- production between the SHRSP and WKY rats. There was a trend towards higher levels of NADH-stimulated O_2^- production in SHRSP but this did not reach statistical significance. Olmesartan appeared to reduce NADH-stimulated O_2^- production to the WKY levels but this reduction was not statistically significant. H + H did not affect the basal or NADH-stimulated O_2^- production.

Again, in order to determine if the difference in O_2^- production between SHRSP and WKY was due to differences in expression levels of vascular NAD(P)H oxidase subunits or Ang II stimulation, the gene expression of p22^{phox}, p47^{phox}, rac1 and AT₁R were measured (Figure 4.11). There were no significant differences in p22^{phox}, p47^{phox}, rac1 or AT₁R gene expression levels between the SHRSP control and WKY. Neither of the drug treatments significantly affected the gene expression of p22^{phox}, p47^{phox}, rac1 or AT₁R.

SHRSP expressed significantly lower *rGstm1* than WKY by approximately 0.6-fold ($p < 0.001$) and *rGstm5* by approximately 0.8-fold ($p = 0.005$; CI = -1.09, -0.37) (Figure 4.12). There were no significant differences in *rGstm2*, *rGstm3* and *rGstm7* between SHRSP control and WKY. Olmesartan significantly increased *rGstm3* expression in SHRSP by approximately 0.5-fold ($p = 0.003$; CI = -1.21, -0.06) and *rGstm7* by approximately 0.4-fold ($p = 0.045$; CI = -1.04, -0.07). Both H + H and olmesartan significantly increased *rGstm5* expression by approximately 0.6-fold ($p = 0.018$; CI = -1.15, -0.13) and 0.7-fold ($p = 0.010$; CI = -1.26, -0.24), respectively. Although H + H increased *rGstm3* and *rGstm7* expression, these were not statistically significant. Neither drug treatments significantly affected the expression levels of *rGstm1* and *rGstm2*.

4.3.2.2. Effect of Drugs on Renal Function and Gene Expression

SHRSP controls demonstrated significantly higher NADH-stimulated O_2^- production in renal cortex and medulla than WKY (Figure 4.13A). The higher NADPH-stimulated O_2^- production in renal cortex and medulla from SHRSP

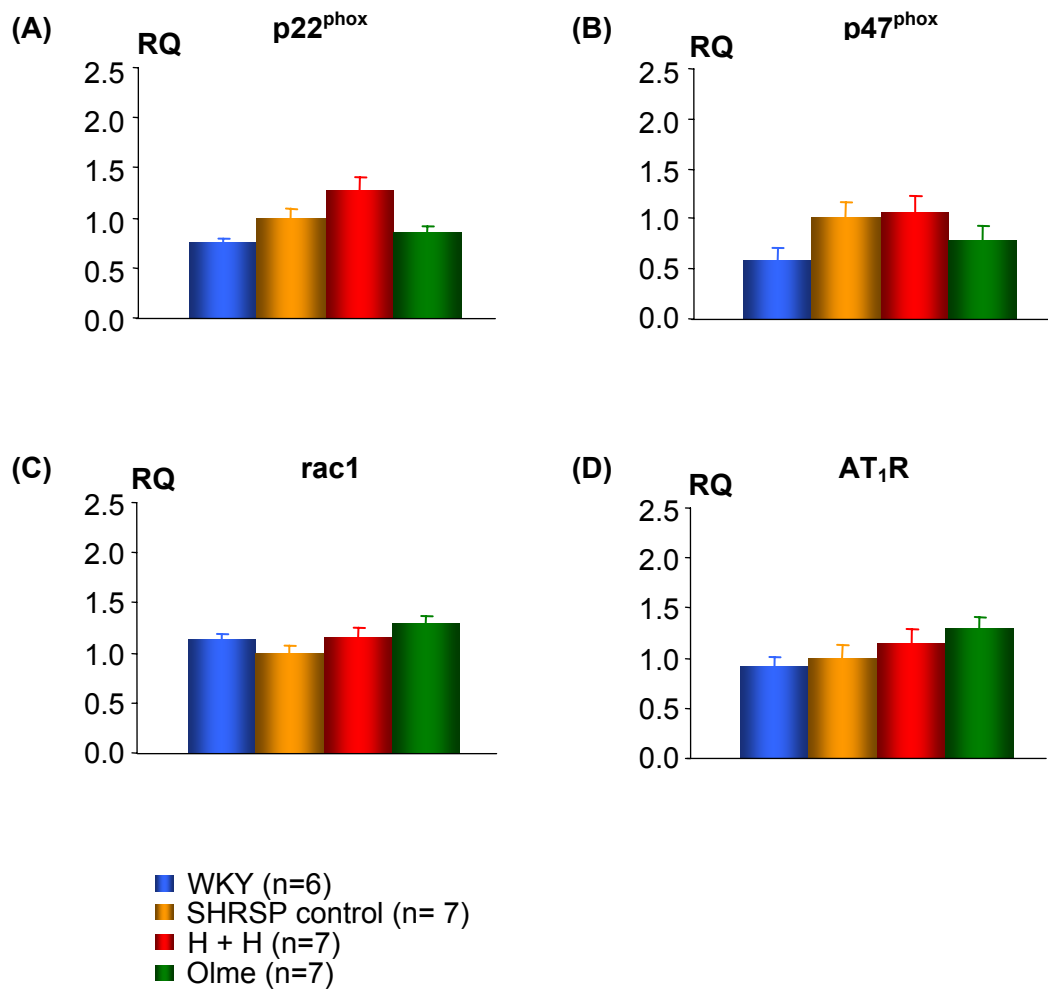


Figure 4.11: Effect of drugs on vascular gene expression in prevention study

Gene expression of p22^{phox}, p47^{phox}, rac1 and AT₁R relative to SHRSP expression levels. RQ = relative quantitation; H + H = Hydralazine + hydrochlorothiazide; Olme = olmesartan.

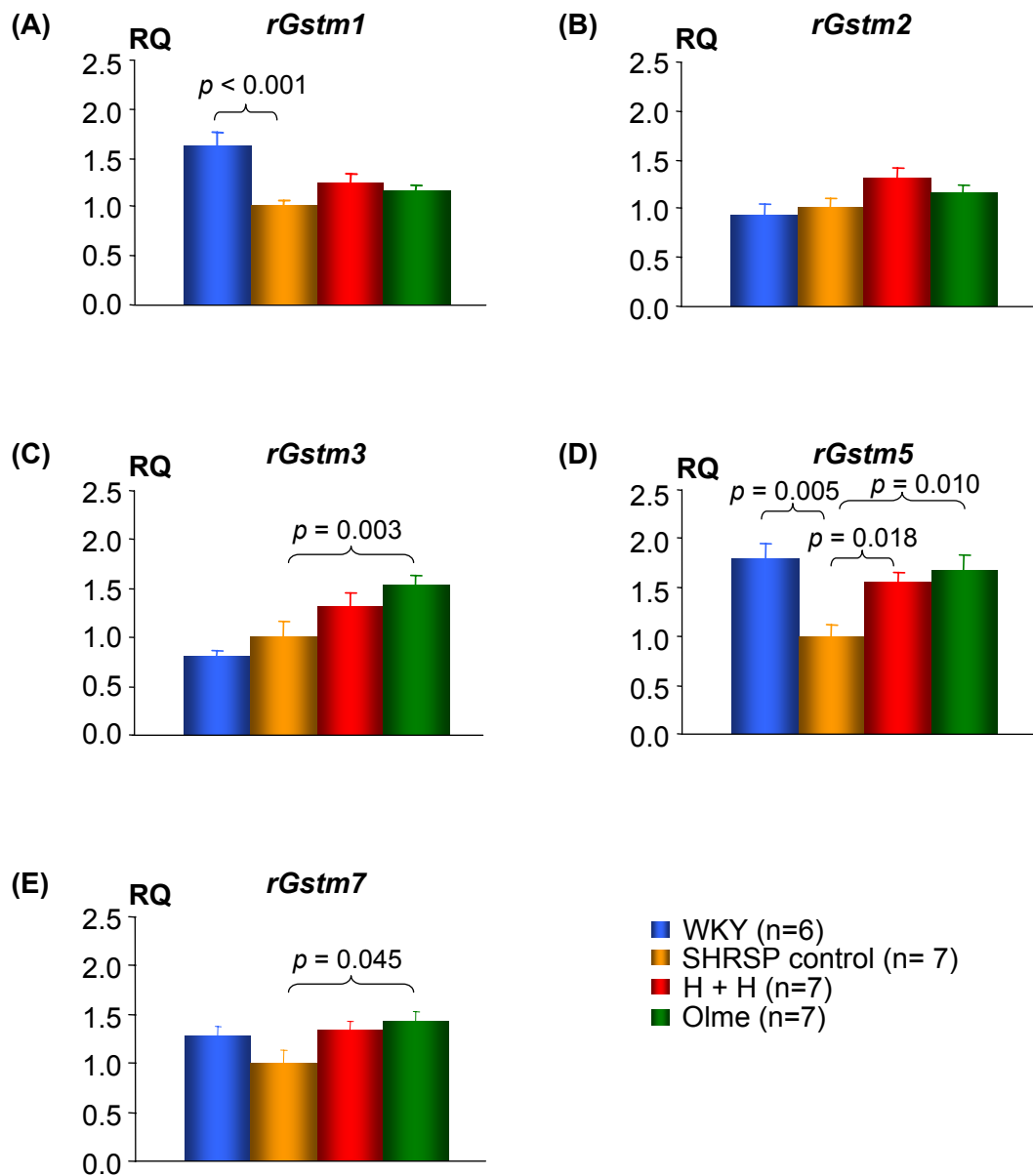


Figure 4.12: Effect of drugs on vascular *rGstm* gene expression in prevention study
 Gene expression of *rGstm1*, *rGstm2*, *rGstm3*, *rGstm5* and *rGstm7* relative to SHRSP expression levels. RQ = relative quantitation; H + H = Hydralazine + hydrochlorothiazide; Olme = olmesartan.

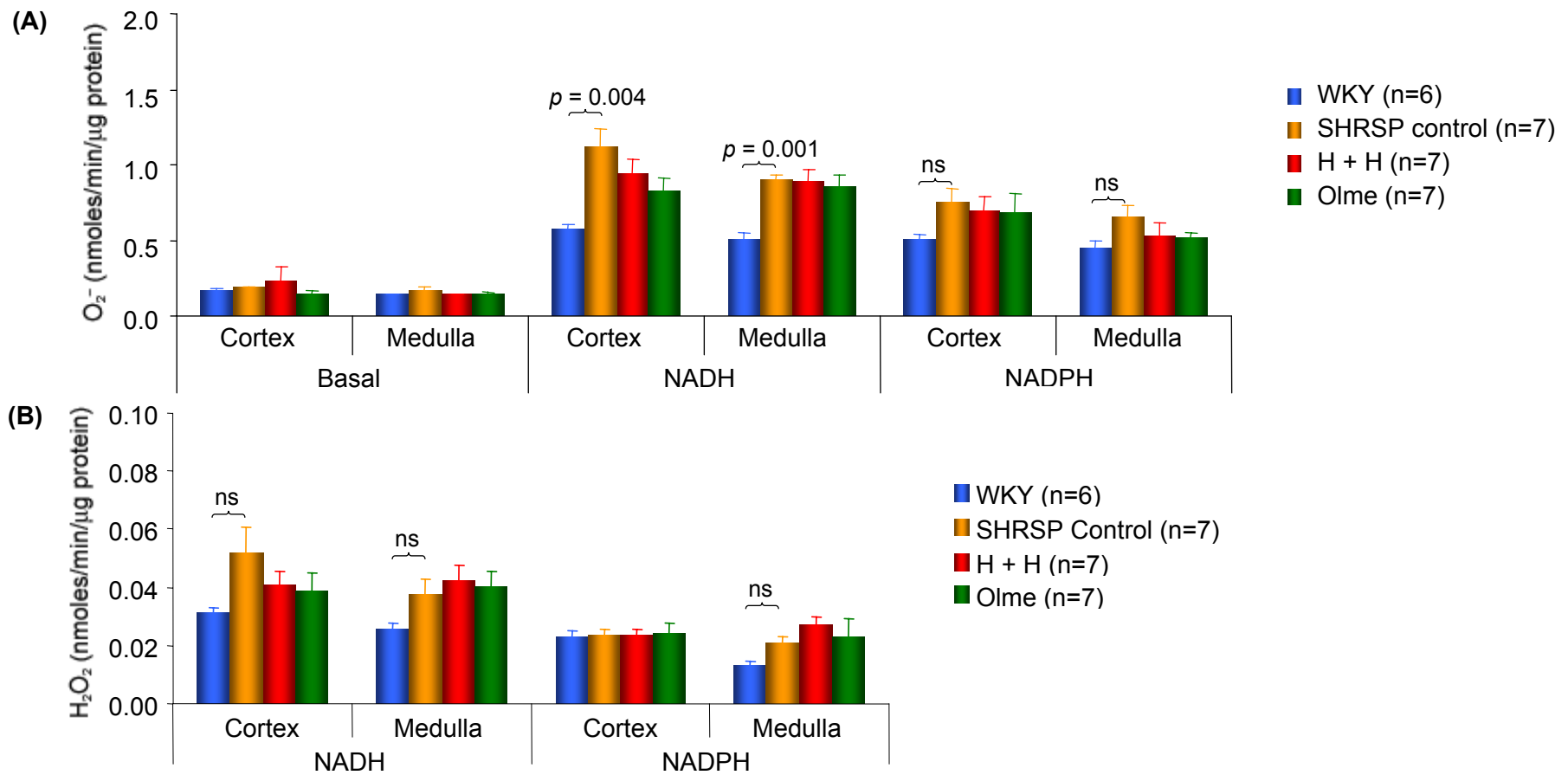


Figure 4.13: Prevention study – Superoxide and hydrogen peroxide production in renal cortex and medulla

(A) Basal, NADH- and NADPH-stimulated O_2^- production in renal cortex and medulla.

(B) H_2O_2 production stimulated with NADH or NADPH in renal cortex or medulla. H + H = Hydralazine + hydrochlorothiazide; Olme = olmesartan; SHRSP = stroke-prone spontaneously hypertensive rat; WKY = Wistar Kyoto; ns = non-significant.

compared to WKY was not significant. There were no significant differences in basal O_2^- production in either cortical or medullary tissues between SHRSP and WKY. Both treatments did not affect the levels of O_2^- production but there was a trend for reduced NADH-stimulated O_2^- production in renal cortex from olmesartan-treated rats. SHRSP control also demonstrated a non-significant trend towards higher H_2O_2 production with NADH-stimulation in renal cortex and medulla, as well as NADPH-stimulation in renal medulla than WKY (Figure 4.13B). As with reversal study, both treatments reduced NADH-stimulated H_2O_2 production in renal cortex but these effects did not reach statistical significance. Both treatments did not affect NADH-stimulated H_2O_2 production in renal medulla or NADH-stimulated H_2O_2 production.

SHRSP untreated controls demonstrated a small (approximately 0.3-fold) but significantly lower $p22^{phox}$ mRNA expression than WKY ($p = 0.023$; CI = $-0.67, -0.08$) (Figure 4.14). Both H + H and olmesartan significantly increased $p22^{phox}$ gene expression ($p = 0.010$; CI = $-0.65, -0.08$ and $p = 0.012$; CI = $-0.62, -0.06$, respectively). There were no significant differences in $p47^{phox}$, *rac1* and *AT₁R* gene expression between SHRSP control and WKY. Olmesartan significantly increased *AT₁R* gene expression by approximately 0.4-fold ($p = 0.012$; CI = $-0.82, -0.14$) while H + H did not affect *AT₁R* gene expression. Both drug treatments did not affect $p47^{phox}$ and *rac1* gene expression.

SHRSP controls expressed significantly lower *rGstm1* than WKY in renal tissue by approximately 5-fold ($p < 0.001$; CI = $-2.97, -2.22$), *rGstm3* and *rGstm5* by approximately 1-fold ($p < 0.001$; CI = $-1.33, -0.57$ and $p < 0.01$; CI = $-1.35, -0.60$, respectively), and *rGstm7* by approximately 0.8-fold ($p < 0.001$; CI = $-1.23, -0.51$) (Figure 4.15). There was no significant difference in *rGstm2* expression level between SHRSP control and WKY groups. Olmesartan treatment significantly increased renal *rGstm5* expression by approximately 0.4-fold ($p < 0.005$; CI = $-0.83, -0.10$) but was not affected by H + H treatment. Both drug treatments did not affect the renal *rGstm1*, *rGstm2*, *rGstm3* and *rGstm7* expression.

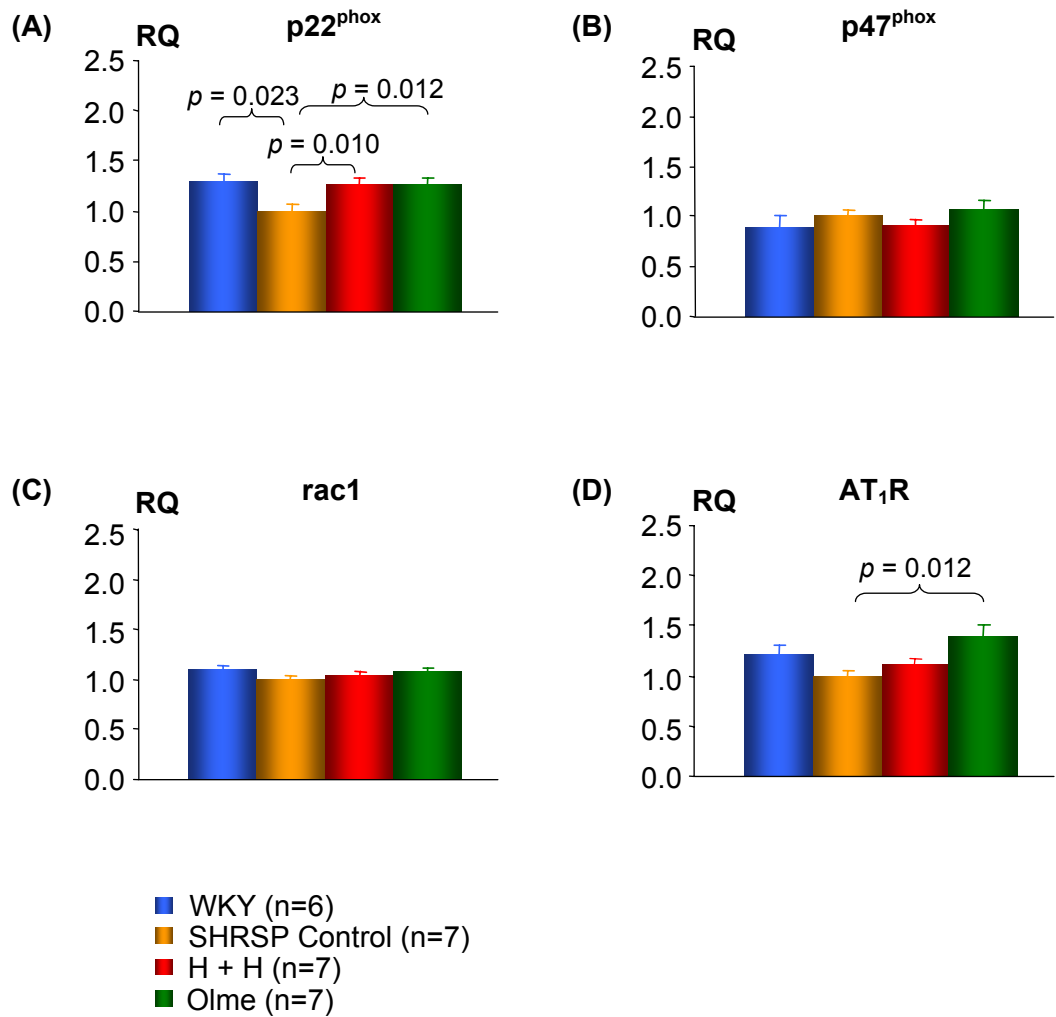


Figure 4.14: Effect of drugs on renal gene expression in prevention study

Gene expression of p22^{phox}, p47^{phox}, rac1 and AT₁R relative to SHRSP expression levels. RQ = relative quantitation; H + H = Hydralazine + hydrochlorothiazide; Olme = olmesartan.

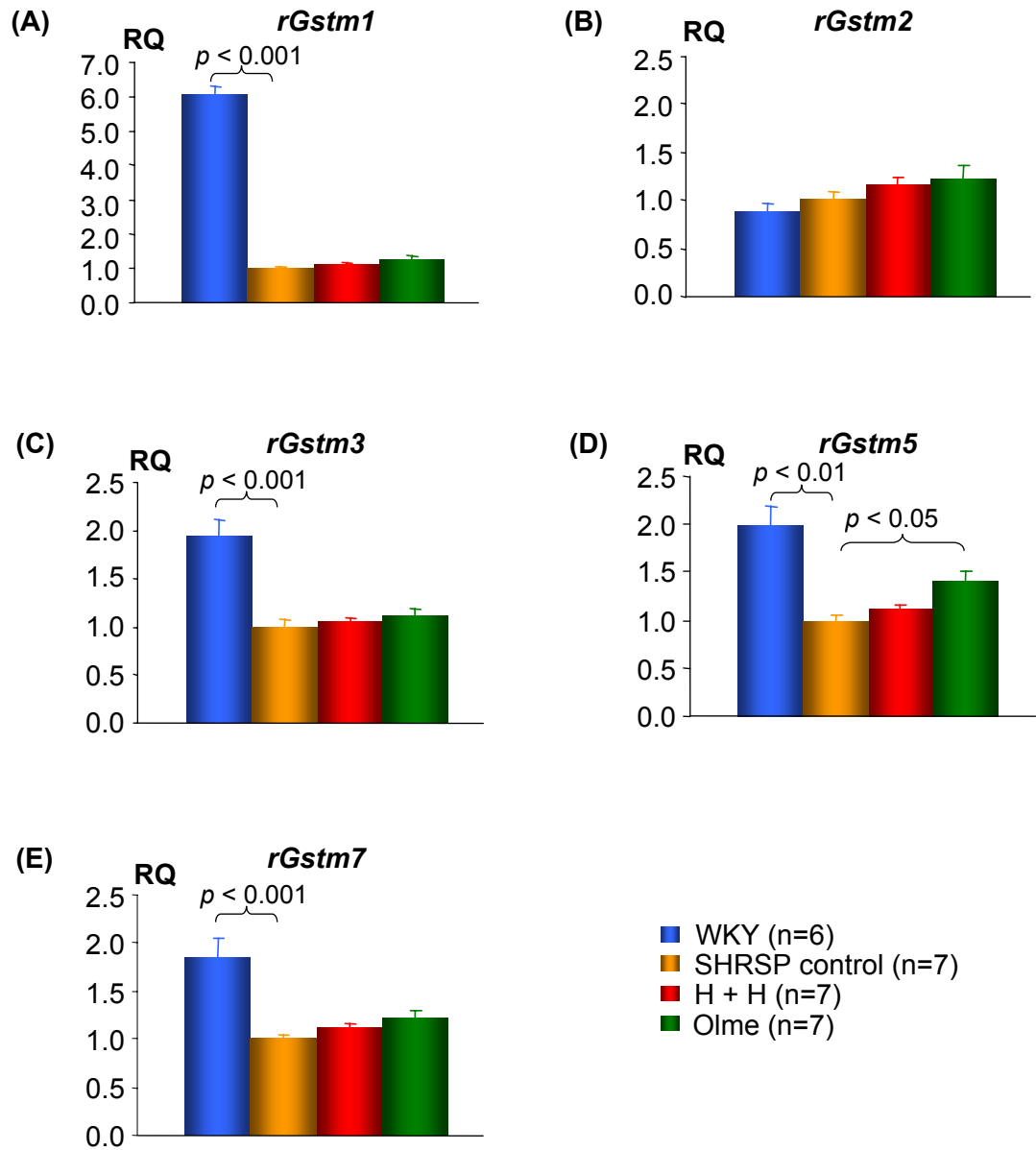


Figure 4.15: Effect of drugs on renal *rGstm* gene expression in prevention study
 Gene expression of *rGstm1*, *rGstm2*, *rGstm3*, *rGstm5* and *rGstm7* relative to SHRSP expression levels. RQ = relative quantitation; H + H = Hydralazine + hydrochlorothiazide; Olme = olmesartan.

4.4. Discussion

Despite significant reductions in SBP by both olmesartan and H + H to equivalent normotensive levels and some improvements in O_2^- levels, this study was unable to show major effects on *rGstm* expression levels, particularly *rGstm1*. This inability to improve *rGstm* expression indicate that the *rGstm* gene defect cannot be modulated by changes in BP.

4.4.1. Vascular Effects of Antihypertensive Treatment

Vascular O_2^- production was significantly higher in SHRSP when compared to WKY in the reversal study. However, vascular O_2^- production was not different between SHRSP and WKY in the prevention study. This observation was unexpected since a previous study from our group has shown higher O_2^- production in abdominal aorta from SHRSP compared to WKY (248). Neither hydralazine plus hydrochlorothizide or olmesartan treatments significantly affect the vascular O_2^- despite lowering BP to normotensive levels. This was unexpected as previous studies have shown reduction in vascular O_2^- production with AT_1R blockade (240;244). However, there was a trend towards reduction in O_2^- in vascular tissue of rats treated with AT_1R blocker.

There was no significant difference in vascular AT_1R , p22^{phox}, p47^{phox} and rac1 expression levels between SHRSP and WKY. Neither treatment affected vascular AT_1R , p22^{phox}, p47^{phox} and rac1 expression levels. These results confirm data from a previous study in male apolipoprotein E knockout mice, where olmesartan did not affect vascular AT_1R , p47^{phox} and rac1 expression nor reduce superoxide production or NAD(P)H oxidase activity (243).

Untreated SHRSP expressed significantly higher vascular *rGstm3* than WKY in the reversal study. This is not surprising since in the previous characterisation chapter, *rGstm3* was shown to increase with age in the SHRSP to a significantly higher level than WKY. There were no differences in vascular *rGstm1*, *rGstm2*, *rGstm5* and *rGstm7* expression in the reversal study. In the prevention study, *rGstm1* and *rGstm5* were significantly higher in WKY thoracic aorta than SHRSP. In contrast to the previous characterisation chapter, the higher vascular *rGstm1* and *rGstm5*

expression in WKY rats of the same age did not reach statistical significance. Both drug treatments significantly increased vascular *rGstm5* expression but only olmesartan treatment significantly increased *rGstm3* and *rGstm7* expression. These results suggest that different control mechanisms may regulate or influence the expression of different vascular *rGstm* isoforms. RAS may influence expression of some of the *rGstm* genes via Ang II. As the improvements in *rGstm* expression were observed in the prevention but not the reversal study, this suggests that once mature levels of BP have been achieved the changes in *rGstm* expression cannot be reversed.

4.4.2. Renal Effects of Antihypertensive Treatment

Generally, data from the current reversal and prevention studies, demonstrated that SHRSP produces higher levels of renal ROS than WKY rats. The levels of ROS production in renal cortex and renal medulla were similar in 16-week-old rats but were higher in renal medulla than renal cortex in 20-week-old rats. This is in agreement with the study by Zou et.al. 2001, in which they showed that renal outer medulla exhibited the greatest enzymatic activities for O_2^- production (249). Increased superoxide concentration within the renal medulla selectively reduced medullary blood flow resulting in chronic hypertension (250), possibly involving other ROS such as H_2O_2 (251). There were trends towards decreased ROS production in renal cortex by both drug treatments when stimulated with NADH and NADPH, the largest effect occurring with olmesartan treatment. The reductions in ROS production were greater in reversal study compared to prevention study. This suggests that some of the renal oxidative stress in hypertension was a consequence of increased BP.

Results from the reversal study showed that SHRSP expressed small but significantly higher levels of $p47^{phox}$ mRNA than WKY. In contrast, SHRSP expressed significantly less $p22^{phox}$ mRNA than WKY in the prevention study. Prevention of BP increase with both drug treatments increased $p22^{phox}$ expression significantly, and olmesartan treatment increased AT_1R expression. These results were surprising as SHRSP was expected to express higher levels of $p22^{phox}$, $p47^{phox}$ and $rac1$, which would be decreased with AT_1R blockers. Despite this, the differences were less than 0.5-fold and may consequently have little biological

importance. Zou et. al. 2001 previously determined that NADPH oxidase and mitochondrial enzymatic sources were responsible for O_2^- production in outer medulla (249). It is also likely that the expected differences in gene expression were more pronounced in the medulla. However, for the current study, whole kidney was homogenised for gene expression measurements therefore the important differences might have been missed.

SHRSP expressed significantly lower renal *rGstm1*, *rGstm3* and *rGstm7* than WKY in both reversal and prevention study. SHRSP also expressed significantly lower *rGstm5* than WKY in the prevention study. This confirms the differential expression of *rGstm* genes observed in the previous chapter. Preventing BP increase with olmesartan increased *rGstm5* expression significantly but only slightly and had no effect on the other *rGstm* family members. This suggests that the differential *rGstm* gene expression was not a secondary effect of high blood pressure. This is further supported by the observation that *rGstm1* gene expression was reduced in SHRSP prior to development of hypertension as reported in the previous chapter and by McBride et. al. 2005 (67). Both drug treatments did not have a great impact on the *rGstm* gene expression, despite improvements in SBP in the reversal study. Okuda et. al. 2002 also previously identified *rGstm1* as a positional and physiological candidate gene for blood pressure regulation (65;66). In one of their studies, short-term treatment with the antihypertensive drugs enalapril or hydralazine decreased the blood pressure of the SHR but did not modify the expression levels of renal *rGstm1* (65). Taken together, these results demonstrated that improvement in BP does not improve *rGstm1* gene expression. The *rGstm* gene family is less consistently influenced by pharmacological interventions due to strain-dependent genetic abnormalities.

CHAPTER 5: GENE – PHENOTYPE INTERACTIONS IN THE OXIDATIVE STRESS PATHWAY

5.1. Introduction

We hypothesise that polymorphisms in enzymes responsible for the balance between ROS species and NO bioavailability influence the risk of developing hypertension and thus coronary artery disease. The aim of this study was to look for association between three polymorphisms in *CYBA* and *NOS3* genes with coronary artery disease and arterial stiffness. *CYBA* and *NOS3* genes are selected as a representative gene on each side of the balance. *CYBA* encodes for p22^{phox} subunit of NAD(P)H oxidase, which produces superoxide anion (the first reactive oxygen species of the reactive oxygen radical cascade) while *NOS3* encodes for eNOS enzyme, which produces NO required for vasodilation. Three arterial stiffness indices were selected for investigating the association between *CYBA* and *NOS3* polymorphisms and arterial stiffness.

5.1.1. *CYBA* Polymorphisms

In recent years, polymorphisms within the 8.5kB long genomic *CYBA* gene localised to chromosome 16q24, encoding the p22^{phox} subunit of NAD(P)H oxidase, have been associated with higher risk of CAD (252). Four types of allelic polymorphisms in the *CYBA* gene were reported by Dinauer et. al. 1990 (253). In addition, there are three other SNPs within the *CYBA* gene (254). Of these, the C242T polymorphism in exon 4 of *CYBA* results in a change from histidine at residue 72 to tyrosine (His72Tyr), in the potential haem-binding site (253). The SNP A640G in the 3' untranslated region (3'UTR) of the mRNA transcript had been suggested to be related to mRNA processing and stability, which may influence p22^{phox} protein biosynthesis (255). The C242T, but not the A640G polymorphism, was first associated with CAD in a Japanese population (256). The authors speculated that the C242T polymorphism might modulate the activity and regulation of NAD(P)H oxidase, which leads to decrease in oxidative stress and thus reduce susceptibility to CAD. In contrast, the A640G, but not the C242T polymorphism, was found to be associated with CAD in the Caucasian population (255). Since then, there have been contrasting results as to whether there was an

association of either of these two SNPs with CAD (257-259). A new polymorphism in the promoter region (A-930G) of the human *CYBA* gene was found to be associated with essential hypertension in the Caucasian population (260). Transfection experiments on rat vascular smooth muscle cells (VSMCs) showed that the G allele produced increased reporter gene expression by 30% in cells from hypertensive rats (260;261). In this study, investigation of polymorphisms A-930G, C242T and A640G as individual SNP as well as haplotype in the West of Scotland population and to determine if there was an association with CAD as single locus polymorphism and as three-SNP haplotype. C242T was reported to be in linkage disequilibrium with A640G in Caucasians (255) but there was no information regarding the linkage disequilibrium score between either C242T or A640G with A-930G. Hence, analysis of linkage disequilibrium between the three SNPs was also undertaken.

5.1.2. NOS3 Polymorphisms

Endothelial nitric oxide synthase (eNOS) is encoded by 21kB *NOS3* gene localised to chromosome 7q36 (262;263). To date, the two most studied polymorphisms due to their transcriptional and functional effects are T-786C in the promoter region and G894T in exon 7. Three linked mutations (T-786C, A-922G and T-1468A) in the 5'-flanking region of *NOS3* gene were associated with coronary spasm in a Japanese population (264). Reporter assays of constructs of the mutations showed that T-786C reduced promoter activity by 52%. The G894T polymorphism results in the production of glutamate or aspartate at position 298 respectively (265;266). The 894T allele produces a protein that is more susceptible to proteolytic cleavage. These polymorphisms had been associated with CAD, acute myocardial infarction, atherosclerosis and hypertension (264;267-275). A third polymorphism consists of either four or five tandem repeats of 27bp in intron 4, known as 4A or 4B respectively, and has been associated with expression levels of eNOS (276). The association between this polymorphism and CAD is less consistent (269;272;277). In this project, associations between these three polymorphisms and CAD as single locus polymorphisms and haplotype was investigated. In addition, it was determined whether different expression levels observed with 4A/4B might be the effect of linkage disequilibrium with T-786C or G894T.

5.1.3. Arterial Stiffness and Vascular Compliance

Arterial stiffness is an intermediate phenotype and can be assessed non-invasively. Arterial stiffness describes rigidity of arterial walls, often expressed as indices such as large (C1) and small artery compliance (C2) and augmentation index (Alx) (*Table 5.1*) (278;279). C1 describes the relationship between pressure change and volume change in the arteries during the exponential component of diastolic pressure decay. C2 describes the relationship between oscillating pressure change and oscillating volume change around the exponential pressure decay during diastole. Alx is the difference between the second and first systolic peaks as a percentage of pulse pressure. Arterial stiffness increases both with age and BP, and is elevated in subjects with other risk factors for CVD (278;280). Arterial stiffness is also related to endothelial function in large and small arteries (281;282). Changes in arterial stiffness can be detected before the appearance of clinically apparent vascular disease (278). Alx is also highly predictive of CV mortality (283).

The first aim of this study was to look for association between the three polymorphisms in CYBA and NOS3 genes with CAD as single locus polymorphisms and haplotypes consisting of 3 polymorphisms. The second aim of this study was to look for association between CYBA and NOS polymorphisms with arterial stiffness indices C1, C2 and Alx as single locus polymorphisms and 3-polymorphisms haplotypes.

5.2. Materials & Methods

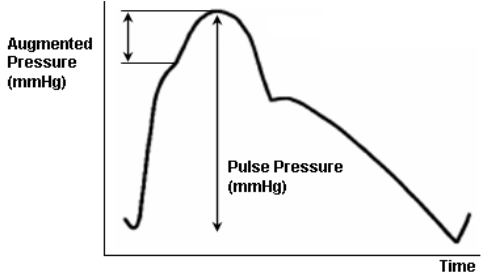
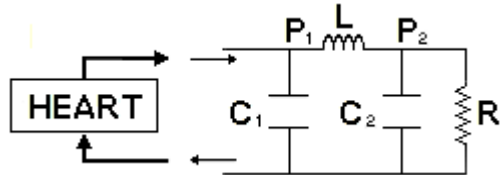
The vascular compliance measurements were carried out by Dr. Christian Delles, Dr. Lukas Zimmerli, Dr. David McGrane and Dr. Russell Drummond. The details for the equipments, chemicals, reagents and consumables used in this study are listed in *Appendix B*.

5.2.1. Subjects

Full ethical approval was attained from the West Ethics Committee, Glasgow and all the subjects had given informed consent for the use of their DNA for

Table 5.1: Indices of arterial stiffness

Terms	Definitions	Formula
Pulse wave velocity (PWV)	Velocity of travel of the pulse along a length of artery with the equation	$\frac{\text{Distance (cm)}}{\Delta t \text{ (s)}}$
Capacitative or “large” artery compliance (C1)	Change in volume (ΔV)/ change in pressure (ΔP) during diastolic decay	$\frac{\Delta V \text{ (cm}^3\text{)}}{\Delta P \text{ (mmHg)}}$
(Windkessel Model)	$\Delta V/\Delta P$ during oscillations around diastolic decay (ml/mmHg)	$\frac{\Delta V \text{ (cm}^3\text{)}}{\Delta P \text{ (mmHg)}}$
Augmentation index (Aix)	Difference in pressure between first and second peaks (ΔP) of the central pressure waveform, expressed as a percentage of PP.	$\frac{\Delta P \times 100\%}{PP}$



R = systemic vascular resistance; L = inertia of the blood; P1 = proximal pressure; P2 = distal pressure. Adapted from Ref. (278;279;284;292)

cardiovascular research. The coronary artery disease (CAD) cohort consisted of patients with angiographically proven obstructive CAD, who were about to undergo coronary artery bypass graft surgery. Patients with evidence of secondary hypertension or hormonal, renal and hepatic abnormalities were excluded from this study. Patients who did not have regular sinus rhythm were also excluded as arrhythmias including atrial fibrillation change the pressure shape. The control subjects were recruited from local universities and a local health club. Control subjects underwent clinical assessment and did not have evidence of CAD or other CVD including hypertension. Each subject had their baseline demographic measurements recorded.

5.2.2. Pulse Wave Analysis

The subjects were placed in the supine position and right radial artery waveforms were acquired with the use of a calibrated proprietary tonometer (model CR-2000 Hypertension Diagnostics Inc.) after a 30min resting period. The subject's arm was stabilised in an angulated wrist support and radial artery waveforms analysed for a 20sec period. The CR-2000 device then utilises the 4 element modified Windkessel model to generate large (C1) and small artery elasticity index (C2) (284;285). For both C1 and C2, the average of four independent readings was calculated. The SphygmoCor device (PWV Medical, Sydney, Australia) was used for estimation of the central augmentation index (AIx) corrected for heart rate, expressed as a percentage of pulse pressure.

5.2.3. DNA samples

Whole blood samples in ethylenediaminetetraacetic acid (EDTA) tubes collected were stored at 4°C for DNA extraction. DNA samples were extracted routinely within a fortnight in batches using the Promega Wizard genomic DNA kit according to the manufacturer's instructions. The DNA samples were re-solubilised in 400µl of 1x Tris borate EDTA (TBE) buffer and quantified as described in section 2.4.3.

5.2.4. PCR

An optimisation PCR with annealing temperature set as a gradient from 50°C to 65°C were run prior to any experimental PCR of the DNA samples to determine the optimal PCR conditions for every polymorphism. The PCR reactions were run on the Peltier Thermal Cycler (PTC-225). The primers for each of the genotype, the sizes of their PCR products and the annealing temperature used are as in *Table 5.2*.

For the *CYBA* A-930G, C242T, *NOS3* T-786C and intron 4 VNTR, a 20µl PCR reaction was set up containing a final concentration of 1.5mM MgCl₂, 1X buffer, 0.2mM dNTPs, 0.5µM of each primer, 0.01u/µl of Qiagen HotStar Taq polymerase and 25ng of DNA. The forward primer used for genotyping of the eNOS intron 4 alleles was tagged with 6-FAM at the 5'-end. For the *CYBA* A640G and *NOS3* G984T, a 20µl PCR reaction was set up containing a final concentration of 1.5mM MgCl₂, 1X buffer, 1X Q-solution, 0.2mM dNTPs, 0.5µM of each primer, 0.01u/µl of Qiagen HotStar Taq polymerase and 25ng of DNA.

5.2.5. Genotyping

5.2.5.1. Genotyping by Sequencing

The *CYBA* A-930G and A640G; and *NOS3* T-786C and G894T were genotyped by direct sequencing as described in section 2.4.6.

5.2.5.2. Genotyping of by RFLP

The PCR products for C242T polymorphism of 348bp were digested with restriction enzyme (RE) *RsaI* at 37°C for 2hr. A 20µl reaction was set up with 10µl PCR products, 1u/µl RE and 1X RE buffer. There is no *RsaI* restriction site in the C242 allele of p22phox while T242 mutation introduces a *RsaI* site digesting the PCR product into 2 fragments of 160bp and 188bp. The digested fragments were resolved in a 2% agarose gel. 14 random samples were amplified and genotypes determined by sequencing. As these were shown to match completely with the

Table 5.2: Genotyping primers for *CYBA* and *NOS3*

Gene	SNPs	Primers	Sequences (5'---3')	AT	PCR size
<i>CYBA</i> (p22phox)	A-930G Promoter	For Rev	CCACCAAGTGCCTCGGATGG TGGACTCCCTGACAGGTGCC	59°C	255bp
<i>CYBA</i> (p22phox)	C242T Tyr72His	For Rev	TGCTTGTGGGTAAACCAAGG GGAAAACACTGAGGTAAGTG	55°C	348bp
<i>CYBA</i> (p22phox)	A640G 3'UTR	For Rev	AGCAGTGGACGCCCATGGAGCCCAA CGCTGCGTTTATTGCAGGTGGGTGC	61°C	258bp
<i>NOS3</i> (eNOS)	T-786C Promoter	For Rev	TGGAGAGTGCTGGTGTACCCCA GCCTCCACCCCCACCCTGTC	62°C	180bp
<i>NOS3</i> (eNOS)	VNTR (27bp) Intron 4	For Rev	*AGGCCCTATGGTAGTGCCTTT TCTCTTAGTGCTGTGGTCAC	57°C	4A: 393bp 4B: 420bp
<i>NOS3</i> (eNOS)	G894T Asp298Glu	For Rev	AAGGCAGGAGACAGTGGATGGA CCCAGTCAATCCCTTTGGTGCTCA	58°C	248bp

*6-FAM dye was tagged to 5'-end of primer

results from RFLP, further analysis of C242T polymorphism were done using RFLP.

5.2.5.3. Genotyping by PAGE Resolution

2 μ l of the PCR products were diluted 1/20, of which 1 μ l were added into 10 μ l of formamide with DNA ladder GeneScan™ 500 Liz™ size standard in a barcoded plate and analysed on the 3730 DNA analyser and GeneMapper v2.0 software. The rest of the un-diluted PCR products were kept at -20°C. When necessary, different dilutions of the PCR products were prepared for analysis on the 3730 DNA analyser.

5.2.6. Statistical Analysis

The linkage disequilibrium (LD) tests were performed using the EMLD software (Author: Qiqing Huang; <https://epi.mdanderson.org/~qhuang/Software/pub.htm>), where the pair-wise haplotype reconstruction and frequencies were estimated based on the expectation-maximisation algorithm. The genotype analyses were performed using the software PHASE version 2.1 (<http://www.stat.washington.edu/stephens/software.html>) (286;287). The genotype analyses for both genes were run with 200 iterations, 5 thinning intervals and burn-in of 200, with the algorithm run repeated ten times. All 153 samples, including both cases and controls, were used to estimate recombination rates. The likelihood ratio statistical test (not affected by HWE) was used to test for differences among the cases and controls. The 2-proportions test was used to test for significance between the two groups for each haplotype combination. ANOVA was used to test for association between each polymorphism and phenotypic traits of CAD.

The haplotype association analysis was carried out using the large artery compliance, small artery compliance and Alx as the phenotypic traits of interest in both genes. This was done using the software whap (Author: Shaun Purcell and Pak Sham; <http://pngu.mgh.harvard.edu/purcell/whap/>). This programme used the likelihood ratio test to determine if any of the haplotypes were significantly associated with the phenotypic traits of interest. The haplotype frequencies

generated by whap programme was similar to the haplotype frequencies generated by PHASE. The whap programme also gives an overall p -value for association between haplotype frequencies and clinical phenotypes, comparing the two groups.

5.3. Results

A significantly higher proportion of the CAD subjects were males and older than the control subjects (*Table 5.3*). The pulse pressure (PP) and Alx were significantly higher in the CAD group. The C2 was significantly lower in the CAD group. There were no statistical difference in SBP, DBP C1 and heart rate between the CAD and control groups. The CAD subjects had significantly higher levels of plasma triglycerides and very low density lipoprotein (VLDL) cholesterol but significantly lower levels of total cholesterol, high density lipoprotein (HDL) cholesterol and low density lipoprotein (LDL) cholesterol.

5.3.1. Genotype and Haplotype Analysis of CYBA Polymorphisms

Odds ratios (OR) were estimated from logistic regression analysis for the genotypes without making any assumptions and with the assumptions for recessive and dominant models. The Hardy-Weinberg equilibrium (HWE) tests (*Table 5.4*) showed that the C242T and A640G polymorphisms were not deviant from HWE, while the A-930G SNP deviated from HWE in both groups ($p \leq 0.05$).

The most common genotypes are -930^{G/G}, 242^{C/T} and 640^{A/G} (*Table 5.4*). The logistic regression analyses found that the -930^{A/A} frequencies were significantly different between the patients and controls ($p = 0.042$) but no evidence of association was found for the C242T and A640G SNPs with CAD. The frequencies of the -930^{A/A} genotype between the two groups were significantly different in the recessive model ($p = 0.011$) but not the dominant model ($p = 0.535$). The T allele at position 242 was previously shown to have a dominant effect (288) but there was no significant difference in genotype frequencies of C242T between the two groups from the current study, even when the dominant model was applied. There was no significant difference in the A640G genotype frequencies between the two groups, even when the recessive or dominant models were employed.

Table 5.3: Baseline characteristics of the study subjects

Characteristics	Control (n=156)	CAD (n=209)	p-value
Gender (M/F)	81/75	161/48	<0.001*
Age (year)	53 ± 11	62 ± 9	<0.001*
Systolic BP (mmHg)	130.4 ± 16.5	132.8 ± 18.4	0.228
Diastolic BP (mmHg)	73.9 ± 9.2	71.9 ± 9.8	0.064
Pulse pressure (mmHg)	56.6 ± 11.1	60.1 ± 12.4	0.011*
C1 (ml/mmHg x 10)	13.88 ± 4.17	14.71 ± 4.80	0.107
C2 (ml/mmHg x 100)	5.58 ± 3.22	4.60 ± 2.70	0.005*
Augmentation Index (%)	22.8 ± 12.2	26.5 ± 11.1	0.009*
Heart Rate (beats/min)	62 ± 10	61 ± 11	0.206
Total cholesterol (mmol/L)	5.15 ± 1.08	4.09 ± 0.91	<0.001*
Triglycerides (mmol/L)	1.33 ± 0.78	1.91 ± 1.08	<0.001*
HDL cholesterol (mmol/L)	1.44 ± 0.37	1.06 ± 0.35	<0.001*
LDL cholesterol (mmol/L)	3.11 ± 1.00	2.16 ± 0.76	<0.001*
VLDL cholesterol (mmol/L)	0.69 ± 0.38	0.87 ± 0.49	0.001*

All data are expressed as mean ± SD. Augmentation index (AIx) has been corrected for the heart rate. The gender distributions in the two groups were compared using the χ^2 test. The other comparisons were made using the 2-sample t-test for normally distributed data and Mann-Whitney U-test for data not following normal distribution. * denotes characteristics that are significantly different between the control and coronary artery disease (CAD) groups. BP = blood pressure; C1 = large artery compliance; C2 = small artery compliance; HDL = high density lipoprotein; LDL = low density lipoprotein; VLDL = very low density lipoprotein

Table 5.4: Single SNP genotype distribution of CYBA gene

	Control	CAD	OR (95% CI)	p-value
A-930G	(n = 136)	(n = 204)		
GG	64 (47.06%)	103 (50.49%)	1.00	
AG	28 (20.59%)	60 (29.41%)	1.33 (0.77 - 2.30)	1.696
AA	44 (32.35%)	41 (20.10%)	0.58 (0.34 - 0.98)	0.042*
HWE	$\chi^2 = 17.570$	$\chi^2 = 13.318$		
<u>Recessive Model</u>				
GG or AG	92 (67.65%)	163 (79.90%)	1.00	
AA	44 (32.35%)	41 (20.10%)	0.53 (0.32 - 0.86)	0.011*
<u>Dominant Model</u>				
GG	64 (47.06%)	103 (50.49%)	1.00	
AG or AA	72 (52.94%)	101 (49.51%)	0.87 (0.56 - 1.35)	0.535
C242T	(n = 138)	(n = 203)		
CC	56 (40.58%)	88 (43.35%)	1.00	
CT	64 (46.38%)	96 (47.29%)	0.95 (0.60 - 1.51)	0.843
TT	18 (13.04%)	19 (9.36%)	0.67 (0.32 - 1.39)	0.283
HWE	$\chi^2 = 0.000$	$\chi^2 = 0.844$		
<u>Recessive Model</u>				
CC or CT	120 (86.96%)	184 (90.64%)	1.00	
TT	18 (13.04%)	19 (9.36%)	0.69 (0.35 - 1.36)	0.285
<u>Dominant Model</u>				
CC	56 (40.58%)	88 (43.35%)	1.00	
CT or TT	82 (59.42%)	115 (56.65%)	0.89 (0.58 - 1.38)	0.611
A640G	(n = 136)	(n = 206)		
AA	37 (27.21%)	43 (20.87%)	1.00	
AG	64 (47.06%)	105 (50.97%)	0.99 (0.59 - 1.67)	0.970
GG	35 (25.74%)	58 (28.16%)	0.70 (0.38 - 1.29)	0.252
HWE	$\chi^2 = 0.192$	$\chi^2 = 0.027$		
<u>Recessive Model</u>				
GG or AG	99 (72.79%)	163 (79.13%)	1.00	
AA	37 (27.21%)	43 (20.87%)	0.71 (0.43 - 1.17)	0.088
<u>Dominant Model</u>				
GG	35 (25.74%)	58 (28.16%)	1.00	
AG or AA	101 (74.26%)	148 (71.84%)	0.88 (0.54 - 1.44)	0.311

The odds ratio (OR) was estimated from logistic regression analysis. * denotes significantly different frequency between the two groups. CAD = coronary artery disease; CI = confidence interval; HWE = Hardy Weinberg equilibrium.

As all the three SNPs studied occur at different allele frequencies. Pair-wise LD score by r^2 makes the assumption of equal allele frequencies (289;290) so only the pair-wise LD score by $|D'|$ is relevant. LD analysis by $|D'|$ showed that C242T and A640G were in relatively low LD in control (0.482) and CAD (0.374) groups. A-930G and C242T or A-930G and A640G were not linked in control (0.034, 0.188 respectively) or CAD (0.018, 0.068 respectively) groups.

The frequencies of three-SNP haplotypes of the *CYBA* gene in the CAD and healthy groups are summarised in *Table 5.5*. The most commonly observed haplotype in both groups is -930^G/242^C/640^G and the least common haplotype was -930^G/242^T/640^G. The frequencies of the other six haplotypes differed slightly between the CAD and control groups in the order of how common or uncommon they were. The comparison of the haplotype frequencies in both groups by the software PHASE gave an overall p -value of borderline significance ($p = 0.06$). 2-proportions test was used to look for significantly different frequencies of each of the haplotype combinations. The most different haplotype between the two groups is the -930^G/242^C/640^G but this did not reach statistical significance.

5.3.2. *CYBA* Gene – Phenotype Interactions

The significance of the influence of *CYBA* polymorphisms as single locus on clinical phenotypes are summarised in *Table 5.6*. A-930G was significantly associated with heart rate in both CAD and control groups. In the control group, the heart rate in subjects with -930^{A/A} was 65 ± 11 beats/min, 61 ± 9 beats/min in subjects with -930^{G/G} and 59 ± 10 beats/min in subjects with -930^{A/G}. In the CAD population, the heart rate in subjects with -930^{A/A} was 62 ± 12 beats/min, 63 ± 10 beats/min in subjects with -930^{G/G} and 56 ± 10 beats/min in subjects with -930^{A/G}. The C242T and A640G polymorphisms were not associated with any of the clinical phenotypes examined. There were also no significant associations between any of the haplotypes with vascular compliance indices C1 ($p = 0.385$), C2 ($p = 0.742$) and Alx ($p = 0.188$).

Table 5.5: Frequency of three-polymorphism haplotypes of the CYBA gene

Haplotype			Control (n=138)	CAD (n=206)	p-value
-930	242	640			
A	C	A	0.088	0.090	0.897
A	C	G	0.176	0.149	0.308
A	T	A	0.089	0.067	0.287
A	T	G	0.067	0.055	0.615
G	C	A	0.159	0.162	0.911
G	C	G	0.214	0.270	0.092
G	T	A	0.173	0.157	0.578
G	T	G	0.033	0.050	0.228
Global permutation test (PAC-likelihood ratio test) for case control comparison					0.06

2-proportions test was used to test for significance between the two groups for each haplotype combination. The overall significance between the two groups was tested using likelihood ratio test that was not based on Hardy-Weinberg equilibrium. CAD = coronary artery disease

Table 5.6: Significance of the association between CYBA polymorphisms and clinical phenotypes as single polymorphisms

	Control (n=139)			CAD (n=246)		
	A-930G	C242T	A640G	A-930G	C242T	A640G
Systolic BP (mmHg)	0.800	0.375	0.484	0.316	0.062	0.447
Diastolic BP (mmHg)	0.605	0.582	0.814	0.093	0.307	0.746
Pulse Pressure (mmHg)	0.519	0.199	0.361	0.939	0.247	0.169
C1 (ml/mmHg x 10)	0.189	0.917	0.682	0.304	0.153	0.168
C2 (ml/mmHg x 100)	0.364	0.135	0.209	0.463	0.448	0.451
Augmentation Index (%)	0.736	0.742	0.938	0.092	0.610	0.242
Heart Rate (beats/min)	0.028*	0.776	0.710	0.005*	0.444	0.665

One-way ANOVA analysis was used to test for association between each polymorphism and phenotypic traits in both groups. CAD = coronary artery disease

5.3.3. Genotype and Haplotype Analysis of *NOS3* Polymorphisms

Similar to *CYBA* polymorphisms, OR were estimated from logistic regression analysis for the genotypes without making any assumptions and with the assumptions for recessive and dominant models. The HWE tests (*Table 5.7*) showed that all three polymorphisms were not deviant from HWE in both groups.

The most common genotypes were -786^{C/T}, 4^{B/B} and 894^{G/G} (*Table 5.7*). The logistic regression analyses found that the G894T polymorphism was not associated with the absence or presence of CAD. However, 894^{T/T} was significantly lower in the CAD group when recessive model was applied ($p = 0.030$). The polymorphisms T-786C and intron 4A/4B were not associated with the absence or presence of CAD, even when the recessive or dominant model was applied.

For the same reason as *CYBA* polymorphisms, only pair-wise LD score by |D'| is of relevance. LD analysis by |D'| showed that T-786C and 4A/4B or 4A/4B and G894T were in relatively high LD in control (0.718 and 0.756, respectively) and CAD (0.695 and 0.751, respectively) groups. T-786C and G894T were in relatively low LD for control (0.404) and CAD (0.484) groups.

The frequencies of three-SNP haplotypes of the *NOS3* gene in the CAD and healthy groups are summarised in *Table 5.8*. The most commonly observed haplotype in both groups was -786^T/4B/894^G while the least common haplotype was -786^C/4A/894^G. The frequencies estimated for the haplotypes -786^C/4A/894^G and -786^T/4A/894^T were less than 5%. There was no significant difference in haplotype frequencies between the two groups. The haplotype -786^T/4A/894^G was significantly more frequent in the CAD than the control groups. The frequencies of the other *NOS3* haplotypes studied were not significantly different between the two groups.

5.3.4. *NOS3* Gene – Phenotype Interactions

The significance of the influence of each *NOS3* polymorphisms and clinical phenotypes are summarised in *Table 5.9*. The T-786C was significantly associated

Table 5.7: Single SNP genotype distribution of NOS3 gene

	Control	CAD	OR (95% CI)	p-value
T-786C	(n = 138)	(n = 206)		
TT	48 (34.78%)	79 (38.35%)	1.00	
CT	63 (45.65%)	90 (43.69%)	0.87 (0.54 - 1.41)	0.565
CC	27 (19.57%)	37 (17.96%)	0.83 (0.45 - 1.54)	0.558
HWE	$\chi^2 = 0.254$	$\chi^2 = 0.346$		
<u>Recessive Model</u>				
TT or CT	111 (80.43%)	169 (82.04%)	1.00	
CC	27 (19.57%)	37 (17.96%)	0.90 (0.52 - 1.56)	0.708
<u>Dominant Model</u>				
TT	48 (34.78%)	79 (38.35%)	1.00	
CT or CC	90 (65.22%)	127 (61.65%)	0.86 (0.55 - 1.34)	0.502
Intron 4A/4B	(n = 139)	(n = 201)		
BB	97 (69.78%)	153 (75.00%)	1.00	
AB	34 (24.46%)	39 (19.12%)	0.73 (0.43 - 1.23)	0.235
AA	8 (5.76%)	12 (5.88%)	0.95 (0.38 - 2.41)	0.916
HWE	$\chi^2 = 1.732$	$\chi^2 = 3.150$		
<u>Recessive Model</u>				
BB or AB	131 (94.24%)	192 (94.12%)	1.00	
AA	8 (5.76%)	12 (5.88%)	1.02 (0.41 - 2.57)	1.039
<u>Dominant Model</u>				
BB	97 (69.78%)	153 (75.00%)	1.00	
AB or AA	42 (30.22%)	51 (25.00%)	0.77 (0.48 - 1.25)	0.287
G894T	(n = 134)	(n = 201)		
GG	62 (46.27%)	88 (43.78%)	1.00	
GT	45 (33.58%)	90 (44.78%)	1.36 (0.84 - 2.20)	1.784
TT	27 (20.15%)	23 (11.44%)	0.59 (0.31 - 1.13)	0.109
HWE	$\chi^2 = 3.559$	$\chi^2 = 0.000$		
<u>Recessive Model</u>				
GG or GT	107 (79.85%)	178 (88.56%)	1.00	
TT	27 (20.15%)	23 (11.44%)	0.51 (0.27 - 0.94)	0.030*
<u>Dominant Model</u>				
GG	61 (45.52%)	88 (43.78%)	1.00	
GT or TT	73 (54.48%)	113 (56.22%)	1.07 (0.69 - 1.67)	1.247

The odds ratio (OR) was estimated from logistic regression analysis. * denotes significantly different frequency between the two groups. CAD = coronary artery disease; CI = confidence interval; HWE = Hardy Weinberg equilibrium

Table 5.8: Frequency of three-polymorphism haplotypes of the NOS3 gene

Haplotype			Control (n = 139)	CAD (n = 206)	p-value
-786	4A/4B	894			
C	A	G	0.028	0.022	0.574
C	A	T	0.112	0.103	0.767
C	B	G	0.157	0.162	0.879
C	B	T	0.127	0.113	0.572
T	A	G	0.143	0.205	0.031*
T	A	T	0.031	0.042	0.538
T	B	G	0.302	0.291	0.759
T	B	T	0.101	0.061	0.063
Global permutation test (PAC-likelihood ratio test) for case control comparison					0.23

2-proportions test was used to test for significance between the two groups for each haplotype combination. The overall significance between the two groups was tested using likelihood ratio test that was not based on Hardy-Weinberg equilibrium. CAD = coronary artery disease

Table 5.9: Significance of the association between NOS3 polymorphisms and clinical phenotypes as single polymorphisms

	Control (n=139)			CAD (n=206)		
	T-786C	4A/4B	G894T	T-786C	4A/4B	G894T
Systolic BP (mmHg)	0.066	0.453	0.615	0.343	0.354	0.470
Diastolic BP (mmHg)	0.823	0.681	0.969	0.395	0.355	0.887
Pulse Pressure (mmHg)	0.018*	0.499	0.433	0.367	0.321	0.388
C1 (ml/mmHg x 10)	0.191	0.174	0.247	0.283	0.779	0.104
C2 (ml/mmHg x 100)	0.037*	0.118	0.838	0.024*	0.792	0.157
Augmentation index (%)	0.514	0.407	0.545	0.474	0.116	0.914
Heart Rate (beats/min)	0.827	0.699	0.130	0.209	0.656	0.593

One-way ANOVA analysis was used to test for association between each polymorphism and phenotypic traits in both groups. BP = blood pressure; CAD = coronary artery disease

with PP in the control group but not the CAD group. In the control group, PP in -786^{C/C} subjects is 53 ± 9 mmHg, 61 ± 14 mmHg in subjects with -786^{T/T} and 55 ± 10 mmHg in subjects with -786^{C/T}. In the CAD group, PP in -786^{C/C} subjects was 58 ± 11 mmHg, 59 ± 12 mmHg in subjects with -786^{T/T} and 61 ± 13 mmHg in subjects with -786^{C/T}.

The T-786C was also significantly associated with small artery compliance index C2 in both control and CAD group. In the control group, C2 in -786^{C/C} subjects was 6.4 ± 2.7 ml/mmHg, 4.5 ± 2.6 ml/mmHg in subjects with -786^{T/T} and 5.5 ± 3.3 ml/mmHg in subjects with -786^{C/T}. In the CAD group, C2 in -786^{C/C} subjects was 4.2 ± 1.6 ml/mmHg, 5.4 ± 3.3 ml/mmHg in subjects with -786^{T/T} and 4.2 ± 2.4 ml/mmHg in subjects with -786^{C/T}.

The intron 4A/4B and G894T were not associated with any of the clinical phenotypes examined. None of the haplotype combinations of the three *NOS3* polymorphisms were significantly associated with C1 ($p = 0.857$), C2 ($p = 0.626$) and Alx ($p = 0.197$).

5.4. Discussion

As expected, CAD patients were mostly males, older and had higher PP. The small artery compliance in CAD patients was lower but not the large artery compliance. The Alx and heart rate was higher in CAD patients than control subjects. The significantly higher levels of triglycerides and VLDL, along with lower levels of HDL in CAD group were expected while the significantly lower levels of total cholesterol and LDL were the result of lipid-lowering drugs used by the CAD patients.

In this study, the frequency of -930^{A/A} genotype was significantly lower in the CAD group without any assumption for dominance and with assumption for recessive model. This result correlated with the transfection experiments reported by Moreno et. al. (260). Although the A-930G was significantly associated with heart rate, the results could be influenced by the β -blockers administered to the CAD patients. The A-930G was not associated with any of the clinical phenotypes investigated. Since the LD score by $|D'|$ between A-930G and C242T or A640G was very low,

any effect of A-930G was probably independent of C242T or A640G. The C242T and A640G polymorphism were not associated with CAD, even in recessive and dominant models. Neither C242T nor A640G was associated with any of the clinical phenotypes investigated. The difference in haplotype frequencies between the control and CAD groups was only of borderline significance. None of the haplotype combinations were associated with vascular compliance indices C1, C2 or Alx.

The results showed that T-786C and intron 4A/4B polymorphisms were not associated with CAD, with and without assumptions of allele dominance. The T-786C was associated with pulse pressure and small artery compliance. Studies showed increased susceptibility of the 894T allele to proteolytic cleavage (265) and decreased eNOS activity (266), and appeared to have dominant effect (275). In contrast, logistic regression analysis in the current study found the 894G allele to be dominant and was associated with CAD. However, there was no association between G894T and any of the clinical phenotypes investigated. The rare 4A allele of intron 4 was strongly linked to the 894G allele of exon 7 and the -786C allele in the promoter polymorphism. The intron 4 and G894T polymorphisms were in complete linkage disequilibrium in both control and CAD subjects, suggesting that previously associated functional effect of the intron 4 polymorphisms (276) may be attributed to T-786C or G894T. There was no significant difference in the haplotype frequencies between the control and CAD groups. There was no association between any of the haplotype combinations with vascular compliance indices C1, C2 or Alx.

In the present study, the comparisons between the control and CAD groups were not adjusted for confounders, most notably the cholesterol levels, gender and age. The lower cholesterol levels in CAD patients were the consequence of lipid-lowering drugs. Adjustments for cholesterol levels would effectively be adjusting for medications. The correlation between gender and age, where the majority of control group are mostly young females while the CAD patients are mostly old men, meant that adjustment for one factor would effectively be adjusting for the other factor as well. Since the patients are on medications, any adjustment for age would also be an adjustment for the cholesterol levels. As most of the data are not significant, adjustments for the confounders would not provide any additional

information. In addition, there is also a risk of over-adjustments in this relatively small study cohort.

Another limitation of the present study is the age difference between patients and controls. At this stage, it cannot be excluded that some of the controls will develop CAD over the next 10 years and therefore would be cases rather than controls. In the group of CAD patients we examined a selected group of elderly but clinically stable patients whereas we did not have access to more critically ill patients who had to undergo emergency operation or indeed died. This may lead to survival bias and data have to be interpreted with caution.

This exploratory study was also not corrected the genetic analysis for repeated measures. Clearly, the association between A-930G of *CYBA* gene or G894T of *NOS3* gene would become non significant. However, the observed associations suggest that further investigation of these two SNPs are required and justified in an adequately powered cohort of patients with CAD or other functional assays.

This is a medium-size collection of patients who are very well phenotyped and have advanced three vessel CAD. However, as we are studying multiple polymorphisms with subtle effects, large numbers are necessary to have adequate power to confirm or refute the stated hypothesis. A major drawback of this study was the number of subjects. The current study was powered for stiffness analysis but more patients and control subjects need to be recruited for genomic analysis. In addition to the three polymorphisms in each gene studied, there were also other polymorphisms within these genes (254;291). Due to the large number of variations in human genome, the net effects of polymorphisms within the same gene or between genes could be cancelled out. *CYBA* and *NOS3* were only two of the many genes that code for proteins involved in maintaining the balance between NO and O_2^- . All the genes of the oxidative stress pathway should be investigated for functional polymorphisms and association with CAD.

CHAPTER 6: CONCLUSIONS

In conclusion, this thesis provides the most detailed characterisation of the *Gstm* gene family in terms of CVD to date. It has confirmed the previously identified reduction in *rGstm1* expression in SHRSP, which could not be improved by antihypertensive treatment despite significant reductions in BP and oxidative stress levels. Previous work from our group identified thirteen polymorphisms in the promoter correlating to reduced *rGstm1* expression (67). Subsequent investigation using luciferase activities of plasmid constructs in our laboratory has recently implicated five of these variants with consistently significant reduction in luciferase activities (293). However, it is still not clear as to how the reduction in renal *rGstm1* gene expression may influence BP regulation in the SHRSP. There are a number of strategies currently being carried out within our group to investigate this further. One of the strategies is transgenic rescue as previously described for *Cd36* (58), with replacement of the *rGstm1* gene in the SHRSP from a normotensive strain, such as WKY or the Brown Norway (BN), followed by full phenotypic analysis. Another strategy extensively used in our group is gene transfer, in which viral vectors may be used to overexpress *rGstm1* gene in the SHRSP (91). A reciprocal study using RNA interference (RNAi) to inhibit normal *rGstm1* activity in the WKY is an additional strategy currently being undertaken by our group (125). Subsequent measurements of BP and markers of oxidative stress will enable us to understand the role of *rGstm1* in the development of hypertension. The results from this project have also shown reduced expression of several members of the *rGstm* gene family in SHRSP. Further investigation should include sequencing of these *rGstm* members in the SHRSP and WKY to ascertain the presence of any functional polymorphisms for further studies.

There is evidence for renal oxidative stress in hypertensive rat models (67;231). Our group have previously also shown significantly higher levels of O_2^- levels in the SHRSP renal medulla and cortex when compared to WKY (67). Similarly, Meng et.al. have shown increased renal cortical and medullary O_2^- production in Dahl-salt sensitive rats (231). In the study by Meng et.al., they have also shown reductions in Mn-SOD and Cu/Zn-SOD in renal cortex and medulla. We suggest that reduced *rGstm* gene family, in particular *rGstm1*, expression is contributing to diminished protection against renal oxidative stress during the development of

hypertension in the SHRSP. This could be further investigated by inducing oxidative stress with NOS inhibition (294), in a normotensive strain such as the WKY. This provides the opportunity to observe effects of renal oxidative stress on *rGstm* gene family. Markers of oxidative stress (such as oxidised lipids), antioxidant capacity (such as [GSH]:[GSSH] ratio) and gene expression levels of other pro-oxidative and anti-oxidative enzymes can also be measured.

In the present study, despite careful characterisation, there are still four *hGSTM* genes as potential orthologues for *rGstm1*. Further investigation for differential expression in vascular or renal tissues from hypertensive patients will therefore be required. The difficulties in obtaining good quality mRNA from surgically manipulated vascular tissues indicates that pre-treatment of tissues will be required to overcome this problem. Culture of endothelial cells (295), VSMCs (296) and adventitial fibroblasts (297) from CAD and control vascular tissues may provide the opportunity to obtain sufficient good quality mRNA and protein for gene expression or oxidative stress measurements for further investigations.

In addition, a relatively small association study identified significant association between CAD and polymorphisms in two key enzymes involved in NO and O_2^- balance. In addition to NAD(P)H oxidase and eNOS, there are other important enzymes (such as SODs) involved in maintaining the balance between NO and O_2^- . Polymorphisms in ecSOD (Arg760Gly) and catalase (C-262T) have been associated with CAD and hypertension (298;299). Various studies have also implicated the *hGSTM1*0* allele as a genetic risk factor for cigarette smoking related CAD risk (201;202). Since it is not possible for RNAi, gene transfer or transgenic strategies to be investigated in the human, the *hGSTM* gene family needs to be investigated in a large scale association study. A large scale population with well-phenotyped CAD and control subjects will be required. The large number of polymorphisms, each imparting small effects can be scored according to pro-oxidative or anti-oxidative effects. With a sufficiently large population study, a range of scores can be assigned and pharmacogenomic therapies can then be designed for individual patients.

Finally, this thesis presents data supporting the GSTM family of enzymes as an important target for further investigation. Moreover future investigations of the

GSTM gene family in rat models and human studies should take into consideration contributions of polymorphisms within the gene family, as well as other genes.

REFERENCES

- 1) World Health Report 2003: Shaping the Future. 2003.
<http://www.who.int/whr/2003/en/index.html>
- 2) Coronary Heart Disease Statistics 2006. 2006.
<http://www.heartstats.org/datapage.asp?id=5739>
- 3) Economic costs of CVD and CHD. 2006.
<http://www.heartstats.org/datapage.asp?id=101>
- 4) The Atlas of Heart Disease and Stroke. 2006.
http://www.who.int/cardiovascular_diseases/resources/atlas/en/index.html
- 5) JBS 2: Joint British Societies' guidelines on prevention of cardiovascular disease in clinical practice. Heart 2005 Dec;91 Suppl 5:v1-52.
- 6) Staessen JA, Wang J, Bianchi G, Birkenhager WH. Essential hypertension. Lancet 2003 May 10;361(9369):1629-41.
- 7) Kannel WB. Elevated systolic blood pressure as a cardiovascular risk factor. Am J Cardiol 2000 Jan 15;85(2):251-5.
- 8) World Health Report 2002 - Reducing Risks, Promoting Healthy Life. 2002.
<http://www.who.int/whr/2002/en/index.html>
- 9) Turnbull F. Effects of different blood-pressure-lowering regimens on major cardiovascular events: results of prospectively-designed overviews of randomised trials. Lancet 2003 Nov 8;362(9395):1527-35.
- 10) Lifton RP, Gharavi AG, Geller DS. Molecular mechanisms of human hypertension. Cell 2001 Feb 23;104(4):545-56.
- 11) Cowley AW, Jr. The genetic dissection of essential hypertension. Nat Rev Genet 2006 Nov;7(11):829-40.
- 12) Unger T. The role of the renin-angiotensin system in the development of cardiovascular disease. Am J Cardiol 2002 Jan 24;89(2A):3A-9A.
- 13) Lavoie JL, Sigmund CD. Minireview: overview of the renin-angiotensin system--an endocrine and paracrine system. Endocrinology 2003 Jun;144(6):2179-83.
- 14) Donoghue M, Hsieh F, Baronas E, Godbout K, Gosselin M, Stagliano N, et al. A novel angiotensin-converting enzyme-related carboxypeptidase (ACE2) converts angiotensin I to angiotensin 1-9. Circ Res 2000 Sep 1;87(5):E1-E9.
- 15) Crackower MA, Sarao R, Oudit GY, Yagil C, Kozieradzki I, Scanga SE, et al. Angiotensin-converting enzyme 2 is an essential regulator of heart function. Nature 2002 Jun 20;417(6891):822-8.

- 16) Gurley SB, Allred A, Le TH, Griffiths R, Mao L, Philip N, et al. Altered blood pressure responses and normal cardiac phenotype in ACE2-null mice. *J Clin Invest* 2006 Aug;116(8):2218-25.
- 17) Igase M, Strawn WB, Gallagher PE, Geary RL, Ferrario CM. Angiotensin II AT1 receptors regulate ACE2 and angiotensin-(1-7) expression in the aorta of spontaneously hypertensive rats. *Am J Physiol Heart Circ Physiol* 2005 Sep;289(3):H1013-H1019.
- 18) Shanmugam S, Corvol P, Gasc JM. Ontogeny of the two angiotensin II type 1 receptor subtypes in rats. *Am J Physiol* 1994 Dec;267(6 Pt 1):E828-E836.
- 19) Burson JM, Aguilera G, Gross KW, Sigmund CD. Differential expression of angiotensin receptor 1A and 1B in mouse. *Am J Physiol* 1994 Aug;267(2 Pt 1):E260-E267.
- 20) Kakar SS, Sellers JC, Devor DC, Musgrove LC, Neill JD. Angiotensin II type-1 receptor subtype cDNAs: differential tissue expression and hormonal regulation. *Biochem Biophys Res Commun* 1992 Mar 31;183(3):1090-6.
- 21) Gasc JM, Shanmugam S, Sibony M, Corvol P. Tissue-specific expression of type 1 angiotensin II receptor subtypes. An in situ hybridization study. *Hypertension* 1994 Nov;24(5):531-7.
- 22) Marteau JB, Zaiou M, Siest G, Visvikis-Siest S. Genetic determinants of blood pressure regulation. *J Hypertens* 2005 Dec;23(12):2127-43.
- 23) Feinleib M, Garrison RJ, Fabsitz R, Christian JC, Hrubec Z, Borhani NO, et al. The NHLBI twin study of cardiovascular disease risk factors: methodology and summary of results. *Am J Epidemiol* 1977 Oct;106(4):284-5.
- 24) Rao RM, Reddy GP, Grim CE. Relative role of genes and environment on BP: twin studies in Madras, India. *J Hum Hypertens* 1993 Oct;7(5):451-5.
- 25) Longini IM, Jr., Higgins MW, Hinton PC, Moll PP, Keller JB. Environmental and genetic sources of familial aggregation of blood pressure in Tecumseh, Michigan. *Am J Epidemiol* 1984 Jul;120(1):131-44.
- 26) Biron P, Mongeau JG, Bertrand D. Familial aggregation of blood pressure in 558 adopted children. *Can Med Assoc J* 1976 Oct 23;115(8):773-4.
- 27) Oparil S, Zaman MA, Calhoun DA. Pathogenesis of hypertension. *Ann Int Med* 2003 Nov 4;139(9):761-76.
- 28) Griffiths AJF, Miller JH, Suzuki DT, Lewontin RC, Gelbart WM. Genetics and the Organism. In: *An Introduction to Genetic Analysis*, 7th Edn. New York. W. H. Freeman and Company Library of Congress. 1999: 1-26.
- 29) Wang WY, Zee RY, Morris BJ. Association of angiotensin II type 1 receptor gene polymorphism with essential hypertension. *Clin Genet* 1997 Jan;51(1):31-4.
- 30) Lajemi M, Labat C, Gautier S, Lacolley P, Safar M, Asmar R, et al. Angiotensin II type 1 receptor-153A/G and 1166A/C gene polymorphisms

- and increase in aortic stiffness with age in hypertensive subjects. *J Hypertens* 2001 Mar;19(3):407-13.
- 31) Hindorff LA, Heckbert SR, Tracy R, Tang Z, Psaty BM, Edwards KL, et al. Angiotensin II type 1 receptor polymorphisms in the cardiovascular health study: relation to blood pressure, ethnicity, and cardiovascular events. *Am J Hypertens* 2002 Dec;15(12):1050-6.
 - 32) Reckelhoff JF. Gender differences in the regulation of blood pressure. *Hypertension* 2001 May;37(5):1199-208.
 - 33) Charchar FJ, Tomaszewski M, Padmanabhan S, Lacka B, Upton MN, Inglis GC, et al. The Y chromosome effect on blood pressure in two European populations. *Hypertension* 2002 Feb;39(2 Pt 2):353-6.
 - 34) Pardell H, Rodicio JL. High blood pressure, smoking and cardiovascular risk. *J Hypertens* 2005 Jan;23(1):219-21.
 - 35) Gordon T, Kannel WB. Drinking and its relation to smoking, BP, blood lipids, and uric acid. The Framingham study. *Arch Intern Med* 1983 Jul;143(7):1366-74.
 - 36) Barnoya J, Glantz SA. Cardiovascular effects of secondhand smoke: nearly as large as smoking. *Circulation* 2005 May 24;111(20):2684-98.
 - 37) Brunner H, Cockcroft JR, Deanfield J, Donald A, Ferrannini E, Halcox J, et al. Endothelial function and dysfunction. Part II: Association with cardiovascular risk factors and diseases. A statement by the Working Group on Endothelins and Endothelial Factors of the European Society of Hypertension. *J Hypertens* 2005 Feb;23(2):233-46.
 - 38) Lucas DL, Brown RA, Wassef M, Giles TD. Alcohol and the cardiovascular system research challenges and opportunities. *J Am Coll Cardiol* 2005 Jun 21;45(12):1916-24.
 - 39) Aguilera MT, de la SA, Coca A, Estruch R, Fernandez-Sola J, Urbano-Marquez A. Effect of alcohol abstinence on blood pressure: assessment by 24-hour ambulatory blood pressure monitoring. *Hypertension* 1999 Feb;33(2):653-7.
 - 40) Blair SN, Goodyear NN, Gibbons LW, Cooper KH. Physical fitness and incidence of hypertension in healthy normotensive men and women. *JAMA* 1984 Jul 27;252(4):487-90.
 - 41) Paffenbarger RS, Jr., Hyde RT, Wing AL, Lee IM, Jung DL, Kampert JB. The association of changes in physical-activity level and other lifestyle characteristics with mortality among men. *N Engl J Med* 1993 Feb 25;328(8):538-45.
 - 42) Sandvik L, Erikssen J, Thaulow E, Erikssen G, Mundal R, Rodahl K. Physical fitness as a predictor of mortality among healthy, middle-aged Norwegian men. *N Engl J Med* 1993 Feb 25;328(8):533-7.

- 43) Wenger NK. Hypertension and other cardiovascular risk factors in women. *Am J Hypertens* 1995 Dec;8(12 Pt 2):94s-9s.
- 44) Hall JE. The kidney, hypertension, and obesity. *Hypertension* 2003 Mar;41(3 Pt 2):625-33.
- 45) Garrison RJ, Kannel WB, Stokes J, III, Castelli WP. Incidence and precursors of hypertension in young adults: the Framingham Offspring Study. *Prev Med* 1987 Mar;16(2):235-51.
- 46) De BG, Ambrosioni E, Borch-Johnsen K, Brotons C, Cifkova R, Dallongeville J, et al. European guidelines on cardiovascular disease prevention in clinical practice. Third Joint Task Force of European and other Societies on Cardiovascular Disease Prevention in Clinical Practice (constituted by representatives of eight societies and by invited experts). *Atherosclerosis* 2004 Apr;173(2):381-91.
- 47) Antihypertensive Drugs. In: Harvey RA, Champe PC, Mycek MJ., editors. *Lippincott's Illustrated Reviews: Pharmacology 2nd Edition*. Philadelphia: Lippincott Williams & Wilkins, 2000: 179-191.
- 48) Pinto YM, Paul M, Ganten D. Lessons from rat models of hypertension: from Goldblatt to genetic engineering. *Cardiovasc Res* 1998 Jul;39(1):77-88.
- 49) Lerman LO, Chade AR, Sica V, Napoli C. Animal models of hypertension: an overview. *J Lab Clin Med* 2005 Sep;146(3):160-73.
- 50) Sun ZJ, Zhang ZE. Historic perspectives and recent advances in major animal models of hypertension. *Acta Pharmacol Sin* 2005 Mar;26(3):295-301.
- 51) Takahashi N, Smithies O. Human genetics, animal models and computer simulations for studying hypertension. *Trends Genet* 2004 Mar;20(3):136-45.
- 52) Okamoto K, Yamori Y, Nagaoka A. Establishment of the Stroke-prone Spontaneously Hypertensive Rat (SHR). *Circ Res* 1974 May;34/35 Supp(I):I-143-I-153.
- 53) Louis WJ, Howes LG. Genealogy of the spontaneously hypertensive rat and Wistar-Kyoto rat strains: implications for studies of inherited hypertension. *J Cardiovasc Pharmacol* 1990;16 Suppl 7:S1-S5.
- 54) Davidson AO, Schork N, Jaques BC, Kelman AW, Sutcliffe RG, Reid JL, et al. Blood pressure in genetically hypertensive rats. Influence of the Y chromosome. *Hypertension* 1995 Sep;26(3):452-9.
- 55) Munroe PB, Caulfield MJ. Genetics of hypertension. *Curr Opin Genet Dev* 2000 Jun;10(3):325-9.
- 56) Aitman TJ, Glazier AM, Wallace CA, Cooper LD, Norsworthy PJ, Wahid FN, et al. Identification of Cd36 (Fat) as an insulin-resistance gene causing defective fatty acid and glucose metabolism in hypertensive rats. *Nat Genet* 1999 Jan;21(1):76-83.

- 57) Pravenec M, Zidek V, Simakova M, Kren V, Krenova D, Horky K, et al. Genetics of Cd36 and the clustering of multiple cardiovascular risk factors in spontaneous hypertension. *J Clin Invest* 1999 Jun;103(12):1651-7.
- 58) Pravenec M, Landa V, Zidek V, Musilova A, Kren V, Kazdova L, et al. Transgenic rescue of defective Cd36 ameliorates insulin resistance in spontaneously hypertensive rats. *Nat Genet* 2001 Feb;27(2):156-8.
- 59) Clark JS, Jeffs B, Davidson AO, Lee WK, Anderson NH, Bihoreau MT, et al. Quantitative trait loci in genetically hypertensive rats. Possible sex specificity. *Hypertension* 1996 Nov;28(5):898-906.
- 60) Stoll M, Kwitek-Black AE, Cowley AW, Jr., Harris EL, Harrap SB, Krieger JE, et al. New target regions for human hypertension via comparative genomics. *Genome Res* 2000 Apr;10(4):473-82.
- 61) McBride MW, Carr FJ, Graham D, Anderson NH, Clark JS, Lee WK, et al. Microarray analysis of rat chromosome 2 congenic strains [erratum appears in *Hypertension*. 2003 May 5;41(6):e13]. *Hypertension* 2003 Mar;41(3 Pt 2):847-53.
- 62) Dutil J, Deng AY. Further chromosomal mapping of a blood pressure QTL in Dahl rats on chromosome 2 using congenic strains. *Physiol Genomics* 2001 Jun 6;6(1):3-9.
- 63) Dutil J, Deng AY. Mapping a blood pressure quantitative trait locus to a 5.7-cM region in Dahl salt-sensitive rats. *Mamm Genome* 2001 May;12(5):362-5.
- 64) Garrett MR, Rapp JP. Multiple blood pressure QTL on rat Chromosome 2 defined by congenic Dahl rats. *Mamm Genome* 2002 Jan;13(1):41-4.
- 65) Okuda T, Sumiya T, Mizutani K, Tago N, Miyata T, Tanabe T, et al. Analyses of differential gene expression in genetic hypertensive rats by microarray. *Hypertens Res* 2002 Mar;25(2):249-55.
- 66) Okuda T, Sumiya T, Iwai N, Miyata T. Difference of gene expression profiles in spontaneous hypertensive rats and Wistar-Kyoto rats from two sources. *Biochem Biophys Res Commun* 2002 Aug 23;296(3):537-43.
- 67) McBride MW, Brosnan MJ, Mathers J, McLellan LI, Miller WH, Graham D, et al. Reduction of *gstm1* expression in the stroke-prone spontaneously hypertension rat contributes to increased oxidative stress. *Hypertension* 2005 Apr;45(4):786-92.
- 68) Ignarro LJ, Buga GM, Wood KS, Byrns RE, Chaudhuri G. Endothelium-derived relaxing factor produced and released from artery and vein is nitric oxide. *Proc Natl Acad Sci U S A* 1987 Dec;84(24):9265-9.
- 69) Garland CJ, Plane F, Kemp BK, Cocks TM. Endothelium-dependent hyperpolarization: a role in the control of vascular tone. *Trends Pharmacol Sci* 1995 Jan;16(1):23-30.
- 70) Shimokawa H, Yasutake H, Fujii K, Owada MK, Nakaike R, Fukumoto Y, et al. The importance of the hyperpolarizing mechanism increases as the

vessel size decreases in endothelium-dependent relaxations in rat mesenteric circulation. *J Cardiovasc Pharmacol* 1996 Nov;28(5):703-11.

- 71) Kelm M. Nitric oxide metabolism and breakdown. *Biochim Biophys Acta* 1999 May 5;1411(2-3):273-89.
- 72) Pohl U, Holtz J, Busse R, Bassenge E. Crucial role of endothelium in the vasodilator response to increased flow in vivo. *Hypertension* 1986 Jan;8(1):37-44.
- 73) Gewaltig MT, Kojda G. Vasoprotection by nitric oxide: mechanisms and therapeutic potential. *Cardiovasc Res* 2002 Aug 1;55(2):250-60.
- 74) Massberg S, Sausbier M, Klatt P, Bauer M, Pfeifer A, Siess W, et al. Increased adhesion and aggregation of platelets lacking cyclic guanosine 3',5'-monophosphate kinase I. *J Exp Med* 1999 Apr 19;189(8):1255-64.
- 75) Pfeifer A, Klatt P, Massberg S, Ny L, Sausbier M, Hirneiss C, et al. Defective smooth muscle regulation in cGMP kinase I-deficient mice. *EMBO J* 1998 Jun 1;17(11):3045-51.
- 76) Sausbier M, Schubert R, Voigt V, Hirneiss C, Pfeifer A, Korth M, et al. Mechanisms of NO/cGMP-dependent vasorelaxation. *Circ Res* 2000 Oct 27;87(9):825-30.
- 77) Cai H, Harrison DG. Endothelial dysfunction in cardiovascular diseases: the role of oxidant stress. *Circ Res* 2000 Nov 10;87(10):840-4.
- 78) Irani K. Oxidant signaling in vascular cell growth, death, and survival : a review of the roles of reactive oxygen species in smooth muscle and endothelial cell mitogenic and apoptotic signaling. *Circ Res* 2000 Aug 4;87(3):179-83.
- 79) Cardillo C, Kilcoyne CM, Quyyumi AA, Cannon RO, III, Panza JA. Role of nitric oxide in the vasodilator response to mental stress in normal subjects. *Am J Cardiol* 1997 Oct 15;80(8):1070-4.
- 80) Dietz NM, Rivera JM, Eggner SE, Fix RT, Warner DO, Joyner MJ. Nitric oxide contributes to the rise in forearm blood flow during mental stress in humans. *J Physiol* 1994 Oct 15;480 (Pt 2):361-8.
- 81) Panza JA, Casino PR, Kilcoyne CM, Quyyumi AA. Role of endothelium-derived nitric oxide in the abnormal endothelium-dependent vascular relaxation of patients with essential hypertension. *Circulation* 1993 May;87(5):1468-74.
- 82) Taddei S, Virdis A, Mattei P, Salvetti A. Vasodilation to acetylcholine in primary and secondary forms of human hypertension. *Hypertension* 1993 Jun;21(6 Pt 2):929-33.
- 83) Taddei S, Virdis A, Mattei P, Ghiadoni L, Sudano I, Salvetti A. Defective L-arginine-nitric oxide pathway in offspring of essential hypertensive patients. *Circulation* 1996 Sep 15;94(6):1298-303.

- 84) Forte P, Copland M, Smith LM, Milne E, Sutherland J, Benjamin N. Basal nitric oxide synthesis in essential hypertension. *Lancet* 1997 Mar 22;349(9055):837-42.
- 85) Cardillo C, Kilcoyne CM, Cannon RO, III, Panza JA. Racial differences in nitric oxide-mediated vasodilator response to mental stress in the forearm circulation. *Hypertension* 1998 Jun;31(6):1235-9.
- 86) Ulker S, McKeown PP, Bayraktutan U. Vitamins reverse endothelial dysfunction through regulation of eNOS and NAD(P)H oxidase activities. *Hypertension* 2003 Mar;41(3):534-9.
- 87) Wigg SJ, Tare M, Forbes J, Cooper ME, Thomas MC, Coleman HA, et al. Early vitamin E supplementation attenuates diabetes-associated vascular dysfunction and the rise in protein kinase C-beta in mesenteric artery and ameliorates wall stiffness in femoral artery of Wistar rats. *Diabetologia* 2004 Jun;47(6):1038-46.
- 88) MRC/BHF Heart Protection Study of antioxidant vitamin supplementation in 20,536 high-risk individuals: a randomised placebo-controlled trial. *Lancet* 2002 Jul 6;360(9326):23-33.
- 89) Yusuf S, Dagenais G, Pogue J, Bosch J, Sleight P. Vitamin E supplementation and cardiovascular events in high-risk patients. The Heart Outcomes Prevention Evaluation Study Investigators. *N Engl J Med* 2000 Jan 20;342(3):154-60.
- 90) Anggard E. Nitric oxide: mediator, murderer, and medicine. *Lancet* 1994 May 14;343(8907):1199-206.
- 91) Alexander MY, Brosnan MJ, Hamilton CA, Downie P, Devlin AM, Dowell F, et al. Gene transfer of endothelial nitric oxide synthase improves nitric oxide-dependent endothelial function in a hypertensive rat model. *Cardiovasc Res* 1999 Aug 15;43(3):798-807.
- 92) Alexander MY, Brosnan MJ, Hamilton CA, Fennell JP, Beattie EC, Jardine E, et al. Gene transfer of endothelial nitric oxide synthase but not Cu/Zn superoxide dismutase restores nitric oxide availability in the SHRSP. *Cardiovasc Res* 2000 Aug 18;47(3):609-17.
- 93) Lerman A, Burnett JC, Jr., Higano ST, McKinley LJ, Holmes DR, Jr. Long-term L-arginine supplementation improves small-vessel coronary endothelial function in humans. *Circulation* 1998 Jun 2;97(21):2123-8.
- 94) Lund DD, Faraci FM, Miller FJ, Jr., Heistad DD. Gene transfer of endothelial nitric oxide synthase improves relaxation of carotid arteries from diabetic rabbits. *Circulation* 2000 Mar 7;101(9):1027-33.
- 95) Griending KK, Sorescu D, Lassegue B, Ushio-Fukai M. Modulation of protein kinase activity and gene expression by reactive oxygen species and their role in vascular physiology and pathophysiology. *Arterioscler Thromb Vasc Biol* 2000 Oct;20(10):2175-83.

- 96) Wolin MS, Gupte SA, Oeckler RA. Superoxide in the vascular system. *J Vasc Res* 2002 May;39(3):191-207.
- 97) Li PF, Dietz R, von HR. Differential effect of hydrogen peroxide and superoxide anion on apoptosis and proliferation of vascular smooth muscle cells. *Circulation* 1997 Nov 18;96(10):3602-9.
- 98) Griending KK, FitzGerald GA. Oxidative stress and cardiovascular injury: Part I: basic mechanisms and *in vivo* monitoring of ROS. *Circulation* 2003 Oct 21;108(16):1912-6.
- 99) Wilcox JN, Subramanian RR, Sundell CL, Tracey WR, Pollock JS, Harrison DG, et al. Expression of multiple isoforms of nitric oxide synthase in normal and atherosclerotic vessels. *Arterioscler Thromb Vasc Biol* 1997 Nov;17(11):2479-88.
- 100) Vasquez-Vivar J, Kalyanaraman B, Martasek P, Hogg N, Masters BS, Karoui H, et al. Superoxide generation by endothelial nitric oxide synthase: the influence of cofactors. *Proc Natl Acad Sci USA* 1998 Aug 4;95(16):9220-5.
- 101) Schmidt HH, Nau H, Wittfoht W, Gerlach J, Prescher KE, Klein MM, et al. Arginine is a physiological precursor of endothelium-derived nitric oxide. *Eur J Pharmacol* 1988 Sep 13;154(2):213-6.
- 102) Palmer RM, Rees DD, Ashton DS, Moncada S. L-arginine is the physiological precursor for the formation of nitric oxide in endothelium-dependent relaxation. *Biochem Biophys Res Commun* 1988 Jun 30;153(3):1251-6.
- 103) Shimokawa H, Flavahan NA, Vanhoutte PM. Loss of endothelial pertussis toxin-sensitive G protein function in atherosclerotic porcine coronary arteries. *Circulation* 1991 Feb;83(2):652-60.
- 104) Cosentino F, Katusic ZS. Tetrahydrobiopterin and dysfunction of endothelial nitric oxide synthase in coronary arteries. *Circulation* 1995 Jan 1;91(1):139-44.
- 105) Cosentino F, Patton S, d'Uscio LV, Werner ER, Werner-Felmayer G, Moreau P, et al. Tetrahydrobiopterin alters superoxide and nitric oxide release in prehypertensive rats. *J Clin Invest* 1998 Apr 1;101(7):1530-7.
- 106) Cai H. NAD(P)H oxidase-dependent self-propagation of hydrogen peroxide and vascular disease. *Circ Res* 2005 Apr 29;96(8):818-22.
- 107) Ronson RS, Nakamura M, Vinten-Johansen J. The cardiovascular effects and implications of peroxynitrite. *Cardiovasc Res* 1999 Oct;44(1):47-59.
- 108) Pryor WA, Houk KN, Foote CS, Fukuto JM, Ignarro LJ, Squadrito GL, et al. Free radical biology and medicine: it's a gas, man! *Am J Physiol Regul Integr Comp Physiol* 2006 Sep;291(3):R491-R511.
- 109) Kone BC. Molecular biology of natriuretic peptides and nitric oxide synthases. *Cardiovasc Res* 2001 Aug 15;51(3):429-41.

- 110) Li H, Poulos TL. Structure-function studies on nitric oxide synthases. *J Inorg Biochem* 2005 Jan;99(1):293-305.
- 111) Papapetropoulos A, Rudic RD, Sessa WC. Molecular control of nitric oxide synthases in the cardiovascular system. *Cardiovasc Res* 1999 Aug 15;43(3):509-20.
- 112) Stuehr DJ. Mammalian nitric oxide synthases. *Biochim Biophys Acta* 1999 May 5;1411(2-3):217-30.
- 113) Alderton WK, Cooper CE, Knowles RG. Nitric oxide synthases: structure, function and inhibition. *Biochem J* 2001 Aug 1;357(Pt 3):593-615.
- 114) Govers R, Rabelink TJ. Cellular regulation of endothelial nitric oxide synthase. *Am J Physiol Renal Physiol* 2001 Feb;280(2):F193-F206.
- 115) Kanazawa K, Kawashima S, Mikami S, Miwa Y, Hirata K, Suematsu M, et al. Endothelial constitutive nitric oxide synthase protein and mRNA increased in rabbit atherosclerotic aorta despite impaired endothelium-dependent vascular relaxation. *Am J Pathol* 1996 Jun;148(6):1949-56.
- 116) Liao JK, Shin WS, Lee WY, Clark SL. Oxidized low-density lipoprotein decreases the expression of endothelial nitric oxide synthase. *J Biol Chem* 1995 Jan 6;270(1):319-24.
- 117) Inoue N, Venema RC, Sayegh HS, Ohara Y, Murphy TJ, Harrison DG. Molecular regulation of the bovine endothelial cell nitric oxide synthase by transforming growth factor-beta 1. *Arterioscler Thromb Vasc Biol* 1995 Aug;15(8):1255-61.
- 118) Yoshizumi M, Perrella MA, Burnett JC, Jr., Lee ME. Tumor necrosis factor downregulates an endothelial nitric oxide synthase mRNA by shortening its half-life. *Circ Res* 1993 Jul;73(1):205-9.
- 119) Wever RM, van Dam T, van Rijn HJ, de Groot F, Rabelink TJ. Tetrahydrobiopterin regulates superoxide and nitric oxide generation by recombinant endothelial nitric oxide synthase. *Biochem Biophys Res Commun* 1997 Aug 18;237(2):340-4.
- 120) Milstien S, Katusic Z. Oxidation of tetrahydrobiopterin by peroxynitrite: implications for vascular endothelial function. *Biochem Biophys Res Commun* 1999 Oct 5;263(3):681-4.
- 121) Hamilton CA, Brosnan MJ, McIntyre M, Graham D, Dominiczak AF. Superoxide excess in hypertension and aging: a common cause of endothelial dysfunction. *Hypertension* 2001 Feb;37(2 Part 2):529-34.
- 122) Brandes RP, Mugge A. Gender differences in the generation of superoxide anions in the rat aorta. *Life Sci* 1997;60(6):391-6.
- 123) Dantas AP, Franco MC, Silva-Antonialli MM, Tostes RC, Fortes ZB, Nigro D, et al. Gender differences in superoxide generation in microvessels of hypertensive rats: role of NAD(P)H-oxidase. *Cardiovasc Res* 2004 Jan 1;61(1):22-9.

- 124) Babior BM. The leukocyte NADPH oxidase. *Isr Med Assoc J* 2002 Nov;4(11):1023-4.
- 125) Ushio-Fukai M, Zafari AM, Fukui T, Ishizaka N, Griending KK. p22phox is a critical component of the superoxide-generating NADH/NADPH oxidase system and regulates angiotensin II-induced hypertrophy in vascular smooth muscle cells. *J Biol Chem* 1996 Sep;271(38):23317-21.
- 126) Ushio-Fukai M, Tang Y, Fukai T, Dikalov SI, Ma Y, Fujimoto M, et al. Novel role of gp91(phox)-containing NAD(P)H oxidase in vascular endothelial growth factor-induced signaling and angiogenesis. *Circ Res* 2002 Dec 13;91(12):1160-7.
- 127) Ray R, Shah AM. NADPH oxidase and endothelial cell function. *Clin Sci* 2005 Sep;109(3):217-26.
- 128) Zalba G, Beaumont FJ, San Jose G, Fortuno A, Fortuno MA, Etayo JC, et al. Vascular NADH/NADPH oxidase is involved in enhanced superoxide production in spontaneously hypertensive rats. *Hypertension* 2000 May;35(5):1055-61.
- 129) Wassmann S, Wassmann K, Nickenig G. Modulation of oxidant and antioxidant enzyme expression and function in vascular cells. *Hypertension* 2004 Oct;44(4):381-6.
- 130) Madamanchi NR, Vendrov A, Runge MS. Oxidative stress and vascular disease. *Arterioscler Thromb Vasc Biol* 2005 Jan;25(1):29-38.
- 131) Rajagopalan S, Kurz S, Munzel T, Tarpey M, Freeman BA, Griending KK, et al. Angiotensin II-mediated hypertension in the rat increases vascular superoxide production via membrane NADH/NADPH oxidase activation. Contribution to alterations of vasomotor tone. *J Clin Invest* 1996 Apr 15;97(8):1916-23.
- 132) Griending KK, Minieri CA, Ollerenshaw JD, Alexander RW. Angiotensin II stimulates NADH and NADPH oxidase activity in cultured vascular smooth muscle cells. *Circ Res* 1994 Jun;74(6):1141-8.
- 133) Berry C, Hamilton CA, Brosnan MJ, Magill FG, Berg GA, McMurray JJ, et al. Investigation into the sources of superoxide in human blood vessels: angiotensin II increases superoxide production in human internal mammary arteries. *Circulation* 2000 May 9;101(18):2206-12.
- 134) Sohn HY, Raff U, Hoffmann A, Gloe T, Heermeier K, Galle J, et al. Differential role of angiotensin II receptor subtypes on endothelial superoxide formation. *Br J Pharmacol* 2000 Oct;131(4):667-72.
- 135) Landmesser U, Cai H, Dikalov S, McCann L, Hwang J, Jo H, et al. Role of p47(phox) in vascular oxidative stress and hypertension caused by angiotensin II. *Hypertension* 2002 Oct;40(4):511-5.
- 136) Mollnau H, Wendt M, Szocs K, Lassegue B, Schulz E, Oelze M, et al. Effects of angiotensin II infusion on the expression and function of NAD(P)H oxidase

and components of nitric oxide/cGMP signaling. *Circ Res* 2002 Mar 8;90(4):E58-E65.

- 137) Pagano PJ, Chanock SJ, Siwik DA, Colucci WS, Clark JK. Angiotensin II induces p67phox mRNA expression and NADPH oxidase superoxide generation in rabbit aortic adventitial fibroblasts. *Hypertension* 1998 Aug;32(2):331-7.
- 138) Seshiah PN, Weber DS, Rocic P, Valppu L, Taniyama Y, Griending KK. Angiotensin II stimulation of NAD(P)H oxidase activity: upstream mediators. *Circ Res* 2002 Sep 6;91(5):406-13.
- 139) Touyz RM, Chen X, Tabet F, Yao G, He G, Quinn MT, et al. Expression of a functionally active gp91phox-containing neutrophil-type NAD(P)H oxidase in smooth muscle cells from human resistance arteries: regulation by angiotensin II. *Circ Res* 2002 Jun 14;90(11):1205-13.
- 140) Wassmann S, Laufs U, Baumer AT, Muller K, Konkol C, Sauer H, et al. Inhibition of geranylgeranylation reduces angiotensin II-mediated free radical production in vascular smooth muscle cells: involvement of angiotensin AT1 receptor expression and Rac1 GTPase. *Mol Pharmacol* 2001 Mar;59(3):646-54.
- 141) Marumo T, Schini-Kerth VB, Fisslthaler B, Busse R. Platelet-derived growth factor-stimulated superoxide anion production modulates activation of transcription factor NF-kappaB and expression of monocyte chemoattractant protein 1 in human aortic smooth muscle cells. *Circulation* 1997 Oct 7;96(7):2361-7.
- 142) Bae YS, Kang SW, Seo MS, Baines IC, Tekle E, Chock PB, et al. Epidermal growth factor (EGF)-induced generation of hydrogen peroxide. Role in EGF receptor-mediated tyrosine phosphorylation. *J Biol Chem* 1997 Jan 3;272(1):217-21.
- 143) Patterson C, Ruef J, Madamanchi NR, Barry-Lane P, Hu Z, Horaist C, et al. Stimulation of a vascular smooth muscle cell NAD(P)H oxidase by thrombin. Evidence that p47(phox) may participate in forming this oxidase in vitro and in vivo. *J Biol Chem* 1999 Jul 9;274(28):19814-22.
- 144) Meier B, Radeke HH, Selle S, Younes M, Sies H, Resch K, et al. Human fibroblasts release reactive oxygen species in response to interleukin-1 or tumour necrosis factor-alpha. *Biochem J* 1989 Oct 15;263(2):539-45.
- 145) De Keulenaer GW, Alexander RW, Ushio-Fukai M, Ishizaka N, Griending KK. Tumour necrosis factor alpha activates a p22phox-based NADH oxidase in vascular smooth muscle. *Biochem J* 1998 Feb 1;329(Pt 3):653-7.
- 146) Brandes RP, Koddenberg G, Gwinner W, Kim D, Kruse HJ, Busse R, et al. Role of increased production of superoxide anions by NAD(P)H oxidase and xanthine oxidase in prolonged endotoxemia. *Hypertension* 1999 May;33(5):1243-9.
- 147) Galle J, Lehmann-Bodem C, Hubner U, Heinloth A, Wanner C. CyA and OxLDL cause endothelial dysfunction in isolated arteries through endothelin-

- mediated stimulation of O₂(⁻) formation. *Nephrol Dial Transplant* 2000 Mar;15(3):339-46.
- 148) Heinloth A, Heermeier K, Raff U, Wanner C, Galle J. Stimulation of NADPH oxidase by oxidized low-density lipoprotein induces proliferation of human vascular endothelial cells. *J Am Soc Nephrol* 2000 Oct;11(10):1819-25.
 - 149) Li WG, Miller FJ, Jr., Zhang HJ, Spitz DR, Oberley LW, Weintraub NL. H₂O₂-induced O₂ production by a non-phagocytic NAD(P)H oxidase causes oxidant injury. *J Biol Chem* 2001 Aug 3;276(31):29251-6.
 - 150) Li WG, Stoll LL, Rice JB, Xu SP, Miller FJ, Jr., Chatterjee P, et al. Activation of NAD(P)H oxidase by lipid hydroperoxides: mechanism of oxidant-mediated smooth muscle cytotoxicity. *Free Radic Biol Med* 2003 Apr 1;34(7):937-46.
 - 151) De Keulenaer GW, Chappell DC, Ishizaka N, Nerem RM, Alexander RW, Griending KK. Oscillatory and steady laminar shear stress differentially affect human endothelial redox state: role of a superoxide-producing NADH oxidase. *Circ Res* 1998 Jun 1;82(10):1094-101.
 - 152) McNally JS, Davis ME, Giddens DP, Saha A, Hwang J, Dikalov S, et al. Role of xanthine oxidoreductase and NAD(P)H oxidase in endothelial superoxide production in response to oscillatory shear stress. *Am J Physiol Heart Circ Physiol* 2003 Dec;285(6):H2290-H2297.
 - 153) Fridovich I. Oxygen toxicity: a radical explanation. *J Exp Biol* 1998 Apr;201 (Pt 8):1203-9.
 - 154) Leopold JA, Loscalzo J. Oxidative enzymopathies and vascular disease. *Arterioscler Thromb Vasc Biol* 2005 Jul;25(7):1332-40.
 - 155) Hayes JD, McLellan LI. Glutathione and glutathione-dependent enzymes represent a co-ordinately regulated defence against oxidative stress. *Free Radic Res* 1999 Oct;31(4):273-300.
 - 156) Mates JM. Effects of antioxidant enzymes in the molecular control of reactive oxygen species toxicology. *Toxicology* 2000 Nov 16;153(1-3):83-104.
 - 157) Zelko IN, Mariani TJ, Folz RJ. Superoxide dismutase multigene family: a comparison of the CuZn-SOD (SOD1), Mn-SOD (SOD2), and EC-SOD (SOD3) gene structures, evolution, and expression. *Free Radic Biol Med* 2002 Aug 1;33(3):337-49.
 - 158) Fennell JP, Brosnan MJ, Frater AJ, Hamilton CA, Alexander MY, Nicklin SA, et al. Adenovirus-mediated overexpression of extracellular superoxide dismutase improves endothelial dysfunction in a rat model of hypertension. *Gene Ther* 2002 Jan;9(2):110-7.
 - 159) Zanetti M, Sato J, Katusic ZS, O'Brien T. Gene transfer of superoxide dismutase isoforms reverses endothelial dysfunction in diabetic rabbit aorta. *Am J Physiol Heart Circ Physiol* 2001 Jun;280(6):H2516-H2523.

- 160) Zanetti M, Sato J, Jost CJ, Gloviczki P, Katusic ZS, O'Brien T. Gene transfer of manganese superoxide dismutase reverses vascular dysfunction in the absence but not in the presence of atherosclerotic plaque. *Hum Gene Ther* 2001 Jul 20;12(11):1407-16.
- 161) Li Q, Bolli R, Qiu Y, Tang XL, Murphree SS, French BA. Gene therapy with extracellular superoxide dismutase attenuates myocardial stunning in conscious rabbits. *Circulation* 1998 Oct 6;98(14):1438-48.
- 162) Chung DJ, Wright AE, Clerch LB. The 3' untranslated region of manganese superoxide dismutase RNA contains a translational enhancer element. *Biochemistry* 1998 Nov 17;37(46):16298-306.
- 163) Kirkman HN, Gaetani GF. Catalase: a tetrameric enzyme with four tightly bound molecules of NADPH. *Proc Natl Acad Sci U S A* 1984 Jul;81(14):4343-7.
- 164) Kirkman HN, Galiano S, Gaetani GF. The function of catalase-bound NADPH. *J Biol Chem* 1987 Jan 15;262(2):660-6.
- 165) Kirkman HN, Rolfo M, Ferraris AM, Gaetani GF. Mechanisms of protection of catalase by NADPH. Kinetics and stoichiometry. *J Biol Chem* 1999 May 14;274(20):13908-14.
- 166) Zamocky M, Koller F. Understanding the structure and function of catalases: clues from molecular evolution and in vitro mutagenesis. *Prog Biophys Mol Biol* 1999;72(1):19-66.
- 167) Muzykantov VR. Targeting of superoxide dismutase and catalase to vascular endothelium. *J Control Release* 2001 Mar 12;71(1):1-21.
- 168) Durand E, Al Haj ZA, Addad F, Brasselet C, Caligiuri G, Vinchon F, et al. Adenovirus-mediated gene transfer of superoxide dismutase and catalase decreases restenosis after balloon angioplasty. *J Vasc Res* 2005 May;42(3):255-65.
- 169) Luo D, Rando TA. The regulation of catalase gene expression in mouse muscle cells is dependent on the CCAAT-binding factor NF-Y. *Biochem Biophys Res Commun* 2003 Apr 4;303(2):609-18.
- 170) Nenoï M, Ichimura S, Mita K, Yukawa O, Cartwright IL. Regulation of the catalase gene promoter by Sp1, CCAAT-recognizing factors, and a WT1/Egr-related factor in hydrogen peroxide-resistant HP100 cells. *Cancer Res* 2001 Aug 1;61(15):5885-94.
- 171) Chen G, Kamal M, Hannon R, Warner TD. Regulation of cyclo-oxygenase gene expression in rat smooth muscle cells by catalase. *Biochem Pharmacol* 1998 May 15;55(10):1621-31.
- 172) Cotgreave IA, Gerdes RG. Recent trends in glutathione biochemistry--glutathione-protein interactions: a molecular link between oxidative stress and cell proliferation? *Biochem Biophys Res Commun* 1998 Jan 6;242(1):1-9.

- 173) Wu G, Fang YZ, Yang S, Lupton JR, Turner ND. Glutathione metabolism and its implications for health. *J Nutr* 2004 Mar;134(3):489-92.
- 174) Richman PG, Meister A. Regulation of gamma-glutamyl-cysteine synthetase by nonallosteric feedback inhibition by glutathione. *J Biol Chem* 1975 Feb 25;250(4):1422-6.
- 175) Arthur JR. The glutathione peroxidases. *Cell Mol Life Sci* 2000 Dec;57(13-14):1825-35.
- 176) Fang YZ, Yang S, Wu G. Free radicals, antioxidants, and nutrition. *Nutrition* 2002 Oct;18(10):872-9.
- 177) Fu Y, Porres JM, Lei XG. Comparative impacts of glutathione peroxidase-1 gene knockout on oxidative stress induced by reactive oxygen and nitrogen species in mouse hepatocytes. *Biochem J* 2001 Nov 1;359(Pt 3):687-95.
- 178) Zhang Y, Handy DE, Loscalzo J. Adenosine-dependent induction of glutathione peroxidase 1 in human primary endothelial cells and protection against oxidative stress. *Circ Res* 2005 Apr 29;96(8):831-7.
- 179) Weiss N, Zhang YY, Heydrick S, Bierl C, Loscalzo J. Overexpression of cellular glutathione peroxidase rescues homocyst(e)ine-induced endothelial dysfunction. *Proc Natl Acad Sci U S A* 2001 Oct 23;98(22):12503-8.
- 180) McCarver DG, Hines RN. The ontogeny of human drug-metabolizing enzymes: phase II conjugation enzymes and regulatory mechanisms. *J Pharmacol Exp Ther* 2002 Feb;300(2):361-6.
- 181) van Bladeren PJ. Glutathione conjugation as a bioactivation reaction. *Chem Biol Interact* 2000 Dec 1;129(1-2):61-76.
- 182) Sheehan D, Meade G, Foley VM, Dowd CA. Structure, function and evolution of glutathione transferases: implications for classification of non-mammalian members of an ancient enzyme superfamily. *Biochem J* 2001 Nov 15;360(Pt 1):1-16.
- 183) Hayes JD, Pulford DJ. The glutathione S-transferase supergene family: regulation of GST and the contribution of the isoenzymes to cancer chemoprotection and drug resistance. *Crit Rev Biochem Mol Biol* 1995;30(6):445-600.
- 184) Frova C. Glutathione transferases in the genomics era: new insights and perspectives. *Biomol Eng* 2006 Sep;23(4):149-69.
- 185) Strange RC, Spiteri MA, Ramachandran S, Fryer AA. Glutathione-S-transferase family of enzymes. *Mutat Res* 2001 Oct 1;482(1-2):21-6.
- 186) Nebert DW, Vasiliou V. Analysis of the glutathione S-transferase (GST) gene family. *Hum Genomics* 2004 Nov;1(6):460-4.
- 187) Hayes JD, Strange RC. Potential contribution of the glutathione S-transferase supergene family to resistance to oxidative stress. *Free Radic Res* 1995 Mar;22(3):193-207.

- 188) Mannervik B, Awasthi YC, Board PG, Hayes JD, Di Ilio C, Ketterer B, et al. Nomenclature for human glutathione transferases. *Biochem J* 1992;282:305-6.
- 189) Mannervik B, Board PG, Hayes JD, Listowsky I, Pearson WR. Nomenclature for mammalian soluble glutathione transferases. *Methods Enzymol* 2005;401:1-8.
- 190) Ross VL, Board PG, Webb GC. Chromosomal mapping of the human Mu class glutathione S-transferases to 1p13. *Genomics* 1993 Oct;18(1):87-91.
- 191) DeJong JL, Chang CM, Whang-Peng J, Knutsen T, Tu CP. The human liver glutathione S-transferase gene superfamily: expression and chromosome mapping of an Hb subunit cDNA. *Nucleic Acids Res* 1988 Sep 12;16(17):8541-54.
- 192) Patskovsky YV, Huang MQ, Takayama T, Listowsky I, Pearson WR. Distinctive structure of the human GSTM3 gene-inverted orientation relative to the mu class glutathione transferase gene cluster. *Arch Biochem Biophys* 1999 Jan 1;361(1):85-93.
- 193) Board PG. Biochemical genetics of glutathione-S-transferase in man. *Am J Hum Genet* 1981 Jan;33(1):36-43.
- 194) Widersten M, Pearson WR, Engstrom A, Mannervik B. Heterologous expression of the allelic variant mu-class glutathione transferases mu and psi. *Biochem J* 1991 Jun 1;276(Pt 2):519-24.
- 195) McLellan RA, Oscarson M, Alexandrie AK, Seidegard J, Evans DA, Rannug A, et al. Characterization of a human glutathione S-transferase mu cluster containing a duplicated GSTM1 gene that causes ultrarapid enzyme activity. *Mol Pharmacol* 1997 Dec;52(6):958-65.
- 196) Board PG. Gene deletion and partial deficiency of the glutathione S-transferase (ligandin) system in man. *FEBS Lett* 1981 Nov 30;135(1):12-4.
- 197) Seidegard J, Vorachek WR, Pero RW, Pearson WR. Hereditary differences in the expression of the human glutathione transferase active on trans-stilbene oxide are due to a gene deletion. *Proc Natl Acad Sci USA* 1988 Oct;85(19):7293-7.
- 198) Benhamou S, Lee WJ, Alexandrie AK, Boffetta P, Bouchardy C, Butkiewicz D, et al. Meta- and pooled analyses of the effects of glutathione S-transferase M1 polymorphisms and smoking on lung cancer risk. *Carcinogenesis* 2002 Aug;23(8):1343-50.
- 199) Engel LS, Taioli E, Pfeiffer R, Garcia-Closas M, Marcus PM, Lan Q, et al. Pooled analysis and meta-analysis of glutathione S-transferase M1 and bladder cancer: a HuGE review. *Am J Epidemiol* 2002 Jul 15;156(2):95-109.
- 200) Abu-Amero KK, Al-Boudari OM, Mohamed GH, Dzimirri N. T null and M null genotypes of the glutathione S-transferase gene are risk factor for CAD independent of smoking. *BMC Med Genet* 2006;7:38.

- 201) de Waart FG, Kok FJ, Smilde TJ, Hijmans A, Wollersheim H, Stalenhoef AF. Effect of glutathione S-transferase M1 genotype on progression of atherosclerosis in lifelong male smokers. *Atherosclerosis* 2001 Sep;158(1):227-31.
- 202) Wang XL, Greco M, Sim AS, Duarte N, Wang J, Wilcken DE. Glutathione S-transferase mu1 deficiency, cigarette smoking and coronary artery disease. *J Cardiovasc Risk* 2002 Feb;9(1):25-31.
- 203) Izzotti A, Cartiglia C, Lewtas J, De Flora S. Increased DNA alterations in atherosclerotic lesions of individuals lacking the GSTM1 genotype. *FASEB J* 2001 Mar;15(3):752-7.
- 204) Inskip A, Elexperu-Camiruaga J, Buxton N, Dias PS, MacIntosh J, Campbell D, et al. Identification of polymorphism at the glutathione S-transferase, GSTM3 locus: evidence for linkage with GSTM1*A. *Biochem J* 1995 Dec 15;312 (Pt 3):713-6.
- 205) Yengi L, Inskip A, Gilford J, Aldersea J, Bailey L, Smith A, et al. Polymorphism at the glutathione S-transferase locus GSTM3: interactions with cytochrome P450 and glutathione S-transferase genotypes as risk factors for multiple cutaneous basal cell carcinoma. *Cancer Res* 1996 May 1;56(9):1974-7.
- 206) Ross VL, Board PG. Molecular cloning and heterologous expression of an alternatively spliced human Mu class glutathione S-transferase transcript. *Biochem J* 1993 Sep 1;294(Pt 2):373-80.
- 207) Tetlow N, Robinson A, Mantle T, Board P. Polymorphism of human mu class glutathione transferases. *Pharmacogenetics* 2004 Jun;14(6):359-68.
- 208) Turella P, Pedersen JZ, Caccuri AM, De Maria F, Mastroberardino P, Lo BM, et al. Glutathione transferase superfamily behaves like storage proteins for dinitrosyl-diglutathionyl-iron complex in heterogeneous systems. *J Biol Chem* 2003 Oct 24;278(43):42294-9.
- 209) Daggett DA, Oberley TD, Nelson SA, Wright LS, Kornguth SE, Siegel FL. Effects of lead on rat kidney and liver: GST expression and oxidative stress. *Toxicology* 1998 Jul 17;128(3):191-206.
- 210) Armstrong RN. Structure, catalytic mechanism, and evolution of the glutathione transferases. *Chem Res Toxicol* 1997 Feb;10(1):2-18.
- 211) Cummings BS, Lasker JM, Lash LH. Expression of glutathione-dependent enzymes and cytochrome P450s in freshly isolated and primary cultures of proximal tubular cells from human kidney. *J Pharmacol Exp Ther* 2000 May;293(2):677-85.
- 212) Armstrong RN. Mechanistic imperatives for the evolution of glutathione transferases. *Curr Opin Chem Biol* 1998 Nov;2(5):618-23.
- 213) Segura-Aguilar J, Baez S, Widersten M, Welch CJ, Mannervik B. Human class Mu glutathione transferases, in particular isoenzyme M2-2, catalyze

- detoxication of the dopamine metabolite aminochrome. *J Biol Chem* 1997 Feb 28;272(9):5727-31.
- 214) Hansson LO, Bolton-Grob R, Massoud T, Mannervik B. Evolution of differential substrate specificities in Mu class glutathione transferases probed by DNA shuffling. *J Mol Biol* 1999 Mar 26;287(2):265-76.
- 215) Patskovsky YV, Patskovska LN, Listowsky I. The enhanced affinity for thiolate anion and activation of enzyme-bound glutathione is governed by an arginine residue of human Mu class glutathione S-transferases. *J Biol Chem* 2000 Feb 4;275(5):3296-304.
- 216) Kuba K, Imai Y, Rao S, Jiang C, Penninger JM. Lessons from SARS: control of acute lung failure by the SARS receptor ACE2. *J Mol Med* 2006 Oct;84(10):814-20.
- 217) Luft FC, Toka O, Toka HR, Jordan J, Bähring S. Mendelian hypertension with brachydactyly as a molecular genetic lesson in regulatory physiology. *Am J Physiol Regul Integr Comp Physiol* 2003 Oct;285(4):R709-R714.
- 218) Bähring S, Rauch A, Toka O, Schroeder C, Hesse C, Siedler H, et al. Autosomal-dominant hypertension with type E brachydactyly is caused by rearrangement on the short arm of chromosome 12. *Hypertension* 2004 Feb;43(2):471-6.
- 219) Jeffs B, Negrin CD, Graham D, Clark JS, Anderson NH, Gauguier D, et al. Applicability of a "speed" congenic strategy to dissect blood pressure quantitative trait loci on rat chromosome 2. *Hypertension* 2000 Jan;35(1 Pt 2):179-87.
- 220) Lander ES, Green P, Abrahamson J, Barlow A, Daly MJ, Lincoln SE, et al. MAPMAKER: an interactive computer package for constructing primary genetic linkage maps of experimental and natural populations. *Genomics* 1987 Oct;1(2):174-81.
- 221) Evans AL, Brown W, Kenyon CJ, Maxted KJ, Smith DC. Improved system for measuring systolic blood pressure in the conscious rat. *Med Biol Eng Comput* 1994 Jan;32(1):101-2.
- 222) Young B, Lowe JS, Stevens A, Heath JW. Urinary System. In *Wheater's Functional Histology A Text and Colour Atlas*. Churchill Livingstone. 2006. 302-327.
- 223) Listowsky I, Rowe JD, Patskovsky YV, Tchaikovskaya T, Shintani N, Novikova E, et al. Human testicular glutathione S-transferases: insights into tissue-specific expression of the diverse subunit classes. *Chem Biol Interact* 1998 Apr 24;111-112:103-12.
- 224) Lai HC, Qian B, Grove G, Tu CP. Gene expression of rat glutathione S-transferases. Evidence for gene conversion in the evolution of the Yb multigene family. *J Biol Chem* 1988 Aug 15;263(23):11389-95.
- 225) Hsieh CH, Tsai SP, Yeh HI, Sheu TC, Tam MF. Mass spectrometric analysis of rat ovary and testis cytosolic glutathione S-transferases (GSTs):

- identification of a novel class-alpha GST, rGSTA6*, in rat testis. *Biochem J* 1997 Apr 15;323 (Pt 2):503-10.
- 226) Cheng H, Tchaikovskaya T, Tu YS, Chapman J, Qian B, Ching WM, et al. Rat glutathione S-transferase M4-4: an isoenzyme with unique structural features including a redox-reactive cysteine-115 residue that forms mixed disulphides with glutathione. *Biochem J* 2001 Jun 1;356(Pt 2):403-14.
- 227) Bermano G, Shepherd RK, Zehner ZE, Hesketh JE. Perinuclear mRNA localisation by vimentin 3'-untranslated region requires a 100 nucleotide sequence and intermediate filaments. *FEBS Lett* 2001 May 25;497(2-3):77-81.
- 228) Nuovo GJ. Co-labeling using in situ PCR: a review. *J Histochem Cytochem* 2001 Nov;49(11):1329-39.
- 229) Chen YC, Cadnapaphornchai MA, Schrier RW. Clinical update on renal aquaporins. *Biol Cell* 2005 Jun;97(6):357-71.
- 230) Srivastava PK, Waxman DJ. Sex-dependent expression and growth hormone regulation of class alpha and class mu glutathione S-transferase mRNAs in adult rat liver. *Biochem J* 1993 Aug 15;294(Pt 1):159-65.
- 231) Meng S, Roberts LJ, Cason GW, Curry TS, Manning RD, Jr. Superoxide dismutase and oxidative stress in Dahl salt-sensitive and -resistant rats. *Am J Physiol Regul Integr Comp Physiol* 2002 Sep;283(3):R732-R738.
- 232) Nakajima T, Elovaara E, Anttila S, Hirvonen A, Camus AM, Hayes JD, et al. Expression and polymorphism of glutathione S-transferase in human lungs: risk factors in smoking-related lung cancer. *Carcinogenesis* 1995 Apr;16(4):707-11.
- 233) Caulfield M, Munroe P, Pembroke J, Samani N, Dominiczak A, Brown M, et al. Genome-wide mapping of human loci for essential hypertension. *Lancet* 2003 Jun 21;361(9375):2118-23.
- 234) Delles C, Braga-Marciano AC, Munroe PB, Padmanabhan S, McClure JD, Brain NJ, et al. Variants of the human mu type glutathion-S-transferase (GSTM) gene family are associated with hypertension. *J Hyper Supp* 2006 Jun;24(S4):S13.
- 235) Gabbiani G, Schmid E, Winter S, Chaponnier C, de CC, Vandekerckhove J, et al. Vascular smooth muscle cells differ from other smooth muscle cells: predominance of vimentin filaments and a specific alpha-type actin. *Proc Natl Acad Sci U S A* 1981 Jan;78(1):298-302.
- 236) Schildmeyer LA, Braun R, Taffet G, Debiassi M, Burns AE, Bradley A, et al. Impaired vascular contractility and blood pressure homeostasis in the smooth muscle alpha-actin null mouse. *FASEB J* 2000 Nov;14(14):2213-20.
- 237) Tortora GJ. The Urinary System. In: *Principles of Human Anatomy*, 8th Edition. New York: Benjamin/Cummings Science Publishing. 1999: 747-769.

- 238) Grunfeld S, Hamilton CA, Mesaros S, McClain SW, Dominiczak AF, Bohr DF, et al. Role of superoxide in the depressed nitric oxide production by the endothelium of genetically hypertensive rats. *Hypertension* 1995 Dec;26(6 Pt 1):854-7.
- 239) McIntyre M, Bohr DF, Dominiczak AF. Endothelial function in hypertension: the role of superoxide anion. *Hypertension* 1999 Oct;34(4 Pt 1):539-45.
- 240) Brosnan MJ, Hamilton CA, Graham D, Lygate CA, Jardine E, Dominiczak AF. Irbesartan lowers superoxide levels and increases nitric oxide bioavailability in blood vessels from spontaneously hypertensive stroke-prone rats. *J Hypertens* 2002 Feb;20(2):281-6.
- 241) Graham D, Hamilton C, Beattie E, Spiers A, Dominiczak AF. Comparison of the effects of omapatrilat and irbesartan/hydrochlorothiazide on endothelial function and cardiac hypertrophy in the stroke-prone spontaneously hypertensive rat: sex differences. *J Hypertens* 2004 Feb;22(2):329-37.
- 242) Mizuno M, Sada T, Ikeda M, Fukuda N, Miyamoto M, Yanagisawa H, et al. Pharmacology of CS-866, a novel nonpeptide angiotensin II receptor antagonist. *Eur J Pharmacol* 1995 Oct 16;285(2):181-8.
- 243) Tsuda M, Iwai M, Li JM, Li HS, Min LJ, Ide A, et al. Inhibitory effects of AT1 receptor blocker, olmesartan, and estrogen on atherosclerosis via anti-oxidative stress. *Hypertension* 2005 Apr;45(4):545-51.
- 244) Yao L, Kobori H, Rahman M, Seth DM, Shokoji T, Fan Y, et al. Olmesartan improves endothelin-induced hypertension and oxidative stress in rats. *Hypertens Res* 2004 Jul;27(7):493-500.
- 245) Ellershaw DC, Gurney AM. Mechanisms of hydralazine induced vasodilation in rabbit aorta and pulmonary artery. *Br J Pharmacol* 2001 Oct;134(3):621-31.
- 246) Wei S, Kasuya Y, Yanagisawa M, Kimura S, Masaki T, Goto K. Studies on endothelium-dependent vasorelaxation by hydralazine in porcine coronary artery. *Eur J Pharmacol* 1997 Mar 5;321(3):307-14.
- 247) Brandes RP, Kreuzer J. Vascular NADPH oxidases: molecular mechanisms of activation. *Cardiovasc Res* 2005 Jan 1;65(1):16-27.
- 248) Kerr S, Brosnan MJ, McIntyre M, Reid JL, Dominiczak AF, Hamilton CA. Superoxide anion production is increased in a model of genetic hypertension: role of the endothelium. *Hypertension* 1999 Jun;33(6):1353-8.
- 249) Zou AP, Li N, Cowley AW, Jr. Production and actions of superoxide in the renal medulla. *Hypertension* 2001 Feb;37(2 Part 2):547-53.
- 250) Makino A, Skelton MM, Zou AP, Roman RJ, Cowley AW, Jr. Increased renal medullary oxidative stress produces hypertension. *Hypertension* 2002 Feb;39(2 Pt 2):667-72.
- 251) Makino A, Skelton MM, Zou AP, Cowley AW, Jr. Increased renal medullary H₂O₂ leads to hypertension. *Hypertension* 2003 Jul;42(1):25-30.

- 252) Soccio M, Toniato E, Evangelista V, Carluccio M, De CR. Oxidative stress and cardiovascular risk: the role of vascular NAD(P)H oxidase and its genetic variants. *Eur J Clin Invest* 2005 May;35(5):305-14.
- 253) Dinauer MC, Pierce EA, Bruns GA, Curnutte JT, Orkin SH. Human neutrophil cytochrome b light chain (p22-phox). Gene structure, chromosomal location, and mutations in cytochrome-negative autosomal recessive chronic granulomatous disease. *J Clin Invest* 1990 Nov;86(5):1729-37.
- 254) Krex D, Ziegler A, Konig IR, Schackert HK, Schackert G. Polymorphisms of the NADPH oxidase P22PHOX gene in a Caucasian population with intracranial aneurysms. *Cerebrovasc Dis* 2003;16(4):363-8.
- 255) Gardemann A, Mages P, Katz N, Tillmanns H, Haberbosch W. The p22 phox A640G gene polymorphism but not the C242T gene variation is associated with coronary heart disease in younger individuals. *Atherosclerosis* 1999 Aug;145(2):315-23.
- 256) Inoue N, Kawashima S, Kanazawa K, Yamada S, Akita H, Yokoyama M. Polymorphism of the NADH/NADPH oxidase p22 phox gene in patients with coronary artery disease. *Circulation* 1998 Jan 20;97(2):135-7.
- 257) Cai H, Duarte N, Wilcken DE, Wang XL. NADH/NADPH oxidase p22 phox C242T polymorphism and coronary artery disease in the Australian population. *Eur J Clin Invest* 1999 Sep;29(9):744-8.
- 258) Ito D, Murata M, Watanabe K, Yoshida T, Saito I, Tanahashi N, et al. C242T polymorphism of NADPH oxidase p22 phox gene and ischemic cerebrovascular disease in the Japanese population. *Stroke* 2000 Apr;31(4):936-9.
- 259) Zafari AM, Davidoff MN, Austin H, Valppu L, Cotsonis G, Lassegue B, et al. The A640G and C242T p22(phox) polymorphisms in patients with coronary artery disease. *Antioxid Redox Signal* 2002 Aug;4(4):675-80.
- 260) Moreno MU, San Jose G, Orbe J, Paramo JA, Beloqui O, Diez J, et al. Preliminary characterisation of the promoter of the human p22(phox) gene: identification of a new polymorphism associated with hypertension. *FEBS Lett* 2003 May 8;542(1-3):27-31.
- 261) San Jose G, Moreno MU, Oliván S, Beloqui O, Fortuno A, Diez J, et al. Functional effect of the p22phox -930A/G polymorphism on p22phox expression and NADPH oxidase activity in hypertension. *Hypertension* 2004 Aug;44(2):163-9.
- 262) Marsden PA, Heng HH, Scherer SW, Stewart RJ, Hall AV, Shi XM, et al. Structure and chromosomal localization of the human constitutive endothelial nitric oxide synthase gene. *J Biol Chem* 1993 Aug 15;268(23):17478-88.
- 263) Robinson LJ, Weremowicz S, Morton CC, Michel T. Isolation and chromosomal localization of the human endothelial nitric oxide synthase (NOS3) gene. *Genomics* 1994 Jan 15;19(2):350-7.

- 264) Nakayama M, Yasue H, Yoshimura M, Shimasaki Y, Kugiyama K, Ogawa H, et al. T-786-->C mutation in the 5'-flanking region of the endothelial nitric oxide synthase gene is associated with coronary spasm. *Circulation* 1999 Jun 8;99(22):2864-70.
- 265) Tesauro M, Thompson WC, Rogliani P, Qi L, Chaudhary PP, Moss J. Intracellular processing of endothelial nitric oxide synthase isoforms associated with differences in severity of cardiopulmonary diseases: cleavage of proteins with aspartate vs. glutamate at position 298. *Proc Natl Acad Sci USA* 2000 Mar 14;97(6):2832-5.
- 266) Persu A, Stoenoiu MS, Messiaen T, Davila S, Robino C, El-Khattabi O, et al. Modifier effect of eNOS in autosomal dominant polycystic kidney disease. *Hum Mol Genet* 2002 Feb 1;11(3):229-41.
- 267) Cai H, Wilcken DE, Wang XL. The Glu-298-->Asp (894G-->T) mutation at exon 7 of the endothelial nitric oxide synthase gene and coronary artery disease. *J Mol Med* 1999 Jun;77(6):511-4.
- 268) Gardemann A, Lohre J, Cayci S, Katz N, Tillmanns H, Haberbosch W. The T allele of the missense Glu(298)Asp endothelial nitric oxide synthase gene polymorphism is associated with coronary heart disease in younger individuals with high atherosclerotic risk profile. *Atherosclerosis* 2002 Jan;160(1):167-75.
- 269) Hibi K, Ishigami T, Tamura K, Mizushima S, Nyui N, Fujita T, et al. Endothelial nitric oxide synthase gene polymorphism and acute myocardial infarction. *Hypertension* 1998 Sep;32(3):521-6.
- 270) Hingorani AD, Liang CF, Fatibene J, Lyon A, Monteith S, Parsons A, et al. A common variant of the endothelial nitric oxide synthase (Glu298-->Asp) is a major risk factor for coronary artery disease in the UK. *Circulation* 1999 Oct 5;100(14):1515-20.
- 271) Hyndman ME, Parsons HG, Verma S, Bridge PJ, Edworthy S, Jones C, et al. The T-786-->C mutation in endothelial nitric oxide synthase is associated with hypertension. *Hypertension* 2002 Apr;39(4):919-22.
- 272) Lembo G, De Luca N, Battagli C, Iovino G, Aretini A, Musicco M, et al. A common variant of endothelial nitric oxide synthase (Glu298Asp) is an independent risk factor for carotid atherosclerosis. *Stroke* 2001;32(3):735-40.
- 273) Miyamoto Y, Saito Y, Kajiyama N, Yoshimura M, Shimasaki Y, Nakayama M, et al. Endothelial nitric oxide synthase gene is positively associated with essential hypertension. *Hypertension* 1998 Jul;32(1):3-8.
- 274) Nakayama M, Yasue H, Yoshimura M, Shimasaki Y, Ogawa H, Kugiyama K, et al. T(-786)--> C mutation in the 5'-flanking region of the endothelial nitric oxide synthase gene is associated with myocardial infarction, especially without coronary organic stenosis. *Am J Cardiol* 2000 Sep 15;86(6):628-34.
- 275) Shimasaki Y, Yasue H, Yoshimura M, Nakayama M, Kugiyama K, Ogawa H, et al. Association of the missense Glu298Asp variant of the endothelial nitric

- oxide synthase gene with myocardial infarction. *J Am Coll Cardiol* 1998 Jun;31(7):1506-10.
- 276) Tsukada T, Yokoyama K, Arai T, Takemoto F, Hara S, Yamada A, et al. Evidence of association of the ecNOS gene polymorphism with plasma NO metabolite levels in humans. *Biochem Biophys Res Commun* 1998 Apr 7;245(1):190-3.
- 277) Wang XL, Sim AS, Badenhop RF, McCredie RM, Wilcken DE. A smoking-dependent risk of coronary artery disease associated with a polymorphism of the endothelial nitric oxide synthase gene. *Nat Med* 1996 Jan;2(1):41-5.
- 278) Mackenzie IS, Wilkinson IB, Cockcroft JR. Assessment of arterial stiffness in clinical practice. *QJM* 2002 Feb;95(2):67-74.
- 279) Woodman RJ, Kingwell BA, Beilin LJ, Hamilton SE, Dart AM, Watts GF. Assessment of central and peripheral arterial stiffness: studies indicating the need to use a combination of techniques. *Am J Hypertens* 2005 Feb;18(2 Pt 1):249-60.
- 280) Dart AM, Kingwell BA. Pulse pressure--a review of mechanisms and clinical relevance. *J Am Coll Cardiol* 2001 Mar 15;37(4):975-84.
- 281) McVeigh GE, Allen PB, Morgan DR, Hanratty CG, Silke B. Nitric oxide modulation of blood vessel tone identified by arterial waveform analysis. *Clin Sci* 2001 Apr;100(4):387-93.
- 282) Wilkinson IB, Qasem A, McEniery CM, Webb DJ, Avolio AP, Cockcroft JR. Nitric oxide regulates local arterial distensibility in vivo. *Circulation* 2002 Jan 15;105(2):213-7.
- 283) London GM, Blacher J, Pannier B, Guerin AP, Marchais SJ, Safar ME. Arterial wave reflections and survival in end-stage renal failure. *Hypertension* 2001 Sep;38(3):434-8.
- 284) Cohn JN, Finkelstein S, McVeigh G, Morgan D, LeMay L, Robinson J, et al. Noninvasive pulse wave analysis for the early detection of vascular disease. *Hypertension* 1995 Sep;26(3):503-8.
- 285) McVeigh GE, Burns DE, Finkelstein SM, McDonald KM, Mock JE, Feske W, et al. Reduced vascular compliance as a marker for essential hypertension. *Am J Hypertens* 1991 Mar;4(3 Pt 1):245-51.
- 286) Stephens M, Smith NJ, Donnelly P. A new statistical method for haplotype reconstruction from population data. *Am J Hum Genet* 2001 Apr;68(4):978-89.
- 287) Stephens M, Donnelly P. A comparison of bayesian methods for haplotype reconstruction from population genotype data. *Am J Hum Genet* 2003 Nov;73(5):1162-9.
- 288) Guzik TJ, West NE, Black E, McDonald D, Ratnatunga C, Pillai R, et al. Functional effect of the C242T polymorphism in the NAD(P)H oxidase

- p22phox gene on vascular superoxide production in atherosclerosis. *Circulation* 2000 Oct 10;102(15):1744-7.
- 289) Hedrick PW. Gametic disequilibrium measures: proceed with caution. *Genetics* 1987 Oct;117(2):331-41.
- 290) Lewontin RC. On measures of gametic disequilibrium. *Genetics* 1988 Nov;120(3):849-52.
- 291) Hingorani AD. Polymorphisms in endothelial nitric oxide synthase and atherogenesis: John French Lecture 2000. *Atherosclerosis* 2000 Feb 15;154(3):521-7.
- 292) O'Rourke MF, Adji A. An updated clinical primer on large artery mechanics: implications of pulse waveform analysis and arterial tonometry. *Curr Opin Cardiol* 2005 Jul;20(4):275-81.
- 293) Polke JM, McBride MM, Nicklin SA, Baker AB, Graham D, Dominiczak AF. Interactions between multiple promoter polymorphisms are required for reduced expression of *Gstm1* in the SHRSP. *J Hyper Supp* 2006 Dec;24(S6)(Supp 6):284.
- 294) Zhou X, Frohlich ED. Differential effects of antihypertensive drugs on renal and glomerular hemodynamics and injury in the chronic nitric-oxide-suppressed rat. *Am J Nephrol* 2005 Mar;25(2):138-52.
- 295) Jaffe EA, Nachman RL, Becker CG, Minick CR. Culture of human endothelial cells derived from umbilical veins. Identification by morphologic and immunologic criteria. *J Clin Invest* 1973 Nov;52(11):2745-56.
- 296) Southgate K, Newby AC. Serum-induced proliferation of rabbit aortic smooth muscle cells from the contractile state is inhibited by 8-Br-cAMP but not 8-Br-cGMP. *Atherosclerosis* 1990 May;82(1-2):113-23.
- 297) Zhang J, Lo C. Regulation of fibronectin expression by PDGF-BB and IGF-I in cultured rat thoracic aortic adventitial fibroblasts. *Cell Biol Int* 1995 Jun;19(6):517-25.
- 298) Chu Y, Alwahdani A, Iida S, Lund DD, Faraci FM, Heistad DD. Vascular effects of the human extracellular superoxide dismutase R213G variant. *Circulation* 2005 Aug 16;112(7):1047-53.
- 299) Forsberg L, Lyrenas L, de FU, Morgenstern R. A common functional C-T substitution polymorphism in the promoter region of the human catalase gene influences transcription factor binding, reporter gene transcription and is correlated to blood catalase levels. *Free Radic Biol Med* 2001 Mar 1;30(5):500-5.

APPENDICES

Appendix A – Recipes for Solutions

DNA extraction solution (100ml)

1M Tris pH 8.0	5ml
0.5M EDTA pH 8.0	20ml
5M NaCl	2ml
10% SDS	10ml

6X nucleic acid loading dye (100ml)

Ficoll-400	15g
Bromophenol blue	0.05g
Xylene cyanol	0.05g

10x Phosphate buffered saline(PBS), pH 7.4 (1L)

10X Tris/EDTA (TE) Buffer, pH 8.0 (1L)

Tris	12.1g
EDTA	3.72g

1x Tris borate EDTA (TBE) Buffer (1L)

NaOH	0.1g
Tris base	10.8g
boric acid	5.5g
EDTA	0.74g

In situ hybridisation 2X prehybridisation buffer (10ml)

DEPC-H ₂ O	5.88 ml
5 M NaCl	2.4 ml
1 M Tris (pH 7.5)	200 µl
50 X Denhardt's	400 µl
250 mM EDTA	80 µl
10 mg/ml Salmon Sperm DNA	1 ml
50 mg/ml Yeast tRNA	40 µl

In situ hybridisation 2X hybridisation buffer (10ml)

DEPC-H ₂ O	6.68 ml
5 M NaCl	2.4 ml
1 M Tris (pH 7.5)	200 µl
50 X Denhardt's	400 µl
250 mM EDTA	80 µl
Salmon Sperm DNA	200 µl
Dextran sulphate	2.0 g
50 mg/ml Yeast tRNA	40 µl

0.01M Citrate Buffer pH 6.0 (make up fresh on day of use)

0.1M trisodium citrate	4.1ml
0.1M citric acid	900µl

Make up to 40ml, pH to 6.0 with 5M NaOH and make up to 50ml

Appendix B – Suppliers and Catalogue Numbers

Equipments

Applied Biosystems Taqman (ABI Prism 7900HT Sequence Detection System)
- Data analysis with software SDS 2.1
Applied Biosystems 3730 DNA Analyzer Bios
- Data Collection Software v3.0
- Data analysis with software Seqscape v2.5
- Data analysis with GeneMapper v2.0
Biorad Fluor-S™ Multimager (gel imaging)
Eppendorf Centrifuge 5415C (microcentrifuge)
Thermo IEC Centra GP8R
Thermo electronic Cryotome
Thermo Shandon Finesse 325 Microtome
Packard TRI-CAR 2100TR (liquid scintillation analyser)
Peltier Thermal Cycler PTC-225

Chemicals and consumables not listed below were purchased from campus store.

Abcam, UK

anti-alpha smooth muscle actin; Cat. No. ab18147
anti-aquaporin 2; Cat. No. ab15082
anti-GAPDH; Cat. No. ab9484
anti-β-actin; Cat. No. ab8226
anti-hGSTM1/2; Cat. No. ab27489
anti-goat IgG*HRP; Cat. No. ab6741

ABGene, UK

384-well PCR plate Thermo fast; Cat. No. AB-1310
0.2ml V-PCR plate; Cat. No. AB-0800
Absolute Q-PCR Seal; Cat. No. AB-1170
Clear adhesive PCR Film, 100 sheets; Cat. No. AB-0558
Nucleofast 96 plate; Cat. No. MN743100.10

Abnova, Taiwan

GSTM1 monoclonal antibody; Cat. No. H00002944-M01
GSTM1 recombinant protein; Cat. No. H00002944-Q01
GSTM2 recombinant protein; Cat. No. H00002946-Q01
GSTM3 recombinant protein; Cat. No. H00002947-P01
GSTM4 recombinant protein; Cat. No. H00002948-P01
GSTM5 recombinant protein; Cat. No. H00002949-Q01

Agar Scientific, UK

Ilford K5 nuclear emulsion; no catalogue number required

Ambion, UK

Human Heart Total RNA, 100µg; Cat. No. 7966
Human Kidney Total RNA, 100µg; Cat. No. 7976
Human Liver Total RNA, 100µg; Cat. No. 7960
Human Testes Total RNA, 100µg; Cat. No. 7972
DNA-free™; Cat. No. 1906
RNAlater; Cat. No. 7021
RNaseZap; Cat. No. 9780

Amersham, UK

35S-UTP; Cat. No. SJ40383

ECL Western blot detection reagents; Cat. No. RPN 2106
Hybond™-C extra (nitrocellulose membrane); Cat. No. RPN137E
Hybond-P (PVDF membrane); Cat. No. RPN 303F
Hyperfilm ECL; Cat. No. RPN 3103K
illustra Nick™ columns; Cat. No. 17-0855-01
Recombinant Protein Molecular Weight Markers (10kDa – 250kDa); Cat. No. RPN 800

Anachem, UK

Kodak NTB2 nuclear emulsion; Cat. No. 8895666

Applied Biosystems, UK

ABI Prism® Big Dye Terminator v3.1 Cycle Sequencing Kit; Cat. No. 4337455
Taqman Universal PCR Master Mix; Cat. No. 4324018
GeneScan™ 500 Liz™ Size Standard; Cat. No. 4322682
Rat β -Actin (VIC-MGB) Gene Expression probe; Cat. No. 4352340E
Rat *Gstm1* (5'-FAM) Gene Expression probe; Cat. No. Rn00755117_m1
Rat *Gstm2* (5'-FAM) Gene Expression probe; Cat. No. Rn00598597_m1
Rat *Gstm3* (5'-FAM) Gene Expression probe; Cat. No. Rn00579867_m1
Rat *Gstm5* (5'-FAM) Gene Expression probe; Cat. No. Rn00597012_m1
Rat *Gstm7* (5'-FAM) Gene Expression probe; customised

Dakocytomation UK

Anti-Rabbit Igs*HRP; Cat. No. P0399

Fisher Scientific, UK

Histoclear; Cat. No. H/0468/17

Genetix, UK

GenCLEAN plate (Dye Terminator Removal 96-Well plate); Cat. No. K1015

Microzone UK

microCLEAN, 5 x 1ml; Cat. No. 2MCL-5

Molecular Probes, Eugene, Oregon, USA

PicoGreen® dsDNA Quantitation Kit; Cat. No. P-7589
RiboGreen™ RNA Quantitation Kit; Cat. No. R-11490

National Diagnostic, UK

Histomount; Cat. No. HS-103

Pierce Biotechnology Inc., UK

BCA protein assay reagent kit; Cat. No. 23227

Promega UK

100bp DNA ladders; Cat. No. G2101
5X Transcription buffer, Cat. No. P118B
Blue *Taq*, 500u; Cat. No. M1665
dNTPs set, 40 μ mol each; Cat. No. U1240
Msp I, 2000u; Cat. No. R6401
Proteinase K; Cat. No. V3021
rATP, 10mM; Cat. No. P1132
rCTP, 10mM; Cat. No. P1142
rGTP, 10mM; Cat. No. P1152
RQ1 DNase, 1000u; Cat. No. M6101
Rsa I, 1000u; Cat. No. R6371
Recombinant RNasin® Ribonuclease Inhibitor, 2500u; Cat. No. N2511
Reverse Transcription System, 100 reactions; Cat. No. A3500

T3 RNA polymerase; Cat. No. P2083
T7 RNA polymerase; Cat. No. P2075
Wizard® Genomic DNA Purification Kit; Cat. No. A1125

Qiagen, UK

HotStar Taq DNA polymerase; Cat. No. 203203
RNeasy Mini; Cat. No. 74104
RNeasy Midi; Cat. No. 75142
RNeasy Maxi; Cat. No. 75162

Roche UK

DNA markers X, 0.07 - 12.2kbp; Cat. No. 90437221
Lightcycler FastStart DNA Master SYBR Green 1; Cat. No. 2239264
Complete EDTA-free protease inhibitors cocktail; Cat. No. 1873580
Sex AI, 200u; Cat. No. 1497995

Sigma-Aldrich, UK

Ammonium hydroxide solution; Cat. No. 320145
APES; Cat. No. A3648
4',6-diamidino-2-phenylindole (DAPI); Cat. No. D9542
DL-dithiothreitol; Cat. No. D0632
Eosin Y solution; Cat. No. 45242
Ethanol ACS reagent; Cat. No. 459844
Glycerol; Cat. No. G8773
Glycine; Cat. No. G8898
Harris Modified Haematoxylin; Cat. No. HHS32
Hydralazine hydrochloride; Cat. No. H1753
Hydrochlorothiazide; Cat. No. H2910
Hydrogen peroxide 30% (w/w) solution; Cat. No. H1009
IgGs from goat serum; Cat. No. I5256
IgGs from rabbit serum; Cat. No. I5006
IgGs from mouse serum; Cat. No. I8765
Kodak Biomax MR (7"x9.5"); Cat. No. Z353949
Mayer's Haematoxylin solution; Cat. No. MHS-1
Nonidet-P40, replaced by Igepal-CA630 Cat. No. I7771
Normal goat serum; Cat. No. G9023
Normal mouse serum; Cat. No. M5905
Normal rabbit serum; Cat. No. R9133
Phosphate buffered saline (PBS) tablets; Cat. No. P4417
Phosphatase inhibitors; Cat. No. P5726-1ML
pUC18 DNA MspI Digest, 26 - 501bp; Cat. No. D-4797
Sodium dodecyl sulphate for Molecular Biology; Cat. No. L4390
Tris-base; Cat. No. T87602
TEMED; Cat. No. T9281

VWR UK

Eppendorf Phase Lock Gel Heavy, 1.5ml; Cat. No. 427356S
Microscope slide boxes 50, pack of 10; Cat. No. 406/0286/00
O.C.T. compound; Cat. No. 361603E

Vector Laboratories, UK

Vectashield; Cat. No. H1000
Vectastain Elite ABC Kit (Universal); Cat. No. PK-6200
VectaMount™ Mounting medium; Cat. No. H5000
DAB (diaminobenzidine tetrahydrochloride) substrate kit; Cat. No. SK-4100

Appendix C - Multiple Alignment of Rat *Gstm* Sequences

		Section 1																					
		(1) 1	10	20	30	45																	
rGstm1	(1)	-----																					
rGstm2	(1)	-----																					
rGstm3	(1)	-----																					
rGstm4	(1)	GGGATCCTACTCCTGCCTCTCTTGGGCTGTGGGTGTGACTCTCTG																					
rGstm5	(1)	-----																					
rGstm6a	(1)	-----																					
rGstm6b	(1)	-----																					
rGstm7	(1)	-----																					
		Section 2																					
		(46) 46	60	70	80	90																	
rGstm1	(1)	-----																					
rGstm2	(1)	-----																					
rGstm3	(1)	-----																					
rGstm4	(46)	ATTTAGGGTTCAAAGTCTCTGAGGAAGGGAAAGGCAGTGCCCGAG																					
rGstm5	(1)	-----																					
rGstm6a	(1)	-----																					
rGstm6b	(1)	-----																					
rGstm7	(1)	-----																					
		Section 3																					
		(91) 91	100	110	120	135																	
rGstm1	(1)	-----TTTG				TCCGGC	CCACGTT																
rGstm2	(1)	-----																					
rGstm3	(1)	-----GGGAAAGGCGGTCTGAAGACCT				TG	ACAGAGTGAAGCC																
rGstm4	(91)	TGGGGTTAGGGCTTTGAGGGCAGGACCGT				TG	CAGGGC	CC	CACCC														
rGstm5	(1)	---AGAAAGGAGGAGGCAGTTCAGTCGCGT				TG	ACCCCG	CC	CACAG														
rGstm6a	(1)	-----																					
rGstm6b	(1)	-----																					
rGstm7	(1)	-----CCAG				CC	CCGCC																
		Section 4																					
		(136) 136	150	160	170	180																	
rGstm1	(18)	TCT	CTGG	TAATCT	G	TATAAAGTCGC	AA	CA	CA	CAGGTCAATTCTG	C												
rGstm2	(1)	-----																					
rGstm3	(37)	AGT	CTGT	T	--	TCT	GG	CAGCTCTCGG	AA	CA	GT	C	GAGGCTAG	AT	TGA								
rGstm4	(136)	ACCT	T	TCCCTTAGT	G	CCTCTTTATA	A	TTCCC	CAGCTCAACT	T	GT	C											
rGstm5	(43)	CGT	CCAG	TATAAA	G	TTAGCCGCC	--	A	CA	GT	C	CATCGCGT	AT	CCC									
rGstm6a	(1)	-GG	CTTC	TCTCCTT	G	TGCACCAGGAT	A	T	AGTT	-	ACAGTT	C	AT	TTA									
rGstm6b	(1)	-----																					
rGstm7	(12)	CAG	CT	ACCC	-	GAG	GG	CTCTAGGATA	AA	G	TCAAAGCTACTC	A	CACC										
		Section 5																					
		(181) 181	190	200	210	225																	
rGstm1	(63)	T	GAAGC	CAAATT	G	GA	AG	ACCA	CAGCG	CC	CAG	AACC	AT	GCC	TATGA								
rGstm2	(1)	--	AGGTTT	GTCTGC	T	CTGT	A	CACCCTA	CC	CAG	CAC	GAT	GCC	TATGA									
rGstm3	(80)	C	ACAGC	CTGTCC	G	T	CAG	ACC	---	CC	CAG	CACC	AT	GCC	CATGA								
rGstm4	(181)	T	GAAGC	CAGTCT	G	GA	AG	ACCA	CAGCA	CC	CAG	AG	CC	AT	GGCTATGA								
rGstm5	(86)	A	GAAGGGGC	TAA	GATC	TCC	CA	AAATGT	C	GTGCT	CC	AG	GT	CTATGG									
rGstm6a	(44)	C	T	AGC	TCC	A	C	AGA	--	AG	C	CAG	AC	AT	GCC	TATGA							
rGstm6b	(1)	-----																					
rGstm7	(56)	G	GA	GC	T	A	GT	GGAC	T	C	AG	T	C	T	C	AGGCA	CC	CAG	C	A	T	GCC	TATGA

Section 6

	(226)	226	240	250	260	270
rGstm1	(108)	TACTGGGA	TACTGGAA	ACGTCCG	CGGGCTG	GACACACC
rGstm2	(44)	CACTGGGTT	ACTGGGAC	ATCCGTGG	GGCTCACG	CCATTCGCC
rGstm3	(119)	CACTGGGTT	ACTGGGAC	ATCCGTGG	GGCTAGCG	CATGCCATC
rGstm4	(226)	TACTGGGA	TATGGAA	CGTTCG	CGGACTT	ACTCACCC
rGstm5	(131)	TTCTGGGTT	ACTGGGAT	ATCCGCG	GGGCTGG	CTCATGCC
rGstm6a	(87)	CTCTGGGTT	ACTGGCAC	ATCCGTGG	GGTTGGG	TCAAGCC
rGstm6b	(11)	CTCTGGGTT	ACTGGGAT	ATCCGCG	GATGGG	TCAAGCC
rGstm7	(101)	CACTGGGTT	ACTGGGAC	ATCCGTGG	GGCTGG	CTCATTCG

Section 7

	(271)	271	280	290	300	315
rGstm1	(153)	TGCTCCTGGA	AATACAC	AGACTCAA	GCTATGAG	GAGAA
rGstm2	(89)	TGTCCTGGA	GTATAC	AGACACA	AAGCTATG	AGGAGTACA
rGstm3	(164)	TGCTCCTGGA	AATACAC	AGACTCAA	GCTATGAG	GAGAA
rGstm4	(271)	TGCTCCTGGA	AATACAC	AGACTCAA	GCTATGAG	GAGAA
rGstm5	(176)	TGCTCCTGGA	GTATAC	AGACTCAA	GCTATGAG	GAGAA
rGstm6a	(132)	TGCTCCTGGA	AATACAC	AGACTCAA	GCTATGAG	GAGAA
rGstm6b	(56)	TGCTCCTGGA	AATACAC	AGACTCAA	GCTATGAG	GAGAA
rGstm7	(146)	TACTCCTGGA	AATACAC	AGACTCAA	GCTATGAG	GAGAA

Section 8

	(316)	316	330	340	350	360
rGstm1	(198)	CCATGGGC	GACGCTCC	CGACTATG	ACAGAGCC	AGTGGCTG
rGstm2	(134)	GCAATGGG	GATGCTCC	CGACTATG	ACAGAGCC	AGTGGCTG
rGstm3	(209)	CCATGGG	AGACGCTCC	CGACTT	TGACAGAG	CCAGTGGCTG
rGstm4	(316)	TCAATGGG	GATGCC	CCAACTT	TGACAGAG	CCAGTGGCTG
rGstm5	(221)	CGTGTGG	GAGGCTCC	TGACTATG	ATAGAGCC	AAATGGCTG
rGstm6a	(177)	CCATGGG	GACGCTCC	CGACTATG	ACAGAGCC	AGTGGCTG
rGstm6b	(101)	CCATGGG	CACGCTCC	CGACTATG	ACAGAGCC	AGTGGCTG
rGstm7	(191)	CCATGGG	CACGCTCC	TGACTATG	ACAGAGCC	AGTGGCTG

Section 9

	(361)	361	370	380	390	405
rGstm1	(243)	AGAAATTCAA	ACTGGGC	CTGGACTT	CCC	CAATCTG
rGstm2	(179)	AGAAATTCAA	ACTGGGC	CTGGACTT	CCC	CAATCTG
rGstm3	(254)	AGAAATTCAA	ACTGGGC	CTGGACTT	CCC	CAATCTG
rGstm4	(361)	AGAAATTCAA	TCTTGGC	CTGGACTT	CCC	CAATCTG
rGstm5	(266)	TGAAATTCAA	GCTAGAT	CTGGATT	TCTAA	CTGCCCTAC
rGstm6a	(222)	AGAAATTCAA	ACTGGGC	CTGGACTT	CCC	CAATCTG
rGstm6b	(146)	ACAAATTCAA	GCTGGAT	CTGGACTT	CCC	CAATCTG
rGstm7	(236)	AGAAATTCAA	ACTGGGC	CTGGACTT	CCC	CAATCTG

Section 10

	(406)	406	420	430	440	450
rGstm1	(288)	TTGATGG	ATCGCG	CAAGAT	TACCCAGAG	CAATGCCAT
rGstm2	(224)	TTGATGG	GTCACACA	AGATCACCCAGAG	CAATGCCAT	CTTGCGCT
rGstm3	(299)	TTGATGG	GTCACACA	AGATCACCCAGAG	CAATGCCAT	CTTGCGCT
rGstm4	(406)	TTGATGG	GTCACACA	AGATCACCCAGAG	CAATGCCAT	CTTGCGCT
rGstm5	(311)	TGGACGG	GAAGACA	AGATCACCCAGAG	TAA	CGCCATCT
rGstm6a	(267)	TCGATGG	GTCACACA	AGATCACCCAGAG	CAATGCCAT	CTTGCGCT
rGstm6b	(191)	TTGATGG	GTCACACA	AGATCACCCAGAG	CAATGCCAT	CTTGCGCT
rGstm7	(281)	TCGATGG	GTCACACA	AGATCACCCAGAG	CAATGCCAT	CTTGCGCT

Section 11

	(451)	451	460	470	480	495																																		
rGstm1	(333)	A	C	C	T	T	G	C	C	C	G	C	A	A	G	C	A	C	A	C	T	G	T	G	T	G	G	A	G	A	G	A	G	G	A	G	A	G	C	
rGstm2	(269)	A	C	C	T	T	G	G	C	C	G	G	A	A	G	C	A	C	A	C	T	T	G	T	G	G	G	A	G	A	G	A	G	G	A	G	A	G	A	G
rGstm3	(344)	A	T	C	T	T	G	G	C	C	G	C	A	A	G	C	A	C	A	C	T	G	T	G	T	G	G	A	G	A	G	A	G	A	G	A	G	A	G	A
rGstm4	(451)	A	C	C	T	T	G	G	C	C	G	G	A	A	G	C	A	C	A	C	T	G	T	G	T	G	G	A	G	A	G	A	G	A	G	A	G	A	G	A
rGstm5	(356)	A	C	A	T	C	G	C	A	C	G	C	A	A	G	C	A	C	A	A	T	G	T	G	T	G	T	G	A	C	A	C	G	A	A	G	A	A	G	A
rGstm6a	(312)	A	C	C	T	T	G	G	C	C	G	G	A	A	G	C	A	C	A	C	T	G	T	G	T	G	A	G	A	G	A	G	A	G	A	G	A	G	A	G
rGstm6b	(236)	A	C	C	T	T	G	G	C	C	G	G	A	A	G	C	A	C	A	C	T	G	T	G	T	G	G	A	G	A	G	A	G	A	G	A	G	A	G	A
rGstm7	(326)	A	T	A	T	T	G	C	C	C	G	A	A	A	G	C	A	C	A	C	T	G	T	G	T	G	G	A	G	A	G	A	G	A	G	A	G	A	G	A

Section 12

	(496)	496	510	520	530	540																																						
rGstm1	(378)	G	G	A	T	T	C	G	T	G	T	G	C	A	G	A	C	A	T	T	G	T	G	G	A	A	C	C	A	G	T	C	A	T	G	G	A	C	C	G	C			
rGstm2	(314)	G	G	A	T	T	C	G	T	G	T	G	C	A	G	A	C	A	T	T	T	T	G	G	A	A	C	C	A	G	T	C	A	T	G	G	A	C	A	C	C	G		
rGstm3	(389)	G	G	A	T	T	C	G	T	G	T	G	C	A	G	A	C	A	T	T	C	T	G	G	A	A	T	C	A	G	T	C	A	T	G	G	A	C	A	C	C	G		
rGstm4	(496)	G	G	A	T	T	C	G	T	G	T	G	C	A	G	A	C	A	T	T	T	T	G	G	A	A	C	C	A	G	T	C	A	T	G	G	A	C	A	C	C	G		
rGstm5	(401)	A	G	A	T	T	C	G	A	G	T	G	C	A	T	C	A	T	G	G	A	A	C	C	A	G	A	T	A	T	G	G	A	C	T	T	C	C	G	C	A			
rGstm6a	(357)	G	A	C	T	C	C	G	T	G	T	G	C	A	T	T	T	T	G	G	A	A	C	C	A	G	C	C	G	T	G	A	C	A	C	T	C	G	T	A				
rGstm6b	(281)	G	G	A	T	T	C	G	T	G	T	G	C	A	T	T	T	T	T	G	G	A	A	A	C	A	G	T	C	A	T	G	G	A	C	A	C	C	C	G	C	A		
rGstm7	(371)	A	G	A	T	T	C	G	T	G	T	G	C	A	T	T	T	T	T	G	G	A	A	C	C	A	G	T	C	A	T	G	G	A	C	A	T	G	T	G	T	C	C	A

Section 13

	(541)	541	550	560	570	585																																									
rGstm1	(423)	T	G	C	A	G	C	T	C	A	T	C	A	T	G	C	T	T	T	G	T	T	A	C	A	A	C	C	G	A	C	T	T	T	G	A	G	A	G	C	A	G	A				
rGstm2	(359)	T	A	C	A	G	T	T	G	G	C	A	T	G	G	T	C	T	G	C	T	A	C	A	G	C	C	T	G	A	C	T	T	T	G	A	G	A	A	G	A	G	A				
rGstm3	(434)	T	G	G	T	G	C	T	G	G	C	A	G	A	C	T	T	T	G	C	T	A	T	A	A	C	C	T	G	A	C	T	T	T	G	A	G	A	A	G	C	T	G	A			
rGstm4	(541)	T	A	C	A	T	C	T	C	A	T	G	A	T	A	G	T	T	T	G	C	T	G	C	A	G	T	C	T	G	A	C	T	T	T	G	A	G	A	G	C	A	G	A			
rGstm5	(446)	T	G	C	A	G	C	T	G	G	T	T	C	G	C	T	C	T	G	C	T	A	C	A	A	T	T	C	T	A	A	C	C	A	C	A	G	A	A	G	C	T	G	A			
rGstm6a	(402)	G	G	C	A	G	C	T	T	C	A	A	T	G	G	T	C	T	G	C	T	A	C	A	G	C	C	T	G	A	G	T	T	T	G	A	A	A	C	G	G	A	C	G	A		
rGstm6b	(326)	T	T	C	A	G	A	T	G	G	C	A	C	A	C	T	C	T	G	C	T	A	C	A	G	C	C	T	G	A	C	T	T	C	G	A	G	A	A	C	G	G	A	C	G	A	
rGstm7	(416)	A	T	C	A	G	C	T	G	G	C	T	A	G	A	G	T	C	T	G	T	T	A	C	A	G	C	C	A	G	A	C	T	T	T	G	A	A	A	C	T	G	A	C	T	G	A

Section 14

	(586)	586	600	610	620	630																																							
rGstm1	(468)	A	G	C	C	A	G	A	G	T	T	C	T	T	G	A	A	G	A	C	C	A	T	C	C	T	G	A	G	A	G	A	T	G	A	A	G	C	T	C	T	A	C	T	
rGstm2	(404)	A	G	C	C	A	G	A	G	T	A	C	T	T	A	G	A	G	G	G	T	C	T	C	C	T	G	A	G	A	G	A	T	G	A	A	G	C	T	T	A	C	T	A	C
rGstm3	(479)	A	G	C	C	A	G	G	T	A	C	C	T	G	G	A	G	C	A	A	C	T	G	C	C	T	G	A	A	T	G	A	T	G	C	G	C	T	T	A	C	T	A	C	
rGstm4	(586)	A	G	C	C	A	G	A	G	T	T	C	T	T	G	A	A	G	T	C	C	A	T	C	C	C	G	G	A	G	A	G	A	T	G	A	A	A	T	C	T	A	T	T	
rGstm5	(491)	A	G	C	C	T	C	A	G	T	A	T	T	T	G	G	A	A	C	A	A	C	T	G	C	C	T	G	C	A	C	A	G	C	T	G	A	A	A	C	A	G	T	T	C
rGstm6a	(447)	A	G	C	C	A	G	A	G	T	A	C	T	T	A	G	A	G	G	G	T	C	T	C	C	T	G	A	C	A	A	G	A	T	G	A	A	G	C	T	C	T	A	C	T
rGstm6b	(371)	A	G	C	C	T	G	A	G	T	T	C	T	T	G	A	A	G	G	G	C	T	C	C	C	A	G	A	T	C	A	G	C	T	G	A	A	G	C	T	C	T	A	C	T
rGstm7	(461)	A	G	G	C	G	A	A	T	A	T	T	T	G	G	A	G	C	A	G	C	T	C	C	C	T	G	G	A	T	G	A	T	G	A	T	G	A	G	A	G	C	T	T	C

Section 15

	(631)	631	640	650	660	675																																							
rGstm1	(513)	C	T	G	A	G	T	T	C	C	T	G	G	G	C	A	A	G	C	A	G	C	C	A	T	G	G	T	T	G	C	A	G	G	G	G	A	C	A	A	G	T	C	A	
rGstm2	(449)	C	C	G	A	A	T	T	C	C	T	G	G	G	C	A	A	G	C	A	G	C	C	A	T	G	G	T	T	G	C	A	G	G	G	A	A	C	A	A	G	A	T	T	A
rGstm3	(524)	C	C	G	A	T	T	C	C	T	G	G	G	C	A	A	G	C	G	G	C	C	A	T	G	G	T	T	G	C	A	G	G	G	G	A	C	A	A	G	T	C	A		
rGstm4	(631)	C	A	G	A	T	T	C	C	T	G	G	G	C	A	A	G	C	G	A	C	C	A	T	G	G	T	T	G	C	A	G	G	G	G	A	C	A	A	G	T	C	A		
rGstm5	(536)	C	G	T	T	G	T	T	C	C	T	G	G	G	G	A	A	T	T	C	A	C	A	T	G	G	T	T	G	C	A	G	A	G	A	A	A	A	G	C	T	G	A		
rGstm6a	(492)	C	T	G	A	G	T	T	C	C	T	G	G	G	C	A	A	G	C	A	G	C	T	A	T	G	G	T	T	G	C	A	G	G	G	A	A	C	A	A	G	A	T	T	A
rGstm6b	(416)	C	C	G	A	T	T	C	C	T	G	G	G	G	C	A	A	G	C	A	G	C	C	A	T	G	G	T	T	G	C	A	G	G	G	G	A	C	A	A	G	A	T	C	A
rGstm7	(506)	C	A	C	A	G	T	T	C	C	T	G	G	G	G	A	A	G	C	A	G	A	C	G	T	G	G	T	T	C	G	T	T	G	T	G	A	A	A	A	G	A	T	T	A

Section 16

	(676)	676	690	700	710	720
rGstm1	(558)	CCTATGTGGATTT	CCTTGCTTAT	GACAT	TCTTGACCAGT	ACCACA
rGstm2	(494)	CGTATGTGGATTT	CTTGTTTAC	GATGT	CCTTGATCA	ACACCGTA
rGstm3	(569)	CCTTTGTGGATTT	ATTGCTTAC	GATGT	TCTTGAGAGGA	ACC AAG
rGstm4	(676)	CCTATGTGGATTT	CCTTGCTTAT	GACAT	TCTTGACCAGT	ACC GTA
rGstm5	(581)	CCTTCGTGGATTT	CTCACTTAT	GACGT	CTTGACCAGAA	T CGTA
rGstm6a	(537)	CCTATGTGGATTT	CCTTGTTTAT	GATGT	CCTCGATAAGC	ACC GTA
rGstm6b	(461)	CCTTTGCA GATTT	CCTTGTC	TATGATGT	CCTTGACCAGC	ACC GAA
rGstm7	(551)	CTTTTGTAGATTT	CCTTGCTTAT	GATAT	CCTTGACCTGC	ACC TTA

Section 17

	(721)	721	730	740	750	765
rGstm1	(603)	TTTGTGAGCC	CAAGTGCCTGGAC	GCCTT	CCCAAAC	CTGAA GGACT
rGstm2	(539)	TATTTGAAACC	CAAGTGCCTGGAC	GCCTT	CCCAAAC	CTGAA GGACT
rGstm3	(614)	TGTTTGAAGGC	CAGTGCCTGGAC	GCCTT	CCCAAAC	CTGAA GGACT
rGstm4	(721)	TGTTTGAAGCC	GAGTGCCTGGAC	GCCTT	CCCAAAC	CTGAA GGACT
rGstm5	(626)	TGTTTGAAGCC	CAAGTGCCTGGAT	GAGTT	CCCAAAT	CTGAA GGCTT
rGstm6a	(582)	TGTTTGAAGCT	CAAGTGCCTGGAC	GCCTT	TCCAAAT	CTGAA GGACT
rGstm6b	(506)	TGTTTGAACC	CAAGTGCCTGGAC	GCCTT	CCCAAAC	CTGAT GGACT
rGstm7	(596)	TATTCGAACC	CAAGTGCCTGGAT	GCCTT	CCCAAAC	CTGAA GGACT

Section 18

	(766)	766	780	790	800	810
rGstm1	(648)	TCTGGCCCGCTT	Y GAGGGCCTGA	AGAAGAT	CTCTG	CCTACATGA
rGstm2	(584)	TCTGGCTCGGTT	T GAGGGCCTGA	AGAAGAT	ATCTG	ACTACATGA
rGstm3	(659)	TCA TAGCGCTT	T GAGGGCCTGA	AGAAGAT	CTCCG	ACTACATGA
rGstm4	(766)	TCTGGCCCGCTT	C GAGGGCCTGA	AGAAGAT	CTCTG	CTTACATGA
rGstm5	(671)	TCA TGTGCGT	TTT GAGGCTT	TGGAGAAGAT	TGCTG	CATTCTG
rGstm6a	(627)	TCA TGGCTCGA	TTT GAGAC	CTTGAGAAGAT	CTCTG	CCTACATGA
rGstm6b	(551)	TCTGGTCCACTT	T GAGGGCCTGA	AGAAGAT	CTCTG	CCTATATGA
rGstm7	(641)	TGTGGCCCGCTT	C GAGGGACTGA	AGAAGAT	CTCTG	TTTACATGA

Section 19

	(811)	811	820	830	840	855
rGstm1	(693)	AGAGCAGCGCT	ACCTCTCAA	CACCTAT	ATTTTCGA	AAGTTGGCC
rGstm2	(629)	AGAGCGGCGCT	TCCTCTCCA	AGCCAAAT	CTTTGCAA	AAGATGGCCT
rGstm3	(704)	AGTCCAGCGCT	TCCTCCA	AAGACCTCT	GTTCACA	AAGATGGCTA
rGstm4	(811)	AGAGTAGCAGCT	TTCTCCA	AAGACCTGT	GTTTACT	AAGATACCGC
rGstm5	(716)	AGTCTGACCGCT	GCTTCAAG	ATGCCAAAT	CAACAAC	AAGATGGCCA
rGstm6a	(672)	AGTCCAGCGCT	TCCTTTCA	GGCCCTGT	GTATTTGA	AAGACAGCGC
rGstm6b	(596)	AGACCAGCGCT	TCCTTCCA	AGTCTGT	GTACTTAA	ACAGGCCA
rGstm7	(686)	AGACCAGCGCT	TCCTCCGG	ACACCCT	ATA TACA	AGGGTGGCTA

Section 20

	(856)	856	870	880	890	900
rGstm1	(738)	AA TGGAGT	AACAAGTAGGCC	-----	T TGCTACA	CTGGCACTCA
rGstm2	(674)	TT TGGAA	CCAAAGTAGC	ACCACAAAGT	CCAGACCTA	GGGATACT
rGstm3	(749)	TT TGGGGCAG	CAAGTAGGACC	CTGACAGG	GTGGCTTT	TAGGAGAAA
rGstm4	(856)	A GTGGGGCA	CTGATTAGGCC	-----	T CGCAT	GCTGGCACTCA
rGstm5	(761)	A GTGGGGT	AACAAG-AGC	ATA-----	TGCTG	AGCTGGAGCTCG
rGstm6a	(717)	T GTGGGGT	AACAAGTAGAG	CG-----	CCC	GTAATACCAAGGGC
rGstm6b	(641)	C GTGGGGCA	ACAAGTAGGACC	CTGCA--	TGGAG	GGCCGGTGA TGG
rGstm7	(731)	CT TGGGGCAA	TAGTAGGGC	TTTGACTCG	GGCAGG	AA GTGGGAAC

Section 21

	(901)	901	910	920	930	945						
rGstm1	(777)	CAG	RG-----A	GGA	CCTGTC	CACATTG-----GAT	CCTGC	AGG	CA-			
rGstm2	(719)	CAT	GA-----GT	GCC	CTGCTGG	CTGTG-----GG-	CCT	AG	CATG			
rGstm3	(794)	GAT	AC-----CAA	ATCT	CCTGGG	TTTGC	CAA	GAG	CCCTA	AGG	AGC	
rGstm4	(895)	CAG	GA-----A	GGA	CCTGTC	CACACTG-----GAT	CCTGC	AGG	CCC			
rGstm5	(798)	CTG	-----CT	GCTGAG	CCAT	CTTTC-----	CCT	CA	AGG	GAC		
rGstm6a	(754)	CAG	GA-----G	GAGAT	TTACT	CTATG	CT--T	GCGG	TCC	ATG	GTG	
rGstm6b	(684)	TAG	GG-----A	GGA	CTGTC	GGCGCC	CTAT	CGC	CCTG	GAC	ACTG	
rGstm7	(776)	CTG	GGGTTCTG	GGA	ACAGT	TGAGA	TTCC	CGT	ATC	CCTG	GCG	CTAC

Section 22

	(946)	946	960	970	980	990									
rGstm1	(812)	---CC	CTGGC-	CTT	CT	-----G	CA	CTGT	GGT	TCTC	---	TCT	-	CCT	
rGstm2	(754)	--G	CTCTGGC-	GCC	CA	-----C	CA	CA-T	GCAG	CCT	---	TCT	-	CCT	
rGstm3	(834)	--G	GCAGGA-	TT	CT	GAG	CCC	CA	GAG	CCATG	TT	---	TCT	CC	
rGstm4	(931)	-TG	GGCAGGA	A	CAG	CACTTTT	G	CA	CTGT	GGCT	CT	GGT	TCT	CTCT	
rGstm5	(829)	-----	CCA-	CC	CT	-----	CT	G	TAA	GCT	TCT	G-	CC	AGCCT	
rGstm6a	(792)	-TG	GGCCCC	A	CTG	GTCCCC	GGC	AT	CT	GTAT	CAG	TCT	TCC	C	
rGstm6b	(724)	-ACT	GGGTC	A	CGG	CTAG	CTTC	CA	GT	-AA	CTG	CTC	--	TAC	ATCAG
rGstm7	(821)	CTT	CTACCT	A	TCC	CTT	CTG	A	CT	GCAG	AA	TG	TCA	AGGG	TCC

Section 23

	(991)	991	1000	1010	1020	1035												
rGstm1	(844)	TC	CTGC	---	TCC	CTT	CTCCA-	G	CTTT	GY	AGCC	C-	CAT	CT	CCT	CA		
rGstm2	(786)	CC	CT	-----	TCC	ATT	-CCT-	G	TT	CCTC	CAT	TC-	CT	CT	TCC	CAG		
rGstm3	(873)	TC	CTTCC	AT	TCC	AGT	CCCCA	A	CC	TTAC	CAG	CT	CAT	TT	TT	TGG		
rGstm4	(975)	CC	TCCC	TA	TCC	TT	CTCCA-	G	CTTT	CT	CAG	CT-	CAT	CT	CCT	CG		
rGstm5	(857)	TG	TCCC	-A	TCC	GAT	CTGG	A	GGG	CCCCG	CACT	CT	GTC	TC	CT	TGC		
rGstm6a	(836)	A	CTCC	G-T	CT	TTCT	CTGAA	A	GGT	G	TAGT	GACT	C	G	CT	TTCT	AC	
rGstm6b	(764)	TC	TCCC	AT	TTT	TT	CTGTC-	T	TTT	CA	TTCT	TT	C	C	TCT	ACA	AG	
rGstm7	(866)	TT	CA	CCC	AG	TCC	TG	CCC	T--	T	CAAG	CC	CT	A	CA	G	CT	AGGC

Section 24

	(1036)	1036	1050	1060	1070	1080															
rGstm1	(884)	A	CC	T-----	C	ACCC	CAGT	CA	TGCC	CAC	ATA	-G	TC	TT	AT	TC					
rGstm2	(823)	CC	CT	-----	T	GCCT	CAGT	CA	AGCC	TCA	GT--	TC	CC	T	GG	TC					
rGstm3	(918)	T	CA	TCAA	AT	-CC	TGCC	AAA	CA	CAG	GC	TCT	TAA	A	-AG	CC	TAG	CA			
rGstm4	(1018)	CC	CT	-----	C	ACCC	CAGT	CA	AGT	CC	CACA	A	-G	TC	CT	AT	TC				
rGstm5	(900)	T	CC	TCCAA	T-A	-A	AC	AG	CAGT	TAA	AT	TAAAA	A	-AAAA	A	AAAA	AAAA				
rGstm6a	(880)	CC	AGCC	---	T	-TT	CTG	TAA	GGG	AG	TTCT	CA	A	-C	TC	AGG	TC	TA			
rGstm6b	(807)	A	CC	TC	---	T	-TG	TT	CCC	CC	TTG	AC	T	CA	A	G	CC	-TC	CAG	T	TC
rGstm7	(908)	CC	CT	GGTT	TT	CTT	TAG	CAA	AGT	G	CCC	T	TC	T	AG	C	T	G	T	TC	

Section 25

	(1081)	1081	1090	1100	1110	1125																
rGstm1	(919)	TC	CCAC	TTTCTTT	-	CAT	AG	TGG	TCC	CCT	TCT	T-	TAT	T	GAC	AC	CT					
rGstm2	(856)	TC	TCCA	-TTTCTT	--	CAT	--	TAG	TCC	CCT	CC	CT-	TG	T	CT	T	G	CC				
rGstm3	(961)	A	CT	CTTT	CCATT	AG	CA	AAA	TAG	C	TT	CTAA	AG-	T	TAA	AG	T	G	CC			
rGstm4	(1053)	TT	CCAC	TTTCTTT	-	CAT	TA	TGA	TCC	CCT	TCT	T	C	T	TA	T	G	G	CA	CC		
rGstm5	(942)	AA	-----																			
rGstm6a	(920)	GT	TCC	CTAA	TGG	TT	CT	TGA	TGT	GT	CAA	TAA	AG	AA	G	G	CT	G	G	AG	CC	
rGstm6b	(847)	G	CT	CC	CTG	TC	CT	CAG	CAA	AG	T	CC	T	TTT	CT	CC	CC	T	G	T	TT	CT
rGstm7	(953)	TG	T	G	CCAC	T	TGA	T	GG	T	TT	C	T	G	T	C	T	G	T	G	T	G

Section 26

(1126) 1126 1140 1150 1160 1170
 rGstm1 (962) TA-AC---ACAACTCACAGTCTTTCTGTGATTTG-AGGTCTG
 rGstm2 (895) T-----GCATCCAACCTTCCCTCACTGATTTCGGAGGACTG
 rGstm3 (1005) C-----GCCCCACCCCTCGAGCTCATGTGATTGGATAGTTGG
 rGstm4 (1097) TA-AC---CATCCTCACAGACTTTCTGTGATTTG-AGGTCTG
 rGstm5 (944) -----
 rGstm6a (965) CA-AT---TGCTGGGCAGGAAGGTATAGGTGGGACTTCCGAGTCC
 rGstm6b (892) GTCAT---GTTCTAACC GTTCTTTCACCTGAGCTTTGAGCACCTT
 rGstm7 (998) AGAGTTGAGACTTCA TCAGCGCTCAGCCTGGGACTCCCATGCTT

Section 27

(1171) 1171 1180 1190 1200 1215
 rGstm1 (1002) C-CCTGAACTCAGTCTCCCT-----
 rGstm2 (933) TACCAGACCCCTGAATCCCT-----
 rGstm3 (1043) CTCCCAACATGTGATTATTTTG-----
 rGstm4 (1137) C-CCTGAACTCAGGCTCCCTAGAAATTAACCCAAAGGTCAATGCTG
 rGstm5 (944) -----
 rGstm6a (1006) AAGAGAAAAGGAGATTTCAGGGGAA-----AGATAGAGGGGCTT
 rGstm6b (934) AACCTGAAGACCCATTCTCC-----CCGGAAGGCAGGCTCGG
 rGstm7 (1043) GTCTGGA GACTGGA GATGCTGATGTATGGAGGTCCCTGCACAGC

Section 28

(1216) 1216 1230 1240 1250 1260
 rGstm1 (1020) -----TAGACTTACCCTAAATGT--AACACT
 rGstm2 (952) -----CAGCCTGGCCTGAGAGAT--TAGA-T
 rGstm3 (1065) -----GGCAGGTGCAGGCTC-CCCGGCAGAT--GGGG-T
 rGstm4 (1181) TCTCAGTGCCAGCCCTCCTTAGAA TTA CCGGAGACTC-AAACT
 rGstm5 (944) -----
 rGstm6a (1044) TTCTGCTGTGCTTCGGAGTAAGAAGGTAACA GTCATG-TAAGGT
 rGstm6b (971) CCTCCAGAGTGGGATGGCCTAGCGTTGTTTGCTCTCTAA TAAGT
 rGstm7 (1088) TCTTTTGGATCTCTCCTGTAAAGCTCGAATCA CACTGGCTCTGGC

Section 29

(1261) 1261 1270 1280 1290 1305
 rGstm1 (1044) GTCTCAGT-GCCAGCCTGTTCCTGG-----TGGGGGAGCTGCCCC
 rGstm2 (975) CTCACTGT-GCTGCCCTGGTCC-----CCAGGAG--GACCC
 rGstm3 (1095) CTATCTGGAGACAGTAGATTGCTAGCAGCTTTGACCACCGTAGCC
 rGstm4 (1225) GTCTCAGT-GCCAGCCTGTTCCT-----CC-TGGAGGAGCTTCCCT
 rGstm5 (944) -----
 rGstm6a (1088) CTTCGGCAGCTAGGGCCGTGGCCTCCGCAACAGGC GGATAGCC
 rGstm6b (1016) ATTACCACACTT-----
 rGstm7 (1133) TCTTGCACTGCCAGCTTTTACTGCGATC---TCCAGTGCCTGCCCT

Section 30

(1306) 1306 1320 1330 1340 1350
 rGstm1 (1083) AGGCCTG-TCATCTTTAA TAAAGCCTGAAA CACMAAAAAAAA
 rGstm2 (1008) A-----TTTATTTGCAA TAAAGTGTGAAC CACAAA-----
 rGstm3 (1140) AAGCCCC-CTTCT-TGCTGTTTCCCGA GACTAGCTATGAGCAG
 rGstm4 (1263) CAGCCTG-TCATCTCTAA TAAAGCCTGAAA CACACTTGCT---
 rGstm5 (944) -----
 rGstm6a (1133) AAGGATGT TGGCAGGGGC TGGCTGATACAAGT CACTAAGTTT AGG
 rGstm6b (1029) -----
 rGstm7 (1175) AGTGACCC TGGCAGACACTGTGTTTACAGGGATTTCA GTTGGATA

Section 31

(1351) 1351 1360 1370 1380 1395
 rGstm1 (1127) AAAAAAAAAAAAAAAAAAAAAA-----
 rGstm2 (1039) -----
 rGstm3 (1183) GTGTGCTGTGTCCCAGCACTTGTCACTGCCTCTGTAACCCGCTC
 rGstm4 (1304) GTGTGTTGTGTCTTTTCTTTTGCT----CTTTAGCCTCTCCAAG
 rGstm5 (944) -----
 rGstm6a (1178) GCAGAGGCAGATGGAGATAATAAACT---GGTAAGAGCACGCCTT
 rGstm6b (1029) -----
 rGstm7 (1220) GCAGGGCTTTGGGACTTCCTTGGCCTCACCTGAGTTTCACAGGAG

Section 32

(1396) 1396 1410 1420 1430 1440
 rGstm1 (1146) -----
 rGstm2 (1039) -----
 rGstm3 (1228) CTACCGCTCTTTCTTCCTGTCTGCTGTGAAGCTGTACCTCCTGACCA
 rGstm4 (1345) CATTTCATGGCTACTTCCAAAGAGTCTGAAGCTCTGAGCCTGTAGTG
 rGstm5 (944) -----
 rGstm6a (1220) TCCAGGCCGTTGTTATCTGAGCCCAGCAATTGTGCCTAGCAGGCA
 rGstm6b (1029) -----
 rGstm7 (1265) GCAGCTGCAGAAGGCTCTGTGGAGCTCAAGGGAGCTTGGATCTC

Section 33

(1441) 1441 1450 1460 1470 1485
 rGstm1 (1146) -----
 rGstm2 (1039) -----
 rGstm3 (1273) CAAACCAGAATAAATCATTCTCCCCGCAAAAAAAAAAAAAAAAAAAAA
 rGstm4 (1390) CCAGGCTCTGAAATGTCTAATGGAATCAGAAGAGCTTTAACATAA
 rGstm5 (944) -----
 rGstm6a (1265) AATTCTAAAGTAA-----
 rGstm6b (1029) -----
 rGstm7 (1310) TTTTATGCTAGCAGCACTGAGGTTTGTACCCAGGTCTCAGGGTT

Section 34

(1486) 1486 1500 1510 1520 1530
 rGstm1 (1146) -----
 rGstm2 (1039) -----
 rGstm3 (1318) AAAAAAAAAAAAAA-----
 rGstm4 (1435) CTTTGG-----
 rGstm5 (944) -----
 rGstm6a (1278) -----
 rGstm6b (1029) -----
 rGstm7 (1355) GGGGATCCAGGCTGGTGGGAGTCCCCAACAGTAAGCCAGGATCCT

Section 35

(1531) 1531 1540 1550 1560 1575
 rGstm1 (1146) -----
 rGstm2 (1039) -----
 rGstm3 (1330) -----
 rGstm4 (1441) -----
 rGstm5 (944) -----
 rGstm6a (1278) -----
 rGstm6b (1029) -----
 rGstm7 (1400) CTCTGCCAGCTGTGCTAGGGCTGCCTTATATCTGTGTCTCCAGGA

Appendix D - Multiple Alignment of Human *GSTM* Sequences

		Section 1				
	(1)	1	10	20	30	45
hGSTM1	(1)	-----				
hGSTM2	(1)	-----				
hGSTM3	(1)	-----				
hGSTM4	(1)	GGCGAGGCCGAGCCCCTCCTAGTGCTTCCGGACCTTGCTCCCTGA				
hGSTM5	(1)	-----				
		Section 2				
	(46)	46	60	70	80	90
hGSTM1	(1)	-----				
hGSTM2	(1)	-----				
hGSTM3	(1)	-----				
hGSTM4	(46)	ACACTCGGAGGTGGCGGTGGATCTTACTCCTTCCAGCCAGTGAGG				
hGSTM5	(1)	-----				
		Section 3				
	(91)	91	100	110	120	135
hGSTM1	(1)	-----				
hGSTM2	(1)	-----				
hGSTM3	(1)	-----				
hGSTM4	(91)	ATCCAGCAACCTGCTCCGTGCCTCCCGCGCCTGTTGGTTGGAAGT				
hGSTM5	(1)	-----				
		Section 4				
	(136)	136	150	160	170	180
hGSTM1	(1)	-----				
hGSTM2	(1)	-----				
hGSTM3	(1)	-----GGCAAGGGA				
hGSTM4	(136)	GACGACCTTGAAGATCGGCCGGTTGGAAGTGACGACCTTGAAGAT				
hGSTM5	(1)	-----				
		Section 5				
	(181)	181	190	200	210	225
hGSTM1	(1)	-----				
hGSTM2	(1)	-----				
hGSTM3	(10)	CGGAGAACGGGGCGGAGGCGGAGTCAGGGCGCCCGCGCGTGGGCC				
hGSTM4	(181)	CGGCGGGCGCAGCGG-GGCCGAGGGGGCGGGTCTGGCGCTAGGTC				
hGSTM5	(1)	-----				
		Section 6				
	(226)	226	240	250	260	270
hGSTM1	(1)	-----CTCTGAGCCCTGCT				
hGSTM2	(1)	-----CCCCGCC				
hGSTM3	(55)	CCGCCCCCTTATGTAGGGTATA-----AAGCCCTTCCTCCGCTCA				
hGSTM4	(225)	CAGCCCTGCGTGCCGGGAACCCAGAGGAGGTCGCAGTTCAAGCC				
hGSTM5	(1)	-----TCCTGGGCCTCTCA-----AAGTCTGAGCCCGCT				

		Section 7				
		271	280	290	300	315
hGSTM1	(15)	CGGTTT----	AGGCCTGTCTG	---	CGGAATCCG--	CACCAACCCAG
hGSTM2	(8)	CCGCTG----	AGGCCTGTCTG	---	CAGAATCCA--	CAGCAACCCAG
hGSTM3	(93)	CAGTTTCCCT	AGTCCTCGAA	GGCT	CGGAAGCCGT	CACCATGTCTG
hGSTM4	(270)	CAGCTG----	AGGCCTGTCTG	---	CAGAATCCGA--	CACCAACCCAG
hGSTM5	(31)	CCGCTG----	ATGCCTGTCTG	---	CAGAATCCG--	CACCAACCCAG
		Section 8				
		316	330	340	350	360
hGSTM1	(51)	CACCATGC--	CCATGATACT	GGGGTACTGGG	CATCCGCGGGGCTG	
hGSTM2	(44)	CACCATGC--	CCATGACACT	GGGGTACTGGAA	CATCCGCGGGGCTG	
hGSTM3	(138)	TGCGAGTCTGT	CTATGCTTCT	CGGGTACTGGGA	TATTCGTGGGCTG	
hGSTM4	(306)	CATCATGT--	CCATGACACT	GGGGTACTGGG	CATCCGCGGGGCTG	
hGSTM5	(67)	CACCATGC--	CCATGACTCT	GGGGTACTGGG	CATCCGTGGGCTG	
		Section 9				
		361	370	380	390	405
hGSTM1	(94)	GCCACCGCCATCCGC	CTTGCTCCTGGA	ATACACAGACT	CAAGCTAT	
hGSTM2	(87)	GCCATTCCATCCGC	CTTGCTCCTGGA	ATACACAGACT	CAAGCTAC	
hGSTM3	(183)	GCGACCGCCATCCGC	CTTGCTCCTGGA	ATTACAGGATA	CCTCTAT	
hGSTM4	(349)	GCCACCGCCATCCGC	CTTGCTCCTGGA	ATACACAGACT	CAAGCTAC	
hGSTM5	(110)	GCCACCGCCATCCGC	TGCTCCTGGA	ATACACAGACT	CAAGCTAT	
		Section 10				
		406	420	430	440	450
hGSTM1	(139)	GAGGAAAAGAA	GTACACGATGGGGGAC	GCTCCTGAT	TATGACAGA	
hGSTM2	(132)	GAGGAAAAGAA	GTACACGATGGGGGAC	GCTCCTGAT	TATGACAGA	
hGSTM3	(228)	GAGGAGAAACG	GTACACGTGCGGGGA	AGCTCCTGACT	TATGATCGA	
hGSTM4	(394)	GAGGAAAAGAA	GTATACGATGGGGGAC	GCTCCTGACT	TATGACAGA	
hGSTM5	(155)	GTGAAAAGAA	GTACACGCTGGGGGAC	GCTCCTGACT	TATGACAGA	
		Section 11				
		451	460	470	480	495
hGSTM1	(184)	AGCCAGTGGCTGA	AATGAAAAATTCAAGCT	GGGCCTGGACTTTCC		
hGSTM2	(177)	AGCCAGTGGCTGA	AATGAAAAATTCAAGCT	GGGCCTGGACTTTCC		
hGSTM3	(273)	AGCCAATGGCTG	GATGTGAAAATTCAAGCT	AGACCTGGACTTTCC		
hGSTM4	(439)	AGCCAGTGGCTGA	AATGAAAAATTCAAGCT	GGGCCTGGACTTTCC		
hGSTM5	(200)	AGCCAGTGGCTGA	AATGAAAAATTCAAGCT	GGGCCTGGACTTTCC		
		Section 12				
		496	510	520	530	540
hGSTM1	(229)	AATCTGCCCTACT	TGATTGATGGG	GCTCACAAAGATCACCCAGAGC		
hGSTM2	(222)	AATCTGCCCTACT	TGATTGATGGG	ACTCACAAAGATCACCCAGAGC		
hGSTM3	(318)	AATCTGCCCTACT	CTCTGGATGGG	AAGACAAAGATCACCCAGAGC		
hGSTM4	(484)	AATCTGCCCTACT	TGATTGATGGG	GCTCACAAAGATCACCCAGAGC		
hGSTM5	(245)	AATCTGCCCTACT	TGATTGATGGG	GCTCACAAAGATCACCCAGAGC		

		Section 13				
		541	550	560	570	585
hGSTM1	(274)	AACGCCATCT	TGTC	TACATTGCC	CGCAAGCACAAAC	CTGTGTGGG
hGSTM2	(267)	AACGCCATCT	TGCG	TACATTGCC	CGCAAGCACAAAC	CTGTGTGGG
hGSTM3	(363)	AATGCCATCT	TGCG	TACATTGCG	CGCAAGCACAAAC	ATGTGTGGT
hGSTM4	(529)	AACGCCATCT	TGTC	TACATTGCC	CGCAAGCACAAAC	CTGTGTGGG
hGSTM5	(290)	AATGCCATCT	TGCG	TACATTGCC	CGCAAGCACAAAC	CTGTGTGGG
		Section 14				
		586	600	610	620	630
hGSTM1	(319)	GAGACAGAAGAG	GAGAAGATTTCGT	GTGGACATTTT	TGGAGAACCAG	
hGSTM2	(312)	GAATCAGAAAG	GAGCAGATTTCGC	GAAGACATTTT	TGGAGAACCAG	
hGSTM3	(408)	GAGACTGAAGA	AGAAAGATTTCGA	GTGGACATCAT	TAGAGAACCAG	
hGSTM4	(574)	GAGACAGAAGAG	GAGAAGATTTCGT	GTGGACATTTT	TGGAGAACCAG	
hGSTM5	(335)	GAGACAGAAGAG	GAGAAGATTTCGT	GTGGACATTTT	TGGAGAACCAG	
		Section 15				
		631	640	650	660	675
hGSTM1	(364)	ACCATGGACAACC	CATATGTCAGCTGG	CCATGATCTGCT	TACAATCCA	
hGSTM2	(357)	TTATGGACAGCC	GTATGTCAGCTGG	CCAACTCTGCT	TATGACCCA	
hGSTM3	(453)	GTAATGGATTTCC	GCACACAAGCTG	ATAAGGCTCTG	TACAGCTCT	
hGSTM4	(619)	GCTATGGACGTCT	CCAATCAGCTGG	CCAGAGTCTG	TACAGCCCT	
hGSTM5	(380)	GTTATGGATTAAC	CAATGGAGCTGT	CAGACTGTGCT	TATGACCCA	
		Section 16				
		676	690	700	710	720
hGSTM1	(409)	GAAATTTGAGAACT	GAAAGCCAAAGT	TACTTGGAGGAA	CTCCTGAA	
hGSTM2	(402)	GATTTTGAAGAACT	GAAACCAGAA	TACTTGCAGGCA	CTCCTGAA	
hGSTM3	(498)	GACCACGAAAACT	GAAAGCCTCAGT	TACTTGGAGAG	AGCTACCTGGA	
hGSTM4	(664)	GACTTTGAGAACT	GAAAGCCAGAA	TACTTGGAGGAA	CTCCTACA	
hGSTM5	(425)	GATTTTGAAGAACT	GAAAGCCAAAT	TACTTGGAGGAA	CTCCTGAA	
		Section 17				
		721	730	740	750	765
hGSTM1	(454)	AAGCTAAAGCTCT	TACTCAGAGTTT	CTGGGGAA	GCGGC	CATGGTTT
hGSTM2	(447)	ATGCTGAAGCTCT	TACTCAGAGTTT	CTGGGGAA	GCAAGC	CATGGTTT
hGSTM3	(543)	CAACTGAAACAAT	TCTCCATGTTT	CTGGGGAA	ATTCT	CATGGTTT
hGSTM4	(709)	ATGATGCAGCACT	TCTCAGAGTTT	CTGGGGAA	GAGGC	CATGGTTT
hGSTM5	(470)	AAGCTAAAGCTCT	TACTCAGAGTTT	CTGGGGAA	GCGGC	CATGGTTT
		Section 18				
		766	780	790	800	810
hGSTM1	(499)	GCAAGGAAACAAG	ATCACCTTTGTA	GATTTTCT	CGTCTATGAT	GTC
hGSTM2	(492)	CTTGGGGAACAAG	ATCACCTTTGTA	GATTTTCA	TGCTTATGAT	GTC
hGSTM3	(588)	GCCGGGGAACAAG	CTCACCTTTGTA	GATTTTCT	CACTATGAT	ATC
hGSTM4	(754)	GTTGGAGACAAG	ATCACCTTTGTA	GATTTTCT	CGCTATGAT	GTC
hGSTM5	(515)	GCAAGGAGACAAG	ATCACCTTTGTA	GATTTTCT	TGCCATGAT	GTC

		Section 19				
		811	820	830	840	855
hGSTM1	(544)	CTTGACCTCCACCGTATATTTGAGCCCAAGTGC TTGGACGCCTTC				
hGSTM2	(537)	CTTGAGAGAAACCAAGTATTTGAGCCCA GCTGCCTGGATGCCTTC				
hGSTM3	(633)	TTGATTCAGAACCGTATATTTGACCCCAAGTGCCTGGATGAGTTC				
hGSTM4	(799)	CTTGACCTCCACCGTATATTTGAGCCCAACTGC TTGGACGCCTTC				
hGSTM5	(560)	CTTGACATGAAGCGTATATTTGAGCCCAAGTGC TTGGACGCCTTC				
		Section 20				
		856	870	880	890	900
hGSTM1	(589)	CCAAATCTGAAGGACTTTCATCTCCGCTTTGAGGCGTTGGAGAAG				
hGSTM2	(582)	CCAAACCTGAAGGACTTTCATCTCCGATTTGAGGCGTTGGAGAAG				
hGSTM3	(678)	CCAAACCTGAAGGCTTTCATGTGCCGTTTTGAGGCTTTGGAGAA				
hGSTM4	(844)	CCAAATCTGAAGGACTTTCATCTCCGCTTTGAGGCGTTGGAGAAG				
hGSTM5	(605)	CTAAACTTGAAGGACTTTCATCTCCGCTTTGAGGCTTTGAGAAG				
		Section 21				
		901	910	920	930	945
hGSTM1	(634)	ATCTCTGCCTACATGAAGTC CAGCCGCTTCCTCCCAAGACCTGTG				
hGSTM2	(627)	ATCTCTGCCTACATGAAGTC CAGCCGCTTCCTCCCAAGACCTGTG				
hGSTM3	(723)	ATCGCTGCCTACTTACAGTC TGATCAGTTCTGCAAGATGCCATC				
hGSTM4	(889)	ATCTCTGCCTACATGAAGTC CAGCCGCTTCCTCCCAAACCTCTG				
hGSTM5	(650)	ATCTCTGCCTACATGAAGTC CAGCCAAATTCCTCCGAGTCTTTTG				
		Section 22				
		946	960	970	980	990
hGSTM1	(679)	TTC TCAAAGATGGCTGTCTGGGGCAACAAGTAGGGCC -- TTGAAG				
hGSTM2	(672)	TTCACAAAGATGGCTGTCTGGGGCAACAAGTAGGGCC -- TTGAAG				
hGSTM3	(768)	AACAACAAGATGGCCAGTGGGGCAACAAGCCTGT --- ATGCTG				
hGSTM4	(934)	TACACAAGGGTGGCTGTCTGGGGCAACAAGTATGCC -- TTGAAG				
hGSTM5	(695)	TTTGGAAAGTCA GCTACATGGAA CAGCAAATAGGGCC CAGTGATG				
		Section 23				
		991	1000	1010	1020	1035
hGSTM1	(722)	GC CAGGAGGTGGGAGTGAGGAGCCCATACT --- CAGCCTGCTGC				
hGSTM2	(715)	GC CAGGAGGTGGGAGTGAGGAGCCCATACT --- CAGCCTGCTGC				
hGSTM3	(809)	AG CAGGAGGCAGACTTGCA GAGC TTGTTTGTGTTT CATCCTG - TCC				
hGSTM4	(977)	GC CAGGAGGTGGGAGTGAGGAGCCCATACT --- CAGCCTGCTGC				
hGSTM5	(740)	- C CAG AAGATGGGAGGAGGAGGAGCCCATACTTG --- CTGCCTGCGAC				
		Section 24				
		1036	1050	1060	1070	1080
hGSTM1	(763)	CCAGGCTGTGCAGCGCAGCTGGACTCTGCATCC CAGCACCTGCCT				
hGSTM2	(756)	CCAGGCTGTGCAGCGCAGCTGGACTCTGCATCC CAGCACCTGCCT				
hGSTM3	(853)	GTAAGGGGT - CAGCGCTCTTGCTTTGCTCTTTT CAATGAATAGCA				
hGSTM4	(1018)	CCAGGCTGTGCAGCGCAGCTGGACTCTGCATCC CAGCACCTGCCT				
hGSTM5	(781)	CC TGGAGGA - CAGC - - - - - CTGACTCCCTGGACCTGCCT				

		Section 25																	
		1081	1090				1100				1110	1125							
hGSTM1	(808)	CCTC	GTTCC	TT	TCTCC	TGTTT	ATTCC	CATCT	TTACT	CCC	AAGA								
hGSTM2	(801)	CCTC	GTTCC	TT	TCTCC	TGTTT	ATTCC	CATCT	TTACT	CCC	AAGA								
hGSTM3	(897)	CTTAT	GTTACT	GGT	GTC	CAGCT	GAGTT	TC	TGGG	TATA	AAGG								
hGSTM4	(1063)	CCTC	GTTCC	TT	TCTCC	TGTTT	ATTCC	CATCT	TTAC	CCC	AAGA								
hGSTM5	(814)	TCTTCC	TTT	T	C	CTTCT	TCTA	CTC	TCT	CTTC	CCC	AAGG							
		Section 26																	
		1126	1140				1150				1160	1170							
hGSTM1	(851)	CTTCATTG	TCC	CTC	TTC	CACT	C	CCCCT	AAAC	CCC	CTGTCC	---	ATG						
hGSTM2	(844)	CTTCATTG	TCC	CTC	TTC	CACT	C	CCCCT	AAAC	CCC	CTGTCC	---	ATG						
hGSTM3	(941)	CTAAAGG	GAAAA	AGG	ATAT	GTGG	AGAA	T	CATC	AAG	ATATGA	AT	T						
hGSTM4	(1106)	CTTATTGG	GG	CTC	TTC	CACT	T	CCCCT	AAAC	CCC	CTGTCC	---	ATG						
hGSTM5	(856)	CCTCATTG	G	CTTC	CTTT	CTT	CTAACA	A	T	CATC	CC	TCCC	CGCAT						
		Section 27																	
		1171	1180				1190				1200	1215							
hGSTM1	(893)	CAGGCC	CTTTGA	AGC	CT	CAGCT	A	CCC	ACT	AT	CCTTC	---	GTGAA						
hGSTM2	(886)	CAGGCC	CTTTGA	AGC	CT	CAGCT	A	CCC	ACT	AT	CCTTC	---	GTGAA						
hGSTM3	(986)	GAA	TCGCTGC	ATAC	TGG	CATT	T	CC	TACT	CC	CAAC	TGAG	TTCA						
hGSTM4	(1148)	CAGGCC	CTTTGA	AGC	CT	CAGCT	A	CCC	ACT	T	CCTTC	---	ATGAA						
hGSTM5	(899)	GAGGC	CTTTAA	AGC	TT	CAGCT	C	CCC	ACT	G	CTTC	---	ATCAA						
		Section 28																	
		1216	1230				1240				1250	1260							
hGSTM1	(934)	CATCCC	TCCC	ATCA	TTA	CCCTT	CCCTGC	-----	ACTAAA										
hGSTM2	(927)	CATCCC	TCCC	ATCA	TTA	CCCTT	CCCTGC	-----	ACTAAA										
hGSTM3	(1031)	AGGG	CTG	TAGGT	CA	TGC	CC	AAG	CCCTG	AGAGTGGGT	ACTAGA								
hGSTM4	(1189)	CATCCC	TCCCA	ACA	CTA	CCCTT	CCCTGC	-----	ACTAAA										
hGSTM5	(940)	AGTCCC	TCC	TAA	CGTC	TT	CC	TTT	CCCTGC	-----	ACTAAC								
		Section 29																	
		1261	1270				1280				1290	1305							
hGSTM1	(969)	GCCAGC	CTGAC	CTTCC	--	TT	CCT	GTTAG	TGGT	TGT	GT	CTGC	TTTA						
hGSTM2	(962)	GCCAGC	CTGAC	CTTCC	--	TT	CCT	GTTAG	TGGT	TGT	GT	CTGC	TTTA						
hGSTM3	(1074)	AAA	AAC	GAGA	TTGCA	CAG	TT	GGAG	AGAG	CAG	G	TGT	GT	TAAA	TGGG				
hGSTM4	(1225)	GCCAGC	CTGAC	CTTCC	--	TT	CCT	GTTAG	TGGT	TGT	AT	CTGC	TTTG						
hGSTM5	(977)	GCC	AAC	CTGAC	TGCTT	--	TT	CCT	G	T	CAG	TGCTT	T	CT	CTT	CTTTG			
		Section 30																	
		1306	1320				1330				1340	1350							
hGSTM1	(1012)	AAGGG	CCTGC	CTG	GCCC	CTC	-	GCC	TGTGG	AGCT	CAGCCC	CGAG	--						
hGSTM2	(1005)	AAGGG	CCTGC	CTG	GCCC	CTC	-	GCC	TGTGG	AGCT	CAGCCC	CGAG	--						
hGSTM3	(1119)	A	CTGG	AGT	CC	CTG	TGAAG	ACT	GGG	TGAGG	ATAA	CA	CAAGT	ATAAA					
hGSTM4	(1268)	AAGGG	CCTAC	CTG	GCCC	CTC	-	GCC	TGTGG	AGCT	CAGCCC	CTGAG	--						
hGSTM5	(1020)	A	GAA	GCC	AGA	CTG	AT	CT	TG	-	AG	CT	CCCT	AGCA	CT	GT	CCT	CA	AAG

Section 31

(1351) 1351 1360 1370 1380 1395
 hGSTM1 (1054) -----CTGTC-CCCGTGTGCA-TGAA--GG-----AG--CAGCA
 hGSTM2 (1047) -----CTGTC-CCCGTGTGCA-TGAA--GG-----AG--CAGCA
 hGSTM3 (1163) -----CTGTG-GTACTGATGGACTTAA--CCGG-----AGTT--CGGAA
 hGSTM4 (1310) -----CTGTC-CCCGTGTGCA-TGA-----AGTT--CGGAA
 hGSTM5 (1064) ACCATCTGTATGCCCTGCTCCCTTTGCTGGTCCCTA---CCCAGCT

Section 32

(1396) 1396 1410 1420 1430 1440
 hGSTM1 (1083) TT-GACTGGTTTACA----GGCCCTGCTCCTGCA-----GCAT
 hGSTM2 (1076) TT-GACTGGTTTACA----GGCCCTGCTCCTGCA-----GCAT
 hGSTM3 (1197) ACCGTCCTGTGTACACATGGGAGTTTAGTGTGATA---AAGGCAG
 hGSTM4 (1334) TT-GACTGGTTTACA----GGCCCTGCTCCTGCA-----GCAT
 hGSTM5 (1109) CC-GTGTGATGCCCA---GTAAA---GCTGGAACCATGCCTGCCATGTCTT

Section 33

(1441) 1441 1450 1460 1470 1485
 hGSTM1 (1116) GGTCCCTGCCCTTA-GGCCTACCTGATGGAAGT-----AAAGCCTC
 hGSTM2 (1109) GGTCCCTGCCCTTA-GGCCTACCTGATGGAAGT-----AAAGCCTC
 hGSTM3 (1239) TATTTTCAACTGGTGGGCTAGCCAAATAGAGTTGGGACAAATTGCTT
 hGSTM4 (1367) GGCCTCCCTGCCCTTA-GGCCTACCTGATCAAAAT-----AAAGCCTC
 hGSTM5 (1153) GTCTTATTCCTGAGGGCTCCCTTGACTCAAGGA---CTGTGCTCG

Section 34

(1486) 1486 1500 1510 1520 1530
 hGSTM1 (1155) AACCACA-----
 hGSTM2 (1148) AACCACAAAAAAATAAATA-----
 hGSTM3 (1284) ACTCATTAAAAATAATAGAGCCCCACTTGACACTATTCACATAAAA
 hGSTM4 (1406) AGCCACAAAAAAATAAATAAAAAAAAAAAAA-----
 hGSTM5 (1194) AATTGTGGGTGGTTTTTTGTCTTCTGTTGTCCACAGCCAGAGCTT

Section 35

(1531) 1531 1540 1550 1560 1575
 hGSTM1 (1162) -----
 hGSTM2 (1167) -----
 hGSTM3 (1329) TTAATCTGGAATTTAAGGCCCAACATTAAACACAAAGCTGTTGAA
 hGSTM4 (1437) -----
 hGSTM5 (1239) AGTGGATGGGTGTGTGTGTGTGTGTGTTGGGGGTGGTGATCAGGC

Section 36

(1576) 1576 1590 1600 1610 1620
 hGSTM1 (1162) -----
 hGSTM2 (1167) -----
 hGSTM3 (1374) ATATTGATGAAAATGTAAGAATTTTGTGACCACGGGGTAGGAGA
 hGSTM4 (1437) -----
 hGSTM5 (1284) AGGTTCATAAATTTCTTGGTCATTTCTGCCCTCTAGCCACATCC

						Section 37
(1621)	<u>1621</u>	<u>1630</u>	<u>1640</u>	<u>1650</u>	<u>1665</u>	
hGSTM1 (1162)	-----					
hGSTM2 (1167)	-----					
hGSTM3 (1419)	AGTTTCTTTAAAGACGTAAAAAGAAAAAACCATAGGCTGCTCTG					
hGSTM4 (1437)	-----					
hGSTM5 (1329)	CTCTGTTCTCACTGTGGGGATTACTACAGAAAGGTGCTCTGTGC					
						Section 38
(1666)	<u>1666</u>	<u>1680</u>	<u>1690</u>	<u>1700</u>	<u>1710</u>	
hGSTM1 (1162)	-----					
hGSTM2 (1167)	-----					
hGSTM3 (1464)	CCTGTGGAGTAGCCATTCTTTATTCTTTTACTTTTTAAATAATA					
hGSTM4 (1437)	-----					
hGSTM5 (1374)	CAAGTTCCTCACTCATTTCGCGCTCCTGTAGGCCGTCTAGAAGTGG					
						Section 39
(1711)	<u>1711</u>	<u>1720</u>	<u>1730</u>	<u>1740</u>	<u>1755</u>	
hGSTM1 (1162)	-----					
hGSTM2 (1167)	-----					
hGSTM3 (1509)	ACAATCACAAAGGAAAGATTTGCCAATTGAATAGGATCAAATTCT					
hGSTM4 (1437)	-----					
hGSTM5 (1419)	CATGGTTCAAAGAGGGGCTAGGCTGATGGGGAAGGGGCTGAGCA					
						Section 40
(1756)	<u>1756</u>	<u>1770</u>	<u>1780</u>	<u>1790</u>	<u>1800</u>	
hGSTM1 (1162)	-----					
hGSTM2 (1167)	-----					
hGSTM3 (1554)	ACAACTTTTCCTAAGGCACCCACAAATAAATGACAAGTGAGACAA					
hGSTM4 (1437)	-----					
hGSTM5 (1464)	GCTCCAGGCAGACTGCCTTCTTTCACCC-TGTCCTGATAGACTT					
						Section 41
(1801)	<u>1801</u>	<u>1810</u>	<u>1820</u>	<u>1830</u>	<u>1845</u>	
hGSTM1 (1162)	-----					
hGSTM2 (1167)	-----					
hGSTM3 (1599)	AAAGCACTAGTATAAAGATTATATAAAGACCTATAAATCATTAAG					
hGSTM4 (1437)	-----					
hGSTM5 (1508)	CCCTGATCTAGATATCCTTCGTGACACTTCTCAATAAAAACGT					
						Section 42
(1846)	<u>1846</u>	<u>1860</u>	<u>1870</u>	<u>1880</u>	<u>1890</u>	
hGSTM1 (1162)	-----					
hGSTM2 (1167)	-----					
hGSTM3 (1644)	ACAACTGAGTTTTTAAAAATGGACAAAATCCATGAACAATTTATA					
hGSTM4 (1437)	-----					
hGSTM5 (1553)	ATCCCACCGTATTGT-----					

Section 43					
(1891)	1891	1900	1910	1920	1935
hGSTM1 (1162)	-----	-----	-----	-----	-----
hGSTM2 (1167)	-----	-----	-----	-----	-----
hGSTM3 (1689)	AAATAGAAATATAGCCAAAAATGTCTAAAAGATGTTTATGATGTA				
hGSTM4 (1437)	-----	-----	-----	-----	-----
hGSTM5 (1568)	-----	-----	-----	-----	-----
Section 44					
(1936)	1936	1950	1960	1970	1980
hGSTM1 (1162)	-----	-----	-----	-----	-----
hGSTM2 (1167)	-----	-----	-----	-----	-----
hGSTM3 (1734)	AGGAATTATCAATTACAACAGTGAGAAACCATATTTCTTCTATC				
hGSTM4 (1437)	-----	-----	-----	-----	-----
hGSTM5 (1568)	-----	-----	-----	-----	-----
Section 45					
(1981)	1981	1990	2000	2010	2025
hGSTM1 (1162)	-----	-----	-----	-----	-----
hGSTM2 (1167)	-----	-----	-----	-----	-----
hGSTM3 (1779)	CGATGAGTAAAAAGTTTCTAAAGTGTTGGCAAGGCTTAGGAAAGT				
hGSTM4 (1437)	-----	-----	-----	-----	-----
hGSTM5 (1568)	-----	-----	-----	-----	-----
Section 46					
(2026)	2026	2040	2050	2060	2070
hGSTM1 (1162)	-----	-----	-----	-----	-----
hGSTM2 (1167)	-----	-----	-----	-----	-----
hGSTM3 (1824)	GATATGCATTTCTGCTGGTCAAGTTGTAAATTAGTATAGCTACT				
hGSTM4 (1437)	-----	-----	-----	-----	-----
hGSTM5 (1568)	-----	-----	-----	-----	-----
Section 47					
(2071)	2071	2080	2090	2100	2115
hGSTM1 (1162)	-----	-----	-----	-----	-----
hGSTM2 (1167)	-----	-----	-----	-----	-----
hGSTM3 (1869)	TTGGAGGACAATTGTAAAATTTAAATCATATCCTATGACCCAGCA				
hGSTM4 (1437)	-----	-----	-----	-----	-----
hGSTM5 (1568)	-----	-----	-----	-----	-----
Section 48					
(2116)	2116	2130	2140	2150	2160
hGSTM1 (1162)	-----	-----	-----	-----	-----
hGSTM2 (1167)	-----	-----	-----	-----	-----
hGSTM3 (1914)	ATTCCATGCTATAAAAACTCATCCATGGCCGGGCTTGTTGGCTCA				
hGSTM4 (1437)	-----	-----	-----	-----	-----
hGSTM5 (1568)	-----	-----	-----	-----	-----

Section 49					
(2161)	<u>2161</u>	<u>2170</u>	<u>2180</u>	<u>2190</u>	<u>2205</u>
hGSTM1 (1162)	-----	-----	-----	-----	-----
hGSTM2 (1167)	-----	-----	-----	-----	-----
hGSTM3 (1959)	CGCCTGTAATCCCAGCACTTTGGGAGGCTGAGGTGGGCAGATCAC				
hGSTM4 (1437)	-----	-----	-----	-----	-----
hGSTM5 (1568)	-----	-----	-----	-----	-----
Section 50					
(2206)	<u>2206</u>	<u>2220</u>	<u>2230</u>	<u>2240</u>	<u>2250</u>
hGSTM1 (1162)	-----	-----	-----	-----	-----
hGSTM2 (1167)	-----	-----	-----	-----	-----
hGSTM3 (2004)	GAGGTCAAGAGATCGAGACCATCCTGGCCAACATGATGAAACCCC				
hGSTM4 (1437)	-----	-----	-----	-----	-----
hGSTM5 (1568)	-----	-----	-----	-----	-----
Section 51					
(2251)	<u>2251</u>	<u>2260</u>	<u>2270</u>	<u>2280</u>	<u>2295</u>
hGSTM1 (1162)	-----	-----	-----	-----	-----
hGSTM2 (1167)	-----	-----	-----	-----	-----
hGSTM3 (2049)	GTTTCTACTAAAAATACAAAAATTAGCTGGGCATGGTGGCATGTG				
hGSTM4 (1437)	-----	-----	-----	-----	-----
hGSTM5 (1568)	-----	-----	-----	-----	-----
Section 52					
(2296)	<u>2296</u>	<u>2310</u>	<u>2320</u>	<u>2330</u>	<u>2340</u>
hGSTM1 (1162)	-----	-----	-----	-----	-----
hGSTM2 (1167)	-----	-----	-----	-----	-----
hGSTM3 (2094)	CCTATAGTCCCAGCTACTCAGGAGGCTGAGGCAGGAGAATTGCTT				
hGSTM4 (1437)	-----	-----	-----	-----	-----
hGSTM5 (1568)	-----	-----	-----	-----	-----
Section 53					
(2341)	<u>2341</u>	<u>2350</u>	<u>2360</u>	<u>2370</u>	<u>2385</u>
hGSTM1 (1162)	-----	-----	-----	-----	-----
hGSTM2 (1167)	-----	-----	-----	-----	-----
hGSTM3 (2139)	GAACCTGGGAGGCAGAGGTTGCAGTGAGCCGAGATCACGCCACTG				
hGSTM4 (1437)	-----	-----	-----	-----	-----
hGSTM5 (1568)	-----	-----	-----	-----	-----
Section 54					
(2386)	<u>2386</u>	<u>2400</u>	<u>2410</u>	<u>2420</u>	<u>2430</u>
hGSTM1 (1162)	-----	-----	-----	-----	-----
hGSTM2 (1167)	-----	-----	-----	-----	-----
hGSTM3 (2184)	CACTCCAGCCTGGCTACAGGGCGAGACTCTGTCTCAAAAAAAAAAA				
hGSTM4 (1437)	-----	-----	-----	-----	-----
hGSTM5 (1568)	-----	-----	-----	-----	-----

Section 55

	(2431)	<u>2431</u>	<u>2440</u>	<u>2450</u>	<u>2460</u>	<u>2475</u>
hGSTM1 (1162)	-----					
hGSTM2 (1167)	-----					
hGSTM3 (2229)	AAAAAAAAAAAAAAAAAAAAACATTCAAAGAGACATATACTAAGATGT					
hGSTM4 (1437)	-----					
hGSTM5 (1568)	-----					

Section 56

	(2476)	<u>2476</u>	<u>2490</u>	<u>2500</u>	<u>2510</u>	<u>2520</u>
hGSTM1 (1162)	-----					
hGSTM2 (1167)	-----					
hGSTM3 (2274)	TCACTGTGGCATTGTCTGTAATGACAAATAAGTGGAAACCGTGTA					
hGSTM4 (1437)	-----					
hGSTM5 (1568)	-----					

Section 57

	(2521)	<u>2521</u>	<u>2530</u>	<u>2540</u>	<u>2550</u>	<u>2565</u>
hGSTM1 (1162)	-----					
hGSTM2 (1167)	-----					
hGSTM3 (2319)	AATACCTGTCAATACTATGGAGTACCATGTGGCAACGGAAGAATG					
hGSTM4 (1437)	-----					
hGSTM5 (1568)	-----					

Section 58

	(2566)	<u>2566</u>	<u>2580</u>	<u>2590</u>	<u>2600</u>	<u>2610</u>
hGSTM1 (1162)	-----					
hGSTM2 (1167)	-----					
hGSTM3 (2364)	AGACTGAACTGTGTGAACTAACATGCAAAGATCCCCAAAACAGGC					
hGSTM4 (1437)	-----					
hGSTM5 (1568)	-----					

Section 59

	(2611)	<u>2611</u>	<u>2620</u>	<u>2630</u>	<u>2640</u>	<u>2655</u>
hGSTM1 (1162)	-----					
hGSTM2 (1167)	-----					
hGSTM3 (2409)	CAGGTGTGGTTGCTCACAGCTGTAATAACAACACCTTCAGAGGCT					
hGSTM4 (1437)	-----					
hGSTM5 (1568)	-----					

Section 60

	(2656)	<u>2656</u>	<u>2670</u>	<u>2680</u>	<u>2690</u>	<u>2700</u>
hGSTM1 (1162)	-----					
hGSTM2 (1167)	-----					
hGSTM3 (2454)	GAGGTGAGAGGATCAGTTGAGGCCAGGAGTTTAAGACCAGCCTGG					
hGSTM4 (1437)	-----					
hGSTM5 (1568)	-----					

Section 61					
(2701)	<u>2701</u>	<u>2710</u>	<u>2720</u>	<u>2730</u>	<u>2745</u>
hGSTM1 (1162)	-----	-----	-----	-----	-----
hGSTM2 (1167)	-----	-----	-----	-----	-----
hGSTM3 (2499)	GCAACATAGTGAGACCCCTGTCTCCCAAAAATTTTTTTTAATTAG				
hGSTM4 (1437)	-----	-----	-----	-----	-----
hGSTM5 (1568)	-----	-----	-----	-----	-----
Section 62					
(2746)	<u>2746</u>	<u>2760</u>	<u>2770</u>	<u>2780</u>	<u>2790</u>
hGSTM1 (1162)	-----	-----	-----	-----	-----
hGSTM2 (1167)	-----	-----	-----	-----	-----
hGSTM3 (2544)	CTGTGCGCAATTGCTCATGCATAGTCCCAGCTACCCAGGAGGCTG				
hGSTM4 (1437)	-----	-----	-----	-----	-----
hGSTM5 (1568)	-----	-----	-----	-----	-----
Section 63					
(2791)	<u>2791</u>	<u>2800</u>	<u>2810</u>	<u>2820</u>	<u>2835</u>
hGSTM1 (1162)	-----	-----	-----	-----	-----
hGSTM2 (1167)	-----	-----	-----	-----	-----
hGSTM3 (2589)	AGGTGGGAGGATCACTTGAGCCCAGGAATTTGAAGCTGCAGTGAG				
hGSTM4 (1437)	-----	-----	-----	-----	-----
hGSTM5 (1568)	-----	-----	-----	-----	-----
Section 64					
(2836)	<u>2836</u>	<u>2850</u>	<u>2860</u>	<u>2870</u>	<u>2880</u>
hGSTM1 (1162)	-----	-----	-----	-----	-----
hGSTM2 (1167)	-----	-----	-----	-----	-----
hGSTM3 (2634)	CTGTGTTCTTGCCACTGCACTCCAATCTGGGTGACTGAGCAAGAC				
hGSTM4 (1437)	-----	-----	-----	-----	-----
hGSTM5 (1568)	-----	-----	-----	-----	-----
Section 65					
(2881)	<u>2881</u>	<u>2890</u>	<u>2900</u>	<u>2910</u>	<u>2925</u>
hGSTM1 (1162)	-----	-----	-----	-----	-----
hGSTM2 (1167)	-----	-----	-----	-----	-----
hGSTM3 (2679)	CCTGTCTCTTAAAAAATAAAAAAGATCTCCAAGCATAGAGAAGA				
hGSTM4 (1437)	-----	-----	-----	-----	-----
hGSTM5 (1568)	-----	-----	-----	-----	-----
Section 66					
(2926)	<u>2926</u>	<u>2940</u>	<u>2950</u>	<u>2960</u>	<u>2970</u>
hGSTM1 (1162)	-----	-----	-----	-----	-----
hGSTM2 (1167)	-----	-----	-----	-----	-----
hGSTM3 (2724)	GTCTGGAGGGAAACACCAAACATAACAGTCTTACTGCAGGCAA				
hGSTM4 (1437)	-----	-----	-----	-----	-----
hGSTM5 (1568)	-----	-----	-----	-----	-----

						Section 67
(2971)	<u>2971</u>	<u>2980</u>	<u>2990</u>	<u>3000</u>	<u>3015</u>	
hGSTM1 (1162)	-----	-----	-----	-----	-----	
hGSTM2 (1167)	-----	-----	-----	-----	-----	
hGSTM3 (2769)	GTGGGATAAAGGCC	CAGACTCCATGGT	GGAAGTTAAAGGGC	ATTT		
hGSTM4 (1437)	-----	-----	-----	-----	-----	
hGSTM5 (1568)	-----	-----	-----	-----	-----	
						Section 68
(3016)	<u>3016</u>	<u>3030</u>	<u>3040</u>	<u>3050</u>	<u>3060</u>	
hGSTM1 (1162)	-----	-----	-----	-----	-----	
hGSTM2 (1167)	-----	-----	-----	-----	-----	
hGSTM3 (2814)	CCAAGTTAAGGCTA	AGACTTGCTTTTCT	AACTAAGAGAATGT	GCT		
hGSTM4 (1437)	-----	-----	-----	-----	-----	
hGSTM5 (1568)	-----	-----	-----	-----	-----	
						Section 69
(3061)	<u>3061</u>	<u>3070</u>	<u>3080</u>	<u>3090</u>	<u>3105</u>	
hGSTM1 (1162)	-----	-----	-----	-----	-----	
hGSTM2 (1167)	-----	-----	-----	-----	-----	
hGSTM3 (2859)	CATGCATTGCTTGT	GTAGTAGAACTAGT	TTTTTAGAAAAGAA	AGC		
hGSTM4 (1437)	-----	-----	-----	-----	-----	
hGSTM5 (1568)	-----	-----	-----	-----	-----	
						Section 70
(3106)	<u>3106</u>	<u>3120</u>	<u>3130</u>	<u>3140</u>	<u>3150</u>	
hGSTM1 (1162)	-----	-----	-----	-----	-----	
hGSTM2 (1167)	-----	-----	-----	-----	-----	
hGSTM3 (2904)	AAACTTAAGAAAC	ACTGACTCCTGTGG	GAGATGACTTGGC	ACCACT		
hGSTM4 (1437)	-----	-----	-----	-----	-----	
hGSTM5 (1568)	-----	-----	-----	-----	-----	
						Section 71
(3151)	<u>3151</u>	<u>3160</u>	<u>3170</u>	<u>3180</u>	<u>3195</u>	
hGSTM1 (1162)	-----	-----	-----	-----	-----	
hGSTM2 (1167)	-----	-----	-----	-----	-----	
hGSTM3 (2949)	CTCCTTTCACAGAG	CAGAGTCTGAATAG	TCTTCAGAGATAG	GCCT		
hGSTM4 (1437)	-----	-----	-----	-----	-----	
hGSTM5 (1568)	-----	-----	-----	-----	-----	
						Section 72
(3196)	<u>3196</u>	<u>3210</u>	<u>3220</u>	<u>3230</u>	<u>3240</u>	
hGSTM1 (1162)	-----	-----	-----	-----	-----	
hGSTM2 (1167)	-----	-----	-----	-----	-----	
hGSTM3 (2994)	GTGGGCCAGATTGCC	CATCCCCTATGGAC	CAGAAGCCAAGGAT	CTC		
hGSTM4 (1437)	-----	-----	-----	-----	-----	
hGSTM5 (1568)	-----	-----	-----	-----	-----	

Section 73

(3241)	<u>3241</u>	<u>3250</u>	<u>3260</u>	<u>3270</u>	<u>3285</u>
hGSTM1 (1162)	-----				
hGSTM2 (1167)	-----				
hGSTM3 (3039)	TCTAGTGATGGTCAGAGGGCCCAAATGGCAGGGATACCCAGTGAT				
hGSTM4 (1437)	-----				
hGSTM5 (1568)	-----				

Section 74

(3286)	<u>3286</u>	<u>3300</u>	<u>3310</u>	<u>3320</u>	<u>3330</u>
hGSTM1 (1162)	-----				
hGSTM2 (1167)	-----				
hGSTM3 (3084)	GTCAGGAGGAATAGTACAGACAGAAGGTGCTAAGCAGACAATTCA				
hGSTM4 (1437)	-----				
hGSTM5 (1568)	-----				

Section 75

(3331)	<u>3331</u>	<u>3340</u>	<u>3350</u>	<u>3360</u>	<u>3375</u>
hGSTM1 (1162)	-----				
hGSTM2 (1167)	-----				
hGSTM3 (3129)	ACTGCCATGTTTTGCCACCCCTGTGAGCAGGGATTAGGTGTTCA				
hGSTM4 (1437)	-----				
hGSTM5 (1568)	-----				

Section 76

(3376)	<u>3376</u>	<u>3390</u>	<u>3400</u>	<u>3410</u>	<u>3420</u>
hGSTM1 (1162)	-----				
hGSTM2 (1167)	-----				
hGSTM3 (3174)	GGCCAGTATCTTGGGCATGGGGGAGCCTTTGGCCAGAAGAGGTAT				
hGSTM4 (1437)	-----				
hGSTM5 (1568)	-----				

Section 77

(3421)	<u>3421</u>	<u>3430</u>	<u>3440</u>	<u>3450</u>	<u>3465</u>
hGSTM1 (1162)	-----				
hGSTM2 (1167)	-----				
hGSTM3 (3219)	AAAGCTCAGAAGTTTTTCAGTCTGATAACTATTGATATAATTTCC				
hGSTM4 (1437)	-----				
hGSTM5 (1568)	-----				

Section 78

(3466)	<u>3466</u>	<u>3480</u>	<u>3490</u>	<u>3500</u>	<u>3510</u>
hGSTM1 (1162)	-----				
hGSTM2 (1167)	-----				
hGSTM3 (3264)	ATAGTGAGGGAGCGGTATGCTCTACCCTTGTGTATTTAAGGCA				
hGSTM4 (1437)	-----				
hGSTM5 (1568)	-----				

Section 79					
(3511)	3511	3520	3530	3540	3555
hGSTM1 (1162)	-----	-----	-----	-----	-----
hGSTM2 (1167)	-----	-----	-----	-----	-----
hGSTM3 (3309)	GGACAGAGAAATTGAGGATGCCCTGGGGCTAGATCGATGATATG				
hGSTM4 (1437)	-----	-----	-----	-----	-----
hGSTM5 (1568)	-----	-----	-----	-----	-----
Section 80					
(3556)	3556	3570	3580	3590	3600
hGSTM1 (1162)	-----	-----	-----	-----	-----
hGSTM2 (1167)	-----	-----	-----	-----	-----
hGSTM3 (3354)	ACCAGAAATCAAAAAGGGAATGCATTATTTATTGCTGTGTAACAC				
hGSTM4 (1437)	-----	-----	-----	-----	-----
hGSTM5 (1568)	-----	-----	-----	-----	-----
Section 81					
(3601)	3601	3610	3620	3630	3645
hGSTM1 (1162)	-----	-----	-----	-----	-----
hGSTM2 (1167)	-----	-----	-----	-----	-----
hGSTM3 (3399)	TGTTAAGAGAGGAGGTAGTTAAGGGATGGATAGGCACATAGAGAG				
hGSTM4 (1437)	-----	-----	-----	-----	-----
hGSTM5 (1568)	-----	-----	-----	-----	-----
Section 82					
(3646)	3646	3660	3670	3680	3690
hGSTM1 (1162)	-----	-----	-----	-----	-----
hGSTM2 (1167)	-----	-----	-----	-----	-----
hGSTM3 (3444)	GGAAGGTCTCAGGAGAAGGGATAGAAAGGAACTATGTTTACAAGA				
hGSTM4 (1437)	-----	-----	-----	-----	-----
hGSTM5 (1568)	-----	-----	-----	-----	-----
Section 83					
(3691)	3691	3700	3710	3720	3735
hGSTM1 (1162)	-----	-----	-----	-----	-----
hGSTM2 (1167)	-----	-----	-----	-----	-----
hGSTM3 (3489)	ACAACGGCAAGACAGTGCCTATACTGCCTCTACAGTTAATAGGAA				
hGSTM4 (1437)	-----	-----	-----	-----	-----
hGSTM5 (1568)	-----	-----	-----	-----	-----
Section 84					
(3736)	3736	3750	3760	3770	3780
hGSTM1 (1162)	-----	-----	-----	-----	-----
hGSTM2 (1167)	-----	-----	-----	-----	-----
hGSTM3 (3534)	AAACGGAAGAAGTTACCCTTAAGCTAGGATGTTGCTCAGAAGTGA				
hGSTM4 (1437)	-----	-----	-----	-----	-----
hGSTM5 (1568)	-----	-----	-----	-----	-----

Section 85					
(3781)	3781	3790	3800	3810	3825
hGSTM1 (1162)	-----	-----	-----	-----	-----
hGSTM2 (1167)	-----	-----	-----	-----	-----
hGSTM3 (3579)	CCATCCCAACTTTGGTGCGGGCACAATAAATCAGCCTAAATGTCC				
hGSTM4 (1437)	-----	-----	-----	-----	-----
hGSTM5 (1568)	-----	-----	-----	-----	-----
Section 86					
(3826)	3826	3840	3850	3860	3870
hGSTM1 (1162)	-----	-----	-----	-----	-----
hGSTM2 (1167)	-----	-----	-----	-----	-----
hGSTM3 (3624)	CTAATTTAACCAGCTCATTATAATGTCATTAAACATGACATTAG				
hGSTM4 (1437)	-----	-----	-----	-----	-----
hGSTM5 (1568)	-----	-----	-----	-----	-----
Section 87					
(3871)	3871	3880	3890	3900	3915
hGSTM1 (1162)	-----	-----	-----	-----	-----
hGSTM2 (1167)	-----	-----	-----	-----	-----
hGSTM3 (3669)	CATTGTGGTTTTAGCACCCCATGGGTTTTGCTTAGGCACTCATG				
hGSTM4 (1437)	-----	-----	-----	-----	-----
hGSTM5 (1568)	-----	-----	-----	-----	-----
Section 88					
(3916)	3916	3930	3940	3950	3960
hGSTM1 (1162)	-----	-----	-----	-----	-----
hGSTM2 (1167)	-----	-----	-----	-----	-----
hGSTM3 (3714)	GGTAATAACCAAGATGGAGTCCCTTTGGCAAACCTTAGGCATGCA				
hGSTM4 (1437)	-----	-----	-----	-----	-----
hGSTM5 (1568)	-----	-----	-----	-----	-----
Section 89					
(3961)	3961	3970	3980	3990	4005
hGSTM1 (1162)	-----	-----	-----	-----	-----
hGSTM2 (1167)	-----	-----	-----	-----	-----
hGSTM3 (3759)	CAGCTGTAGTACCCCAAGAAGAAAATGTTACTTCTCTCATCTGGG				
hGSTM4 (1437)	-----	-----	-----	-----	-----
hGSTM5 (1568)	-----	-----	-----	-----	-----
Section 90					
(4006)	4006	4020	4030	4040	4050
hGSTM1 (1162)	-----	-----	-----	-----	-----
hGSTM2 (1167)	-----	-----	-----	-----	-----
hGSTM3 (3804)	CAAAACCCACAGAAGACTTCCAGCTTCTGCCACATAAAAGACAC				
hGSTM4 (1437)	-----	-----	-----	-----	-----
hGSTM5 (1568)	-----	-----	-----	-----	-----

Section 91

(4051) 4051 4060 4070 4080 4095
hGSTM1 (1162) -----
hGSTM2 (1167) -----
hGSTM3 (3849) AGAACACAGACGCCTTACTGGCAACCTGCTTTCAAGACCCCTGTC
hGSTM4 (1437) -----
hGSTM5 (1568) -----

Section 92

(4096) 4096 4110 4120 4130 4140
hGSTM1 (1162) -----
hGSTM2 (1167) -----
hGSTM3 (3894) TTTGCTGAGAGCTTTCCTTTTTCCCAATAAATTCTACTCTGCCCT
hGSTM4 (1437) -----
hGSTM5 (1568) -----

Section 93

(4141) 4141 4150
hGSTM1 (1162) -----
hGSTM2 (1167) -----
hGSTM3 (3939) ACTCACTCTC
hGSTM4 (1437) -----
hGSTM5 (1568) -----